THESIS AND ABSTRACT

CALHM6: Function in the innate immune system and role in infectious diseases

By Sara Danielli



Linacre College, University of Oxford

Kennedy Institute of Rheumatology, NDORMS

Thesis submitted in fulfilment of the requirements for the degree of Doctor in Philosophy, University of Oxford

Michaelmas Term 2021

Abstract

CALHM6: Function in the innate immune system and role in infectious disease

By Sara Danielli

Innate myeloid cells, such as macrophages and dendritic cells (DC), regulate the type, the magnitude, and the duration of the immune response. Macrophages and DCs do so, by instructing the functions of effector cells, such as natural killer (NK) cells. NK cells effector functions are important in the killing of virus or bacterial-infected and malignantly transformed cells. NK cells also participate in the production of cytokines like IFN-γ, IL-10 and TNF after viral, fungal or bacterial infection.

CALHMs (calcium homeostasis modulator) are a family of membrane proteins recently identified as voltage-gated oligomeric ion- and ATP-channels. CALHM1 and 3 specifically, form a channel that localises in the synapse between taste bud cells and neurons, where it is important for the formation of a synaptic structure. Interestingly, a single member of the CALHM family, CALHM6 is expressed almost exclusively in immune cells. Like other CALHMs, CALHM6 forms a higher order complex, composed by up to 11 oligomers, with a channel-like structure. Previous studies show that CALHM6 is required for the instruction of antitumour effector responses in NK cells, but its role in infections and its mechanism of action remains unknown.

In this work we show that in myeloid cells, CALHM6 is highly induced on myeloid cells in response to pathogen derived signals and is inhibited by anti-inflammatory cytokines. Also, while the structure of CALHM6 resembles a higher oligomeric version of the CALHM1/3 channel, we show that its gating is different as it does not release ATP in response to the same stimuli that open CALHM1/3.

To understand the function of CALHM6, we generated CALHM6 deficient mice (*Calhm6*$^{-/-}$). To test whether CALHM6 plays a role in the immune response to infections we challenged WT and *Calhm6*$^{-/-}$ mice with *Listeria monocytogenes* (*L. monocytogenes)* an intracellular gram-positive bacterium that elicits a strong innate immune response and require NK cells derived IFN-γ for its clearance by activated macrophages. *Calhm6*$^{-/-}$ mice fail to control *L. monocytogenes* burden at peak infection. This is not caused by an intrinsic failure of macrophages in killing *Listeria* but it is likely driven by an early deficiency in NK-derived IFN-γ, that causes a delay in the kinetic of the innate immune response.

It is well appreciated that the most efficient activation of NK cells *in vivo* requires their direct priming/interaction with activated macrophages/DC. *Calhm6*$^{-/-}$ mice are specifically unable to activate

NK cells in a DC- and macrophage-dependent manner. Bone marrow derived macrophages from *Calhm6*$^{-/-}$ mice fail to upregulate mRNA expression of synaptic-associated genes when stimulated with pro-inflammatory stimuli. This together with our findings that CALHM6 relocates to the macrophage-NK cell interface *in vitro*, suggests that CALHM6 localises in the immunological synapse between innate and NK cells, where it forms a channel that is important in the innate cell-mediated instruction of NK cell activation.

Acknowledgements

This thesis is the result of four years of struggles, lockdowns and more failed hypothesis that I would wish on anyone, but this is not why I will remember my DPhil with fondness for the rest of my life. First and foremost, I will remember those years as full of excitement, discoveries, and personal growth, especially because I had the luck to spend them with the most amazing bunch of people I could hope for.

None of this would have been possible without the unconditional support of my supervisor that has stuck with me, especially when time were though, always keeping my passion for this job alive. All throughout Jelena has been a mentor, a friend, and a bottomless source of knowledge. I was also lucky enough to have great colleagues that made my life in the lab easy and enjoyable. I cannot thank them enough for their intellectual generosity and their willingness to sit through three hours of lab meeting just to come up with a reasonable explanation for my constantly puzzling data.

I will not even try to distil in a few sentences my gratitude for my partner David because it would take more than the word limit of this document to do him justice. He is my best reason to go back home in the evening and be cheerful, no matter what happened in the lab. He is the source of my resilience and he is always been there to remind me that we are not defined by our jobs.

My family deserves a special mention at the beginning of this thesis, even if I am pretty sure they still have no idea what my job his. It is only through their support and their staunch conviction that access to education was the most important instrument that they could provide me to guarantee my happiness that this work was possible. And after many years I am glad to say that they were right.

If it is not the journey but the friends that you make along the way that counts, then mine has been an invaluable journey. Every member of my home-away-from-home crew has gifted me with moments of true joy and personal growth. I will cherish the memory of our every dinner, night out, concert, birthday and late night scientific and philosophical discussion for many years to come. The ones I was sober enough to remember at least. They say that if you are the most interesting person in the room then you are in the wrong room, well, that never happened when I was with the OxFam. My friends showed me how to be kind, self-confident, passionate and caring, and I became a better person for it.

"If you trust in yourself, and believe in your dreams, and follow your star…you'll still get beaten by people who spent their time working hard and learning things and weren't so lazy."

Terry Pratchett

1 Contents

Abstract 2

By Sara Danielli 2

Acknowledgements 4

2 Abbreviations 11

3 Introduction 15

3.1 The CALHM family 15

3.1.1 Discovery of CALHMs as a new family of membrane ATP channel 15

3.1.2 CALHMs in taste sensing 17

3.1.3 CALHMs in the central nervous system 23

CALHMs in the immune system 25

3.1.4 25

3.2 Natural killer cell activation in viral and bacterial infection 30

3.2.1 Definition, development and subsets of NK cells 30

3.2.2 Activation of NK cells 32

3.2.3 NK cells effector responses: cytotoxicity 45

3.2.4 NK effector responses: secretion of pro-inflammatory cytokines 47

3.3 Listeria monocytogenes 48

3.3.1 Cell biology of *L. monocytogenes* 49

3.3.2 Innate response to *L. monocytogenes* 50

3.3.3 Sensing of *L. monocytogenes* 51

3.3.4 Innate cells in *L. monocytogenes* immune response 52

3.3.5 Adaptive responses to *L. monocytogenes* 55

3.4 Thesis hypothesis and Aims 58

4 Materials and methods 59

4.1 Cell cultures 59

4.1.1 Bone marrow collection 59

4.1.2 Bone marrow derived macrophages generation 59

4.1.3 BMDC generation 59

4.1.4 HEK293T cells 60

4.1.5 Plat-E cells 60

4.2 In vitro cell stimulation 60

4.2.1 Pro- and anti-inflammatory stimuli for BMDM/BMDC 60

4.2.2 Listeria infection 60

4.2.3 NK cell activation with soluble factors or PMA 61

4.3 Quantitative real-time PCR 61
4.4 Immunoblots 62
4.4.1 SDS page 62
4.4.2 Native BluePAGE gel 63
4.5 *Calhm6*$^{-/-}$ mouse strains 63
4.5.1 Generation of *Calhm6*$^{-/-}$ mouse strains 63
4.5.2 Genotyping PCR 64
4.6 Flow cytometry 64
4.6.1 Single cell suspension from spleen 64
4.6.2 Single cell suspension from thymus 64
4.6.3 Flow cytometry staining 65
4.7 In vivo *L. monocytogenes* infection 65
4.7.1 Primary *L. monocytogenes* infection 65
4.7.2 L. monocytogenes re-challenge 66
4.8 In vivo Poly(I:C) injection 66
4.9 Cytokine measurement 66
4.9.1 Serum collection 66
4.9.2 ELISA assay 67
4.9.3 LEGENDplex 67
4.10 H3N2 Influenza virus infection 68
4.11 Griess Assay for NO2- measurement 68
4.12 In vitro *L. monocytogenes* infection 68
4.13 *in vitro* co-culture experiments 69
4.13.1 BMDM/BMDC-NK cells co-culture 69
4.13.2 F4/80^{+}-NK1.1^{+}CD3^{-} cell co-culture 69
4.13.3 Whole spleen culture 70
4.14 Overexpression of CALHM6 70
4.14.1 Plasmid generation 70
4.14.2 HEK293T transfection 70
4.14.3 BMDM transduction 71
4.15 Confocal imaging 71
4.15.1 CALHM6-GFP imaging 72
4.15.2 BMDM-NK synapse imaging 72
4.15.3 Opsonisation of sRBC 72
4.15.4 BMDM-beads or BMDM-sheep RBC synapse imaging 73
4.16 phagocytosis and endocytosis assay 73

4.16.1 sRBC phagocytosis 73
4.16.2 Zymosan Phagocytosis 74
4.16.3 Dextran endocytosis 74
4.17 De-glycosylation 75
4.18 ATP release assays 75
4.18.1 ATP release from BMDM 75
4.18.2 ATP release from transfected HEK 293T cells or transduced BMDM 75
4.18.3 ATP released from transfected Plat-E cells 76
4.19 Inflammasome activation 76
4.20 Table1: Primers for qPCR 76
4.21 Table 2: Primers for genotyping 77
4.22 Table 3: list of reagents 77
5 CALHM6 regulation in the innate immune system 81
5.1 Introduction: 81
5.1.1 Calhm6 regulation in the immune system 82
5.1.2 Generation of a CALHM6 transgenic mice 83
5.2 Chapter aims: 83
5.3 Results 84
5.3.1 CALHM6 is mostly expressed in innate immune cells, especially monocytes and macrophages 84
5.3.2 CALHM6 is upregulated by pro- and downregulated by anti-inflammatory stimuli 87
5.3.3 *Calhm6* expression is boosted by IFN-γ pre-treatment 90
5.3.4 Generation and characterisation of a *Calhm6*$^{-/-}$ mouse 92
5.4 Discussion 98
5.4.1 CALHM6 expression at steady state 98
5.4.2 CALHM6 expression in BMDM versus BMDC 99
5.4.3 Regulation of *Calhm6* expression by pro- and anti-inflammatory signals 100
5.4.4 Generation of *Calhm6*$^{-/-}$ mice 102
5.5 Limitations of the study 103
5.6 Conclusions 104
6 Role of CALHM6 in infection 106
6.1 Introduction 106
6.1.1 CALHM6 role in NK cell activation 106
6.1.2 Choosing murine models of infection 107
6.2 Aims 109
6.3 Results 110

6.3.1 *Calhm6-/-* mice fail to produce IFN-γ in the early stage of *L. monocytogenes* infection 110
6.3.2 IFN-γ but not granzyme B production is impaired in *Calhm6*$^{-/-}$ mice 113
6.3.3 *Calhm6*$^{-/-}$ mice fail to control the early phase of *L. monocytogenes* infection 115
6.3.4 *Calhm6*$^{-/-}$ mice are more susceptible to *L. monocytogenes* even when exposed to lower doses of infection 117
6.3.5 *Calhm6*$^{-/-}$ mice can compensate IFN-γ production at peak infection 119
6.3.6 CALHM6 absence causes a shift in the kinetic of the immune response 122
6.3.7 *Calhm6*$^{-/-}$ mice can efficiently clear *L. monocytogenes* in the later phase of the infection 124
6.3.8 Absence of CALHM6 does not impair memory response to *L. monocytogenes* infection 126
6.3.9 CALHM6 is not required for control of the flu virus H3N2 infection *in vivo* 128
6.3.10 *Calhm6*$^{-/-}$ NK cells are capable of producing normal levels of IFN-γ in response to contact-independent, soluble stimuli 130
6.3.11 *Calhm6*$^{-/-}$ macrophages are capable of responding to Poly(I:C) and developing normal Type I IFN responses *in vivo*. 133
6.3.12 *Calhm6*$^{-/-}$ macrophages and DC are capable of responding to *L. monocytogenes* and developing normal pro-inflammatory and anti-microbial response *in vitro*. 135
6.3.13 CALHM6 expression in CD11c^{+} cells is not required for NK-dependent IFN-γ production 140
6.3.14 *In vitro* models of co-culture between macrophages/DC and NK cells are not suitable to study the role of CALHM6 in NK cells activation. 144
6.4 Discussion 147
6.4.1 CALHM6 is important for NK cell-derived early production of IFN-γ in infections 147
6.4.2 CALHM6 is important for the control of *L. monocytogenes* in the early phases of infection 149
6.4.3 CALHM6 is not important for T cell priming, function and immunological memory formation 150
6.4.4 CALHM6 is important for the accessory cell-mediated activation of NK cells 151
6.4.5 *Calhm6*$^{-/-}$ mice can control H3N2 Influenza A infection efficiently 153
6.5 Limitation of the study 154
6.6 Conclusions 156
7 Mechanism of CALHM6 function in macrophages 157
7.1 Introduction 157
7.1.1 The CALHM6 proteins function 158
7.1.2 Phagocytosis and endocytosis in macrophages 159
7.2 Aims 160

7.3 Results 160
7.3.1 *Calhm6*$^{-/-}$ macrophages fail to upregulate synaptic pathway related genes in response to inflammatory stimuli. 161
7.3.2 CALHM6 polarises to the contact synapses of macrophages 165
7.3.3 CALHM6 is not requires for phagocytosis or endocytosis in macrophages 171
7.3.4 CALHM6 forms a higher order molecular complexes similar to those make by other members of CALHM family. 174
7.3.5 CALHM6 channel does not open in response to the same stimuli that open the CALHM1/3 channel 177
7.3.6 CALHM6 does not act as a P2X7R chaperone 180
7.4 Discussion 182
7.4.1 CALHM6 is a synaptic protein in macrophages 182
7.4.2 CALHM6 forms a channel-like structure similar to other CALHM proteins 187
7.4.3 CALHM6 channel does not open in response to the same conditions that open CALHM1 188
7.4.4 CALHM6 is not a chaperone for ATP receptor P2X7 in BMDM 190
7.5 Limitations 191
7.6 Conclusions 192
8 Future directions 194
8.1 Determine if CALHM6 is an ATP or ion channel in macrophages 195
8.2 Define in which cell type CALHM6 is important in vivo 196
8.2.1 Generation of conditional KO mice 196
8.2.2 Unbiased approach to the study of macrophage and NK transcriptome in *Calhm6*$^{-/-}$ mice 196
8.3 Define CALHM6 role at the immune synapse 197
8.3.1 Avoid artefact caused by CALHM6 overexpression 197
8.3.2 Imaging the immune synapse 197
8.4 Investigate further the physiological consequences of delayed innate responses in *Calhm6*$^{-/-}$ mice 198
8.4.1 Establish how CALHM6 affect the accessory cell response to Poly(I:C) 198
8.4.2 Test how delayed innate responses in *Calhm6*$^{-/-}$ mice affect their response to a subsequent co-infection. 198
8.5 Define the interactome of CALHM6 199
8.6 Test possible functional interaction between CALHM6 and other CALHM proteins 199
9 Final comments 200
10 List of figures 206
11 Appendix 208

11.1 Untreated BMDM 208
11.2 Poly(I:C) stimulated BMDM 208
11.3 LPS stimulated BMDM 210
11.4 LPS and IFN-γ stimulated BMDM 212
11.5 Zymosan stimulated BMDM 213
11.6 Zymosan + IFN-γ stimulated BMDM 214
12 References 217

2 Abbreviations

ATP - adenosine triphosphate

P2XR - P2X receptors

P2YR - P2Y receptors

CALHM - calcium homeostasis modulator channel

NT – N terminal

GPCR – G-protein coupled receptors

T1R – taste receptors type 1

T2R – taste receptors type 2

AD - Alzheimer's disease

PLCβ2 - phospholipase Cβ2

IP_3 - 1,4,5-inositol triphosphate

TRPM5 – transient receptor potential channel M5

ENaC - amiloride-sensitive epithelial sodium channels

Aβ – amyloid-β

LOAD – late onset Alzheimer

ERK1 - extracellular signal-regulated kinases 1

ERK2 - extracellular signal-regulated kinases 2

APP - amyloid precursor protein

DC - dendritic cells

PAMP - pathogen associated molecular patterns

LPS – lipopolysaccharide

Poly(I:C) - Polyinosinic:polycytidylic acid

IFN – interferon

NK – natural killer

SNP – single nucleotide polymorphism

IS – immunological synapse

PRR - pattern recognition receptors

IRF - interferon regulatory transcription factor

uNK – uterine NK

TNF – Tumour necrosis factor

ILC – innate lymphoid cell

NCAM - neural cell adhesion molecule

GM-CSF - granulocytes macrophage colony-stimulating factors

MCMV – murine cytomegalovirus

MHC - major histocompatibility complex

NKG2 - C-type lectin natural killer group

ITIM - immunoreceptor tyrosine-based inhibitory motifs

KIR - killer cell immunoglobulin-like receptors

SHP - Src homology-containing tyrosine phosphatase

ITAM - immunoreceptor tyrosine-based activation motif

NCR - natural cytotoxic receptors

DAP - DNAX-activating protein

Rae-1α - retinoic acid early inducible-1 family of proteins

MIC - MHC class I chain-related

HA – hemagglutinin

TLR - toll-like receptors

APC – antigen presenting cell

TCR – T cell receptor

cDC – classical DC

pDC – plasmacytoid DC

BMDC – bone marrow derived DC

NLR – NOD-like receptor

dsRNA – double stranded RNA

LN – lymph node

WP – white pulp

RP – red pulp

Treg – T regulatory cells

RBC – red blood cell

TF – transcription factor

TGF – transforming growth factor

TRIF – TIR-domain-containing adaptor protein inducing IFNβ

NLRP – NOD-, LRR- and pyrin domain-containing protein

TRAIL – TNF-related apoptosis-inducing ligand

FasL – Fas ligand

HMGB1 - High mobility group box protein 1

MTOC – microtubule- organizing centre

LAMP – lysosomal-associated membrane protein

DISC – death-inducing signalling complex

InlA – internalin A

InlB – Internalin B

Plc – phospholipase

Com – DNA uptake competence system

cGAS – cyclic GMP-AMP synthetase

STING – stimulator of interferon genes

NOD – nucleotide-binding oligomerization domain

GlcNAc - N-acetylglucosamine

MurNAc - N-acetylmuramic acid

MZM – marginal zone macrophages

MMM – marginal metallophilic macrophages

PALS – periarteriolar sheet

BM – bone marrow

RPMI – Rosewell Park memorial institute

FBS – foetal bovine serum

DMSO – dimethyl sulfoxide

BMDM – bone marrow derived macrophages

mGM-CSF – mouse GM-CSF

DMEM – Dulbecco's Modified Eagle Medium

MOI – multiplicity of infection

PMA – phorbol 12-Myristate 13-Acetate

ELISA – enzyme-linked immunosorbent assay

cDNA – complementary DNA

DTT – dithiothreitol

SDS – sodium dodecyl sulphate

WB – western blot

DDT – dichlorodiphenyltrichloroethane

RT – room temperature

PFA – paraformaldehyde

BHI – brain hearth infusion

FACS – Fluorescence-activated cell sorting

sRBC – sheep RBC

SIV – simian immunodeficiency virus

WT – wild type

Immgene - Immunological Gene Project

scRNA – single cell RNA

RPM – red pulp macrophages

IFNGR – IFN-γ receptor

FcgR – Fc gamma receptor

ISRE – interferon stimulated response element

CFU – colony forming unit

i.p. – intraperitoneally

MZ – marginal zone

PFU – plaque forming units

ISG – interferon stimulated genes

DEG – differentially expressed gene

KEGG – Kyoto Encyclopaedia of Genes and Genome

PNGase – Peptide-N-Glycosidase F

iBMDM – immortalised BMDM

CNS – central nervous system

TM – trans-membrane helix

AAM – alternatively activated macrophages

CAM – classically activated macrophages

3 Introduction

3.1 The CALHM family

3.1.1 Discovery of CALHMs as a new family of membrane ATP channel

Adenosine triphosphate (ATP) is a metabolite well known as the primary source of energy for cellular processes, but its importance does not end in the cytoplasm. Once considered mainly a danger signal released by dying cells[1,2], extracellular ATP is also actively released by many cell types to function as a pleiotropic messenger for intercellular communication[3,4]. ATP is an ideal signalling molecule; it is water soluble so it can quickly be released, and the strong concentration gradient created between extracellular and intracellular environment allows for a high signal to noise ratio[5,6]. Extracellular ATP is sensed by two classes of receptors: ligand-gated cationic channels called P2X receptors (P2XR), and G-coupled protein P2Y receptors (P2YR)[3,7]. As a signalling molecule, extracellular ATP has been implicated in the synaptic transmission in both the immune system[1,7] and the brain[3,8]. ATP induced signalling is important in pain perception[9], taste sensing,[10] and in mounting the appropriate inflammatory response against pathogens and tumours[1,7]. ATP can be released via ATP-containing vesicles, or via dedicated ATP channels, such as connexin hemichannels, pannexins, volume regulated anion channels, maxi-anion channels, or calcium homeostasis modulator channels (CALHMs)[5]. Members of the CALHM family have only recently been identified as non-selective plasma membrane channels that are permeable to ATP and are regulated by extracellular Ca^{2+}, membrane voltage, temperature and mechanical pressure[11–14]. Their importance in intercellular communication and in the neuronal, neuro-muscular, and immune system is increasingly evident.

Proteins from the CALHM family, previously known as FAM26[15], are highly conserved in vertebrates[11,16] and are encoded by six genes in humans and mice. In humans the six genes are divided in two clusters: the first containing *CALHM1, CALHM2* and *CALHM3*, is located on chromosome

10q24.33, while *CALHM4, CALHM5* and *CALHM6* are on chromosome 6q22.1[17]. CALHMs lack evolutionary relationships with other known gene families but, their four transmembrane domains, suggest some structural similarities with Pannexins, Connexins and Innexins[18], all of which are well-characterised transmembrane ATP channels[19]. CALHMs function is conserved through evolution down to a single *Calhm* gene, CLHM-1, which is present in *Caenorhabditis Elegans*[16,20]. CLHM-1, is expressed in *C. Elegans* excitable cells, like neurons and body-wall muscles where its loss leads to diminished muscular coordination. Expression of human CALHM1 in CLHM1 KO *C. Elegans* can rescue the phenotype, demonstrating that CALHMs function is highly conserved[16].

Proteins of the CALHM family span the plasma membrane; all CALHMs have four transmembrane domains, with cytosolically disposed C- and N-termini (NT)[18]. Like pannexins and connexins, CALHM proteins oligomerise to form channels with a wide pore, that can be permeable to ATP, Ca^{2+}, and to other monovalent ions with lower affinity[10,21]. Unlike Pannexin and Connexins though, the transmembrane helices are arranged in a counter clockwise fashion that creates a trapezoid-like protein with helices T2 and T4 in contact with the lipid bilayer while T3 and T1 are internal[22], thus the arrangement of the monomers in the channel is very different from the one of any other known ATP channel[22–25]. The channels' oligomerisation is quite heterogeneous: CALHMs channels are made of either eight (CALHM1 and CALHM3)[11,21], ten (CALHM4, CALHM5 and CALHM6)[22,25] or eleven (CALHM2, CALHM4 and CALHM6)[22,26] with some rarer forms that can go up to 13 subunits[25] and can be homo- or hetero-oligomers (Figure 1). The relatively big pores formed can be gated by the α-helix that faces the internal side of the pore, as it is likely the case in CALHM1/CALHM3 and CLHM1[26,27] or, Cryo-EM studies have suggested, by a lipid gate[22,25]. Structural studies suggest that the non-glycosylated CALHM proteins, CALHM2 CALHM4 and CALHM5, have the potential, at least *in vitro*, to form connexin-like gap junctions, either between the two adjacent cells (CALHM2)[26], or between the two intracellular sides of the channel, linking the two intracellular membranes (CALHM4 and CALHM5)[22,25] (Figure 1)

but this remains to be formally tested in cells[11,21,22,26] and could be due to artefacts caused by protein overexpression in non-physiological cell-types.

In mice and humans, CALHM proteins display a variety of expression profiles between tissues that may account for their different functions *in vivo*. CALHM1 and CALHM3, are expressed in type II taste bud cells as well as fungiform $ENaC^+$ taste cells[10–12,28] and are also expressed in human brains, however low-to-none in mouse brain[29]. CALHM2 is more ubiquitously expressed, even if *Calhm2*$^{-/-}$ mice mostly display brain-specific phenotypes[30], probably because the higher expression registered is in the brain and, in particular, microglia[31]. Substantial expression of several CALHM proteins (CALHM2, CALHM4 and CLAHM6) have also been ascertained in human placenta, but it is not clear exactly in which cell type[22]. CALHM6, is the only CALHM that is highly expressed in immune cells[32,33], making it an outlier.

The ability of CALHMs to open in response to diverse stimuli (change in membrane voltage, Ca^{2+} concentration, temperature and mechanical pressure)[5,11,13–15,26,34,35], and the different compounds that can go through the channels (ATP, Ca^{2+}, monovalent cations)[10,21,36], make CALHMs versatile channels, on par with pannexins and connexins. Although the significance of CALHM functions was brought to the fore only about a decade ago, they have already been implicated in multiple diseases with unmet clinical needs, such as Alzheimer's disease (AD), depression, autoimmune diseases, infections, and cancer[30,33,37–41]. We hope that our study will provide new insights into CALHM6 functions in the immune system and lay the path for the design of novel therapies.

3.1.2 CALHMs in taste sensing

The most striking and well-studied physiological role of CALHMs is in taste perception. Mice that lack CALHM1 lose preference for sweet and umami. These mice show also partial avoidance for bitter flavours[12] and reduction in avoidance for high concentration of NaCl[42]. There is also loss of preference for fat-rich food, higher than in mice without CD36, a taste receptor for fatty acids[43,44]. In consequence, *Calhm1*$^{-/-}$ mice consume less food, weigh less, and have a shorter lifespan[45].

In mice and humans, food is tasted on the tongue by specialised cellular structures, the taste buds. Each taste bud contains clusters of 50-100 of three types of taste bud cells[46]: Type I, II and III. Type II cells expressing CALHM1 and CALHM3, are specialised for sweet, umami and bitter flavours[10,11,47]. The ability to sense these flavours confers an evolutionary advantage: sweet and umami compounds are typical of nutrient rich food, while bitter compounds, mostly plant alkaloids, can be toxic so give rise to an avoidance reaction. Type II taste bud cells form stable synapses with sensory neuronal axons and sense flavours via G-protein coupled receptors (GPCRs). Of the GPCRs, taste receptors type 1 (T1Rs) sense sweet and umami taste, while Type II (T2Rs) sense bitter[48]. Every Type II cell has only one specific type of GPCR, but the downstream activation is the same for every cell. After binding their ligands, GPCRs activate phospholipase Cβ2 (PLCβ2) that converts PIP2 into 1,4,5-inositol triphosphate (IP_3) and diacylglycerol. IP_3, in turn, binds its receptor IP_3R_3 causing release of Ca^{2+} from the endoplasmic reticulum, elevating intracellular Ca^{2+} concentration. Release of Ca^{2+} activates the Transient receptor potential channel M5 (TRPM5), selective for monovalent cations, and causes membrane depolarisation[46]. Taste buds are then activated by membrane depolarisation, triggering the opening of voltage-gated channel CALHM1/CALHM3[11], allowing the release of ATP into the synaptic cleft. Finally, the ATP released is sensed by the P2X7 receptors on sensory neurons, and thereby activating these neurons (Figure 2)[10,12]. Thus, the ATP in this system works as a neurotransmitter, and CALHM1 works as the ATP release channel. This atypical synapse that does not contain vesicles has been deemed a “channel synapse” and it is the only one of its kind whose function is known[10,28].

The sensing of salt (NaCl) can also open CALHM1 channel. Sensing, in this case, is mediated by amiloride-sensitive epithelial sodium channels (ENaC) opening that causes membrane depolarisation and consequent CALHM1 channel opening, independently of Ca^{2+} signalling[28].

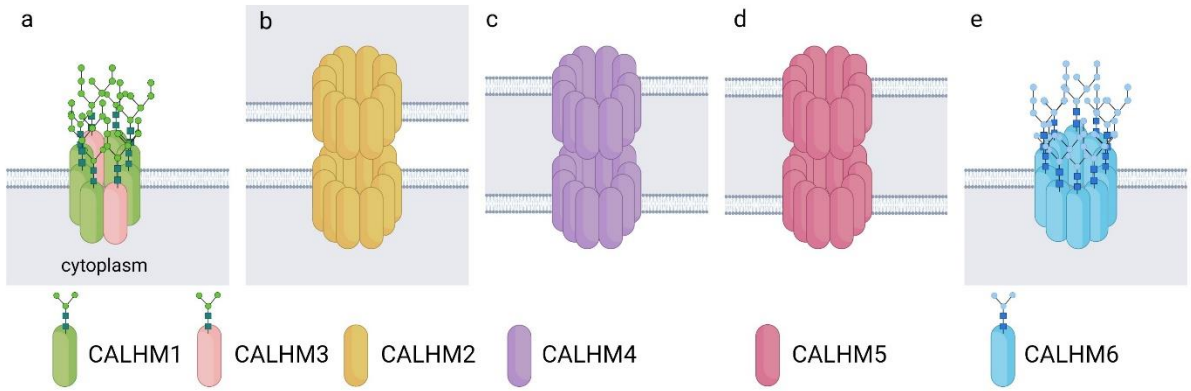


FIGURE 1: Oligomeric structure of CALHM proteins. Schematic rendition of the channel structure of CALHM1/3 a), CALHM2 b), CALHM4 c) CALHM5 d) and CALHM6 e) channels. CALHM1 forms an octameric channel in chickens and killfishes. In humans the functional channel contains both CALHM1 and CALHM3. CALHM2 forms undecameric channels. Human CALHM4, CALHM5 and CALHM6 form both decamers and undecamers, with a preference for decamers in the case of CALHM6. CALHM1, CALHM3 and CALHM6 are N-glycosylated on one extracellular loop residue. Due to glycosylation, the proteins only form hemichannels. CALHM2, CALHM5 and CALHM4 are not glycosylated in Cryo-EM conditions and have the potential to form gap-like junctions. CALHM2 interacting on the extracellular side, CALHM4 and CALHM5 on the intracellular one.

The opening of CALHM1 has a steep dependence on the membrane voltage (-10 mV threshold) and the amount of ATP released is proportional to the magnitude of the current[10,21], although *in vitro* some molecular transport through the channel can occur even in the absence of ionic currents[49]. Unlike the ATP release via pannexins[18], the release of ATP via CALHM is pulsatile and dependent on discrete action potentials[11]. Interestingly, even though CALHM1 is a poorly selective channel: its functional diameter of 12.8-14.2 Å makes it permeable to mono and divalent ions (order of selectivity Ca^{2+}:Na^{+}:K^{+}:Cl^{-} :: 11:1.2:1:0.6)[17,21,35], CALHM1 opening does not lead to increase in intracellular Ca^{2+}, or severe depolarisation. This is because, in taste bud cells, the channel operates in a presynaptic compartment enriched with ATP-producing mitochondria. The localised high concentration of ATP at the presynaptic membrane where CALHMs operate explains the specificity for ATP in type II taste bud synapses (Figure 2)[10,50].

Most of the studies on individual CALHMs were initially performed in cell lines or *in vitro* models, such as *Xenopous Laevis* oocytes, over-expressing a single CALHM protein. This was not ideal as when expressed alone, CALHM1 ATP channel does not recapitulate the opening kinetics measured *in vivo*. A study by Ma and colleagues[11] offered a possible solution to this conundrum. They showed that *in vivo* CALHM3 forms a complex with CALHM1 in taste bud cells, and when expressed in oocytes CALHM1/3 hetero-oligomeric channel displays kinetics that are indistinguishable from the *in vivo* one[11,51]. Consistent with this, *Calhm3*$^{-/-}$ mice, like *Calhm1*$^{-/-}$ ones, have reduced preference for sweet, salt and umami and reduced avoidance of bitter taste[11,28].

The mechanisms of voltage-dependent opening of the CALHM1/3 channel are not entirely understood. In CALHM1, the NT loop does not work as a plug as in the Connexin equivalent[27]. In CALHM2, however, akin to Connexins, the NT tail is critical to keep the channel in the closed state when it is bound by the CALHMs inhibitor Ruthenium Red as shown by Choi and colleagues[26]. For both CALHM1 and CALHM2, normal levels of extracellular Ca^{2+} concentration stabilise the closed structure of the channel[26]. In CALHM1 this is due, at least partially, to the Asp121 residue exposed on the second

extracellular loop. Mutation of Asp121 eliminates the ability of Ca^{2+} to close the channel[21]. Post-translational modification of CALHM1 is required for normal function[52] as mutation of its glycosylation site completely abolished it, possibly because of its effect on protein folding and cellular localisation[36,53]. Also the absence of post-translational palmitoylation affects the kinetic of the gating and its affinity for lipid rafts[52]. Several studies indicate that, pharmacologically, CALHM1 is unique: traditional Pannexins and Connexins inhibitors, like probenecid and heptanol, do not inhibit currents generated by CALHM1 opening[12,17]. The same is not true for nonselective ion channel blockers, like ruthenium red, which efficiently blocks the currents generated by open CALHM1, CALHM2 and CALHM3[11,21,26].

CALHM1 and CALHM3 functions beyond taste sensing are poorly understood, taste cells are not only present in taste buds: bitter sensory cells have been identified in the alimentary canal, pancreas, brain, and in the airway epithelium[54,55], partly because they can help in the identification of bitter compounds produced by dangerous bacteria[54,56]. All these cells express TRPM5 and, studies show, CALHM1/CALHM3 channels can also relay signals in some such cell type like tanycytes and ciliated epithelial cells[57]. In hypothalamic tanycytes (radial glia-like cells that respond to nutrient signals), as example, CALHM1 together with Pannexin1, is required for the release of ATP upon sensing of the amino acid L-arginine, and the CALHM inhibitor Ruthenium red reduces this response[57]. Thus, a role of CALHMs in the synaptic transmission of taste sensing will likely be a common theme for all organs where taste sensing channels are found.

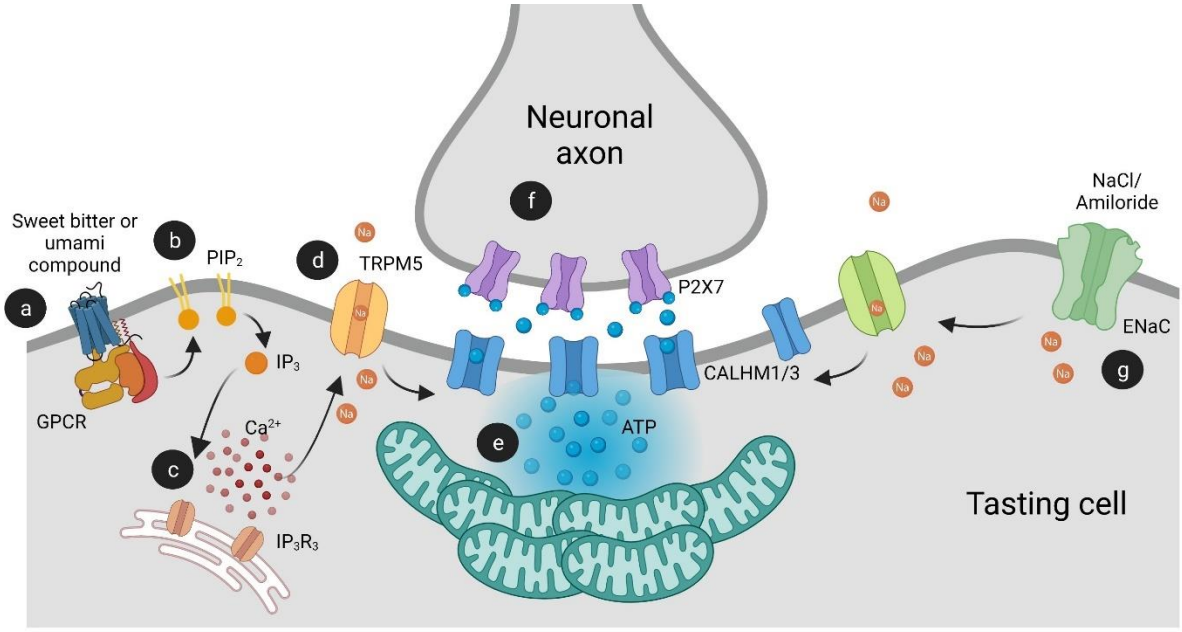


FIGURE 2: CALHM1/3 channel in taste sensing. a) Bitter, sweet and umami compounds are sensed by GPCRs on Taste Bud Cells' membranes. b) After GPCR activation, PLCβ2 gets activated and converts PIP_2 into IP_3 and diacylglycerol. c) IP_3 binds its receptor IP_3R3 on the endoplasmic reticulum, causing the release of the stored Ca^{2+}. d) The increase in cytoplasmic Ca^{2+} concentration triggers the opening of the TRPM5 channel and Na^+ selectively passes through TRPM5 causing membrane depolarisation. e) Membrane depolarisation opens CALHM1/3 channel. CALHM1/3 is surrounded by atypical mitochondria that create an ATP-rich environment; so, ATP gets released into the synaptic cleft in response to CALHM1/3 channel opening. f) Released ATP binds to P2X7 receptors activating the sensory neuron. g) Alternative CALHM6 activation pathway in sodium taste sensor cells: Na^+ entry through ENaC channels causes depolarisation that drives voltage-dependent CALHM6 opening and neurotransmission.

3.1.3 CALHMs in the central nervous system

CALHM1 first became of interest about ten years ago when Dreses-Werringloer and colleagues identified CALHM1 as the possible cause of the strong association of the 10q24.33 region with AD[15]. CALHM1 was considered as a possible causative AD gene due to its high expression in the hippocampus, where the first symptoms of AD are detected and a P86L (rs2986017) variation in CALHM1 had been found to be significantly associated with AD patients[15,37,58,59]. AD is the most common type of dementia and its burden is expected to increase with the aging of the general population, there are no biomarkers for early diagnosis, and it is currently incurable. An increasing body of data links AD with glial and microglial changes that drive neuroinflammation, but abnormal amyloid-β (Aβ) metabolism is still the major hallmark of the disease[60]. As of today there is no consensus on the association between CALHM1 P86L and AD; a meta-analysis performed soon after CALHM1 identification suggested a link with late onset AD (LOAD)[38], but other studies failed to find any association between the P86L variation and LOAD[61–67]. Regardless, the 10q24.33 region that hosts CALHM1, 2 and 3 has been associated with schizophrenia[68], temporal lobe epilepsy[69], and spontaneous Creutzfeldt-Jakob diseases[70] and, as such, this suggest an involvement of CALHM proteins in neuronal diseases[31].

Mechanistically, these first studies on CALHM1 suggested that it could act as a Ca^{2+} permeable channel, in 'add back' experiments (initial depletion of extracellular Ca^{2+}, to open the channel, then add back Ca^{2+} in the medium, to see if it can pass through the open channel)[15,36,71]. In this model CALHM1 opening leads to the activation of the extracellular signal-regulated kinases 1 and 2 (ERK1/2), a central event in Ca^{2+}-dependent signal transduction during neuronal function[36]. Calcium signalling is known to be involved in the regulation of amyloid precursor protein (APP)[72] processing, and thus, under Ca^{2+} 'add-back' conditions, expression of CALHM1 (but not disease associated P86L mutant) significantly decreased total extracellular Aβ accumulation[15,37]. These results suggest that CALHM1 may control APP proteolysis in a Ca^{2+}-dependent manner, a process that is disrupted in AD. While 'add

back' experiments may reflect the low calcium concentration that is found in neural tissues and in the synaptic cleft[73], they do not recapitulate the known voltage-dependent mechanism of CALHM opening described for taste bud cells. This might explain why it has been difficult to reproduce the association of CALHM1 with AD and Aβ accumulation *in vivo.*

Two *Calhm1*$^{-/-}$ mouse strains were created separately by removing the whole gene[29] or just exon one[74], in both cases mice exhibit normal brain architecture without loss of synapses[29]. While both studies showed no differences in learning ability, one of the studies, showed a severe impairment in memory flexibility, as assessed in the Morris water maze test, and a significant disruption of long-term potentiation[74]. The study suggests that the differences could be due to CALHM1 control of the the N-methyl-D-aspartate and the α -amino-3-hydroxy-5-methyl-4-isoxazolepropionate receptors phosphorylation, both associated with memory flexibility[36,74]. These results are puzzling seeing that in one of the studies, low to no *Calhm1* mRNA was reported in mouse brains[29]. Unfortunately, none of these groups has assessed *Calhm1*$^{-/-}$ or *Calhm2*$^{-/-}$ mice response to pain: due to the role of ATP in pain sensing and its dependence on Ca^{2+}, CALHM1 has been suggested as a druggable target for the control of neuralgia[75] and ischemic brain damage[76].

The investigations of CALHM proteins in brains were not restricted to CALHM1. CALHM2 is also expressed in the brain and especially in astrocytes and microglia[30,31]. In the first study involving *Calhm2*$^{-/-}$ mice, germline and astrocyte-specific *Calhm2* deletion was generated[30] in which *Calhm2* deficiency resulted in reduced brain ATP concentrations, neural dysfunction and a depression-like behaviour. Imbalance in ATP concentration in the brain is known to lead to depression-like behaviour[77,78] which, in *Calhm2*$^{-/-}$ mice was rescued either by continuous intraperitoneal ATP replenishment or by a direct single injection of ATP into the hippocampus [30]. A more recent study from Cheng and colleagues, generated microglia specific *Calhm2*$^{-/-}$ mice and proposed a link between CALHM2 expression in mouse brains and AD[31]. CALHM2 levels are increased in AD brains of mice and humans, and *Calhm2*$^{-/-}$ mice have reduced Aβ plaques, increased microglial-phagocytosis and a

general alleviation of the cognitive impairment typical of AD. Cheng and colleagues argue that the amelioration of AD symptoms in microglia specific *Calhm2*$^{-/-}$ mice is due to a reduction in neuro-inflammation caused by lower levels of P2X7, an ATP receptor, presented on the surface of microglia. CALHM2, they argue, function as a chaperon for P2X7 that when in the plasma membrane, can bind ATP and trigger microglial NLRP3 activation, inflammasome formation, the release of pro-inflammatory cytokines like IL-1β, and a decrease in the phagocytotic rate of microglia[31]. This study suggests that CALHM proteins could have functions other than that of ATP channels. In this case CALHM2 acts as a chaperone to help the expression of another protein, an ATP receptor, on the plasma membrane.

Collectively, the published data point to the involvement of CALHM1 and CALHM2 in neuronal and microglial excitability and ATP and/or Ca^{2+} homeostasis. It is known that imbalances in ATP and Ca^{2+} signalling can inflict pain[9,79] and memory loss, and it can impact long term cell survival[8,80]. Further studies are needed to better understand the role of CALHMs in the central nervous system and its therapeutic potential.

3.1.4 CALHMs in the immune system

The functions of CALHM proteins in the immune system are largely unexplored. It is possible that the ATP release ability of CALHM1 participate in the clearance of infective pathogens. The CALHM1 channel is expressed in nasal epithelial cells, where it can release ATP in response to mechanical stresses. *In vitro* this causes an intensification in ciliary beat frequency that allows effective mucociliary clearance of parasites[34]. This process highlights a new mechanism for CALHM1 opening, that has also been shown in pig bladders[13], wherein hypotonic stress caused CALHM1-dependent release of ATP. In both models CALHM1 plays a role that is complementary to Pannexin channels[13,34].

The most puzzling of all CALHMs is CALHM6, which has a distinct expression profile and function compared to the other family members. Unlike other CALHMs, CALHM6 is largely expressed on $CD45^{+}$,

hematopoietic cells. *Calhm6* mRNA is detected in a wide range of immune effector cells such as T cells, NK cells, B cells, but the highest expression is on innate cells, especially monocytes and macrophages[32,33].

In 2010, Ebihara and colleagues[32], identified CALHM6 as a membrane protein induced on dendritic cells (DC) and macrophages upon recognition of pathogen associated molecular patterns (PAMP), such as bacterial lipopolysaccharide (LPS) or synthetic viral RNA mimic Polyinosinic:polycytidylic acid (Poly(I:C))[32]. The expression of CALHM6 required the induction of type I interferons (IFNs) upon pathogen recognition, as IFN receptor (*Ifnar1*)-deficient mice, or pathogen derived signals that failed to induce IFNs, failed to upregulate CALHM6 expression[33,81,82]. Upregulation of CALHM6 on DCs turned out to be important for DC-mediated activation of natural killer (NK) cells[83]. NK cells are innate effector cells that contribute to the elimination of cancer cells, as well as virus- or bacteria-infected cells. NK cells can be activated directly by malignantly transformed cells and pathogens or indirectly by myeloid accessory cells, such as DCs and macrophages. Once activated, NK cells secrete proinflammatory cytokines, like IFN-γ, and cytotoxic molecules, like granzyme B[84–86]. Ebihara and colleagues showed that CALHM6, initially called INAM (IFN regulatory factor 3-dependent NK-activating molecule), was required to induce IFN-γ secretion, but not cytotoxicity, from NK cells[32]. Another study reproduced these findings showing that CALHM6 is also induced on DCs upon recognition of tumour cell membrane carbohydrates via Dectin-1[87], and that CALHM6 upregulation contributes to DC-mediated NK cell IFN-γ secretion in anti-tumour responses (Figure 3). Subsequently, *Calhm6*$^{-/-}$ mice were generated and demonstrated the antimetastatic function of this protein in response to Poly(I:C) therapy[33]. *Calhm6*$^{-/-}$ mice are healthy, but the NK cell-dependent IFN-γ production is impaired. This causes poor antitumour immunity against IFN-sensitive metastases[33] and the failure of Poly(I:C) based anti-cancer immunotherapy[33].

The role of CALHM6 in the immune defences against pathogens and in immune mediated inflammatory diseases is otherwise unexplored, but it has been suggested in several correlational

studies[88]. In a simian immunodeficiency virus infection model, pre-infection levels of CALHM6 in PBMCs inversely correlated with viral load and directly correlated with IFN-γ[41], thus, suggesting a role for CALHM6 in virus clearance *in vivo*. Several single nucleotide polymorphisms (SNPs) that alter CALHM6 expression have been associated with autoimmune diseases: ulcerative colitis is associated with a SNP that is thought to increase CALHM6 expression[89], whilst steroid-sensitive nephrotic syndrome is associated with a SNP thought to decrease CALHM6 expression[90]. Increased CALHM6 expression is also a prognostic biomarker for a good response to glucocorticoid therapy in rheumatoid arthritis patients[91]; the same therapy is used to treat ulcerative colitis. Collectively, these studies link CALHM6 to diseases that are sensitive to steroid treatments, albeit, without evidence for direct cause-effect relationship thus far.

The mechanism of CALHM6 action, and its potential role as an ATP channel in the immune response, have not been investigated within the hematopoietic system. Protein structure and cellular localisation of CALHM6 are compatible with membrane ATP channels such as CALHM1 and CALHM2[17,92]. Unlike CALHM1 though, changes in membrane voltage or extracellular Ca^{2+} concentration are not sufficient to cause the passage of currents or molecules through the CALHM6 channel, when expressed in placenta cells[22]. This is probably due to the plug made of transmembrane domain 1 (TM1) of CALHM6 that appears to be pointing towards the middle of the pore under the 60^{o} angle, with a possible lipid-like density in the intercellular facing part of the channel, just underneath the TM1, in the Cryo-EM resolved structure[22]. The mechanism of channel opening and its function thus remain unknown.

ATP is an important signalling molecules in immune defence, its autocrine and paracrine signal elicit pro-inflammatory responses via activation of innate and adaptive cells[93,94]. For example, ATP is important in DC-mediated activation of T cells that occurs through the formation of the immunological synapses (IS)[95,96]. Like in the taste buds, the IS that are formed between DC and T cells or between DC and NK cells are rich in mitochondria, which are crucial for the supply of local ATP and ATP-mediated

activation of effector T and NK cells[97–99]. In our study we will try to decipher whether CALHM6 localises to the IS between DC/macrophages and NK cells, and, akin to other CALHMs, forms a membrane channel for ATP and/or Ca^{2+} that controls innate activation of NK cells during infection. To accomplish this, we will select infectious models, or their experimental mimics, where early immune defences are known to depend on interferons and on cross-talk between myeloid cells and NK cells to investigate CALHM6 function.

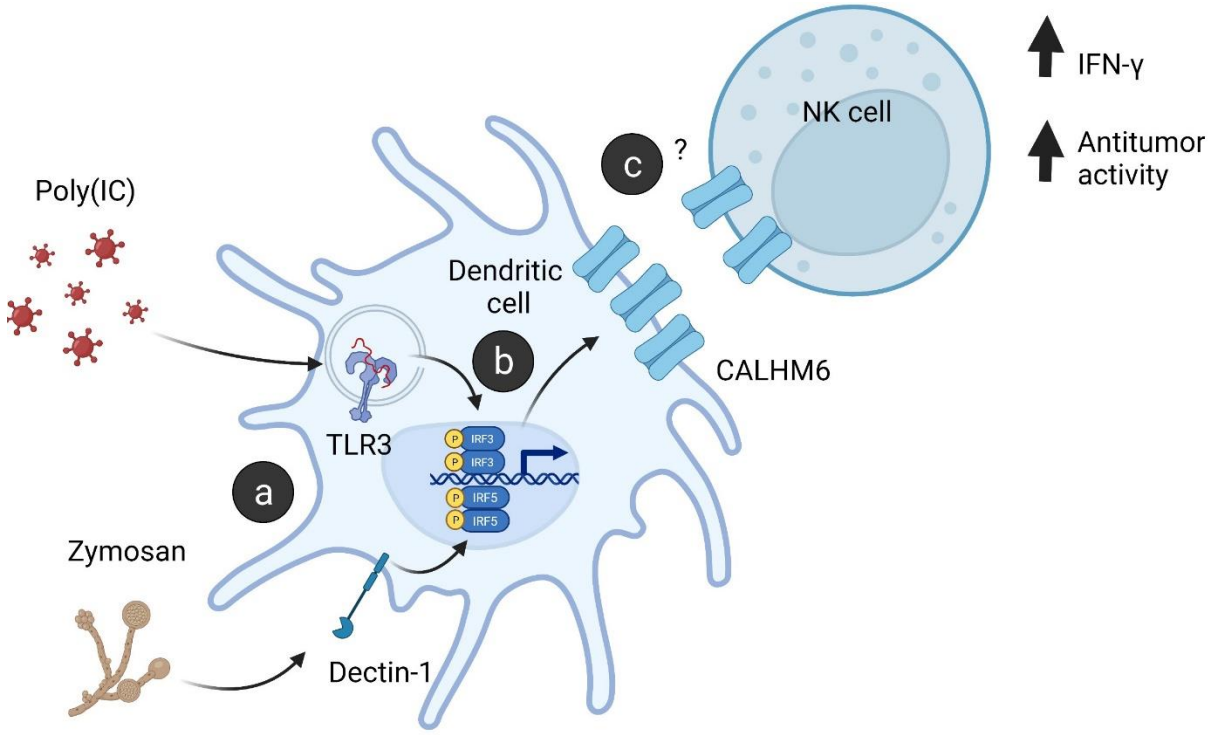


FIGURE 3: Function of CALHM6 in the immune system. a) Double strand RNA analogue, Poly(I:C), and N-Glycan structure like zymosan activate DCs by binding to their pattern recognition receptors (PRR), TLR3 and Dectin 1, respectively. (b) PRR ligation activates interferon regulatory transcription factor 3 (IRF3) and IRF5 that translocate in the nucleus and promotes, among others, *Calhm6* mRNA expression. c) Activated DCs form immunological synapses with NK cells. In response, NK cells produce immunoregulatory cytokines such as IFN-γ and increase pro-apoptotic activity. NK cells in *Calhm6*$^{-/-}$ mice produce less IFN-γ in response to activated DCs and NK cells antimetastatic activity is thwarted.

3.2 Natural killer cell activation in viral and bacterial infection

3.2.1 Definition, development and subsets of NK cells

NK cells are innate effector immune cells that are particularly important in the immune defence against viruses, intracellular bacteria and cancer. They were first identified in the 1960s as cytotoxic cells[100] but it took over ten years of further studies to characterise them as a separate population that had both cytotoxic and pro-inflammatory roles, thanks to their ability to produce cytokines[101]. NK cells are morphologically characterised as large granular lymphocytes[102] mostly derived from BM even if a small percentage can also originate in secondary lymphoid organs[103,104].

Today NK cells are defined as CD3-CD56^{+} in human and CD3-NK1.1^{+} in mouse strains that express NK1.1 (C57BL/6, FVB/N, and NZB), and in other strains as CD3-CD49b^{+}[105]. In humans and mice the transcription factors T-bet and Eomesodermin control their differentiation[106]. NK cells are a relatively small percentage of the total lymphocyte in the body, in mouse peripheral blood they represent between 2-7% of lymphocytes while in humans they are less than 18%[105,107]. NK cells are also present in secondary lymphoid and other organs, in human they constitute about 20-30% of total hepatic lymphocytes and 10% of mouse and human lungs[105,107]. Interestingly, NK cells are particularly abundant in human uterus and placenta, where they constitute 50-90% of total lymphoid cells. Uterine NK (uNK) cells are a distinctive subset that does not show killer activity but has immunosuppressive phenotypes[105]. uNK cells produce angiogenic factors, like vascular endothelial growth factor C and interleukin 8 (IL-8), that keep them non-cytotoxic while assisting in the vascular remodelling necessary during foetal growth[108–110]. NK cells are very similar to the IFN-γ and tumour necrosis factor (TNF)-producing Innate lymphoid cells 1 (ILC1), but their distinct developmental pathway and cytotoxic function set them apart from the ILC lineage[111].

Different subsets of NK cells have been identified, in human most NK cells express the neural cell adhesion molecule NCAM (CD56) and some also express high levels of the activating Fc receptor

CD16[112,113]. These subpopulations have different functions and localisation in the body, most circulating NK cells are $CD56^{dim}CD16^{+}$ and represent a more mature NK cell-stage and are capable of producing some IFN-γ and large amount of perforin and granzyme B when activated[114,115] so they can perform both cytotoxic and pro-inflammatory effector function. In contrast $CD56^{bright}CD16^{-}$ are more common in secondary lymphoid organs and they are preferentially cytokine-producing NK cells[116]. Mouse NK cells do not express CD56 and their maturation have been defined through the membrane proteins CD27 and CD11b. CD27 somewhat recapitulates the profile of CD56, it is first upregulated after NK cell maturation and its expression is dimmed in the final stages when CD11b is higher[117]. Functionally, in their final stage as $CD11b^{+}CD27^{dim}$ NK cells are in replicative senescence but otherwise have the same characteristics of double positive $CD11b^{+}CD27^{+}$ and like $CD56^{dim}CD16^{+}$, $CD11b^{+}CD27^{dim}$ are more abundant in blood than in lymphoid organs[118].

In vivo, NK cells can recognise virus-infected and cancerous cells through their "loss of self" phenotype and can kill them via the formation of a lytic IS through which perforins and granzymes are secreted[107]. NK cells also recognise parasites directly and use the same enzymes to kill them[119]. Alternatively, activated NK cells can secrete several cytokines to modulate the immune response, IFN-γ, TNF and granulocytes macrophage colony-stimulating factors (GM-CSF) are the most abundant[105]. For this reasons, the activation of NK cells is beneficial in several infection models, NK depleted mice are clearly more susceptible to Murine cytomegalovirus (MCMV)[107], and NK cells can recognise and kill cells infected with influenza, flavoviruses and poxivirus[120–122]. Despite this, individuals with NK cells-specific deficiencies do not have heightened sensitivity to viral or bacterial infections[123], although there is an association with increased susceptibility to herpesviruses and other select viral pathogens, increased risk of virus-induced cancers and fungal infections[123–125]. This does not necessarily mean that NK cells are not required for the correct function of the immune system, it is possible that their function is concealed by our societal high hygiene level and low overall infection rate[107].

3.2.2 Activation of NK cells

To exert their cytotoxic or pro-inflammatory functions NK cells first need to be activated. Activation can be direct, mediated by the ligation of NK cell receptors with infected/cancerous cells or with an invading pathogen, or NK cells can be indirectly activated by accessory cells like macrophages or DC.

3.2.2.1 Direct activation of NK cells

NK cells have the ability of killing autologous cells that are undergoing stresses like viral infection, DNA damage response, senescence or tumour development[105]. This process needs to be tightly regulated to avoid NK cells attacking healthy cells leading to autoinflammatory diseases. For this purpose, NK cells activation needs to be "licenced" by the absence on the target cells of ligands recognised as self[126]. The main of these inhibitory signals expressed by healthy cells is the major histocompatibility complex (MHC) class I that is expressed in all the cells of the organism but can be downregulated following stress. NK cells express a wide range of receptors that can be inhibitory or activating and need to act in concert to determine the demeanour of NK cells. The Ly49 family of receptors, member of the type II transmembrane proteins containing carbohydrate recognition domains superfamily, are some of the best-known receptors expressed by NK cells that can recognise MHC I and inhibit NK cell activation[127]. There are several members of this family in mice: Ly49A, C, I and P all have inhibitory functions[105]. Humans do not express Ly49 proteins but their equivalent killer cell immunoglobulin-like receptors (KIR), that can recognise HLA molecules[128]. Another important receptor on NK cell membrane that has inhibitory functions is the C-type lectin natural killer group member A (NKG2A) that recognises the non-classical MHCs HLA-E in humans and Qa1 in mice[129,130]. All these inhibitory receptors signal through the immunoreceptor tyrosine-based inhibitory motifs (ITIM) present in their domain, that is phosphorylated upon binding of the appropriate ligand and recruits several phosphatases like Src homology-containing tyrosine phosphatase 1 (SHP-1) and SHP-2 that proceed to dephosphorylate the immunoreceptor tyrosine-based activation motif (ITAM) motifs on NK cell activating receptors[131]. Thus, ITIM is the ultimate controller of NK cell activation.

While inhibitory receptors signal through ITIM to block activation, NK cells also express a plethora of germline-encoded activation receptors that signal through ITAM or the tyrosine-based signalling motif YINM[113,132]. Among the receptors that signal through ITAM there is the low-affinity Fc receptor FcγRIIIa (CD16), and the family of the natural cytotoxic receptors (NCR) that can recognise a wide variety of bacterial and viral targets as well as tumour transformed cells[105]. From the NCR family mice only express NKp46 while humans also have NKp44, and 30[133]. Other receptors signalling through ITAM are KIR family members, including KIR2DS and KIR3DS in humans[105,133]. Of these activating receptors only CD16 can act alone to trigger activation, all the others need adaptor proteins containing the intracellular ITAM domain to function, like proteins FcεRI-γ, DNAX-activating protein of 12 kD (DAP12) and CD3-ζ[134,135]. Upon ligation with their receptors, ITAM is tyrosine-phosphorylated by Src family kinases. This recruits the tyrosine kinases Syk and Zap70, leading to the activation of MAP, ERK and to an intracellular calcium spike. This in turn, triggers actin remodelling towards cytotoxic synapse formation[136]. Non ITAM-dependent signalling happens through adaptor like YINM expressing DAP10[132] that can be phosphorylated by Src proteins after is bound by Grb2-Vav1[137]. Through a Syk-independent pathway YINM phosphorylation leads to PI(3)K activation and phosphorylation of Jak2, STAT5, Akt and ERK[105,138]. This mobilises lytic granules towards the membrane and increases pro-inflammatory cytokines production via transcription factors like AP-1 and NFkB[139]. NKG2D is one of the main receptors to signal through DAP10 and DAP12, it targets structural homologs of MHC like the like retinoic acid early inducible-1 family of proteins ε (Rae-1α-ε) in mice[140] or MHC class I chain-related protein A (MICA) and B (MICB) and UL16-binding proteins in humans[141], all well known to be upregulated in several tumours[142,143]. Other non-ITAM receptors are 2B4 in mice and humans, and Ly49D and Ly49H in mice[105,132]. The signal from these activating receptors can result into different outcomes and, in cases like NKG2D and 2B4, the synergy of the two receptors acting together creates a cytotoxic response that is bigger than the sum of the single signals[139]. Rarely the engagement of a single receptor is sufficient for the complete activation of NK cells[132].

No matter which activator receptors are engaged though, the ITIM domain dominates over all the other signals[113,131,144] to avoid targeting of cells recognised as self. Because NK cells can kill targets that do not express MHC I they can clear intracellular pathogens that evade CD8 T cell lysis by interfering with MHC I loading.

Finally, NK cells can also be directly activated by pathogens through the same receptors used to recognise stressed or cancerous cells. For example the influenza A protein hemagglutinin (HA) is recognised by NKp46[120] while MCMV binds Ly49H directly[145]. While most cases of direct activation involve viruses, there are examples of bacterial activation: *Mycobacterium bovis* for example, can stimulate NCR and drive cytotoxicity[146]. NK cells also encode toll-like receptors (TLR) proteins that can directly be triggered by bacteria like *Kleibsella pneumoniae* and by the bacterial protein flagellin[147].

3.2.2.2 Indirect activation of NK cells

While NK cells can directly be activated by contact with stressed and cancerous cells or even with parasites, the most efficient form of activation following infection is indirect, and dependent on signals provided by accessory cells[148]. This indirect activation is similar to immune priming of adaptive cells; it is mediated by both cytokines and chemokines produced by stimulated or infected accessory cells[105,119] and by the formation of an IS in which accessory cells concentrate ligands for NK cell receptors and exchange contact signals[148].

3.2.2.1.1 Accessory cells: dendritic cells

The main accessory cells for NK cells activation are macrophages and DC, they are both myeloid cell types widely distributed in the organism that act as sentinels. Macrophages and DC sense the environment for the presence of foreign invaders, stress signals, and changes in the metabolic environment or cell composition. Macrophages and DC respond to threats by initiating and regulating adaptive and innate immunity.

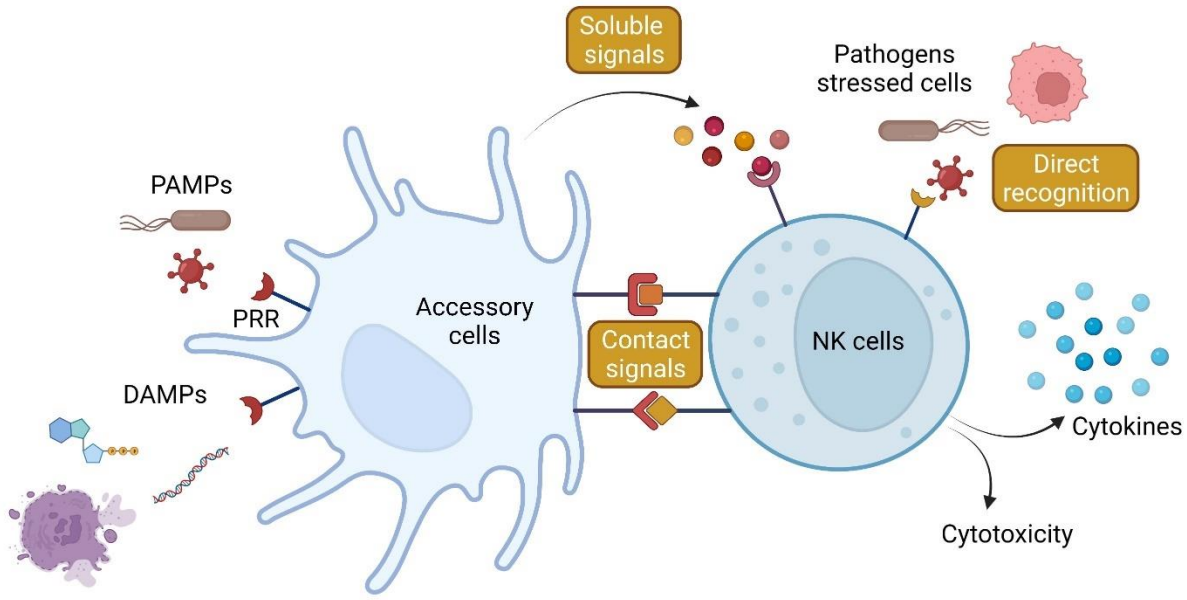


Figure 4: Activation of NK cells. Activation of NK cells can happen by direct recognition of pathogens in the extracellular environment or cells that show signs of stress due to viral or intracellular bacterial infection as well as tumour cells. Alternatively, NK cells can be activated indirectly by accessory cells that have been in turn activated by infection or inflammation and can form an IS with NK cells in which contact and soluble signals are exchanged.

DC were first discovered in 1973 by Ralph Steinman[149] and in the following years they were defined as specialised antigen presenting cells (APC)[150]. DCs are the most efficient cells at capturing and processing antigens, converting them into peptides and presenting them to T cells on their MHC molecules, aiming to select T cell that express pathogen-specific T cell receptors (TCR)[151]. The discovery of DC functions connected innate and adaptive immunity as theorised first by Metchnikov[152] and later by Janeway Jr[153].

Compared to humans mouse DC populations are better defined, due the difficulty of working with primary human tissue-derived DC, so most studies, especially in the beginning, focused on blood DC[151]. In mice we can define two major population of "classical" DC (cDC), cDC1 and cDC2, widely distributed in the body[154,155]. These two cell types are usually distinguished by the expression of surface molecules, some cDC1 express CD8αα in secondary lymphoid organs[155] and compared to cDC2 have higher CD103, CD24 and Flt3, and lower CD11b and other macrophages markers[156]. cDC2 are the most abundant and the most heterogeneous subset and express CD4[157] and Sirpa[156]. Other non-classical DC subpopulations are the type I IFN-producing plasmacytoid DC (pDC) and the macrophage-like Langherans cells in the skin[154]. Extremely useful for *in vitro* studies during the years, have been monocyte or bone marrow-derived DC (BMDC). First used by Lanzavecchia and Sallusto[158] they differentiated $CD34^+$ BM cells using GM-CSF and obtained DC-like cells.

In their sentinel role DC are key to the early detection of infections, partly because they are positioned in classical pathogen entry sites like lungs[159], intestine lumen and lamina[160,161]. Sensing of pathogens is carried out by germline encoded PRR that can bind small molecular motifs conserved in a wide variety of microbes, called PAMPs[162]. The main PRR can be found on the cell surface, endosomal membranes or in the cytosol. These are TLRs, C-type lectin receptors, RIG-I like receptors and NOD-like receptors (NLRs), together they can sense both extracellular and intracellular PAMPs. In their sentinel role cDC do not only respond to PAMP, but also to self-ligands produced by damaged cells, like ATP or filamentous actin[163,164], nevertheless these signals are less efficient at triggering bona-fide

cDC activation and mostly function in synergy with PAMPs[165]. The ability of cDC to respond to specific PAMP is partially regulated by the level of expression of PRR; for example TLR4, the ligand for LPS, is equally expressed in cDC subsets[166], while only cDC1 express high levels of TLR3 that sense dsRNA and makes them more responsive to specific viruses and capable of producing more IL-12[167,168]. Thanks to the DNGR-1 receptor cDC1 are also more sensitive to the presence of extracellular filamentous actin released by dead cells[169].

DC in the body exist in two different states, a quiescent one, in which they are present at the barrier where they only receive tonic survival signals like Flt3 and type I IFN[170,171] or, after they have encountered stimulatory factors, an activated and mature state. DC maturation involves upregulation of MHC and co-stimulatory molecules like CD86, CD80 and CD40 as well as CCR7 that allows migration towards lymphoid tissue[154]. The necessity of activated DC to migrate to secondary lymphoid organs and in particular lymph nodes (LN), in order to present acquired antigens, is one of the main differences between DC and macrophages, that are quite sessile[151]. Mouse studies have shown that without migration, DC cannot generate proper T cell response in response to several antigens[172,173]. After infection we can find two distinct DC populations in the LN, one resident with lower MHC and higher CD11c expression, activated by soluble antigens[174], and one population migrating from the tissue that express markers of maturation[156]. In the spleen, resident populations have been identified both in the white (WP) and in the red pulp (RP)[175] but the DC still maintain their migratory phenotype and can move from the RP to the T cell zone after activation[167,176].

The main difference between quiescent and activated cDC is their ability to interact with other cells, being these T cells, B cells[177], NK cells, or others[178,179]. Once in the LN or in the WP, mature DC can perform the function for which they have been mostly studied: the priming of T cells. This is done not only by forming an IS through which they can present antigens bound to MHC molecules ,but also by providing co-stimulatory signals like CD86 and CD40[151]. Many of the co-stimulatory signals are the same used by cDC to activate NK cells in the spleen[148]. Production of instructive cytokines like IL-6, IL-

12, IL-10, IL-15 and TGFb[180–182] is also an important factor. Traditionally cDC1 have been considered poised to elicit a Th1-type response: cDC1 are the only DCs that can activate the CTL CD8 T cells, as shown by *Batf3*$^{-/-}$ mice[156] while cDC2 give rise more to Th17- and Th2-type responses. This is partially because they express high levels of TLR5 that stimulates IL-23 production after activation[183]. It is possible that, more than the cDC type, it is the signal that binds the PRRs that defines DC activation[184] taking advantage of the functional plasticity of cDC subpopulations.

Mature DCs do not necessarily have pro-inflammatory activity, they are also important for tolerance, for example in the thymus, where resident cDC present self-antigen to maturating T cells to negatively select the auto-reactive ones[185]. Outside the thymus, cDC have a role in inducing the conversion of CD4 into T regulatory cells (T_{reg})[186] and are key for the maintenance of the LN structural integrity, without them there is a marked reduction in LN cellularity caused by poor vascularisation[187,188].

3.2.2.1.2 Accessory cells: macrophages

Like DC, macrophages are sentinel cells. Their main function is to sense environmental cues, both physiological and pathological, in response to which they can engage effector cells and orchestrate a response that drive inflammation or is oriented towards maintenance of homeostasis or resolution of inflammation[189]. Unlike DC, one of the main functions of macrophages is phagocytosis: they can phagocyte apoptotic cells, senescent cell debris and invading pathogens[190,191]. Macrophages activity avoids the accumulation of antigenic macromolecules from dead cells[192,193] and recycle important cellular components and products, like heme from red blood cells (RBC)[194] or lung surfactant[195]. Macrophages are present in small numbers in most tissues[190] where, thanks to their protruding dendrites, form a cellular network particularly apt to survey the surrounding environment[190]. The first to notice the existence of ameboid cells capable of engulfing foreign material was Metchnikoff during his observation of starfishes[196], this shows how macrophages are present even in very primitive animals and their phagocytic activity pre-date the appearance of a developed immune system[197].

Initial studies of the role of macrophages had focused on monocyte-derived infiltrating macrophages, because of their role in immunity and their relative ease of collection and *in vitro*-production. More recently, fate mapping studies in mice have shown that, unlike DCs, most tissue resident macrophages originated in the yolk sac[198,199] and are maintained by self-renewal[200]. Tissue resident macrophages have different traits, depending on the microenvironment to which they are exposed. The determination of the tissue-resident phenotype is controlled by a hierarchy of transcription factors (TF)[201,202] the most general of which are PU.1 and CEBPβ that control the maintenance of the macrophage lineage[202,203]. The expression of other TF is determined by tissue-specific signals, like transforming growth factor TGF-β in the brain or retinoic acid in the omentum[189]. Tissue resident macrophages can have different names and functions based on their location, brain macrophages termed microglia have the function of prune neurons[204], splenic macrophages can phagocytes huge quantities of senescent RBC[194] and osteoclasts, multinucleated macrophages that line the bone endosteum[205], promote angiogenesis and osteoblasts formation[206].

Most of the phagocytosis carried out by macrophages is immunologically silent and independent from other immune cells[207], but if phagocyted debris are loaded with danger signals like nuclear proteins, DNA, nucleotides or other DAMPs[208] or PAMPs[207] this can cause activation of macrophages that leads to increased surface expression of activating receptors and production of pro-inflammatory molecules needed to orchestrate downstream inflammatory responses. Like DC, macrophages express a variety of TLR and intracellular PRR[209,210] that when engage PAMP or DAMP, can produce “classically activated macrophages ”, historically designed as M1[207], in contrast with “alternatively activated macrophages ” called M2, that encompass basically any other type of macrophages with very different physiologies[207,211].

In addition to being sentinel cells, M1 macrophages can also act as effectors. Activated by TNF and IFN-γ they acquire increased microbicidal and tumouricidal activity and secrete high levels of pro-inflammatory molecules[212]. *In vivo,* the IFN-γ necessary to stimulate the effector function of

macrophages is usually provided by activated NK cells at early stages and maintained by the engagement of Th1 cells during the adaptive response[207]. Exposure of macrophages to IFN-γ not only stimulates cytokines secretion and expression of activating receptors on the plasma membrane[148], but also increases production of superoxide anions and oxygen and nitrogen radicals used for pathogen killing[213], explaining macrophages increased microbicidal activity. Unsurprisingly, mice and humans with mutations in the IFN-γ pathway are more susceptible to bacterial, viral and protozoal infections[214].

Signal integration between different PRR, or between PRR and cytokines, specifies the magnitude and the type of macrophage responses. For example, when mice are stimulated with TNF and IFN-γ before *Leishmania.* infection, the macrophages can efficiently kill the parasites, much better then when the stimulation is limited to IFN-γ, showing the necessity of both signals for efficient activation[215]. In this model both signals are necessary because *Leishmania* does not express any PAMP that can be recognised by macrophages. More typically during infection, engagement of TLRs that act through MyD88 (like LPS) or through the TIR-domain-containing adaptor protein inducing IFNβ (TRIF) (like Poly(I:C))[216], causes the release from macrophages of TNF and IFNβ that act in an autocrine fashion, and synergise with NK- or T cell-derived IFN-γ to allow effective macrophage activation. Another example of signal integration in macrophage activation can be found in the inflammasome pathway. Inflammasome activation follows a two-step stimulation process, step one, priming, is done by ligands like TNF or PAMPs and it is followed by step 2, triggering, done by signals indicating cell damage or pathogen invasion. Both steps are needed to licence the activation of a cytosolic sensor called NOD-, LRR- and pyrin domain-containing protein 3 (NLRP3), and the effector enzyme Caspase-1, to initiate the high inflammatory cell death termed pyroptosis and the release of pro-inflammatory cytokines like IL-1β and IL-18[217]. Thus, classically activated inflammatory macrophages are key sentinels and also effectors of innate immunity which activation needs to be carefully regulated because the cytokines that they produce, like IL-1β, IL-6 and IL-23, have been associated with tissue damage and expansion

of Th17 cell population[218] that can contribute to immunopathology like rheumatoid arthritis[219] and inflammatory bowel disease[208].

While the pro-inflammatory function of macrophages is the most well-studied[189,190], of equal if not greater importance is the role of macrophages in the maintenance of homeostasis and tissue repair. For example, by continuously sampling their microenvironment, macrophages can sense various metabolites[220] and directly alter the metabolism of target cells controlling insulin and fatty acid metabolism[221]. By phagocyting RBC they grant a constant supply of heme[194] and can also produce growth factors like nerve growth factor and neurotrophin 3 in the brain[204]. Macrophages presence in every tissue and organ allows them to monitor both local and systemic changes and organise their response so to maintain the organism at homeostasis[154].

3.2.2.1.3 Immunological synapse between accessory cells and NK cells

The IS is a highly organised structure formed between two immune cells to facilitate inter-cellular communication by polarising ligand-receptor contacts and release of soluble stimuli in the synaptic cleft. The first concept of synapse as a nexus of communication was coined to describe neuronal function, but unlike the neuronal synapse the IS is not permanent and terminally differentiated but transient and happens when patrolling effector cells, like T cells and NK cells, encounter activated accessory cells that express specific receptors or antigens[96,222].

When accessory cells are activated, the contact between their ligands and NK cells causes polarisation of the cytoskeleton towards the contact site and the formation of an actin ring where cell-cell adhesion is facilitated by integrins (ICAM-1, ICAM-3) and intracellular adhesion molecules (LFA-1) reorganising around the synaptic cleft[223,224]. This actin remodelling seems to be more important on the macrophage/DC side than in the NK cells side for activating IS[225]. The importance of accessory cells for the activation of NK cells is clearly demonstrated by the fact that, isolated NK cells, fail to respond to pathogen stimulation but are instead activated in the presence of other cells from secondary lymphoid organs[226–228]. For ideal NK cell activation both contact and soluble signals need to be exchanged at the

IS, as shown by semi-permeable membrane experiments[226,227] as well as cytokine blocking ones[148,226,229,230].

NK cells are often the main sources of IFN-γ in very early stages of the immune response. Thus, lack of NK cells activation is deleterious following infections with *Listeria monocytogenes*, *Plasmodium chabaudi*, *Leishmania donovani* and other pathogens[231–233]. Of the soluble factors produced by accessory cells, the most important to drive NK cell activation and early IFN-γ production, is IL-12[231,234]. As shown by Borg and colleagues, the secretion of IL-12 from DC is dependent on the IS formation because IL-12 is trafficked inside endosomes and released into the synaptic cleft[223]. While IL-12 is important for NK activation, also synergy between other cytokines can significantly increase IFN-γ production[235]. One of these cytokines IL-18, is produced mostly by macrophages and released through a non-canonical pathway dependent on inflammasome activation[236], like IL-12, IL-18 polarises at the IS during NK cell activation[237] and the two cytokines can synergise to boost IFN-γ production[237,238]. Other stimuli released by DC and macrophages can stimulate NK cell activation and IFN-γ release: type I IFN, TNF and T-cells derived IL-2 are the main ones[148]. These cytokines have various effects on NK cells activation, type I IFN for example, increases IFN-γ production and induces NKG2D as well as TNF-related apoptosis-inducing ligand (TRAIL) and Fas ligand (FasL) upregulation, helping NK cells to respond to viral infections[119,239]. The case of the IL-15 cytokine is an interesting one, it also synergises with IL-12 to induce IFN-γ production but, unlike IL-12 and IL-18, is not secreted freely but it is trans-presented by accessory cells at the synapse, bound to IL-15Rα[182,240]. Thus, the IS is not just a hub for the clustering of contact signals but also works to concentrate soluble ones required for the dialogue between accessory cells and NK cells.

The contact signals presented to NK cells by accessory cells are the same that are used by NK cells to recognise lysis targets. TLR stimulation and bacterial infection, like with *L. monocytogenes* or *M. tuberculosis*, increase the expression of classic stress or cancerous signals in macrophages: Rae-1α-ε in mice, MICB and ULBP1/2/3 in humans[225,241–243]. Other classic NK cell-ligands are upregulated in

infected and stimulated accessory cells and are used in synergy with soluble factors to activate effector NK cells, CD40 from DC binds CD40L stimulating IFN-γ production[244] and ligation of CD48 by 2B4 stimulates IFN-γ production and NK cell proliferation[225,245,246]. After 2B4 stimulation, NKG2D/DAP10, CD3ζ and ICAM-1 are recruited and cluster in the NK cell immune synapse[247]. DC expression of CX3CL1 upregulates NKG2D and NKp46[248,249] that also clusters at the IS[250]. Macrophages also present F4/80 to NK cells and, if this contact is disrupted NK cells activation is impaired[244,251]. It is clear that macrophages and DC express a large array of stimulants, both soluble and contact-dependent that in case of cellular stress can be used to fine tune the activation of NK cells (Figure 5).

Signals produced by accessory cells can also serve to dampen the immune response and terminate NK cell activation. The main cytokines for this purpose are TGF-β and IL-10, produced by both macrophages and DC[105,148,247]. TGF-β can inhibit the production of IFN-γ, TNF and GM-CSF[252] as well as downregulate activating molecules like NKG2D[253], reducing both cytotoxicity and cytokines production of NK cells[230,254]. IL-10 is more efficient in reducing cytokines production, especially IFN-γ, and its neutralisation can increase resistance to infections like listeriosis[230,255,256].

3.2.2.1.4 Bidirectional crosstalk between accessory cells and NK cells.

The communication between accessory cells and NK cells is not a one-way road. Cytokines produced by NK cells after activation can influence macrophage/DC maturation and antimicrobial and antitumour effector responses, as discussed above. Activated NK cells can control the size of accessory cell population by cytotoxic lysis of immature DCs (a process called “DC editing”) and of highly activated macrophages[102,247]. The main way in which NK cells induce maturation of DC is by producing the soluble factors IFN-γ, TNF and the High mobility group box protein 1 (HMGB1)[237,257]. Once matured DC express high levels of the CD80 and CD86 ligands, can produce IL-12 and have enhanced ability to stimulate other NK cells and naive T cells[257]. CD86 expressing cells are less likely to be killed by NK cells via NCR receptors[258,259], in a process in which the amount of MHC is also a main discriminatory factor[102].

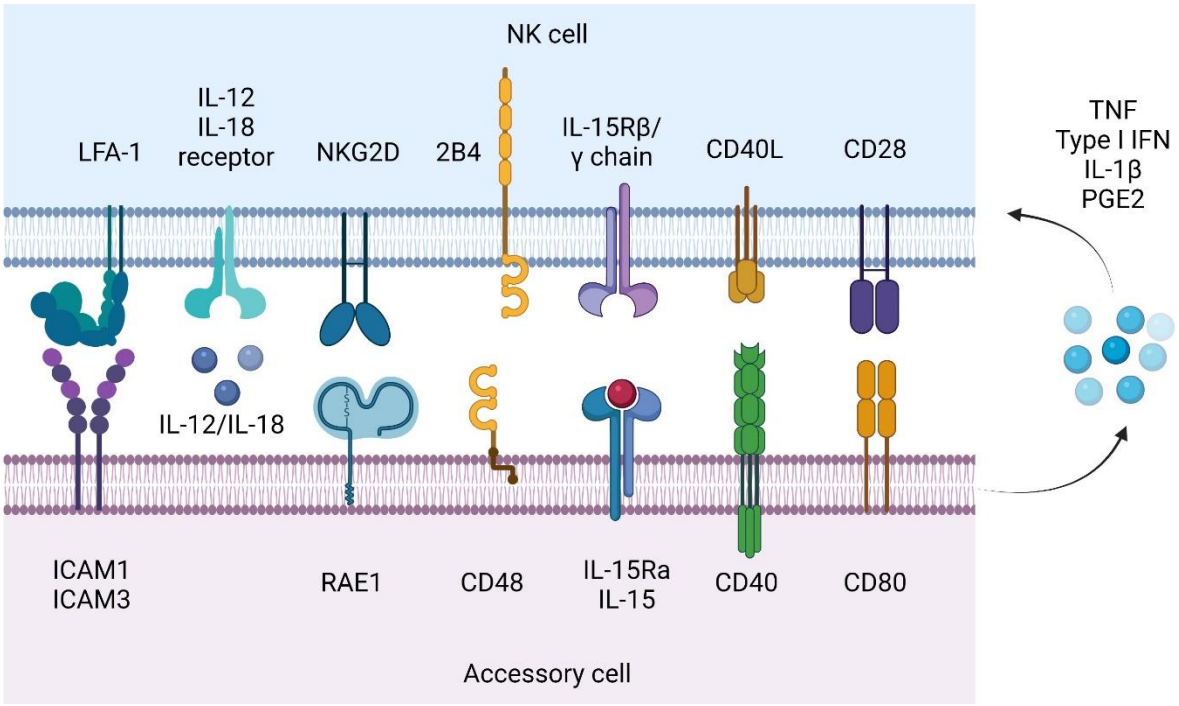


Figure 5: Schematic representation of a murine accessory cell-NK cell activating immune synapse. Integrins ICAM-1/3 can contact LFA-1 on NK cells to strengthen the cell-cell contact and organise the IS structure. In the synaptic cleft accessory cells secrete the soluble cytokines IL-12 and IL-18 while IL-15 is presented bound by its ligand IL-15ra. NKG2D can bind to Rae-1α-ε while 2B4 binds CD48. The CD40L and CD28 common to NK and T cells bind respectively CD40 and CD80 on the accessory cells. Other soluble stimuli released from accessory cells independently of synapse formation (type I IFN, TNF, IL-1b, PGE2) also help the activation of NK cells.

The “DC editing” mechanism is important for the organism: in *Chlamydia* infection for example, depletion of NK cells alters the maturation profile of DCs causing worst infection outcome[260]. NK cells are also capable of killing macrophages activated with high doses of LPS *in vitro*. According to Nedvetzki and colleagues[225], coincubation with these “over-activated” macrophages increases NKp30/44/46 expression and subsequent cytotoxicity in NK cells[225]. The same phenomenon has been studied in alveolar macrophages infected with *M. tuberculosis*, in this case the cytotoxicity is driven by NKG2D-ULBP1 ligation[242]. NK cells can also terminate DC and MF activation without killing them, by producing enough IL-10 to block IL-12 production, thus establishing a negative feedback loop[255,256]. The macrophage and NK cell crosstalk at the synapse is so quick and finely tuned that it is difficult to disentangle the timing and order of activities of the cells on each other[148].

3.2.3 NK cells effector responses: cytotoxicity

Once activated NK cells recognise a target (e.g. infected, stressed, cancerous cells or extracellular pathogens), proceed to form a cytotoxic IS through which trigger the target’s apoptotic or pyroptotic cell death, via the cleavage of Gasdermins protein that form large pore in the cell membrane[261,262]. Cytotoxic killing is a process that happens in stages, first the cytotoxic IS is formed thanks to the presence of the LFA-1-ligand ICAM-1 on the target’s plasma membrane as well as the ligation of several activating receptors. As shown on a bilayer model by Liu and colleagues, 2B4 segregated in the central region of the IS, surrounded by NKGD2, in a bull’s eye structure reminiscent of cytotoxic T cell killing[263]. After the IS is formed, reorganisation of the cytoskeleton is triggered and the microtubule-organising centre (MTOC) polarises underneath it, thanks to PI3K and kinesin-1 action[264,265]. MTOC shift is followed by Golgi and lysosomes associated with myosin IIA[266], to allow trafficking of vesicles towards the synaptic cleft[267,268]. The lysosomes that have been trafficked to the IS, can then dock and fuse with the membrane releasing their content in the synaptic cleft. The vesicle fusion with the membrane can be seen by the increase in lysosomal-associated membrane protein (LAMP) 1 and LAMP-2 on the surface of NK cells[105,269]. Released lytic granules contain perforin, granulysin and

several granzymes, the first two are pore-forming proteins used to allow granzymes to reach the cytoplasm of target cells[119]. Perforin insert itself in cholesterol rich membranes where it creates a large channel formed by more than 20 subunits[270] while granulysin preferably binds cholesterol-free membranes[271]. Granzymes are serine-proteases that, once in the cytoplasm, can cleave caspase molecules, in particular Caspase 3 and 8, and trigger the apoptotic death of the target[272,273]. The same set of proteins can also be used by NK cells to kill extracellular pathogen directly although the sequence of events is less clear in this case[119] and the process seems to happen more slowly than in the cytotoxic IS[274]. Perforin and granulysin can also form holes directly in some bacterial membranes, like in the case of mycobacteria[275]. Once inside the bacteria granzymes cleave proteins necessary for bacterial protein synthesis and metabolism[276]. In some tumours, granzymes can also cleave gasdermins (pore forming proteins), causing a pro-inflammatory form of target cell death, called pyroptosis[261].

NK cells cytotoxicity is not only mediated by granzymes, they can also kill target cells by engaging so-called death receptors[277]. This is obtained by the binding of CD95 (Apo/Fas) to FasL on the NK plasma membrane or thanks to TRAIL that can bind several TRAILs receptor on target cells. Upon activation of Fas with FasL a death-inducing signalling complex (DISC) is recruited, this complex allows the cleavage of caspases thanks to its death effector domain[278]. The cleavage of effector caspases 8 and 1 initiate the apoptotic module causing the death of the target cell[277,278]. The same fate is caused by the binding of TRAIL, that also brings the formation of the DISC and leads to the activation of a caspase cascade, as well as non-apoptotic signalling including NF-κB activation. FasL can even exercise action at a distance when it is secreted inside lytic granules with Granzyme B[279]. Both processes are beneficial in the context of anti-tumour immune response[280].

3.2.4 NK effector responses: secretion of pro-inflammatory cytokines

Activated NK cells can orchestrate the immune response not only by killing infected and transformed cells, but by being a source of cytokines and chemokines that influences the function of other innate and adaptive cells and helps with the recruitment of circulating cells to the site of the injury. NK cells mostly produce Th1-type cytokines[113] and are the main producers of IFN-γ in the early stages of *L. monocytogenes* and MCMV[229,281] infection, thus establishing a pro-inflammatory feedback loop for macrophages and DC to produce more IL-1β, IL-18, TNF and upregulate ligands like CD86[105,247]. Many other cytokines are secreted by activated NK cells: TNF, GM-CSF, IL-5, IL-13 and IL-10 as well as chemokines: CCL3, CCD4, CCL5, XCL1 and CXCL8 to attract myeloid and effector cells to the site of the injury[282,283]. Some of the cytokines produced are required to clear infections, like GM-CSF that is important for the clearance of *C. albicans*[284] but not all the cytokines have pro-inflammatory properties, for example IL-10 produced after IFN-γ in later stages of *L. monocytogenes* infection breaks the pro-inflammatory feedback loop between NK cells and macrophages/DC by reducing the amount of IL-12 and IFN-γ produced[256,285,286]. NK cells are then important not only in the initiation but also in the resolution of infection.

3.3 Listeria monocytogenes

L. monocytogenes is a gram positive rod-shaped bacteria first discovered in 1929 in guinea pigs and rabbits[287,288]. *Listeria* thrives in many diverse environments like soil, water and several human foods[289], making it a problem for the food industry. Because of its capacity of overcoming food preservation practices[290] most cases of *L. monocytogenes* infections are foodborne. *Listeria* infection typically manifests as easily manageable gastroenteritis but, in the case of very small children, elderly or immunocompromised people and pregnant women, can turn into a serious infection with 20-30% mortality[287]. This is due to the ability of *L. monocytogenes* to cross the defensive barriers of the body: in the gut it can cross the intestinal barrier and lead to sepsis, in the brain can cross the blood-brain barrier resulting in bacterial meningitis and can also cross the fetoplacental barrier, resulting in abortion, pregnancy complication or neonatal infections[287,289]. *L. monocytogenes* is facultatively anaerobic and can grow at low temperatures, low pH and high salt concentrations[288]. Its adaptability, together with its genetic tractability and easiness to culture[291], makes it a good model for *in vitro* infection work[289].

While *L. monocytogenes* is an excellent model for the study of systemic bacterial infections, mice cannot recapitulate human food borne listeriosis. In mice oral infection is inefficient because they do not express the protein that can be bound by bacterial Internalin in the gut, so the bacterium cannot pass the intestinal barrier. The creation of humanised mouse strains has made possible to study foodborne *L. monocytogenes* diseases in mice[292] but the majority of the studied published are still based on intravenous or intraperitoneal infection models that mimic systemic *L. monocytogenes* infection. Interestingly, not all strains of mice respond equally to *L. monocytogenes*, of the two most common strains used BALB/c are susceptible while C57BL/6 the mice used in our study, are resistant[291]. In this case the difference in resistance is due to IL-12 and IL-15 production in early stages of *L. monocytogenes* infection. DSc from C57BL/6 express more IL-12p40 as well as *Il15* already 3 h post-infection, thus also upregulating IFN-γ production more efficiently[293]. This disparity in cytokine

production can be linked to differences in TLR expression and general levels of DC maturation between the strains[294]. The importance of the IFN-γ production in early *L. monocytogenes* infection is confirmed by the disappearance of the increased resistance of C57BL/6 mice following infection with LLO-deficient *L. monocytogenes* strains that cannot escape the vacuole of naïve macrophages[295].

3.3.1 Cell biology of *L. monocytogenes*

Once ingested, *L. monocytogenes* passes the intestinal epithelial barrier mainly via directional transcytosis across goblet cells. These cells are important because they expose the Internalin A (InlA) ligand E-cadherin, as shown by Nikitas and colleagues[296], in this way bacteria can reach the lamina propria shielded from the extracellular environment without eliciting an immune response. From the lamina propria *Listeria* can then disseminate via lymph and blood to other organs like spleen and liver[288]. The great advantage that *L. monocytogenes* has on the host is its ability to enter both professional and non-professional phagocytes. Professional phagocytes are macrophages, present in the lamina propria, that engulf *L. monocytogenes* thanks to their natural ability to phagocyte bacteria and their expression of CD64 that can act as additional receptor for *L. monocytogenes*[297]. In non-phagocytic cells, entry is induced by the binding of InlA and/or InlB to respectively E-cadherin and Met[298,299]. Met is a protein tyrosine kinase, and receptor for the hepatocyte growth factor[299], while E-cadherin is a cell–cell adhesion molecule[298], both are mostly expressed in epithelial cells. When Internalines bind their ligands on the host cells, they trigger actin remodelling causing bacterial uptake through endocytosis, a process mediated by the ArpP2/3 actin-nucleation complex[300]. Once internalised *L. monocytogenes* can evade the vacuole and replicate in the cytoplasm. The evasion from the vacuole is mediated by the bacterial protein listeriolysin (LLO) and two phospoholipases: PlcA and PlcB[301,302]. In macrophages the phagosome containing *Listeria* is fused to lysosomes to create phagolysosomes, in which, due to low pH, active oxygen and nitrogen species and enzymes, the bacteria is killed, so evasion mediated by LLO is particularly important[303,304]. LLO is part of a family of pore-forming cholesterol-dependent cytolysins present in several gram-positive bacteria[302], the pore-

forming activity of LLO is optimal at low pH, making it fully active in the phagosome but not in the cytoplasm[305,306], so the bacterium avoids killing the host cell once it has escaped to the cytoplasm. A functional DNA uptake competence (com) system and in particular comK are also helping *Listeria* to escape the vacuole[307]. Once in the cytoplasm, the bacteria cause dramatic cellular alterations. The expression of the surface protein Actin assembly-inducing protein on Listeria surface, can mediate asymmetric host actin polarisation, creating actin structure termed "comets" that propel *L. monocytogenes* through the cytoplasm and allow the spread of the bacterium from one cell to the adjacent ones[308]. Like for *L. monocytogenes* cell entry, this process requires the mediation of the Arp2/3 complex, in this case composed by a different protein subset[300]. Formins have also been shown to participate in formation of actin comet tails and their stability[309] especially diaphanous-related formins are important for cell-cell spread of *L. monocytogenes*[310]. These formins create protrusions on the cell membrane, where the bacterium is closer to the membrane, permeabilisation by LLO then mediates local damage that causes presentation of the inner leaflet of the membrane in the extracellular environment. This stimulates efferocytosis of neighbouring cells, especially macrophages expressing T cell immunoglobulin and mucin domain-containing protein 4[311], thus allowing *L. monocytogenes* to spread in the organism.

3.3.2 Innate response to *L. monocytogenes*

Sub-lethal systemic infections of *L. monocytogenes* in mice are usually cleared in the first 7-10 days. In the early response the innate immune system is the key player, with innate cells required to keep *L. monocytogenes* replication and spread under control[291]. Even if the innate immune system is sufficient to slow bacterial infection though, an effective adaptive response is required for sterilising immunity: SCID mice develop chronic infection and are not capable to clear the bug[312].

3.3.3 Sensing of *L. monocytogenes*

Sensing of *L. monocytogenes* by innate immune cells is mediated by extra- and intracellular PRR because bacteria is able to survive and replicate both inside and outside host cells[291]. In human infections the first exposure of immune cells to *L. monocytogenes* happens in the lamina propria after the bug has passed the intestinal barrier. Extracellular *Listeria* sensing in macrophages and DC is mostly driven by MyD88-dependent TLR, as shown by Edelson and Unanue[313], in particular TLR2 and TLR5. TLR2 recognises gram positive cell wall elements[314] and when engaged, activates NF-kB through MyD88 upregulating the expression of IL-6, TNF and IL-12[315]. Seki and colleagues demonstrated that lack of TLR2 causes decreased cytokine production in response to *L. monocytogenes*[316]. The flagellin-binding TLR5 also recognises *L. monocytogenes in vitro*, but its importance is less clear-cut *in vivo* seeing that *Listeria* evades immune responses by downregulating flagellin at 37° C[291,317]. Finally, the CLEC5A member of the C-type lectin receptor family is also important for immunity against *L. monocytogenes,* a study found that *Clec5a*$^{-/-}$ mice infected with L. monocytogenes produce less , IL-1β, IL-17A, and TNF as well as fewer IL-17A^{+} γδ T cells and develop severe liver necrosis.[318]. The same study suggested that CLEC5A could bind N-acetylglucosamine (GlcNAc) and N-acetylmuramic acid (MurNAc) disaccharides from L. monocytogenes walls because exogenous addition of GlcNAc or MurNAc *in vitro* inhibited CLEC5A binding to Listeria cell wall extract[318]

Once *L. monocytogenes* has escaped the phagosome and entered the cytoplasm it can trigger intracellular PRR: NLRP3[319] and NLRC4[320] sense LLO, the bacterial protein p60 and flagellin, while *Listeria* nucleic acids are sensed by either cyclic GMP-AMP synthetase/stimulator of interferon genes (cGAS/STING), AIM2- like receptors, or RIG-I-like receptors[291]. Nucleotide-binding oligomerisation domain 1 (NOD1) and NOD2 can also detect *L. monocytogenes*, especially in the gut[321]. The sensing of *Listeria* by cytoplasmic PRR can lead to NF-kB activation and increased expression of pro-inflammatory cytokines and chemokines in the case of cGAS/STING and NODs[321,322], or to the secretion of IL-1β and IL-18 following pyroptotic death in case of AIM2 or NLRs activation[320].

3.3.4 Innate cells in *L. monocytogenes* immune response

Innate immune cells are the first barrier that the immune system puts in place to stem *L. monocytogenes* infections. Macrophages come in contact with *L. monocytogenes* first, due to their role as professional phagocytotic cells. In the intravenous (i.v.) mouse infection model it is splenic marginal zone macrophages (MZM) and marginal metallophilic macrophages (MMM) that first engulf the bacteria[323,324] in order to contain widespread spleen infections[323,325]. Kupffer cells in the liver have a similar function and also limit the spread of *L. monocytogenes*[325]. Macrophages that have phagocyted *Listeria* proceed to kill the bug by exposing it at the low pH, the oxygen and nitrogen radicals and the enzymes present in the phagolysosome[304,326]. This killing is only possible in macrophages that have been primed by IFN-γ, largely provided by NK cells, and some by $CD8^+$ T cells, otherwise *L. monocytogenes* can efficiently escape the phagosome and instead, use macrophages as a vector of infection[304,327]. Mice and humans that lack or have mutations in genes of the IFN-γ pathway, are susceptible to listeriosis and more prone to recurrent infections[328,329]. Reflecting the need for an IFN-γ rich environment early in the disease, the peak of IFN-γ production is only 24 to 48 h post-infection[285,291,330].

Macrophages not only help the host by phagocyting bacteria but once infected, can also produce high levels of chemokines and cytokine. The bacterial protein p60 for example, induces inflammasome activation causing release of IL-1β and IL-18[331], IL-1β activates effector immune cells as well as non-immune cells, while IL-18 is an important stimulant of IFN-γ production[316]. Macrophages are also a major source of IL-12 once triggered by *L. monocytogenes* encounter with TLRs[332]. IL-12 that is required to induce IFN-γ secretion in NK, NKT and T cells[333,334]. The effect of IL-12 on effector cells is evident because absence of IL-12 results in increased bacterial burden 3 days after infection, when the effector cells should have already been activated to kill bacteria and infected cells[335,336]. Macrophages also produce TNF that acts as autocrine stimulus[337] and works in concert with IFN-γ to initiate a Th1 adaptive response.

Splenic DC are infected at very early stages of Listeriosis, possibly by direct transfer from infected macrophages. 9 hours after i.v. infection Listeria-positive DC are already migrating towards the periarteriolar sheet (PALS) in the WP to initiate the activation of T cells[338]. DC are key for the transfer of *L. monocytogenes* to the T cell zone, in *Baft3*$^{-/-}$ mice that do not express CD8α^{+} cDC, the bacteria never reach the white pulp and the generation of *Listeria*-specific T cells is impaired[339]. In order to activate T cells, DC upregulate co-stimulatory molecules, present *L. monocytogenes*-specific peptides on MHC molecules, and produce soluble stimuli like IL-12, IL-18[256,335] and type I IFN[340,341]. Production of type I IFN must be tightly regulated, while it is important for the initiation of immune response against intracellular pathogens, too much type I IFN has anti-inflammatory properties in *L. monocytogenes* infection[256,285]. Excess of IFN-α or IFN-β induces T cell apoptosis[342] , IL-10 expression[285,343] and downregulation of TNF[344]. This is possibly an artefact of the murine i.v. infection model that exposes the mice to very high levels of bacteria in a short time, thus stimulating the production of levels of type I IFN that are not common in a foodborne infection[291].

L. monocytogenes also stimulates the production of chemokines like CXCL1, CXCL2 and CXCL8, that recruit immune cells to the site of infection[291,345]. The first cells to arrive on site are neutrophils, that appears within just 30 minutes after i.v. inoculation and peak 4 hours later[346], driven by the chemokine receptor CXCR2[345]. Neutrophils are capable of engulfing extracellular bacteria and killing them with their granules. Antibody-mediated depletion of neutrophils affects the clearance of *L. monocytogenes*[347]. Neutrophils are followed by infiltrated monocytes driven by CCL2, CCL3, and CCL7[348,349], after 24 h infection foci are no more surrounded by neutrophils but by monocytes and the inability to switch between the two cell types increases susceptibility to *L. monocytogenes*[350]. It is possible that monocytes are required to prevent excessive activation of neutrophils and consequent tissue damage.

NK cells are the main source of IFN-γ in early primary *L. monocytogenes* infections[255,333,351,352]. They can be activated by infected macrophages or DCs[148], and the IFN-γ produced is important for

enhancing accessory cells activation as well as helping T cell priming in the white pulp[291]. NK cells start producing IFN-γ 12 hours post-infection, but already after 24 hours a wide variety of cells can produce it[352]. This is probably the reason why several studies have found that ablation of NK cell does not worsen the phenotype of *L. monocytogenes* infection, and it can even enhance mice resistance in some cases[255,353]. Perona-Wright and colleagues explained this paradox by showing that 4 days post-infection, NK cells are a major source of the anti-inflammatory cytokine IL-10[354], so NK cells have also immunoregulatory functions that might work against the host in experimental models of *Listeria* infection.

Other cells that are poised to produce IFN-γ after IL-12 and IL-18 stimulation in primary infections, are T lymphocytes that have a memory phenotype without having encountered *L. monocytogenes* before, termed "virtual memory" $CD8^+$ T cells, and NKT cells[333,355,356]. Virtual memory cells can secrete IFN-γ 16 to 24 hours post-infection[355,357] and their numbers correlates directly with innate resistance to Listeriosis in mice[333,355]. NKT cells are a small subset of cells that is in-between NK cells and T cells, they express an invariant TCR that recognises lipid antigens. Few days after L*. monocytogenes* infection NKT are a significant source of IFN-γ, and could help the activation of DC[335].

The early immune response to *L. monocytogenes* is controlled by a network of innate cells that need to act in concert to enhance each other action. While the response to i.v. *L. monocytogenes* infection in the spleen has been intensively studied and the role of NK cells mostly elucidated, there are still areas of confusion regarding exactly which cells are important for the activation of NK cells, as well as the location of the activation. Most of the studies focus on DC-activated NK cells but, considering how quickly NK cells start to produce IFN-γ, is possible that macrophages are the most important cells in early activation. Also, NK cells localise in the RP together with macrophages and only later can they migrate in the WP to enhance activation of T cells. The use of i.v. infection that generates a very quick and strong immune response unlike the one typical of foodborne infections might be the reason why

Type I IFN and IL-10 production from NK cells so elevated, and studies on more physiological models of *L. monocytogenes* infection might be needed to entirely clarify the role of NK cells in Listeriosis.

3.3.5 Adaptive responses to *L. monocytogenes*

The innate immune response does not only keep bacterial replication in check and stop the infection from spreading too fast but it also creates the right conditions to generate *Listeria*-specific adaptive immune cells that are effective in clearing *L. monocytogenes*[358]. Primary infections give rise to T and B cells that persist in the organism and, upon reinfection, allow for a more efficient control of the pathogen in the first few hours[303]. Because *L. monocytogenes* is an intracellular bacterium, the humoral response is not a major actor in the secondary infection: transfer of sera from immune mice does not confer resistance[359] and *L. monocytogenes* infected mice do not have a robust antibody response[360].

3.3.5.1 Primary L. monocytogenes infection

The priming of T cells requires 3 distinct signals that can all be delivered by antigen presenting cells (APC): signal 1 is the recognition by the TCR of a cognate antigen that is presented on a cell surface by MHC I or MHC II proteins. The second signal requires the binding of co-stimulatory protein expressed by accessory cells, like CD86 or CD40[361]. Finally, T cell activation is influenced by the local concentration of soluble pro-inflammatory stimuli like IL-12 or IFNs[303,362]. Activation of T cells happens through the formation of an APC-T cell IS similar to the NK cells one, that requires TCR recognition[148]. During primary *L. monocytogenes* infection, the $CD8^+$ T cell population begins to proliferate and 3 to 4 days post-infection, a *Listeria*-specific population is detectable. This population peaks typically after 7-8 days[363]. $CD8^+$ Listeria-specific T cells recognise peptides presented on the MHC Ia/b proteins that are ubiquitously expressed on host cells and normally present self-protein cleaved in the cytoplasm and loaded in the ER. When cells are infected with *L. monocytogenes*, bacterial peptides are presented by MHC I to T cells, in particular peptides derived from LLO (91-99) and p60 (84-92) become immunodominant[364]. An expanded population of *L. monocytogenes*-specific T cells can then traffic

through the body and, upon recognition of specific MHC::peptide complexes, produce IFN-γ[365] and initiate cytotoxicity[365–367]. Like for the cytotoxic process that we have described in activated NK cells, T cell-mediated cell killing requires the formation of a cytotoxic IS and can be mediated by granule exocytosis[367] and Fas-FasL ligation[366]. Lysis of infected cells is beneficial because it exposes intracellular bacteria to the phagocytic action of macrophages and neutrophils that carry out the killing. As the infection subside, the population of activated $CD8^+$ T cells dwindle, most of them die and the remaining develop a long lasting memory phenotype that help with subsequent infections[365].

$CD4^+$ T cells, also named T helper cells, also expand and contract during *L. monocytogenes* infection at the same rate $CD8^+$ T cells do[363]. $CD4^+$ T cells recognise peptides presented by the MHC II proteins, only expressed in professional APCs and upregulated during infections[368]. MHC II bind peptides derived from extracellular antigens, LLO is the most common source of peptides that binds MHC II and is recognised by T cells in *Listeria* infection [369]. Activated $CD4^+$ T cells are particularly efficient at producing pro-inflammatory cytokines. In the case of *L. monocytogenes* infection, the main products are IFN-γ and TNF. This is because IL-12 and Type I IFN are signal 3 molecules that push $CD4^+$ towards a Th1 phenotype. Defects in the production of either one of them results in fewer IFN-γ^+ $CD4^+$ T cells in mice[370].

The vast majority of the T cell findings in *L. monocytogenes* infection models have been obtained after i.v. injection, a model that does not recapitulate the human diseases that is slower and involves more tissues because it happens thorough the intestinal epithelium. As an example of the differences between i.v. and physiological infection, Pepper and colleagues found that, when mice are infected through a mucosal route, about 10% of the $CD4^+$ T cell population had a Th17 phenotype, while in in i.v. infection virtually every $CD4^+$ is a Th1 cell[371].

3.3.5.2 Secondary L. monocytogenes infection

When a secondary challenge with *L. monocytogenes* occurs, mice are significantly more resistant, this is mostly due to the presence of memory T cells that recognise *Listeria* antigens and move to control

the infection already in the first 6 hours[372]. The subsequent expansion of specific T cells also happens rapidly and the final number of effector cells is higher than during the primary infection[363,373].

The generation of $CD8^+$ T cells can be followed after primary infection by increase in the surface marker IL-7R and decrease of KLRG1 levels[374], cells so identified are precursor memory cells that will generate long-lasting immunity by maintaining their phenotype thanks to epigenetic modifications[375]. The presence of both IL-2 and IL-12 is required for the generation of efficient memory cells[374,376], in this context IL-2 works as a growth factor to sustain T cell proliferation upon reinfection[377]. The lack of specific markers that define $CD4^+$ T memory cells generation has made the study of this cell type challenging in the *Listeria* infection system[291]. Once activated, memory T cells fight *L. monocytogenes* infection with the same mechanisms that they adopt during primary infections: $CD4^+$ T cells mostly producing IFN-γ and TNF[378] and $CD8^+$ T cells exercising their cytotoxic action.

The large body of published studies on the immune response to *L. monocytogenes* infection gives us perhaps the most complete biological understanding that we have of any host-pathogen interaction, although this is mostly limited to two mouse models: BALB/c and C57BL/6. The great majority of the studies have focused on the role of the innate immune system, in particular in spleen and liver, and of $CD8^+$ T cells. While this is understandable considering the importance of both components in the outcome of *L. monocytogenes* infections, future studies will be needed to address the real importance of populations such as $CD4^+$ and B cells in the human infection. There is also more work to do in understanding what are the major sources of susceptibility in humans, why very young and very old people are more at risk of dying by listeriosis and how exactly *L. monocytogenes* is capable of crossing the trans-placental barrier to cause foetal infection and create complications in pregnant women. Regardless, *L. monocytogenes* remains a powerful experimental tool to understand the molecules that allow the cross-talk between macrophages/DC and NK cells the biology of IFN production, the crosstalk between DC and T cells, and the immune control of bacterial infections and this are the reasons why we used *Listeria* in our study.

3.4 Thesis hypothesis and Aims

In this thesis we set out to test the **hypothesis that CALHM6 acts as a synaptic membrane ion channel that mediates innate instruction of NK cell activation during infection.** To address this hypothesis, we pursued the following three Aims:

Aim 1: Characterise the regulation of CALHM6 expression in the innate immune system.

Aim 2: Characterise the requirement for CALHM6 in innate instruction of effector responses in the early phases of infection.

Aim 3: Describe the mechanism of Calhm6 function in macrophages.

4 Materials and methods

4.1 Cell cultures

4.1.1 Bone marrow collection

To obtain bone marrow (BM) from mice we collected leg bones and proceeded to clean from muscle tissue and sterilise them in ethanol 70%. The epiphyses were removed and the BM flushed out with a 30 G syringe into Roswell Park Memorial Institute (RPMI) 1640 complete medium (10% low endotoxin heat inactivated foetal bovine serum (FBS), 100 units/ml penicillin, 100 µg/ml streptomycin and 5.84 µg/ml glutamine, 1 % HEPES from 1 M stock, 1 mM Sodium pyruvate and 1 µg/ml β-mercaptoethanol). The cells so obtained were centrifuged to remove the supernatant and resuspended in 2 ml freezing medium (90% FBS, 10% dimethyl sulfoxide (DMSO)), moved into 2 cryovials then slowly cooled down to -80^{o}C before being transferred to liquid nitrogen storage.

4.1.2 Bone marrow derived macrophages generation

To generate mouse bone marrow derived macrophages (BMDM), frozen BM cells from one mouse leg were cultured in 100 mm non-TC-treated square dishes in 15 ml complete RPMI 1640 medium with 50 ng/ml rhM-CSF. Cells were incubated at 37^{o}C in 5% CO_2. On day five, 5 ml of complete medium with 50 ng/ml rhM-CSF were added to the culture. At day seven, the cells were lifted with cold PBS and used for experiments.

4.1.3 BMDC generation

Mouse BMDC were generated from frozen bone marrow cells; one mouse leg was cultured in two 10 cm ø petri dishes in 10 ml complete RPMI 1640 medium with 10 ng/ml mouse GM-CSF (mGM-CSF). Cells were incubated at 37°C in 5% $C0_2$. On day two and five, 5 ml complete medium with 10 ng/ml

mGM-CSF were added to the culture. On day seven, only the cells in suspension were collected for experiments.

4.1.4 HEK293T cells

HEK293T cells kindly provided by the Midwood lab (Kennedy Institute of Rheumatology, Oxford, UK), were maintained in 10 cm ø TC plates in 10ml of complete Dulbecco's Modified Eagle Medium (DMEM) supplemented with 10% heat inactivated FBS 100 units/ml penicillin and 100 µg/ml streptomycin, 5.84 µg/ml glutamine and 1% HEPES from 1 M stock. Cells were grown at 37°C in 5% CO_2.

4.1.5 Plat-E cells

Plat-E cells, were grown in 10 cm ø TC plates in 10ml of complete DMEM without HEPES. Every week 10 µg/ml of Blasticidin and 1 µg/ml of Puromycin were added to the culture to select competent cells. The cells were grown at 37°C in 5% CO_2. Plat-E cells were not kept in culture for more than a month to maximise transfection efficiency.

4.2 In vitro cell stimulation

4.2.1 Pro- and anti-inflammatory stimuli for BMDM/BMDC

Unless specifically stated, for in vitro stimulation of BMDM and BMDC we used LPS 100ng/ml, Zymosan 100 µg/ml, Poly(I:C) 50µg/ml, IFN-γ 10ng/ml, TGF-β 10 ng/ml, IL-10 10 ng/ml and IL-4 10 ng/ml, for the duration of the stimuli see figures and figure legends.

4.2.2 Listeria infection

For in vitro *L. monocytogenes* stimulation, BMDM were cultured overnight with antibiotic-free complete medium, 100.000 cell/well in a flat bottom 96 well plate. Frozen, stationary phase, OVA expressing *L. monocytogenes* (kindly donated by the Gerard's lab, Kennedy Institute of Rheumatology,

University of Oxford) were diluted in complete medium to obtain a multiplicity of infection (MOI) of 1 and added to the BMDM. To synchronise the infection the plates were spin down for 3 min at 300 g. Cells were placed in the incubator for an hour, then *L. monocytogenes* left in the supernatant was washed away with warm medium and the supernatant was supplemented with 5 µg/ml Gentamicin, to make sure that only intracellular *L. monocytogenes* was present in the culture. Cells were infected with *L. monocytogenes* for 6 h in total.

4.2.3 NK cell activation with soluble factors or PMA

Single cell suspension obtained from spleen was stained for flow cytometry with live/dead stain, αCD3 and αNK1.1 conjugated antibody. $NK1.1^{+}CD3^{-}$ cells were isolated from naïve spleen with fluorescent assisted cell sorting to obtain a NK cell pure population. 200.000 $NK1.1^{+}CD3^{-}$ cells so obtained were plated in a U bottom 96 well plate straight after sorting and stimulated with PMA/Ionomycin 1:500 (Phorbol 12-Myristate 13-Acetate 40.5 µM, Ionomycin (670 µ)), Il-12 (50 ng/ml), TNF (50ng/ml) and or IL-18 (50ng/ml) for 6h. Supernatant was collected and IFN-γ concentration measured by enzyme-linked immunosorbent assay (ELISA).

4.3 Quantitative real-time PCR

RNA was extracted from BMDM or $F4/80^{+}$ macrophages isolated with magnetic beads using a RNeasy Mini kit according to manufacturer instructions. 1.5-3x10^{6} starting cells were used for BMDM RNA extraction. Complementary DNA (cDNA) was obtained by using 1 µg of starting RNA in 10.5 µl were possible. For the reverse transcriptase reaction, we used 1 µl oligo-dT, the RNA was heated up to 70°C for 3 min and quickly cooled down on ice to allow annealing of oligo-dT. 8.5 µl of reaction buffer containing: 4 µl First-strand buffer, 2 µl dNTP (10 mM), 2 µl dithiothreitol (DTT) (100 mM) and 0.5 µl SMART MMLV Reverse Transcriptase were added to the RNA mix. The machine used for the temperature cycling was a c1000 Touch Thermal Cycler (Bio Rad). Primers for quantitative PCR (see

Table 1) were mainly ordered from KiCqStart Primers (Merck) and SYBR Green reaction buffer was used for the amplification reaction. The machine used to collect the data was a ViiA 7 Real-Time PCR system.

4.4 Immunoblots

The antibodies used for western blot analysis were: FAM26F, HA, FLAG, pCAMKII, CAMKII, and GAPDH. As secondary antibody we used peroxidase-conjµgated AffiniPure Goat Anti-Mouse IgG or goat Anti-Rabbit IgG.

4.4.1 SDS page

Cells were lysed in sodium dodecyl sulphate (SDS) lysis buffer (2% SDS 66mM, TRIS pH 7.4) or, for non-denaturing lysis conditions, in Triton buffer (50 mM Tris pH7.4, 150 mM NaCl, 1 % Triton X-100 with 1:25 cOmplete Protease inhibitor Cocktail) cells collected in Triton buffer were left on ice for 30 min before collection and then centrifuged at 10.000 g for 15 min, before supernatant collection. Before western blot (WB) run, lysates were mixed with 4x Laemmli sample buffer containing the specified amount of DTT. Unless otherwise indicated, samples were boiled at 95°C for 5 min. Proteins were separated by being run on an SDS PAGE gels 4-20%, then transferred to nitrocellulose membrane using a Trans-Blot Turbo machine (Bio Rad). Membranes were blocked at room temperature for 1 h in with 5% non-fat milk in TBST wash buffer (Tris-buffered saline (50 mM Tris/HCl, 150 mM NaCl, pH 7.6) containing 0.1% Tween 20) and then incubated with primary antibodies overnight at 4°C (FAM26F 1:100, pCAMKII, CAMKII 1:1000) or 1 h at room temperature (HA 1:1000, FLAG 1:5000, GADPH 1:1000) in 2.5% milk in TBST. Membranes were washed for 1 h in TBST and incubated with HRP-conjugated secondary antibodies (goat anti-mouse or goat anti-rabbit, 1:5000 dilution) at room temperature for 1 h in 2.5% milk in TBST. Non-specific secondary bound antibodies were washed with TBST for an hour and membrane used for chemiluminescence detection (ECL/ECL-Plus reagent) on X-ray films. When

we needed to ensure equal loading, membranes were re-probed with the loading control antibody GAPDH.

4.4.2 Native BluePAGE gel

For Native BluePAGE gel, cells were lysed in 50 µl cold 1X NativePAGE Sample Buffer containing 1% Digitonin or 1% dichlorodiphenyltrichloroethane (DDT) in the presence of cOmplete protease inhibitor cocktail. Lysates were incubated on ice for 15 min and centrifuged at 13000 g for 30 min at 4°C. just before the run NativePAGE 5% G-250 sample additive was added to the samples then run on NativePAGE Bis-Tris gels in NativePAGE dark blue running buffer.

4.5 Calhm6$^{-/-}$ mouse strains

4.5.1 Generation of *Calhm6*$^{-/-}$ mouse strains

Calhm6$^{-/-}$ mice were obtained by crossing C57BL/6N FAM26F$^{fl/fl}$ mice, generated by Jelena Bezbradica Mirkovic, in the Medzhitov lab (Yale School of Medicine, New Haven, CT) using ES cells from EUCOMM repository, with the C57BL/6J PGK$^{Cre/-}$ line kindly donated by the Arnon's lab (Kennedy Institute of Rheumatology, Oxford, UK). The progeny was then intercrossed to remove the PGKcre allele and generate the final *Calhm6*$^{-/-}$ and WT controls. In order to generate CD11c-conditional KO mice we crossed our original Calhm6$^{fl/fl}$ mice with a flippase-expressing C56BL/J strain to excise the LacZ-containing cassette that interferes with the production of complete CALHM6. The mice were then crossed with an Itgax$^{cre/-}$ expressing strain to obtain Itgax$^{cre/-}$Calhm6$^{fl/fl}$ mice that had specific deletion of CALHM6 in CD11c^{+} cells. We also generated a rag$^{-/-}$Calhm6$^{-/-}$ strain by crossing C57BL/6N FAM26F$^{-/-}$ mice with C57BL/6J rag$^{-/-}$ mice.

All animals are housed under specific-pathogen-free conditions in individually ventilated cages.

4.5.2 Genotyping PCR

Biopsies for genotyping PCR reaction were collected from mouse ears. DNA was extracted from biopsies by overnight lysis in 500 µl Lysis Buffer (1M Tris pH 8, 5 M NaCl, 0,5 M EDTA, 10% SDS in water) with 400 µg/ml of Proteinase K at 56°C. The next day 250 µl of 6M NaCl buffer were added and samples incubated on ice for 10 min. Biopsies were centrifuged at 10.000 rpm for 10 min at 4°C. Supernatant was transferred to a clean tube and mixed with the same volume of isopropanol for DNA precipitation and incubated for 15 min at RT. DNA was centrifuged at 13.000 rpm for 10 min, dried, and resuspended in water. DNA extracted was used for PCR with One Taq MM and amplified products run on a 1.5% agarose. SYBR safe was use to visualise DNA bands under UV lights.

4.6 Flow cytometry

4.6.1 Single cell suspension from spleen

Single cell suspensions from mouse spleens were obtained by collecting spleens in complete RPMI 1640 medium and cutting them with surgical blades to obtain small fragments then digested with Collagenase (1:25) and DNAse I (1:250) at 37°C for 30 min. The cells obtained were filtered through a 70 µm nylon mesh. RBC were lysed by incubation for 7 min on ice with RBC Lysis Buffer and the splenocytes were then used for experiments. To measure intracellular IFN-γ and Granzyme B the spleens were harvested in complete RPMI medium containing 5 µg/ml Brefeldin The obtained cell suspensions were cultured in round bottom 96 well plates ($2x10^6$ cells/well) in the same medium.

4.6.2 Single cell suspension from thymus

Single cell suspension from thymus was obtained by collecting the organ in complete RPMI medium and mashing it through a 70 µm nylon mesh with the help of a syringe plunger. The cells obtained were then resuspended and used for flow cytometry.

4.6.3 Flow cytometry staining

For flow cytometry staining $2x10^6$ cells per condition, were possible, were used. Cells were washed twice in PBS and stained with 1:1000 live/dead staining in PBS for 20 min, after 3 more PBS washes cells were blocked for 10 min in FACS buffer (PBS, 3% FCS, 0.05% (w/v) sodium azide, 1mM EDTA) supplemented with 0.5% normal mouse serum and 1:200 Fc blocking antibodies. Surface membrane staining was then performed by adding fluorescently conjugated antibodies (see Table 2 for reagent list) to the cells in a 1:200 dilution in FACS staining buffer (with normal mouse serum and Fc block). For intracellular protein staining, extracellularly stained cells were washed and permeabilised with Fixation/Permeabilisation buffer for 20 min. After the permeabilization cells were kept in a saponin-containing buffer to keep the membrane permeable for the duration of the staining. Blocking was done for 10 min in saponin-containing buffer supplemented with 0.5% normal mouse serum and 1:200 Fc blocking antibodies. Antibodies against intracellular proteins were then added to the cells and incubated for 30 min. At the end of the staining the cells were fixed at with 4% PFA for 5 min on ice. For IFN-γ and Granzyme B staining cells were always kept in buffers containing 5µg/ml of Brefeldin A to block protein secretion. The entire staining protocol was carried out on ice and, during incubation, in the dark. Stained cells were run on a LSRII flow cytometer.

4.7 In vivo L. monocytogenes infection

4.7.1 Primary *L. monocytogenes* infection

OVA expressing *L. monocytogenes* was grown in brain heart infusion (BHI) broth without antibiotics at 37°C on a shaker until reached log phase. Log phase was measured by absorbance (OD 0.8-1.0 at OD600). Log phase *L. monocytogenes* was washed and re-suspended in PBS right before injection, concentration of *L. monocytogenes* was calculated using the OD and confirmed by culturing *L. monocytogenes* overnight on BHI agar plates. WT and *Calhm6*$^{-/-}$ mice were inoculated with $3x10^5$ or $3x10^4$ CFU of log phase *L. monocytogenes* via intraperitoneal injection. Weight was monitored every

day at the same time of the injection. Mice were sacrificed 1, 3 or 7 days later, blood was collected at day 1 and 3 spleen was collected and weighted at day 1, 3 and 7. For determination of CFU, splenocytes were lysed by centrifugation with Precellys beads (1.4 mm) at 10000 rpm on a Quiashredder for 10 min in 1 ml PBS. 100 µl of the lysate obtained was plated in several dilutions on BHI-Agar coated plates without antibiotics and incubated at 37°C for 24/48 hours. Bacterial colonies were counted automatically with ImageJ software and *L. monocytogenes* CFU load per spleen was calculated based on the number of colonies, the spleen weight and the dilution factor.

4.7.2 L. monocytogenes re-challenge

Mice infected with $3x10^5$ CFU of *L. monocytogenes* were left to recover for six weeks. After 42 days the same mice were re-challenged with $3x10^6$ CFU IP. The weight was monitored every day and on day 3 mice were sacrificed and spleen and one lobe of liver collected and weighted. CFU in the organs were determined as illustrated before.

4.8 In vivo Poly(I:C) injection

WT and *Calhm6*$^{-/-}$ mice were injected IP with 100 or 200 µg Poly(I:C) or 100 µl PBS per mouse. Mice were sacrificed 3 or 12 hours later and spleen collected in complete RPMI 1640 medium with Brefeldin A. Single cell suspension was obtained and cells plated $2x10^6$ cells/well in round bottom 96 well plate and incubated for 4 hours at 37°C in 5% CO_2 in the presence of Brefeldin A. Intracellular IFN-γ and Granzyme B production was measured by flow cytometry.

4.9 Cytokine measurement

4.9.1 Serum collection

For serum cytokine measurements, mouse blood was extracted by heart puncture with a 27 G needle. To avoid coagulation the mice were sacrificed two by two. Blood was left at room temperature for

half an hour to coagulate, and centrifuged at 10000 g for 10 min at 4°C in order to separate the serum from the coagulated blood cells and complement.

4.9.2 ELISA assay

Cytokines in supernatant and serum were measured with ELISA assay. For IFN-γ and IL-1β ELISA assays, high binding optically clear flat-bottom 96 well plates were coated overnight PBS at 4°C with capture antibody. Plates were washed in wash buffer (PBS, 0.05% Tween 20) before being blocked with ELISA/ELISPOT Diluent. Samples and standards were incubated in the plate for at least 2 hours at RT before being washed and incubated for 1 hour in detection antibody, then washed again. Colorimetric reaction was obtained by adding Avidin-HRP followed by Tetramethylbenzidine substrate solution. The colorimetric reaction was stopped with stop solution (2 N H_2SO_4) and absorbance measured with a FLUOstar Omega microplate reader. For IL-18 measurement we used pre-coated plates from and the biotin-conjugated antibody was added together with the samples according to manufacturer instructions.

4.9.3 LEGENDplex

We used the LEGENDplex Mouse Inflammation Panel to measure 13 different cytokines in serum. This is a bead-based immunoassay that use beads of different sizes and brightness to capture specific cytokines. The assay works with the principle of sandwich immunoassays: the cytokine concentration in serum correlates with the fluorescence intensity of the cytokine-specific beads. We performed the assay according to manufacturer instruction. In brief the serum was diluted two-fold in assay buffer solution and 25 µl of serum were incubated with 15 µl of assay beads for 2 h at RT. After washes the beads were incubated with 15 µl of detection antibodies and incubated for an hour before adding SA-PE reagent for 30 min. Beads were washed twice and immediately run on an LSR II flow cytometer where different bead populations could be disentangled and cytokine concentration calculated based on their fluorescence compared to standard samples.

4.10 H3N2 Influenza virus infection

H3N2 virus was kindly donated by the Arnon lab (Kennedy Institute of Rheumatology, Oxford, UK). For infection with influenza, mice were anesthetized with isoflurane, and 30 µL of H3N2 dilution ($1x10^4$ PFU) were inoculated intranasally. Mice were monitored for weight loss daily at the same time of the first inoculation. On day 4 mice were sacrificed and lungs collected. Single cell suspension was obtained from the lungs via mechanical disruption and the same number of cells per sample were lysed in RLT buffer. RNA from the lungs was extracted using the RNeasy kit and reverse-transcribed using SMART MMLV Reverse Transcriptase with oligo-dT. qPCR was performed using H2N3 and HPRT specific primers. HPRT was used as a housekeeping gene.

4.11 Griess Assay for NO measurement

$1x10^6$ BMDM per condition were plated 1 day before the experiment and stimulated overnight with LPS or Poly(I:C), three technical replicates per conditions were assessed. 50 µl of supernatant from the cell culture were used for the measurement and a standard curve was created starting from a 0.1 M sodium nitrite solution. Samples were mixed with Sulfanilamide solution (1% sulphanilamide in 5% phosphoric acid) and incubated for 10 min at room temperature before 50 µl of N-1-naphthylethylenediamine dihydrochloride were added on top as specified in manufacturer instructions. Absorbance was measured in a FLUOstar Omega microplate reader.

4.12 In vitro L. monocytogenes infection

For in vitro *L. monocytogenes* infection, WT and *Calhm6*$^{-/-}$ BMDM were plated into 24 well TC dishes at a density of $3x10^5$ cells/well in 2 ml antibiotic-free complete RPMI1640 medium, then left naïve or treated with 50 ng/ml IFN-γ overnight. 100 µl of PBS containing stationary phase *L. monocytogenes* were added to the cells (MOI 1), plates were spun down at 1000 g for 5 min and left in the incubator for 30 min. The medium was then replaced with complete medium plus 10 µg/ml of Gentamicin in order to kill extracellular bacteria. After 30 min the medium was replaced with complete medium plus

5 µg/ml of Gentamicin. 0, 4, and 8 h later cells were briefly lysed in a 0.1% Triton X-100 in PBS solution so as to lyse the cells without killing the intracellular bacteria. The cell lysates were plated on BHI-Agar plates in 3 serial dilutions. Colonies were counted automatically with ImageJ software *L. monocytogenes* load per well was calculated based on the number of colonies and the dilution factor.

4.13 *In vitro* co-culture experiments

4.13.1 BMDM/BMDC-NK cells co-culture

NK cells were freshly isolated from WT and *Calhm6*$^{-/-}$ spleen with a MagniSort mouse KN cell Negative Selection Kit. In brief after obtaining single cell suspension from spleen, cells were resuspended 1x10^{7} cells/100 µl in cell separation buffer (PBS, 3% FCS, 10mM EDTA). MagniSort enrichment Antibody cocktail was added to the cells and incubated for 10 min at RT followed by washing and MagniSort Negative selection beads. Magnetic selection was then performed to allow removal of unlabelled cells. NK cells thus obtained were plated in U bottom 96 well plates 300.000 cell/well. 150.000 BMDM or BMDC were added on top of the NK cells (200 µl final volume of complete RPMI 1640 medium) and the cells were treated with Poly (IC) 50ng/ml or left untreated. Supernatant was collected 24 h later and IFN-γ measured by ELISA.

4.13.2 F4/80^{+}-NK1.1^{+}CD3^{-} cell co-culture

F4/80^{+} cells were obtained from *Rag*$^{-/-}$ and *Rag*$^{-/-}$*Calhm6*$^{-/-}$ mouse spleens by using the MagniSort Mouse F4/80 Positive selection kit. The splenocytes that were not magnetically selected were stained for flow cytometry in order to isolate NK cells (NK1.1^{+}CD3^{-}). Fluorescence-activated cell sorting (FACS) was performed on a BD FACSAria III machine. 100.000 F4/80^{+} cells were co-cultured with 200.000 NK1.1^{+}CD3^{-} cells in a 96 well U bottom plate. Cells were stimulated with Poly(I:C) 50 ng/ml or left untreated. Supernatant was collected 24 hours later and used for IFN-γ ELISA.

4.13.3 Whole spleen culture

Single cell suspension was obtained from *Rag*$^{-/-}$ and *Rag*$^{-/-}$*Calhm6*$^{-/-}$ spleens. 300.000 cells/well were plated in U bottom 96 well plates. Final volume of the culture was 200 µl of complete RPMI 1640 medium. Cells were treated with Poly(I:C) 50 ng/ml or left untreated for 24 hours before the supernatant was harvested.

4.14 Overexpression of CALHM6

4.14.1 Plasmid generation

CALHM6, CALHM6-HA, CALHM6-FLAG and CALHM6-ΔNH-HA plasmids were all generated in our lab from pMIG plasmid backbones kindly donated by the Schroder lab (The University of Queensland, Australia) containing HA or FLAG tag and GFP as a reporter gene. CALHM6 sequence was amplified from WT mouse mRNA and inserted in the plasmid using BamHI and NotI restriction enzymes. CALHM6-eGFP plasmid and its empty vector control were ordered from VectorBuilder and came on a pMMLV background. All plasmids contained a bacterial resistance gene for ampicillin. DH5a *E. coli* were used for plasmid amplification. *E. coli* were transformed with plasmids and grown in LB Agar plates with Ampicillin for selection. Plasmids were then purified with a Qiagen Plasmid Maxi kit.

4.14.2 HEK293T transfection

HEK293T were plated for transfection 300.000 cell/well in a TC treated 6 well plate overnight in complete DMEM medium. Transfection was undertaken when the cells were 60% confluent. Transfection mix was prepared by combining 2 µg of plasmid in 250 µl of OptiMEM to 3 µl of Lipofectamine2000 in 250 µl of OptiMEM. The mix was incubated for 20 min and carefully added on top of HEK293T cells. The cells were harvested 24 h post-transfection. Transfection efficiency was based on %GFP^{+} cells measured by flow cytometry.

4.14.3 BMDM transduction

In order to generate the retroviral viruses necessary to transduce BMDM our plasmids were first transfected into Plat-E cells a Retroviral Packaging cell line based on the HEK293T line. Plat-E cells express the retroviral proteins gag, pol and env[379]. $2.5x10^6$ Plat-E cells were plated in a 10 cm ø TC coated plate in complete medium without Blasticidin or Puromycin and cultured overnight. Transfection mix was prepared by combining 20 µg of plasmid in 1,5 ml of OptiMEM to 30 µl of Lipofectamine2000 in 1.5 ml of OptiMEM. The mix was incubated for 20 min and carefully added on top of Plat-E cells. The next day BM cells were harvested from mice and cultured in a 15 cm non-TC coated square plate in 15 ml of complete RPMI medium with 50 ng/ml M-CSF while Plat-E media was replaced with 10 ml of complete RPMI before cells were moved to a 32°C incubator to allow the replication of the retrovirus. Two days after Plat-E transfection, Plat-E supernatant was collected and passed through a 0.45 Millex-HA syringe filter to remove cells and debris and 200 µl 1M HEPES, 3 µl polybrene (10 mg/ml), and 50 ng/ml M-CSF were added to the supernatant. The BM cells plated the day previous were collected and about 10x106 cells added to the 10 ml Plat-E supernatant containing the retrovirus. The cells suspension obtained was plated in a non-TC coated 6 well plate (2.5 ml/well) and centrifuged for 2 h at 1000 g in a 32°C centrifuge to facilitate infection. After the spin, wells were topped up with 2 ml of fresh complete RPMI medium with 50 ng/ml M-CSF. This process was repeated the following day. On day 5 of incubation 2ml of warm complete RPMI media with 50 ng/ml M-CSF were added on top. BMDM were harvested on day 7. Successfully transduced cells were GFP positive.

4.15 Confocal imaging

All cell culture images were taken on an Olympus 880 microscope with a 60x magnification and analysed in ImageJ. In order to quantify polarisation images were blinded and CALHM6 was considered polarised to the synapse when GFP immunofluorescence was present around the actin structure defining the synapses.

4.15.1 CALHM6-GFP imaging

Transduced BMDM were grown overnight on a coverslip, 300.000 cells/well without Poly-L-lysisne. Cells were treated with Poly(I:C) (50 μg/ml) and IFN-γ (10 ng/ml) for 6h before supernatant was removed and cells washed twice with warm PBS. BMDM were fixed in 4% PFA for 10 min at RT. PFA was then washed thrice. Cells were permeabilised with a solution of 0.1% Triton X-100 in PBS for 20 min at RT then washed three times in PBS. To avoid unspecific staining cells were blocked in blocking buffer (5% FCS in PBS, 0.2% NaN_3, 1:200 Fc block and 1% mouse serum) for 30 min at RT. Blocking buffer was removed and phalloidin staining added (Phalloidin 1:200 (AF555) in PBS, 5%FCS, 0.2% NaN3). Cells were then washed five times in PBS before being mounted on slides with ProLong anti-fade DAPI. Slides were dried overnight in the dark and stored at 4oC.

4.15.2 BMDM-NK synapse imaging

To visualise IS, transfected BMDM were first plated and treated as described above. To obtain NK cells spleens were collected from WT mice and splenocytes stained for flow cytometry with Live/dead staining, αCD3 and αNK1.1 antibody. NK cells were isolated by FACS on an Aria III machine ($CD3^-NK1.1^+$ gate). 300.000 NK cell/well were added on top of the BMDM and the plates were centrifuged for 2 min at 300g to synchronise the NK-BMDM cell contact. The coculture so obtained was then placed back in the incubator. After 0, 10, 20 or 40 min the supernatant was removed and replaced directly with 4% PFA for 10 min at RT. The staining was carried out as previously described.

4.15.3 Opsonisation of sRBC

To generate the IgG2a antibody necessary to opsonise sRBC we used the TIB-111 cell line from the American Type Culture Collection, a B-lymphocyte hybridoma kindly provided by the Medzhitov lab (Yale School of Medicine, Connecticut). TIB-111 cells were cultured in complete DMEM medium (DMEM, 10% FCS, 100 units/ml penicillin, 100 μg/ml streptomycin and 5.84 μg/ml glutamine) and

grown at 37°C in 5% CO_2. IgG2a rich supernatant was collected after 7+ days of cell proliferation. Opsonisation of sheep red blood cells (sRBC) was obtained by resuspending 300x10^6 cells in 2 ml IgG2a rich medium and incubating it on a shaker for 2 h at RT. sRBCs were always used fresh within 2–3 weeks of purchase. Control SRBCs were kept in 2 ml of DMEM containing 10% FBS. sRBC were then washed twice in complete RPMI medium before being added to the BMDM.

4.15.4 BMDM-beads or BMDM-sheep RBC synapse imaging

For BMDM-sheep RBC (sRBC) co-culture, sRBC were first labelled with PKH26 to be visible under the microscope: 1x10^8 sRBC opsonised or not, were placed in a 15ml tube and washed in PBS twice. 1ml of Diluent C was used to resuspend sRBC and another 1ml of Diluent C with 4 µl of the PKH26 ethanolic dye solution was add on top and mixed well. sRBC were incubated for 2 min on a shaker before the labelling reaction was stopped by adding 2 ml of FBS. sRBC were then centrifuged, resuspended in complete RPMI medium and moved to a new tube. For BMDM-beads co-culture, polystyrene beads were washed three times in complete medium before being resuspended at the right concentration to be used for the co-culture. Both sRBC and beads were added to the cells to obtain a final 10:1 ratio to the BMDM, both co-cultures were centrifuged for 2 min at 300g to synchronise the contact and the plates were placed back in the incubator. Cells were fixed in 4% PFA for 10 min 0, 10, 20 and 40 min after centrifugation, the staining was obtained like described before but, in the case of sRBC we used phalloidin conjugated with AF594 to minimise overlap with PKH26 staining.

4.16 Phagocytosis and endocytosis assay

4.16.1 sRBC phagocytosis

BMDM were plated at a density of 5×10^5 cells/well in a 12-well TC dish, in complete RPMI medium, 24 h before the experiment. On the day of the experiment, fresh sRBC were labelled with PKH26 and opsonised or left naïve. sRBCs were then added into BMDM-containing wells at an sRBC/BMDM ratio

of 20:1. Plates were incubated at 37 °C and after 5, 15 or 45 min the medium was aspirated, the cells washed gently with PBS at 4 °C, and 0.5 ml RBC lysis buffer was used for 5 min at 4°C to remove non-phagocyted sRBC. The BMDM were then washed and lifted with 0.5 ml of Tripsin-EDTA, lifting reaction was blocked on ice and BMDM washed twice in PBS before being fixed in 4% PFA for 5 min at 4°C and analysed by flow cytometry.

4.16.2 Zymosan Phagocytosis

BMDM were plated at a density of 5×10^5 cells per well of a 12-well TC dish, in complete RPMI medium, 1 d before the experiment. Just before starting the experiment pHrodo Red Zymosan Bioparticles Conjugate for Phagocytosis were resuspended in culture medium, vortexed twice for 30 s and 25 µg of Zymosan were added to the BMDM. The phagocytic reaction was stopped after 0, 5, 10, 20 or 40 minutes by removing the supernatant and adding ice cold PBS. Cells were washed three times with PBS to remove non phagocyted Zymosan and then detached from the plate with 0.5 ml of Tripsin-EDTA. BMDM were fixed in 4% PFA for 5 min at 4°C and analysed by flow cytometry.

4.16.3 Dextran endocytosis

BMDM were plated 24 h before the experiment as described previously. Shortly before the experiment pHrodo Red Dextran 10,000 MW, was resuspended in complete RPMI medium and vortexed thoroughly. 50 µg/ml of Dextran were added to the BMDM and cells incubated at 37 (°C). After 0, 10 and 20 min the supernatant was removed and cells washed in ice cold PBS for three times. Cells were then detached from the plate with 0.5 ml of Tripsin-EDTA, washed and fixed in 4% PFA for 5 min at 4°C and before being analysed by flow cytometry.

4.17 De-glycosylation

300.000 BMDM from WT and *Calhm6*$^{-/-}$ were resuspended in 50 µl of PBS and 9 µl of the cell suspension were used for the experiment. 1 µl of Glycoprotein Denaturing Buffer (10X) was added to the cells and the sample was denatured by heating it at 100°C for 10 min then chilled on ice. 2 µl of GlycoBuffer 2 (10X), 2 µl 10% NP-40 and 6 µl H2O were added to the cells for a total volume of 20 µl. 1 µl of PNGase F was then added and the samples and incubated on a gentle shaker for 20 h at 4 (°C). Laemmli buffer was added to the samples that was split in 2: half was run on an SDS page gel as such while 20mM of DTT were added to the other half.

4.18 ATP release assays

4.18.1 ATP release from BMDM

BMDM from WT and *Calhm6*$^{-/-}$ mice were plated with a density of 100.000 cells/well in a 96 well flat bottom plate in complete RPMI with M-CSF the day before the experiment. On the day of the experiment BMDM were stimulated with IFN-γ for 6h to upregulate CALHM6 expression or left untreated. To measure ATP release, the RPMI medium was replaced with 100 µl of warm low Ca^{2+} Isotonic Buffer (150 mM NaCl, 5 mM KCl, 10 mM HEPES, 10 mM glucose, 2.5 mM EDTA, pH adjusted to 7.4) 1 mM/ml of the ATPase inhibitor ARL67156 was added to the isotonic buffer. BMDM were then cultured for 20 min at 37°C in the isotonic buffer and final ATP concentration was measured by adding 10 µl of supernatant to 90 µl of ENLITEN buffer, luciferase activity was measured on a FLUOstar plate reader.

4.18.2 ATP release from transfected HEK 293T cells or transduced BMDM

For this experiment we used HEK296T cells transfected with CALHM6-HA or CALHM1-HA containing vectors or empty vector as described before or BMDM transduced with HA or CALHM6-HA containing vector, (only GFP^+ cells sorted by FACS). HEK293T cells 24 h after transfection or freshly sorted BMDM

were re-plated at a density of 100.000 cell/well in a 96 well flat bottom plate and left to adhere. To measure ATP release, the supernatant was removed and substituted with low $Ca2^{+}$ Isotonic Buffer and ATP concentration measured like described above.

4.18.3 ATP released from transfected Plat-E cells

Plat-E cells were transfected with HA alone, CALHM6-HA, CALHM6-ΔNH-HA or CALHM1-HA plasmids as previously described. Two days after transfection cells were plated 100.000 cells/well in a 96 well flat bottom plate and left to attach for a few hours. The supernatant was removed and replaced with 100 µl of low Ca^{2+} Isotonic buffer, Excess K^{+} buffer (117,5 mM KCl, 37,5mM NaCl, 10mM HEPES, 10mM Glucose) or Isotonic buffer with calcium (140 mM NaCl, 5 mM CaCl, 10 mM HEPES, 10 mM Glucose) and Ionomycin (25 µM). All buffers contained the ATPase inhibitor ARL67156. ATP release was measured like described above.

4.19 Inflammasome activation

WT and *Calhm6*$^{-/-}$ BMDM were plated at a density of 100.000 cell/well in a flat bottom 96 well plate the day before the experiment. On the day of the experiment cells were treated with Poly(I:C) 50 µg/ml or LPS 100 ng/ml and after 1h or 4h nigericin 5 µg/ml or ATP 5-2.5 µg/ml were added into the well. After 1 h cell-free supernatant was collected and used to assess the level of cell death by performing an LDH Assay: 20 µl of supernatant were mixed with 20 µl of LDH reaction mix, the reaction was incubated at room temperature for 5 min and stopped with the addition of Stop Solution. 100% cell death for normalisation was obtained by lysing 2 experimental wells with 0.1% Triton X-100. To measure cell death the plate was read on the plate reader at 450 nm wavelength.

4.20 Table1: Primers for qPCR

GENE	FORWARD	REVERSE
Calhm1	TGAGATCTATGATGGGAACTG	CAATGTCAATGTAGTGGGAC
Calhm2	AGTATGAGTCTCAGCTCTTC	AGTAATGTTTGAGGCACTTG
Calhm3	TGATGGTGGAGGAGTGGC	GCACACACAAAACACTTGCC
Calhm4	CACAGATACCAGTCACAAATG	CGATGTCTAATAAGAAGTTGGG
Calhm5	GATAACACAGTGGGAAACTG	CTTACAAATCGTGGCAGACC
Calhm6	CTCTTTCTACCAATGTGCTG	CTATCAGAATCCAACCGAAC
Hprt	GTTGGATACAGGCCAGACTTTGTTG	CCAGTTTCACTAATGACACAAACG
Ifna14	TCTCTCTCAGGTAAACAGTG	TAGACTCCTTCTGCAATGAC
Ifna4	CAAAATCCTTCCTGTCCTTC	ATGATAGAGCTACTACTGGTC
Ifnb1	AACTCTGTTTTCCTTTGACC	AACTTCCAAAACTGAAGACC
Il10	CAGGACTTTAAGGGTTACTTG	ATTTTCACAGGGGAGAAATC
Il1r2	GAAGAGACTTCTTTGACTGTG	AAAACTATGTGGAAGTGTCG

4.21 Table 2: Primers for genotyping

GENE	FORWARD	REVERSE
Calhm6 1	GTGTAGCAAAGCCTCAGGACAGGT	
Calhm6 2	CCAACTGACCTTGGGCAAGAACAT	
Calhm6 3	CACACCTCCCCCTGAACCTGAAA	
Calhm6 7	CTTTCTGCCCAATCCTCCTG	
Calhm6 8	GTTTCCCTAACTGGGCTGTC	
Cd11c-Control	CAAATGTTGCTTGTCTGGTG	GTC AGTCGAGTGCACAGTTT
Cd11c-Cre	ACT TGG CAG CTG TCT CCA AG	GCG AAC ATC TTC AGG TTC TG
Flp	ATAGCAGCTTTGCTCCTTCG	TGGCTCATCACCTTCCTCTT
Flp-Control	CTAGGCCACAGAATTGAAAGATCT	GTAGGTGGAAATCTAGCATCATCC
Lacz Cassette	GGTAAACTGGCTCGGATTAGGG	TTGACTGTAGCGGCTGATGTTG
Pgk-Cre	CGT TTT CTG AGC ATA CCT GGA	ATT CTC CCA CCG TCA GTA CG
Rag	TGGATGTGGAATGTGTGCGAG	CATTCCATCGCAAGACTCCT
Rag-Control	TCTGGACTTGCCTCCTCTGT	CATTCCATCGCAAGACTCCT

4.22Table 3: list of reagents

REAGENT	BRAND	CAT. NUMBER
1kb+ DNA ladder	Fisher	10787018
1m Hepes	Fisher	15630056
1x Pbs	Fisher	10010023
2-mercaptoethanol	Thermo Scientific	31350010
4-20% miniprotean tgx precast gels 12 well	Bio-Rad	4568095
4-20% miniprotean tgx precast gels 15 well	Bio-Rad	4568096
4x Laemmli Sample Buffer, 1610747	Bio-Rad	1610747
Actin red 555	Fisher	R37112

Advantage Ultrapure PCR Deoxynucleotide Mix (10 Mm Each Dntp), 4x100 Ul	Takara Bio Europe SAS	639125
Alexa fluor® 647 goat anti-mouse igg	BioLegend	405322
Alt kit (for liver damage measurement in mouse serum	Sigma Aldrich	MAK052-1KT
Ampicilin	Sigma	A9518-25G
Anti-f4/80 microbeads ultrapure, mouse	Miltenyi Biotec	130-110-443
Apc Anti-Mouse Cd215 (Il-15rα) Antibody	BioLegend	153505
Apc anti-mouse nk-1.1 antibody	BioLegend	108710
Arl 67156 trisodium salt atpase	Bio-Techne (R&D Systems)	1283/10
BAFILOMYCIN A1, 10 µg	Fisher Scientific	NC0515789
Bamhi hf	NEB	R3136S
Bd cytofic/cytoperm	BD	554722
Bhi agar	Sigma-Aldrich	70138-500G
Blasticidine s hydrochloride	Sigma	15205-100MG
Brain heart infusion agar (bhi),biochemika	Sigma-Aldrich Co Ltd	70138-500g
Brefeldin 1000x Protein Secretion Inhibitor	BioLegend	420601
Calcium chloride	Merk	K44296278 333
Camkii (pan) antibody	Cell Signaling Technology	3362S
Cd11b-bv711	BioLegend	101242
Cd11c-pe	BioLegend	117307
Cd19-apccy7	BioLegend	115530
Cd3-pe cy7	BioLegend	100220
Cd4-pe dazzle	BioLegend	100566
Cd8-bv605	BioLegend	100743
Cell Activation Cocktail (Without Brefeldin A) 500x	BioLegend	423302
Ceramic beads ck14	Precellys	P000912-LYSKO
Clarity ecl	Bio-Rad	1705061
Clarity ecl max	Bio-Rad	170-5062
Complete edta-free protease inhibitor tablets	Sigma	11873580001
Cytotox 96® non-radioactive cytotoxicity assay (ldh assay)	Promega	G1780
Diluent c for general membrane labeling	Thomas Scientific	C914J95
Dmem	Sigma-Aldrich	R8758
Dmso (cell culture)	Sigma	D2650-100ML
Dnase i, grade ii	Sigma-Aldrich Co Ltd	10104159001
Dntp set	NEB	N0446S
Dtt	Sigma	GE17-1318-02
Dynabeads™ protein g for immunoprecipitation	Thermo Scientific	10004D
Ebioscience 1x Rbc Lysis Buffer-200 Ml	Life Technologies	00-4333-57
Enliten rluciferase/luciferin reagent	Promega	FF2021
F4/80-fitc	BioLegend	123108
Fam26f antibody clone g-12	Santa Cruz	sc-515780
First strand buffer	TaKara	S4992

Flag ab mouse m2	Sigma	F3165-.2MG
GAPDH	CST	2118S
Gentamicin solution bioreagent	Sigma-Aldrich Co Ltd	G1397-10ML
Glycerol	Fisher	BP229
Glycine	Sigma	G8898-1KG
Goat anti rabbit igg hrp	Jackson Immuno/Stratech scientific	111-035-144-JIR
Goat anti-mouse igg1-hrp; 1.0 ml	SouthernBiotech	1071-05
Granzyme b-fitc	BioLegend	515403
Griess reagent kit	Insight Biotechnology Ltd	30100
H_2so_4	Sigma	320501-1L-D
Ha ab mouse	Merck Millipore	05-904
Hcl	Sigma	H1758-100ML
Hek 293t Cells	Sigma Aldrich	12022001-1VL
Ifng-pe	BioLegend	505808
Ionomycin, calcium salt	Thermo Fisher	I24222
Isopropanol	Sigma-Aldrich	I9516-500ML
Latex beads, polystyrene	Sigma	LB30-1ML
Lb broth with agar (lennox), powder mic&	Sigma	L2897-1KG
Liberase th	Sigma-Aldrich Co Ltd	5401135001
Lipofectamine 2000	Fisher (Invitrogen)	11668019
Live/dead® fixable near-ir dead cell stain kit, for 633 or 635 nm excitation	Thermo Fisher	L10119
L-lysine monohydrochloride,reagent grade, ≥98%	L5626-100G	General Supply
Ly6c-pe dazzle	BioLegend	128044
Ly6g-bv605	BioLegend	127639
M il1b elisa	eBioscience	88-7013-77
Magnisort™ mouse cd11c positive selection kit	eBioscience	8802-6861-74
Magnisort™ mouse cd49b positive selection kit	eBioscience	8802-6862-74
Magnisort™ mouse f4/80 positive selection kit	eBioscience	8802-6863-74
Magnisort™ mouse nk cell negative selection kit	eBioscience	8804-6828-74
Mouse ifng elisa	eBioscience	88-7314-77
Mouse il-18 elisa	eBioscience	BMS618-3TEN
Ms columns	Miltenyi Biotec	130-042-201
Mtnf elisa	eBioscience	88-7324-77
Multiscreen-ha filter plate. 0.45 um. Clear. Sterile	Millipore	MAIPS4510
Nacl	Sigma	S7653-5KG
Naoh	Sigma	72068-100ML
Nativepage novex 4-16% bis-tris protein gels, 1.0	BioRad	BN1002BOX
Nativepage running buffer kit-1 kit	Fsher	BN2007
Nativepage sample prep kit-1 kit	Fisher	BN2008
Neb 5-alpha competent e. Coli (high efficiency)	NEB	C2987H
Normal mouse serum	Fisher	10410
Noti hf	NEB	R3189S
Oligo(dt)12-18 primer	Fisher	18418012

Optimem	Fisher	31985070
Pe Anti-Mouse P2x7r [1f11] 25 Ug	Biolegend	148703
Pen/strep glutamine	Fisher	10378016
Perm wash	BD	554723
Phospho camkii (thr286) (d21e4) rabbit mab	Fisher Scientific	NC0855761
Phrodo™ red e. Coli bioparticles™ conjugate for phagocytosis	Thermo Scientific	P35361
Phrodo™ red e. Coli bioparticles™ conjugate for phagocytosis	Thermo Scientific	P35361
Phusion polimerase	NEB	M0530S
Pierce 16% formaldehyde (w/v), methanol-free-10 x	Fisher (Pierce)	28908
Pkh26 red fluorescent cell linker mini kit for general cell membrane labeling	Sigma	MINI26-1KT
Plate cells	Cambridge Bioscience Ltd	RV-101
Pngase f (glycerol-free) recombinant	NEB	P0709S
Polybrene	Merck Millipore	TR-1003-G
Polyinosinic-polycytidylic acid sodium salt,tlr ligand tested	Sigma-Aldrich	P1530-25MG
Ponceaus stain proteomics grade	VWR	K793-500ML
Powerup sybr green master mix-5 x 5 ml	Fisher	A25777
Precision plus protein™ dual color standards	Bio Rad	1610394
Prolong® diamond antifade mountant with dapi	Fisher	P36971
Proteinase K	Fisher	BP1700-100
Purified rat anti-mouse cd16/cd32	BD	553142
Puromycin dihydrochloride	Sigma	P8833-25MG
Qiagen plasmid plus maxi kit (25)	Qiagen	12963
Qiaquick gel extraction kit	Qiagen	28704
Recombinant human tnf (carrier-free)	PeproTech	300-01A
Recombinant mouse ifn-γ (carrier-free)	BioLegend	575304
Recombinant mouse il-10 (carrier-free)	BioLegend	575804
Recombinant mouse il-12 (p70) (carrier-free)	BioLegend	577004
Recombinant mouse il-4 (carrier-free)	BioLegend	574304
Recombinant mouse tgf-β1 (carrier-free)	BioLegend	763104
Recombinant murine gm-csf	PeproTech	250-05
Rneasy mini kit (250)	Qiagen	74106
Rpmi-1640 without l-glut,no hepes	Fisher	21870076
Sds Solution,20% W/V,1000ml	Bio-Rad	1610418
Sheep blood in alsevers solution liquid oxoid	Fisher Scientific UK Ltd	12977755
Smart mmlv reverse transcriptase 20000	Takara Bio Europe SAS	639524
Sodium (meta)periodate,bioultra, ≥99.5% (rt)	Sigma-Aldrich	71859-25G
Sodium azide	Sigma	71290-10G
Sodium phosphate monobasic,bioreagent, for molecular biology, anhydrous, ≥98%	Sigma-Aldrich	S3139-250G
Sodium pyruvate	Fisher	11360070

Sybr safe	BIOTIUM	41003
Sybr safe 10 000	Fisher	S33102
T4 dna ligaze	NEB	M0202L
Transblot midi nitroceluloze transfer kit for 40 blots	Bio-Rad	1704271
Tris (trizma base)	Sigma	T6066-1KG
Triton X100	Sigma	T9284-500ML
Trypsin/edta	Corning	25-051-CI
Tween20	Sigma	P1379-500ML
Ultracomp ebeads™ compensation beads	eBioscience	01-2222-42
Ultrapure agarose	Invitrogen	16500-500
Up lps	Invivogen	tlrl-peklps
V-bottom plate for legendplex™ assay	BioLegend	740379
X-Ray Film 18x24 Pk of 100	Scientific Laboratory SL	MOL7016
Zymosan a from saccharomyces cerevisiae	Sigma-Aldrich	Z4250-250MG

5 CALHM6 regulation in the innate immune system

5.1 Introduction:

5.1.1 *Calhm6* regulation in the immune system

Previous studies have shown that *Calhm6* is mostly expressed in CD45^{+} cells[32,33] and the only organs in which *Calhm6* expression is detectable are spleen, thymus and lymph nodes. Even there, the expression was only detectable after Poly(I:C) stimulation[33]. Therefore, to obtain a comprehensive understanding of CALHM6 role in the immune defence, we set up to study its expression and regulation in mouse immune cells. Several *in vivo* studies during the years have shown how *Calhm6* upregulation is linked to inflamed states in different organisms like humans[39,40,312,380,381], non-human primates[41,382] and pigs[383]. Several different pathologies can cause upregulation of *Calhm6*: viral and bacterial infections like simian immunodeficiency virus, West Nile virus,[382–384], tuberculosis or septicemic mieloidosys[312,380], T-cell mediated kidney rejection[385] and even in autoimmune diseases like villitis of unknow origin and Sjögren's syndrome[39,40]. GWAS studies have also linked SNPs that increase *Calhm6* expression with susceptibility to ulcerative colitis [89].

Macrophages have a large number of receptor for PAMP and DAMP that, when stimulated, can activate specific modules that could be deemed pro- or anti-inflammatory[386,387]. Macrophages can also respond to pro- or anti-inflammatory cytokines and chemokines produced by the tissue environment or by the macrophages themselves[388,389], thus achieving a finer control over the type and duration of the downstream immune response. Traditionally, *in vitro* stimulated macrophages can be activated to polarise towards different functional states of activation. Pro-inflammatory stimuli. LPS and IFN-γ give rise to pro-inflammatory (classically activated) macrophage state, while anti-inflammatory stimuli, like IL-4 or IL-10, generate a range of other/alternative macrophage states[390]. While this distinction has long been deemed artificial and inadequate to describe the wide range of macrophage activated states[386], it remain interesting for us to assess in which one of these modules *Calhm6* is expressed and possibly plays a role. In this chapter we will describe how a variety of pro- and anti-inflammatory stimuli can regulate the expression of *Calhm6* in our chosen murine model.

5.1.2 Generation of a CALHM6 transgenic mice

Due to the difficulty in understanding the role and mechanism of function of a protein in a complete organism, fundamental to biological discoveries during the years has been the study of organism lacking specific proteins. Mice have been the organism of choice for most modern immunological studies due to their closeness to homo sapiens, their relatively small size that allow for easy maintenance, the number and frequency of their offspring and the availability of reagents that allow studies of immune system in this experimental model. Since 1980 when the first transgenic mouse was created thanks to the use of viral construct microinjected in oocytes via bacterial plasmids and then implanted in pseudopregnant females[391,392], the technology behind transgenic mice has remarkably improved. One of the main milestones of this animal model was the application of the Cre-lox recombination system from bacteriophage P1, discovered by Sternberg, to gene deletion[393,394]. This is a powerful and versatile tool that allows scientists to delete or express specific DNA sequences containing the lox cassette only in the presence of a Cre recombinase protein. What makes the system so versatile is the possibility of expressing a Cre recombinase gene under specific promoters in different mouse cells or organs. These strains can then be crossed with the lox cassette-containing mice. This process generates knockout genes that can be relegated to specific tissues, cell types or stages of development. In this chapter we will show how we used the Cre-lox system to generate a CALHM6 deficient mouse line.

5.2 Chapter aims:

- To Identify what are the best cells to study CALHM6 *in vitro* and *in vivo*
- To investigate how pro- and anti-inflammatory stimuli regulate *Calhm6* expression

- To create a murine model to study CALHM6 function *in vivo*.

5.3 Results

5.3.1 CALHM6 is mostly expressed in innate immune cells, especially monocytes and macrophages

To characterise expression of *Calhm6* mRNA in human and mouse immune system I started by looking at available online datasets. The immunological Gene Project (Immgen)[395] allowed me to access RNAseq and single cells RNA (scRNA) sequencing data for mouse resident and circulating immune cells and human circulating blood cells. In Figure 6.a we can see a gene skyline representation of *Calhm6* expression in mouse immune cells at steady state from the ImmGe ULI RNAseq database. Basal levels of *Calhm6* mRNA are present in most immune cells, including $CD4^+$ and $CD8^+$ T cells, $CD8^+$ DCs and marginal zone B cells. By far though, the highest expression of *Calhm6* at steady state is in splenic red pulp macrophages (RPM) and blood $Ly6c^+$ monocytes. Similarly, when I looked at RNA seq results from naïve human blood in the ULI RNAseq database (Figure 6.b) we can see that several B cell populations express *Calhm6* but the highest expression is in $CD16^+$ non-classical monocytes[1] and, to a lesser extent, in classical monocytes and DCs. The same pattern of expression is confirmed in human PBMCs by scRNA seq (Figure 6.c), in this case highest expression is in $CD16^+$ monocytes followed by DCs, $CD14^+$ monocytes and B cells. My analysis confirms previous published data from mouse spleen, that *Calhm6* is expressed in most immune cells, but is highest in innate cells such as macrophages, monocytes and DC[33].

I aimed to understand *Calhm6* expression and function using mouse models in the context of infection, so I next proceeded to examine *Calhm6* expression in our WT mouse following immune stimulation. *Calhm6* is upregulated by several inflammatory stimuli such as IFN, or PAMP that are able to induce Type I IFN. Poly(I:C) in particular has been linked to strong *Calhm6* induction[32,33]. To characterise *Calhm6* expression in primary myeloid cells, I injected WT mice intraperitoneally with Poly(I:C). After

6 hours F4/80^{+} (macrophages) and CD11c^{+} (DC) were magnetically isolated from spleens and *Calhm6* expression in these population measured by qPCR (Figure 6.d). Interestingly *Calhm6* upregulation is much higher in splenic macrophages than in DC. Kasamatsu et al.[33] showed that CALHM6 on either macrophages or DC has a potential to boost the activation of NK cells, but most of the initial study on CALHM6 focused on its role in DC. Similarly, Ebihara et al.[32] used model of BMDC overexpressing CALHM6 to show its role in Poly(I:C) dependent anti-tumour activity of NK cells. To define which *in vitro* generated innate immune cell type, BMDC or BMDM, express the highest CALHM6 level and would be the most relevant cell type for our follow up studies, I checked the expression levels of CALHM6 in these two populations (Figure 6.d). Surprisingly BMDC barely express measurable levels of CALHM6, even after 24h stimulation with IFN-γ and Poly(I:C). BMDM on the other hand, show marked upregulation of CALHM6 already after 6h of stimulation. This is the reason why I decided to focus our *in vitro* study of CALHM6 expression and function in BMDM.

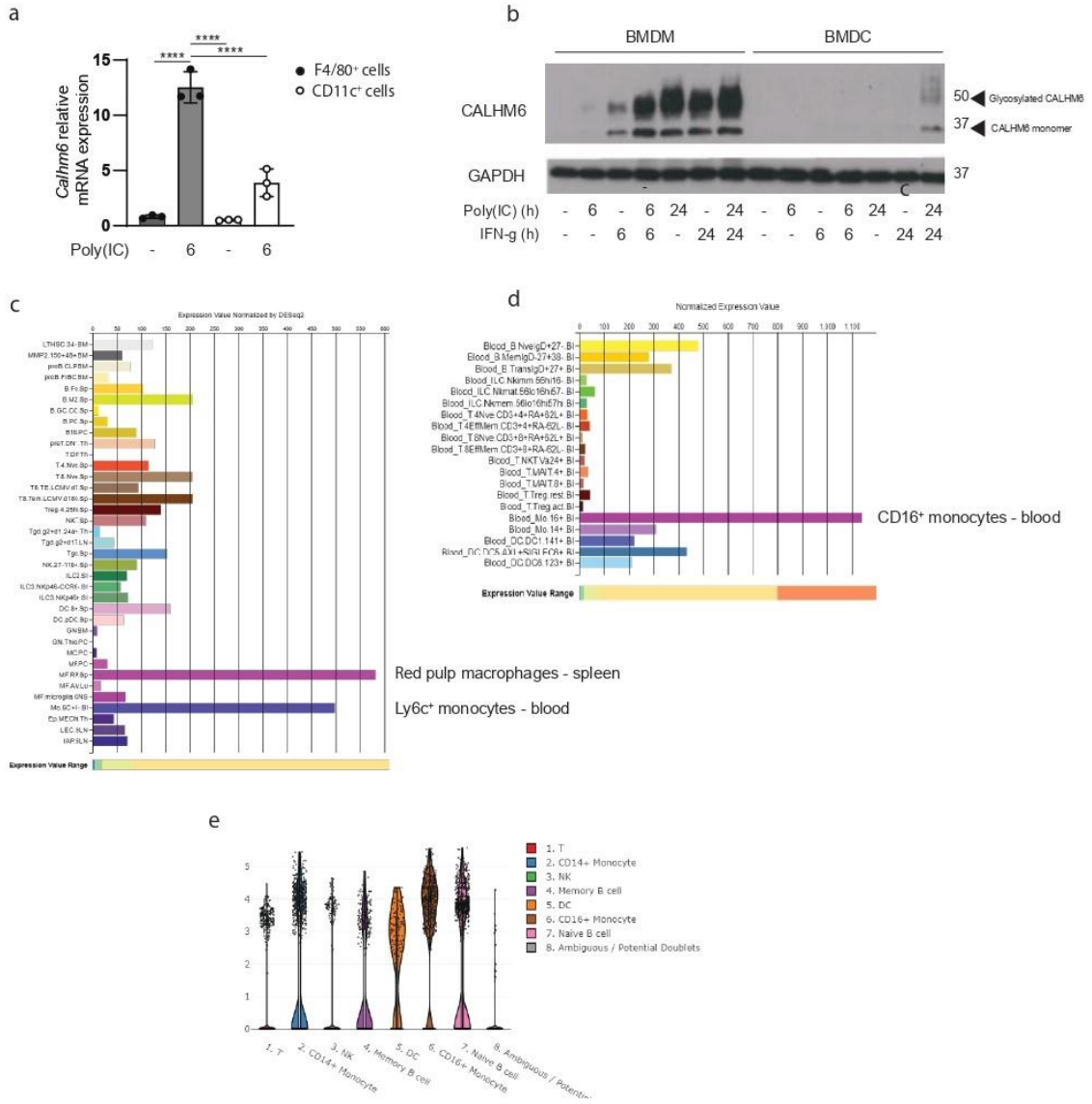


FIGURE 6. *Calhm6* expression in immune cells. a) *Calhm6* mRNA expression measured by qPCR in F4/80^{+} and CD11c^{+} cells magnetically isolated from the spleen of mice injected with Poly(I:C) (0.5 mg/mouse) or PBS for 6h. *Calhm6* mRNA expression was measured by qPCR (n=3 vs 3, one-way ANOVA with multiple comparisons). b) Immunoblot analysis of CALHM6 expression in BMDM and BMDC were stimulated for 6 or 24h with Poly(I:C) (50 µg/ml) and or LPS (100 ng/ml). (Representative of 2 independent experiments, n=2). CALHM6 is detected by a specific antibody as a precursor form of 37 kDa and a higher, glycosylated form of about 50 kDa. c) *Calhm6* expression in mouse immune cell from reference population (ImmGen ULI RNASeq database). d) *Calhm6* expression in human blood cells (ImmGen ULI RNASeq database). e) *Calhm6* expression in single cell sequencing analysis of human blood mononuclear cells (ImmGen). Poly(I:C)Poly(I:C)

5.3.2 CALHM6 is upregulated by pro- and downregulated by anti-inflammatory stimuli

Calhm6 upregulation in full organs and several immune cell types[33] is dependent on stimulation with PAMPS, in particular Poly(I:C) (that signals trough TLR3) and Zymosan (that signals through Dectin1 and TLR2/TLR6)[2]. To confirm these data in our *in vitro* system, and to define other signals that up- or down-regulate the expression of CALHM6 or any other member of the family, I measured CALHM mRNA and/or protein expression in BMDM from WT mice. For this purpose, BMDM were stimulated for 6 and 24h with LPS, Poly(I:C), Zymosan or left untreated. mRNA levels of all the members of the CALHM family were measured by qPCR (Figure 7.a).I could confirm published data[33]: *Calhm6* is the only gene of the CALHM family upregulated by pro-inflammatory stimuli at 6 and 24h post-stimulation in BMDMs. Unlike previously published data[33], though, here I show that LPS also upregulates CALHM6. LPS control over CALHM6 expression seems to be the first one to dwindle while Poly(I:C) maintains constant levels of *Calhm6* mRNA for at least 24h. I also measured protein levels of CALHM6 in BMDM (Figure 7.b) by WB, after a time course of LPS or IFN-γ stimulation. I picked IFN-γ because an earlier Microarray study[396] showed *Calhm6* upregulation after *in vitro* IFN-γ stimulation of BMDMs. The results show how CALHM6 protein is already detectable at 2 h, post-IFN-γ , and 4 h, post-LPS. IFN-γ -induced CALHM6 expression was sustained over 24 h, but LPS control over CALHM6 was lost by this time. As LPS is known to induce a strong IL-10 negative feedback loop to limit excessive inflammation, I next tested how CALHM6 would respond to stimuli generally defined as anti-inflammatory. BMDM were, this time, stimulated with TGF-β, IL-4 and IL-10 alone or together with LPS for 8 h. Gene expression of all *Calhm*s was measured by qPCR (Figure 7.c). None of the anti-inflammatory stimuli upregulated mRNA of *Calhm6* or any other *Calhm* family member, but they all significantly downregulated *Calhm6* levels induced by LPS. The same pattern was true for the CALHM6 protein: when BMDM were stimulated with LPS or IFN-γ, in combination with TGF-b (Figure 7.d), TGF-β significantly reduced CALHM6 upregulation. When TGF-β was administered together with LPS and IFN-γ the reduction was more effective than when it was added to the culture 4h after the first pro-

inflammatory signal. Taken together these results indicate that CALHM6 behaves like an early pro-inflammatory protein, being upregulated in the first phases of the response to a PAMP or a pro-inflammatory IFNs, but also being subject to the control by anti-inflammatory stimuli.

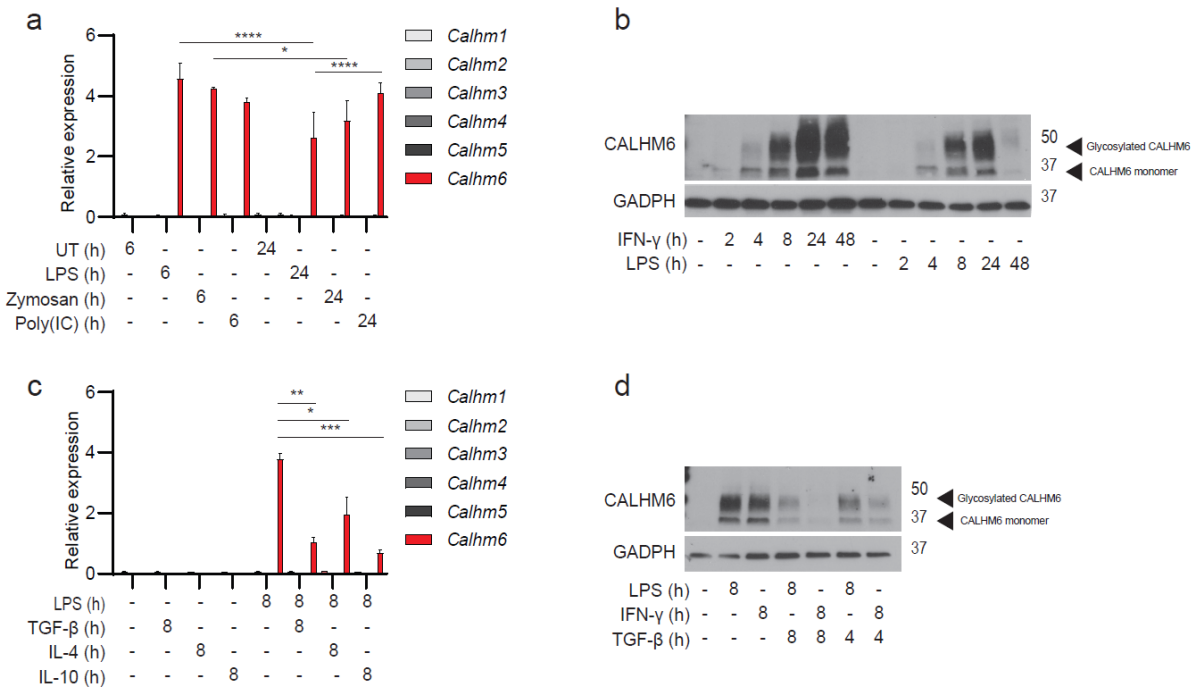


FIGURE 7. *Calhm6* expression is induced by pro- and suppressed by anti-inflammatory cytokines. a) BMDMs were stimulated for 6 or 24 h with LPS (100 ng/ml) Zymosan (100 µg/ml) or Poly(I:C) (50 µg/ml). *Calhms* mRNA expression was measured by qPCR. (Representative of 2 independent experiments, n=6. One-way ANOVA with multiple comparisons). b) Immunoblot analysis of CALHM6 expression in BMDMs stimulated with LPS or IFN-γ (10ng/ml) for 2 to 48 h. (Representative of 3 independent experiments, n=3). c) BMDMs were stimulated for 8 h with LPS, alone or together with recombinant TGF-β (10 ng/ml), IL-10 (10 ng/ml) or IL-4 (10 ng/ml). *Calhms* mRNA expression was measured by qPCR. (Representative of 3 independent experiments. n=9. One-way ANOVA with multiple comparisons). d) Immunoblot analysis of CALHM6 expression in BMDMs stimulated with LPS or IFN-γ with or without TGF-β for 8h. (representative of 3 independent experiments. n=3).

5.3.3 *Calhm6* expression is boosted by IFN-γ pre-treatment

Macrophage responses to external stimuli are dependent on the signal integration of signal-transduction pathway expressed by the cells. We know from work previously published by member of our lab, that *Calhm6* expression is boosted in mouse macrophages by the concomitant activation of the IFN-γ receptor (IFN-γR), that signal through the Jak-STAT pathway and the receptor for the Fc fragment of immunoglobulin (FcgR) that acts via the ITAM adaptor[3]. Because *Calhm6* gene promoter contains STAT1 and interferon-stimulated response element (ISRE) binding sites[92], I wanted to investigate if synergistic upregulation of CALHM6 expression was a prerogative of the IFN-γR/FcgR pathway interaction or if IFN-γ could also increase CALHM6 expression when detected together with other PAMP. For these experiments I stimulated BMDMs with Poly(I:C), that upregulates *Calhm6* signals through TICAM/TRIF, and Zymosan that upregulates *Calhm6* through Dectin1[4,5] and possibly through TLR2/6, in the presence or absence of IFN-γ . To mimic natural cytokine-mediated priming of BMDMs, IFN- γ was administered for 6 hours before Poly(I:C) (Figure 8.a) or Zymosan (Figure 8.b). The cells were then collected at different time points and *Calhm6* expression measured by qPCR. In both cases IFN-γ pre-treatment significantly increased the level of *Calhm6* mRNA expression, up to 8 hours in the case of Poly(I:C) and for at least 24 hours in the case of Zymosan. These results show how CALHM6 expression is finely regulated in the immune system; macrophages primed with pro-inflammatory cytokines are more prone to express high levels of *Calhm*. This once again points to CALHM6 being an important molecule in the early response to infection that needs to be upregulated quickly especially when the macrophages are exposed to several pro-inflammatory stimuli at the same time, skewing them towards a rapid and strong pro-inflammatory response.

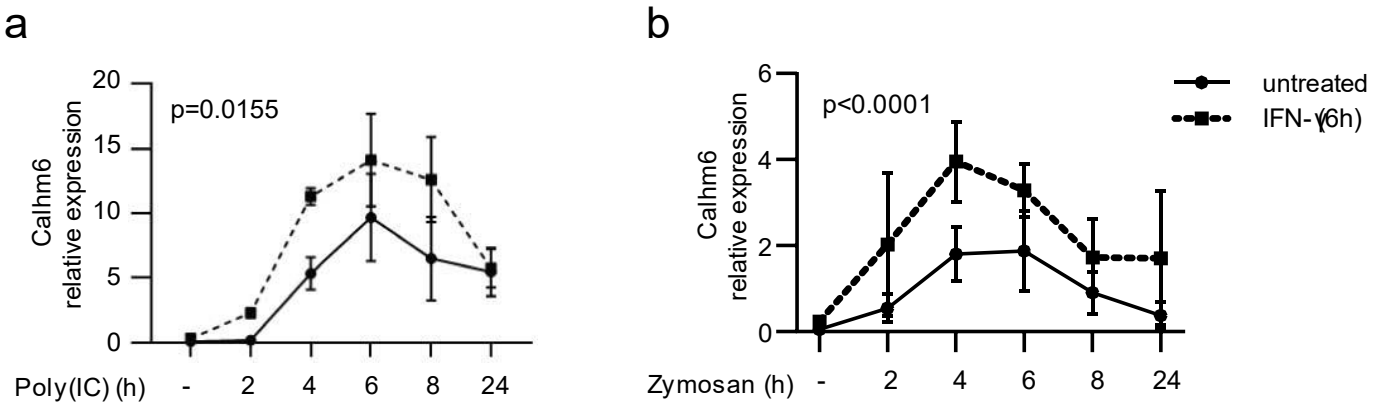


FIGURE 8. *Calhm6* expression is boosted by IFN-γ pre-treatment. a). Naïve or IFN-γ (10 ng/ml) primed (6 h) BMDMs were stimulated with a) Poly(I:C) (Results of one experiment, n=3. Two-way ANOVA analysis) or b) Zymosan for 2 to 24h. *Calhm6* mRNA expression was measured with qPCR. (Pooled results from 2 independent experiments n=2, two-way ANOVA analysis, data generated by Dr E. Pantazi).

5.3.4 Generation and characterisation of a *Calhm6*$^{-/-}$ mouse

To elucidate the biology of CALHM6 and in particular its role in infection *in vivo*, our lab generated conditional CALHM6-deficient mice carrying LacZ reporter allele, using ES cells from the EUCOMM repository[6] (Figure 9.a). To generate a complete *Calhm6*$^{-/-}$ we crossed C57BL/6N *Calhm6*$^{fl/fl}$ with the C57BL/6J PGKCre line, to delete the floxed CALHM6 embryonically[7], in all tissues. PGKcre was then bred out of the colony to eliminate any interferences of a Cre protein with possible phenotypes. The resulting *Calhm6*$^{-/-}$ and WT lines are then generated from the same heterozygous parents, to ensure a common genetic background. Lines were subsequently maintained in the same facility, but in separate cages. The lines were refreshed periodically by breeding it with C57BL/6J mice from The Jackson Laboratory. Following Cre deletion exon 2 of the CALHM6 protein is removed, thus removing the C-terminal cytoplasmic region and transmembrane domains of the protein (amino acid 198 to 364). This mouse is similar to the one used by Kasamatsu et al. in their 2014 work but it was generated independently. CALHM6 deletion in our transgenic mice, was confirmed by PCR on ear biopsies DNA and stimulated BMDM, and with WB of IFN-γ stimulated BMDM (Figure 9.b). *Calhm6*$^{-/-}$ and WT mice were born at the expected mendelian ration and did not show any macroscopic phenotype in specific pathogen-free conditions. To confirm that there were no differences in the development of the immune system between WT and *Calhm6*$^{-/-}$ mice we analysed the immune cell composition of spleen and thymus in 8 weeks old sex matched mice (work performed by Dr Eirini Pantazi). In Figure 9.c we can see that there is no difference in adaptive cell numbers as well as innate cell (Figure 9.d) in spleen. The same is true for the thymus (Figure 9.e): we can find the same amount of $CD4^+$, $CD8^+$ or double positive cells in WT and *Calhm6*$^{-/-}$ (see figure 10 for spleen adaptive cell, figure 11 for spleen innate and Figure 12 for thymus cell flow cytometry gating strategy). Taken together these results show that CALHM6 is not important for the heathy development of C57BL/6 mice or for the maturation of their immune system. Considering that CALHM6 seems to be mostly expressed early after immune stimulation

this does not come as a surprise. The mice used in the study are specific pathogen free and grown in sterile conditions in individually ventilated cages thus unlikely to have encountered situation in which immune system activation would have been required for survival.

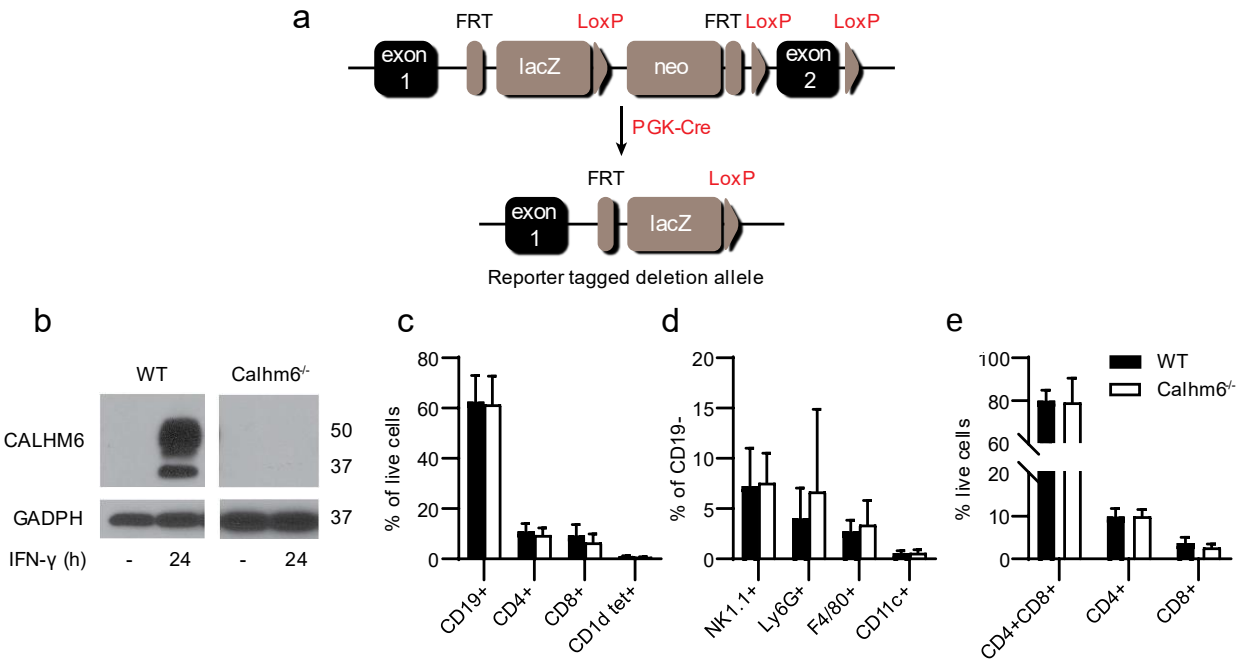


FIGURE 9: Generation and characterisation of *Calhm6*$^{-/-}$ mice. a) Scheme of the gene cassette used to generate *Calhm6*$^{-/-}$ mice. In PGK-Cre strain, Cre is driven by the early acting PGK-1 promoter, the recombinase is under dominant maternal control. b) BMDM from WT and *Calhm6*$^{-/-}$ mice stimulated with IFN-γ (10 ng/ml) for 24h. The cell lysate as used for Immunoblot of CALHM6. Cells from c) and d) spleen or e) thymus of 8 to 12-week-old WT and *Calhm6*$^{-/-}$ mice were run on a flow cytometer. Single cell suspensions were stained with a lymphoid (c and e) or innate d) panel. Represented are the % of total live cells (c and e) or of CD19^{-} cells d) of the population analysed (pooled results from 3 independent experiments n=19 vs 16. Multiple T test FDR 1%) (Data generated by Dr Eirini Pantazi).

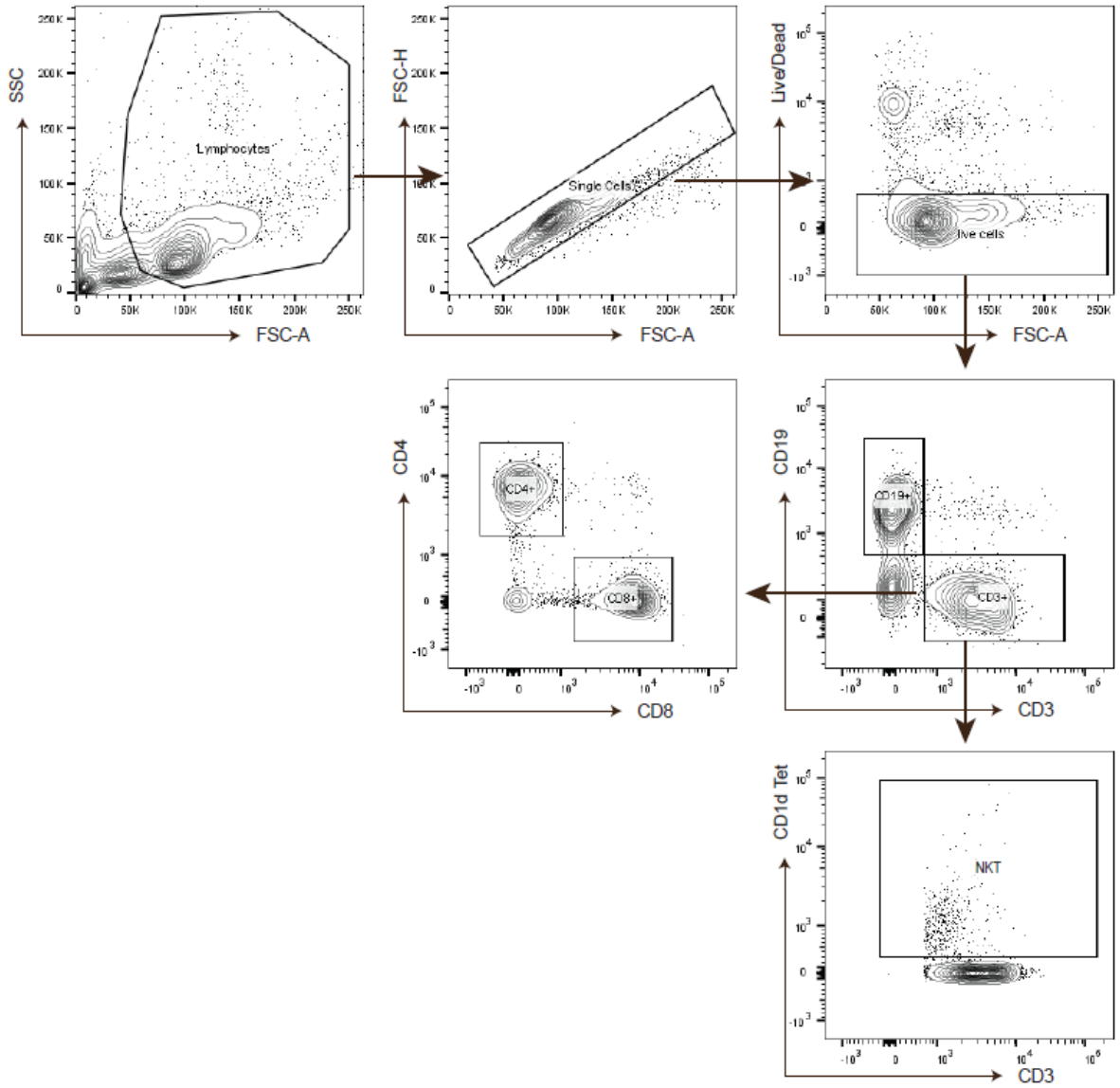


FIGURE 10: Flow cytometry gating strategy for spleen adaptive cells (data generated by Dr Eirini Pantazi)

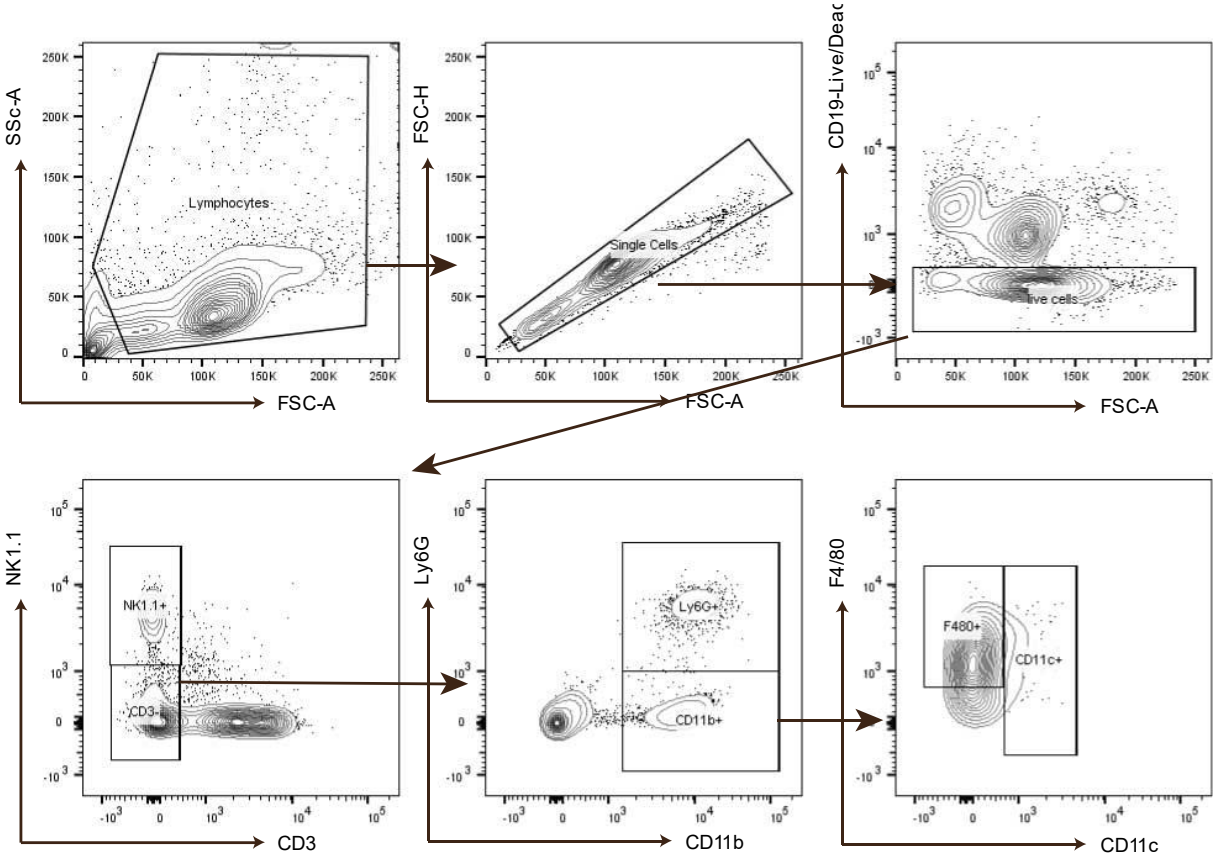


FIGURE 11: Flow cytometry gating strategy for spleen innate cells (data generated by Dr Eirini Pantazi)

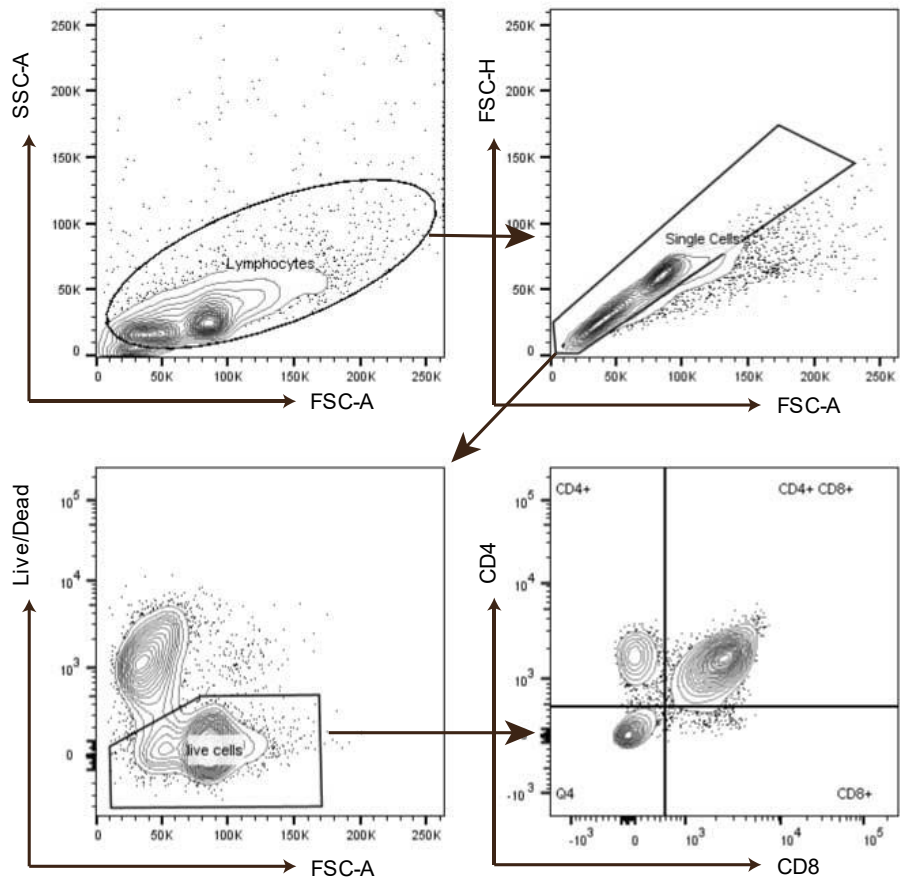


FIGURE 12: Flow cytometry gating strategy for thymus (data generated by Dr Eirini Pantazi)

5.4 Discussion

5.4.1 CALHM6 expression at steady state

By using available online database we showed that the main expression of CALHM6 at steady state is in innate cells, in particular circulating monocytes and RPM, these results are in line with previous reports[32,33]. This, together with the fact that after TLR stimulation upregulation of *Calhm6* is strong and happens quickly, suggest the profile of a fast-acting protein that needs to be present in the very early phases of infection. *Calhm6* presence in both RPM and monocytes could be linked with the function that these cells carry out. RPM are a long-lived resident population present in the red pulp zone of the spleen that is $F4/80^+$ in mice[397]. The RP constitute the majority of the spleen tissue and it has the task of cleaning circulating blood by removing senescent, opsonised or dead blood cells and recycling their iron content[175]. For example, the RBC that have lost CD47 are removed from the blood by red pulp macrophages via eritrophagocytosis[398]. While the immune function of RPM has not yet been completely elucidated, they can be the first cells in the organism to encounter pathogens, especially blood-born ones like *Plasmodium falciparum* in human and *Plasmodium chabaudi* in mice, so they are capable of quickly producing pro-inflammatory cytokines like TNF and high amounts of type I IFNs early in the infection[397,398]. Confirming that the role of RBM in immunity is still mostly unknown, some studies suggest that in response to TLR-agonists and zymosan, RPM are a source of anti-inflammatory cytokines, like IL-10 and TGF-β. Other, *in vitro* experiments show that RPM are capable of presenting antigens to T cells but without triggering their proliferation[399,400]. The RP is also rich in many other leukocytes, including a large number of monocytes[397] that are poised to be rapidly activated upon injury or infection[401].

Monocytes are mononuclear blood leukocytes that can differentiate in macrophages or DC by migrating to peripheral tissue during infections. For this purpose, monocytes display several chemokines and adhesion receptors, like Gr-1 and CCR2, that facilitate their recruitment. Interestingly monocytes are a key player in modulating inflammation by producing cytokines like IL-1β, TNF and IL-

6 in the very early phases of infection[401]. Two population are identified in human and mouse monocytes, deemed canonical and non-canonical. Human canonical monocytes are $CD14^{++}CD16^{+}$, non-canonical $CD14^{+}CD16^{++}$ and an intermediate population is also present[402]. In mice the surface markers used to distinguish the two populations are Ly6C and CD43 with canonical monocytes being $Ly6C^{++}CD43^{+}$ and the non-canonical $Ly6C^{+}CD43^{++}$[403]. We see from the gene expression data that *Calhm6* is more abundant in non-canonical monocytes that present more mature phenotype and are higher in CX3CR1 expression[402]. These monocytes can also sense viral nucleic acid and initiate the immune response[404] while they carry out intraluminal surveillance and neutrophil recruitment[405]. Non-canonical monocytes have been defined as "patrolling" monocytes[406] for their role in keeping the vasculature in check and mediating the removal of damaged endothelial cells[404405]. While their role is generally considered anti-inflammatory, they are the first monocytes to migrate following *L. monocytogenes* infection when they produce high levels of TNF[407]. Similarly to RPM, monocytes have some ability to perform antigen presentation to T cells in the spleen[406]. The functional similarity between RPM and monocyte function in the early immune response suggests that *Calhm6* expression is important in cells that perform patrolling-like behaviours and might need to upregulate pro-inflammatory pathways at a very short notice. This seems to be also confirmed by the fact that CALHM6 expression *in vitro* starts to dwindle already after 24/48 hours, suggesting a protein only important in the first phases of the response.

5.4.2 CALHM6 expression in BMDM versus BMDC

In this chapter we also showed for the first time, that in response to IFN and PAMP, BMDM can upregulate CALHM6 expression substantially more than BMDC. In our model CALHM6 expression was barely detectable in BMDC, even after 24 .,mh of IFN-γ and Poly(I:C) combined stimulation. Both BMDM and BMDC are derived from the same strain of WT mice collected at the same stage of development and differentiated for 7 days. BMDM are differentiated by being exposed to M-CSF while BMDC are exposed to GM-CSF. Consistent with *in vitro* results, we also showed that *Calhm6* mRNA

was significantly higher in splenic F4/80^{+} macrophages than in CD11c^{+} DCs, after 3 hours of intraperitoneal Poly(I:C) stimulation. This difference in expression between macrophages and DC was surprising when we consider that, out of the only two papers previously published about CALHM6 function, the first one published by Ebihara et al. in 2010[32] was almost entirely based on overexpression of *Calhm6* in BMDC. Our results could indicate that the model used in the study was not physiological. Subsequent experiments performed by Kasamatsu et al. and published in 2014[33] looked at CALHM6 expression in WT vs *Calhm6*$^{-/-}$ mice. Results in this case are more nuanced and show that the highest CALHM6 expression is in F4/80^{+} macrophages as well as CD8^{+}DCs thus being closer to our own results.

The GM-CSF used to differentiate BMDC is a cytokine that can act on myeloid cells and enhance their survival or their activation/differentiation. *In vivo* it is mostly associated with inflammation and pain. The GM-CSF receptor signals through JAK2/STAT5 and ERK[408]. While it is usually pro-inflammatory, it has been shown *in vitro* that it can disable cells inflammatory function in a dose-dependent manner via activation of the AKT/mTOR/mTORC1 signalling cascade[409]. Cells generated *in vitro* with high doses of GM-CSF though, produced higher levels of cytokines than ones generated with low doses[410]. While we did not investigate why CALHM6 expression is so reduced in BMDC it is possible that GM-CSF act as an inhibitor of *Calhm6* expression. In a recent pre-published study, Bosteels at al.[411] while studying inhaled GM-CSF treatment efficacy in Covid19 disease show a significant increase of *Calhm6* in lungs of mice that are *Csf2*$^{-/-}$ (the gene of GM-CSF). *Calhm6* was especially increased in the macrophage population of this mouse.

5.4.3 Regulation of *Calhm6* expression by pro- and anti-inflammatory signals

We have shown in this chapter that both *Calhm6* mRNA and CALHM6 protein are upregulated by pro-inflammatory stimuli and downregulated by anti-inflammatory ones. The upregulation of CALHM6 happens quickly in BMDM with the protein already appearing 2 hours after stimulation. This again

suggest that we are dealing with a protein involved in the early inflammatory response. While previous studies had already shown that Poly(I:C) and Zymosan[33,87] could upregulate *Calhm6* in mouse cells, contrary to our finding Kasamatsu et[33] al showed that LPS was not a good stimulus for *Calhm6*. This discrepancy could be due to the fact that in the 2014 paper they measured the levels of *Calhm6* in total spleen and not in innate immune cells alone[33]. Some of our data, not shown in this work, confirm that we can see upregulation in primary splenic immune cells after LPS stimulation *in vitro*. Kasamatsu et al. did not see upregulation of *Calhm6* with Pam3CSK, R837 or CpG stimulation. These are TLR agonists for, respectively, TLR1/TLR2, TLR7 and TLR9, and it was not dissected why they failed to induce CALHM6. One transcription factor that has been associated with the control of *Calhm6* is IRF3[32]. As IRF3 is activated by TRIF, this could be the pathway used by TLR4 and TLR3 but not TLR1/TLR2 to upregulate *Calhm6*. Zymosan on the other hand upregulates *Calhm6* through the Dectin1/IRF5 pathway[87]. IRF7 is not involved in the control of *Calhm6*[32], and this may at least in part explain why R837 and CpG stimulation have no control over CALHM6 expression[412].

In this chapter we showed for the first time that anti-inflammatory stimuli like TGF-β, IL-4 and IL-10 are all capable of downregulating *Calhm6* expression. This is unsurprising because all these cytokines are involved in the "alternative" activation of macrophages[390,413] and *Calhm6* is a signature gene of the LPS, LPS+IFN-γ treated pro-inflammatory macrophages[414]. TGF-β action in skewing the BMDM toward an alternative activation is such that, even when added after 4 h of LPS or IFN-γ stimulation, can still reverse *Calhm6* upregulation.

We also show for the first time *in vitro* that IFN-γ positively upregulates CALHM6 expression. This is likely caused by the presence in the promoter region of ISRE and STAT binding sites[415], making *Calhm6* susceptible to IFN-γ stimulation.

IFN-γ does not only upregulate *Calhm6* alone but, when paired with Poly(I:C) or zymosan, boosts its expression and/or the duration of its upregulation. It is important for macrophages to be able to integrate more than one signal in response to inflammatory stimuli to create a large range of specific

responses starting from a relatively small number of receptors. In our case it is clear that while PAMP, signals of a pathogenic invasion, successfully upregulate *Calhm6*, the response to a pro-inflammatory cytokine like IFN-γ works as a positive feedback for the immune system activation[388] and unleashes the full extent of CALHM6 production. IFN-γ is one of the most important activators of macrophages and it signals primarily through the common JAK-STAT pathway, that causes Stat1 dimerisation and translocation to the nucleus to activate transcription of IFN-γ -regulated genes, many of which are transcription factors[388]. One of the main effects of IFN-γ in macrophages is the priming of the microbicidal effector function, increasing, for example, their capacity to produce iNOS and to respond to LPS. It is possible that a similar functional synergy exists for IFN-γ-TLR3 and IFN-γ-Dectin 1 signal integration. In both cases, IFN-γ priming increased upregulation of *Calhm6* [416] by these PAMP. Our results are consistent with reports that macrophage primed with IFN-γ produce more TNF in response to Dectin-1 stimulation, thus suggesting that IFN-γ can prime macrophages responses to fungal products as well[417].

5.4.4 Generation of *Calhm6*$^{-/-}$ mice

For this study we generated a new line of CALHM6 conditional KO mice. *Calhm6*$^{fl/fl}$ mice were initially crossed with a PGKCre strain that causes embryonic deletion of the loxP-cassette. Resulting progeny lack the entirety of CALHM6 exon 2, and the protein is not detectable at all in mouse tissue and BMDM. The mouse strain generated by us is similar to the one created in the Seya lab in 2014[1] that also lacks exon 2. Like the Seya mouse, ours does not show any defect in breeding, growth, or development of the immune system. It is interesting to confirm that CALHM6 is not required for the development of healthy mice in SPF conditions and individually ventilated cages, but it does not come as a surprise. As we have already discussed, CALHM6 function seems to be linked to its induction after pro-inflammatory stimulation and very few cells express it at steady state. Other mice that lack protein essential for the correct function of the immune system in infection do not show any phenotype in normal housing conditions. This is, for example, true of mice deficient for IL-1β[418], IL-6[419] or IL-18[420] all

genes whose function in the immune defence has been well established but that are not required for homeostasis. We were also pleased to confirm that deficiency in CALHM6 does not cause placental defect: there are no differences in the number of siblings between WT and *Calhm6*$^{-/-}$ mice. Once again this could be due to the absence of pathogen infections during gestation. A study recently performed in human placenta has shown how the expression of 3 members of the CALHM family, 2, 4 and 6 is quite high in this tissue[22]. While the study does not differentiate between CD45^{+} and other cells we could speculate that the expression of CALHM6 in the placenta is concentrated in resident macrophages and possibly in the NK cells that are quite abundant in this tissue[421]. The reported upregulation of *Calhm6* in villitis of unknow aetiology[40] (inflammation of the chorionic villi, which are the structures covering the surface of the placenta) and the importance that NK cells have in the pre-natal immune system[107,421] makes it an interesting tissue to consider for future studies.

5.5 Limitations of the study

While it would have been interesting to measure CALHM6 expression level *in vivo* in several immune populations, both adaptive and innate, this turned out to be impossible to achieve by flow cytometry. The only commercially available antibody of which we could confirm the validity (Santa Cruz, clone G-12) although working sufficiently well for WB analysis, was not good enough for flow cytometry staining. The antibody recognises the C-terminal intracellular portion of the protein that *in vivo* interlocks with the adjacent monomer, it is possible that the epitope is masked in the physiological three-dimensional conformation. While it was possible to obtain more accurate data of *Calhm6* mRNA expression in immune population by sorting the cells and performing qPCR, we reasoned that this was beyond the scope of our work. We were mostly interested in defining if CALHM6 behaved as a pro-inflammatory molecule, it does, and in defining which cell type could be more useful for our subsequent *in vitro* experiment, BMDM. For the same reason, while we used several TLR ligands that we suspected had an effect in upregulating *Calhm6*, we did not focus our attention on a full spectrum of pro-inflammatory stimuli and neither we investigated through which signalling pathway this

stimulation controlled *Calhm6* expression. Even though this is a very interesting question our focus was on identifying the functional role of CALHM6 in the immune response and its mechanism of action. For this we needed to: a) identify a cell that expresses CALHM6; b) identify relevant signal that upregulates CALHM6 expression; and c) generate CALHM6 deficient mice, which we did. These tools set the stage for functional studies in subsequent chapters.

Even though we were pleased with the *Calhm6*$^{-/-}$ mice that we generated, it was not ideal to have to cross 2 different inbred mouse lines: C57BL/6N (background of *Calhm6*$^{fl/fl}$) and C57BL/6J (background of *PGKCre*). Both are C57BL/6 strains but they do differ in several SNPs (source The Jaxon laboratories). To avoid the possibility that random SNP could cause unwanted differences in the result comparisons, we generated our own WT controls mice from the same breeder parents as the *Calhm6*$^{-/-}$. Subsequent WT and *Calhm6*$^{-/-}$ lines were maintained in the same colony but were not littermates. While co-housed in the same exact conditions and in the same room we decided to create two different lines to minimise genotyping and animal use in line with principles of 3R. For this reason, throughout the work the strains were refreshed by back-breeding with WT from the Jackson Lab and key experiments were repeated with the new colony generated.

5.6 Conclusions

In this first chapter I showed how CALHM6 is mostly expressed in innate immune cells. Only monocytes and RBM express a substantial amount of *Calhm6* mRNA at steady state. F4/80^{+} macrophages highly upregulate *Calhm6* in response to stimulation, much more so than CD11c^{+} DCs. Consistent with this result, BMDM have a much higher expression of CALHM6 than BMDC

I also demonstrated that in BMDM, pro-inflammatory stimuli upregulate *Calhm6* while anti-inflammatory ones downregulate it and the upregulation is even stronger when cells are primed with IFN-γ.

At the beginning of our study, we also generated a new mouse line that is deficient for the *Calhm6* gene. The mouse is healthy and has a normal immune system.

I will use the knowledge generated in this chapter to study the role of CALHM6 in infection disease and its function in macrophages.

6 Role of CALHM6 in infection

6.1 Introduction

6.1.1 CALHM6 role in NK cell activation

The limited amount of published literature that investigates CALHM6 suggests an IRF3 dependent role in NK cell production of IFN-γ in anti-tumour defences. CALHM6 was first identified by Ebihara[32] and colleagues in 2010 as a Poly(I:C) inducible protein important for NK cell activation. The study lacked a proper *Calhm6*$^{-/-}$ model but showed that CALHM6 overexpression rescued the ability of *Irf3*$^{-/-}$ BMDC to activate NK cells and produce IFN-γ. Four years later a work from the same lab[33] used a genetically modified mouse to demonstrate that *in vivo Calhm6*$^{-/-}$ NK cells do not produce the same amount of IFN-γ in response to Poly(I:C). Thanks to the use of an *in vitro* model in which macrophages/DC and NK cells were co-cultured for 24 hours after Poly(I:C) stimulation Kasamatsu et al. also showed that CALHM6 presence was important in both macrophages/DC and NK cells for the correct activation of NK cells, albeit it appeared more important in macrophages/DC than NK cells[33]. Both papers used a cancer disease model to test if the absence of CALHM6 was deleterious for the generation of an anti-tumour immune response. In the more physiological of the two models WT and *Calhm6*$^{-/-}$ mice were implanted with modified forms of B16 melanoma cells, that are susceptible to NK cell lysis. The mice were then left untreated or periodically injected with Poly(I:C). Poly(I:C) has been used as an adjuvant in tumour immunotherapy and studies showed that in melanoma models it drives the inhibition of lung metastasis in a IFN-γ and NK cell dependent-fashion[422,423]. The study shows no difference in primary tumour growth but Poly(I:C) treated *Calhm6*$^{-/-}$ mice had more metastasis in the lung than WT controls[33]. Therefore, the authors of the study proposed CALHM6 as a new target for cancer immunotherapy. Knowing that the role of NK cells and IFN-γ in the immune system is much larger and not restricted to protection against cancer[84,86,388], in this chapter we are going to investigate what is the role of CALHM6 in the protection from bacterial and viral infection.

6.1.2 Choosing murine models of infection

Choosing the right model is important in the investigation of protein function, due to the large number of possible pathogens that we could investigate we decided to focus on those where macrophages, NK cells and IFN-γ are known to be important for the clearance of the infection (*L. monocytogenes*) and those that are sensed via TLR3 (*Influenza*) in the expectation that they would trigger upregulation of CALHM6 *in vivo*.

6.1.2.1 *Listeria monocytogenes*

L. monocytogenes is a food-borne gram-positive bacteria that can cause dangerous infection in children, elderly, immunocompromised and pregnant people[288]. It is one of the best known model of infection available to study in a lab[289]. Studies on *L. monocytogenes* lead to the discovery of cell-mediated immunity[424] and it has been an invaluable model for the understanding of DC-mediated T cell activation[303]. Most relevant for our work, we know that early on after *L. monocytogenes* infection (e.g. 12-24 hours post infection) IFN-γ is produced in abundance and the main producers of this IFN-γ are NK cells[255,330,425,426]. NK cell-derived IFN-γ allows the activation of antimicrobial programmes in macrophages[304,427], this is important because MZM are some of the earliest cells to be infected by blood-borne *L. monocytogenes*[230,324,428]. Once it has entered the macrophage by phagocytosis, *L. monocytogenes* can evade macrophage-mediated lysosomal killing by evading from the vacuole to the cytosol[288,429] mostly thanks to the virulence factor LLO[304]. Once *L. monocytogenes* has invaded the cytosol it can replicate, thus overwhelming the macrophages that are then used by *Listeria* to efficiently spread to other cells. On the contrary, if macrophages are primed by IFN-γ they can kill and control the *L. monocytogenes* in the vacuole fast enough to limit/reduce the spread [304,427]. It has been shown that after IFN-γ priming both peritoneal macrophages and BMDM, restrict *L. monocytogenes* growth by stopping its escape form the vacuole[327,430]. Retention of *Listeria* in the vacuole and subsequent bacterial killing is obtained mostly via IFN-γ dependent upregulation of iNOS that creates increased levels of nitric oxide in the vacuoles[431,432]. Our purpose in this chapter is to investigate

whether CALHM6 is required for NK cell activation and IFN- γ production during infection and if so, does the lack of IFN-γ affects *Calhm6*$^{-/-}$ mice response to *L. monocytogenes* infection

6.1.2.2 *Influenza A*

According to the literature the main stimulus that upregulates CALHM6 is Poly(I:C)[32,33]. Poly(I:C) is a TLR3 agonist that mimics viral infection by being analogue to double-stranded RNA. TLR3 and its downstream signalling are key to protective immunity against viruses[433]. This is the reason why we decided to use Influenza A as a model of infection in our *Calhm6*$^{-/-}$ mice. Influenza A is a virus very relevant for human health, it can cause infections that vary from a mild sore throat to lethal pneumonia. Thousands of people die every year from Influenza in developed countries and pandemics of zoonotic origins occur regularly[434]. These pandemics are usually associated with antigenically different strands for which the general population has no pre-existing immunity[434]. Influenza A viruses are single-stranded RNA viruses, despite this, TLR3 is an important PRR for Influenza A *in vivo*. This could be due to the double-stranded RNA produced as an intermediate stage of replication[435]. This dsRNA intermediate is recognised by TLR3 and the subsequent response is TRIF and PI3K/AKT but not MyD88 dependent[436]. A study from Pichlmair and colleagues though, shows how Influenza does not produce dsRNA *in vivo*[437] and TLR3 instead, is involved in the recognition of virus-infected cells phagocyted by macrophages[438,439]. TLR3 role in Influenza appears to be quite complicated and not necessarily beneficial. *Tlr3*$^{-/-}$ mice infected with influenza virus have a survival advantage, despite a higher viral load. This is probably due to the higher level of inflammation found in WT mouse lungs, that can be debilitating for the mice[440]. There is a partial benefit in having TLR3 in the immune response though, when both TLR3 and TLR7 or MyD88 are absent mice succumb to the infection much quicker[441], suggesting a redundant function for the receptors. The H3N2 viral strain used in this work derives from the human H3N2 strain originated in Hong Kong and Singapore[442], this strain is a recombinant of the Hong Kong virus with a high-yield laboratory strain (A0/PR/8) and is routinely used in mice infection. In this chapter we will test whether the lack of CALHM6 upregulation downstream of TLR3 activation causes differences in the outcome of H3N2 infections in *Calhm6*$^{-/-}$ mice.

6.2 Aims

1. To verify if CALHM6 is important for NK cell activation in bacterial and/or viral infection models

2. To define the role of CALHM6 in bacterial and/or viral models of infection

3. To identify in which cell type CALHM6 is important in bacterial and/or viral models of infection

6.3 Results

6.3.1 *Calhm6*$^{-/-}$ mice fail to produce IFN-γ in the early stage of *L. monocytogenes* infection

To understand CALHM6 physiological role in infectious disease I used listeriosis as a model for bacterial infection. WT and *Calhm6*$^{-/-}$ mice were injected with 3x10^5 CFU of *L. monocytogenes* IP. The mice were sacrificed 18 hours later when the IFN-γ production from NK cells is at its peak[330,428] (Figure 13.a). To measure intracellular cytokines, single cell suspension was obtained from spleens and cells were cultured for additional 4 hours incubation in Brefeldin A, a product of the *Penicillium Brefeldianum* fungus that blocks ER transport and protein sectretion[443]. In this way IFN-γ accumulated in the cytoplasm so as to visualise it by flow cytometry after intracellular staining (Figure 13.b and c, gating strategy figure 14). NK cells from *Calhm6*$^{-/-}$ mice produced significantly less IFN-γ than their WT counterpart and the defect in IFN-γ production was limited to NK cells (figure 13.d). To check that this defect was not specific for *L. monocytogenes* infection I injected the mice with 100 µg Poly(I:C) IP (Figure 13.e). Once again, the amount of IFN-γ produced by NK from *Calhm6*$^{-/-}$ mice was drastically reduced (Figure 13.f and g) in the NK cells. This recapitulates the results obtained by Kasamatsu et al.[33] in their 2014 study. My results show that CALHM6 is important for IFN-γ production from NK cells in response to infection.

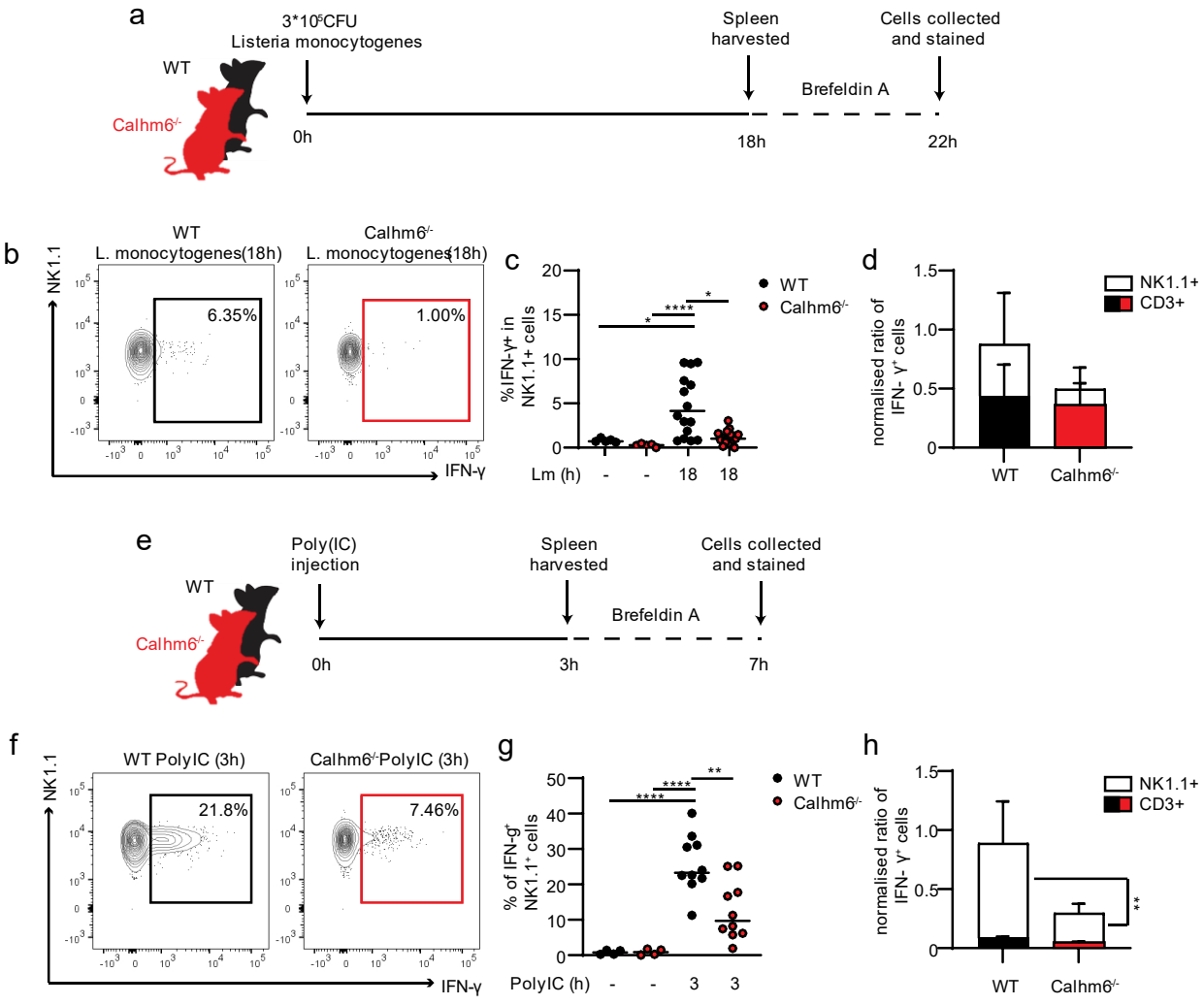


FIGURE 13: CALHM6 is important for IFN-γ production in early response to infection a) Experimental scheme: WT and *Calhm6*$^{-/-}$ mice were injected IP with 3x10^5 CFU of *L. monocytogenes* or PBS. After 18 h spleens were collected, single cell suspension was prepared, and cells incubated for 4 h with Brefeldin A (5 µg/ml) before intracellular staining for flow cytometry. b) Representative flow cytometry panels, c) pooled frequency of IFN-γ$^+$ cells in NK1.1$^+$ cells from WT and *Calhm6*$^{-/-}$ mice and d) normalised ratio of IFN-γ$^+$ cells that are NK1.1$^+$ or CD3$^+$ (Pooled results from 4 independent experiments, n=5, 5, 16 and 17. One-way ANOVA with multiple comparisons). e) Experimental scheme: WT and *Calhm6*$^{-/-}$ mice were injected IP with Poly(I:C) (100 µg/mouse) or PBS for 3 h, spleens were collected and processed like in Figure 3a. f) Representative flow cytometry panels, g) pooled frequency of IFN-γ$^+$ in NK1.1$^+$ cells of WT vs *Calhm6*$^{-/-}$ mice and h) normalised ratio of IFN-γ$^+$ cells that are NK1.1$^+$ or CD3$^+$ (Pooled results from 4 independent experiments, n=4, 4, 10 and 10. One-way ANOVA with multiple comparisons)

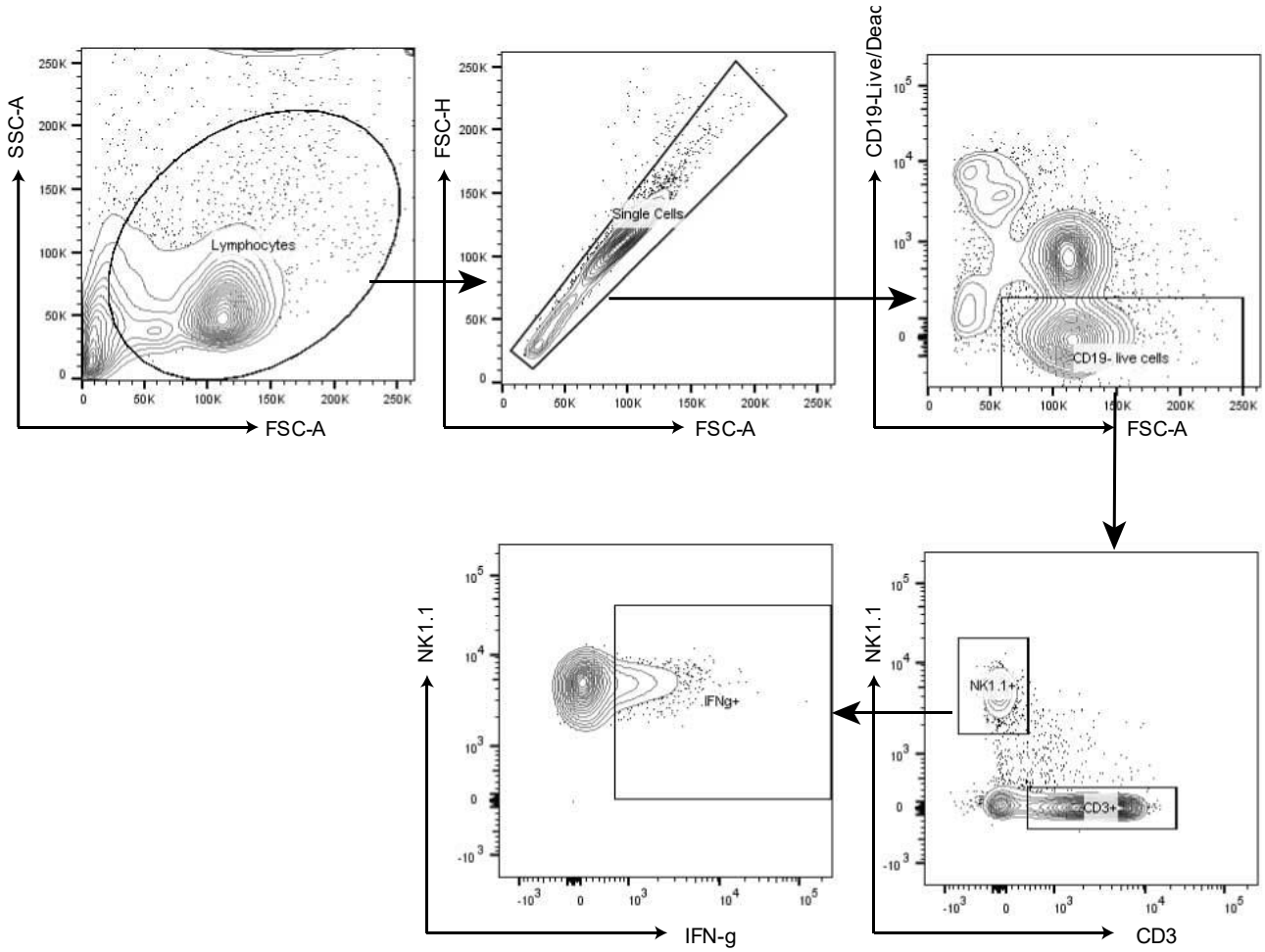


Figure 14: Flow cytometry gating strategy for splenic IFN-γ^{+} NK cells

6.3.2 IFN-γ but not granzyme B production is impaired in *Calhm6*$^{-/-}$ mice

NK cells have a double role in the defence from infection. Cytotoxic NK cells upregulate Granzymes and Perforin proteins used to trigger lysis of target cells that can be infected or cancerous. Alternatively, NK cells can control infection and inflammation by producing pro- or anti-inflammatory cytokines like IFN-γ or IL-10. Previous studies show that the cytotoxic activity of NK cells is not impaired by the lack of CALHM6[32,33], so I tested these findings by measuring intracellular levels of Granzyme B in NK cells after Poly(I:C) injection (Figure 15.a) as a proxy for cytotoxic activity. Flow cytometry results (Figure 15.b and c) demonstrate that only IFN-γ but not Granzyme B levels are reduced in *Calhm6*$^{-/-}$ cells. It appears that, after Poly(I:C) injection, there are two distinct subset of activated cells, one "cytotoxic" that upregulates Granzyme B and another "pro-inflammatory" that produces IFN-γ. There is very little overlap between these two populations. So CALHM6 seems to be specifically implicated in the IFN-γ producing pro-inflammatory state of NK cells but not in their cytotoxicity.

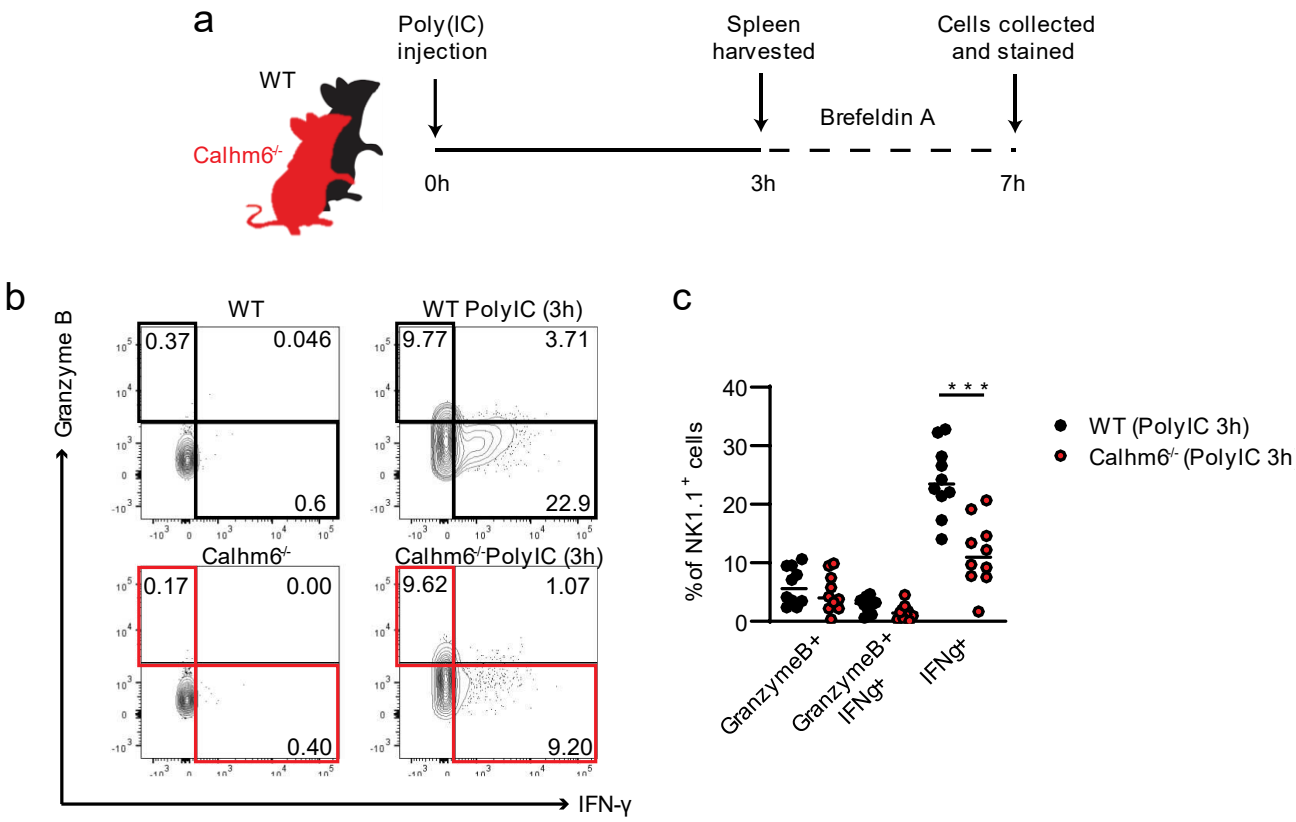


FIGURE 15: CALHM6 deficiency impairs IFN-γ but not Granzyme B production from NK cell in early stages of infection a) Experimental scheme: WT and *Calhm6*$^{-/-}$ mice were injected IP with Poly(I:C) or PBS. After 3h spleens were collected, single cell suspension was prepared, and cells incubated for 4 h with Brefeldin A (5 µg/ml) before intracellular staining for flow cytometry. b) Representative flow cytometry panels and c) pooled percentage of IFN-γ^{+} and or Granzyme B^{+}, NK1.1^{+}. (Pooled results from 2 independent experiments, n=2, 2, 10 and 10. One-way ANOVA with multiple comparisons).

6.3.3 *Calhm6*$^{-/-}$ mice fail to control the early phase of *L. monocytogenes* infection

I chose *L. monocytogenes* as an experimental model because the innate immune response is very important to control the magnitude of bacterial replication in the early stages of infection[303] . This is because IFN-γ produced by NK cells[255,330,335,444] activates macrophages and allows them to efficiently kill phagocyted *L. monocytogenes* [304,431,445]. With these considerations in mind, I decided to check whether the early lack of IFN-γ in *Calhm6*$^{-/-}$ mice influenced their ability to control *L. monocytogenes* infection. WT and *Calhm6*$^{-/-}$ mice were infected with *L. monocytogenes* i.p. and bacterial levels were measured in the spleen 24 and 72 h post-infection (Figure 16.a). Unsurprisingly, there was no difference in spleen bacterial burden 24 h post-infection (Figure 16.b), at this stage the role of IFN-γ and macrophages has been shown to be minimal[285,446], but 72 h later *Calhm6*$^{-/-}$ mice had a significantly higher bacterial burden in the spleen (Figure 16.c) and they were generally more susceptible to the infection as shown by the significantly greater weight loss (Figure 16.d). These results demonstrate that *Calhm6*$^{-/-}$ mice are more susceptible to L. monocytogenes infection and fail to control the bug load at the same rate as WT mice do, at least in the early phases of infection.

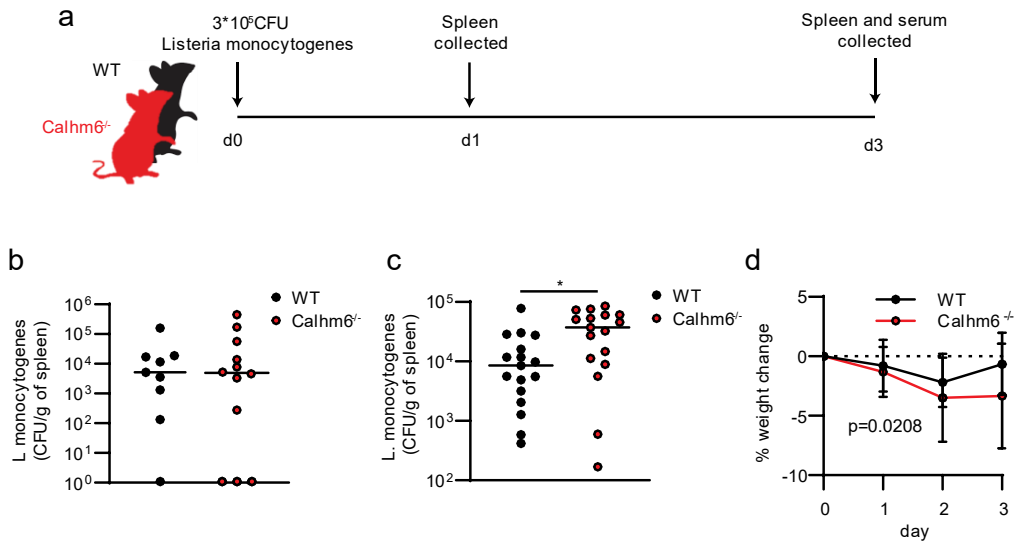


FIGURE 16: *Calhm6*$^{-/-}$ mice fail to control early stages of *L. Monocytogenes* infection. a) Experimental scheme: WT and *Calhm6*$^{-/-}$ mice were infected IP with 3x10^5 CFU of *L. monocytogenes*. At day 1 and 3 mice were sacrificed, and spleen collected. Spleens were mechanically lysed, and the lysate was grown on antibiotic-free BHI agar plates for 24 h at 37°C before CFU count. CFU/g of spleen after b) 24 h of infection (pooled results from 2 independent experiments n= 9 vs 12, Mann Whitney test) or c) 72 h of infection (pooled results from 2 independent experiments n= 16 vs 17, Mann Whitney test). d) Weight was monitored every 24h (two-way ANOVA).

6.3.4 *Calhm6*$^{-/-}$ mice are more susceptible to *L. monocytogenes* even when exposed to lower doses of infection

Some inflammatory processes are dispensable or less required at lower doses of *L. monocytogenes* infection[335,447], for example IL-12 production is dispensable for very low doses of infection[448]. Thus, we tested whether CALHM6 is still required for bacterial control in response to low-dose *L. monocytogenes* infection. *Calhm6*$^{-/-}$ and WT mice this time were infected with only $3x10^4$ CFU i.p. (Figure 17.a) and bacterial burden in the spleen was measured again at day 3 (Figure 17.b). Like for the ten-fold higher dose, *Calhm6*$^{-/-}$ mice early control of bacterial infection was suboptimal and we recovered higher CFU count in the spleen again, when compared to WT mice. We conclude that CALHM6 is required for the efficient clearance of low-dose L. monocytogenes

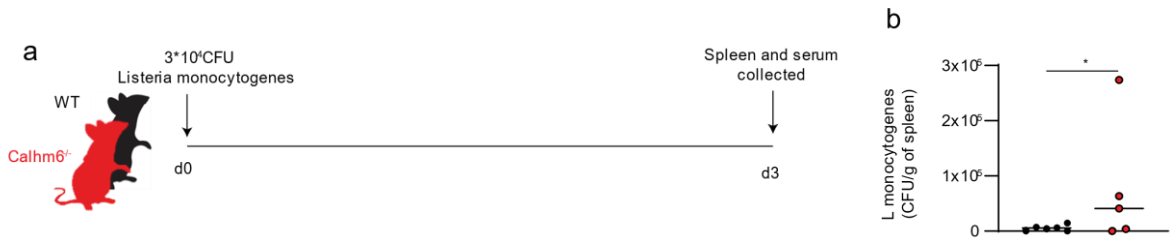


FIGURE 17: *Calhm6*$^{-/-}$ mice fail to control early stages of *L. Monocytogenes* infection even with a lower initial burden of infection. a) Experimental scheme: WT and *Calhm6*$^{-/-}$ mice were infected IP with 3x10^4 CFU of *L. monocytogenes*. At day 3 mice were sacrificed, and spleens collected. Spleens were mechanically lysed, and the lysate was grown on antibiotic free BHI agar plates for 24 h at 37°C before CFU count. b) CFU/g of spleen after 24h of infection (representative experiment from 4 independent experiments n=17 vs 20, Mann Whitney test).

6.3.5 *Calhm6*$^{-/-}$ mice can compensate IFN-γ production at peak infection

While the innate immune system is important for the early response to *L. monocytogenes* infection complete clearance of the bacteria only happens in later stages after the adaptive response has shifted into gear[303]. I therefore tested whether *Calhm6*$^{-/-}$ mice, after an initial failure to control the bacterial burden , could achieve *L. monocytogenes* clearance. First, we tested whether by day 3 of infection the defect in IFN-γ production by NK cells was still present. As shown in Figure 18.a and b, by day 3 there was no longer significant difference in IFN-γ production between *Calhm6*$^{-/-}$ and WT NK cell; on the contrary there seems to be slightly more IFN-γ in the *Calhm6*$^{-/-}$ cells. Following up on these results I tested the systemic concentration of a variety of cytokines at day 3. Interestingly, we could see that some of the pro-inflammatory cytokines: IFN-γ and IL-6 were upregulated in *Calhm6*$^{-/-}$, confirming our flow cytometry data, while the anti-inflammatory IL-10 was higher in the WT mice (Figure 18.c, d and e). None of the other cytokines measured in serum showed any difference (Figure 19.a to j). The difference in pro-inflammatory cytokines at this stage could have been caused by the higher bacterial load present in the *Calhm6*$^{-/-}$ mice although when we considered IFN-γ concentration and CFU load in the spleen (Figure 18.f) we could not see any significant correlation. Otherwise the higher IFN-γ could indicate a shift in the kinetic of *L. monocytogenes* response. We know that in WT mice IFN-γ production from NK cells peaks after 20-24 hours[12,43] while IL-10 is preferentially produced by NK cells three days post-infection[13,44–46]. If the absence of CALHM6 causes a delay in IFN-γ production is possible that what we see is the result of a delayed IFN-γ production peak

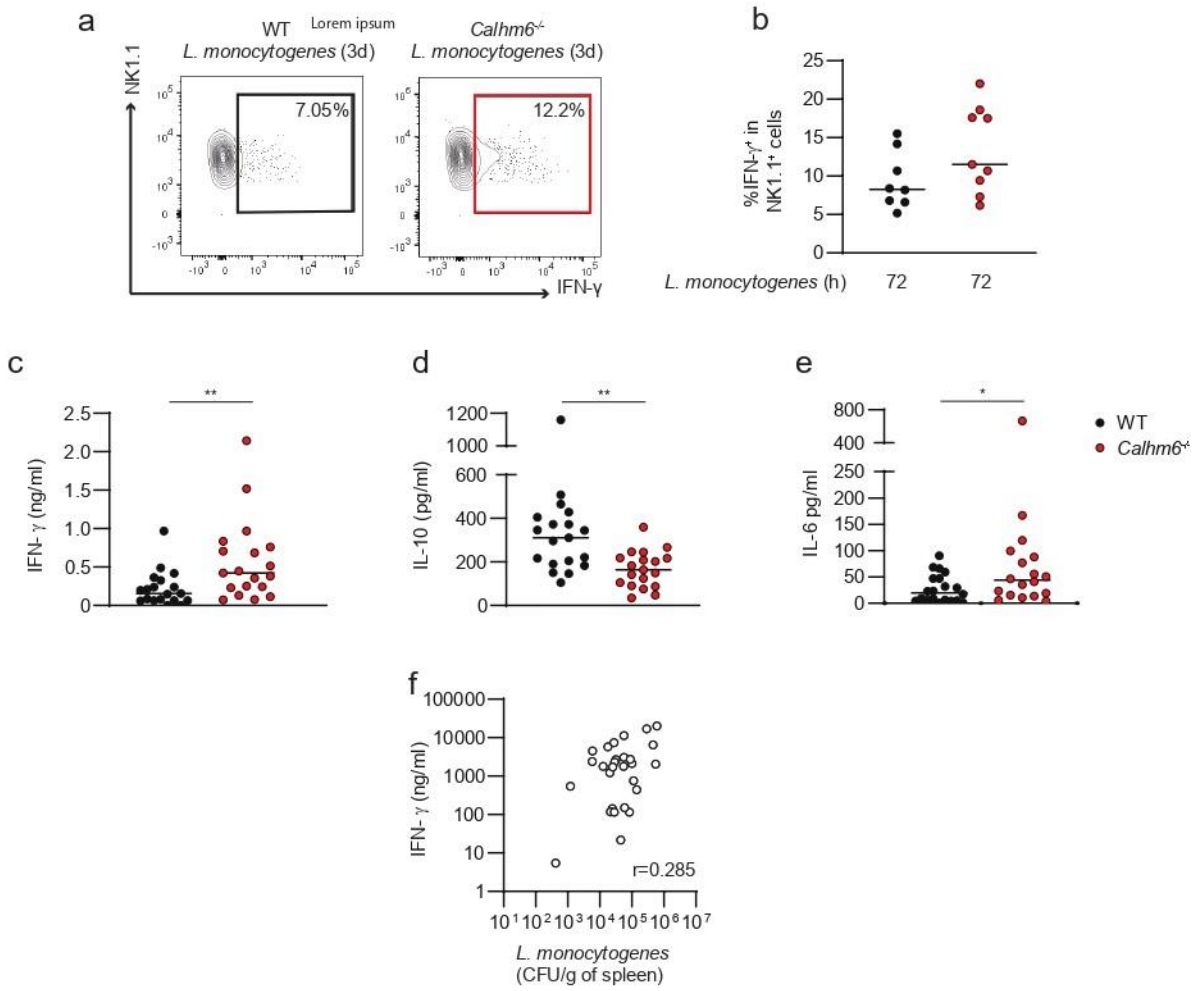


FIGURE 18: *Calhm6*$^{-/-}$ NK cells can produce normal levels of IFN-γ at peak infection allowing for *L. monocytogenes* clearance. WT and *Calhm6*$^{-/-}$ mice were infected i.p. with 3x10^5 CFU of *L. monocytogenes*. At day 3 and mice were sacrificed, and spleen and serum collected. Single cell suspension was made from day 3 spleen, cells were cultured for 4h in Brefeldin A and stained for intracellular cytokines flow cytometry a) representative flow cytometry panels b) pooled frequencies of IFN-γ$^+$ NK1.1$^+$ cells. (Pooled results from 2 independent experiments n= 8 vs 9, Mann Whitney test). Serum collected from the mice was run on a LEGENDplex Mouse Inflammation Panel assay to determine c) IFN-γ, d) IL-10 and e) IL-6 concentration. (pooled results of 2 independent experiment n=16 vs 17, Mann Whitney test). f) correlation between *L. monocytogenes* CFU in spleen and IFN-γ in blood at day 3 post-infection.

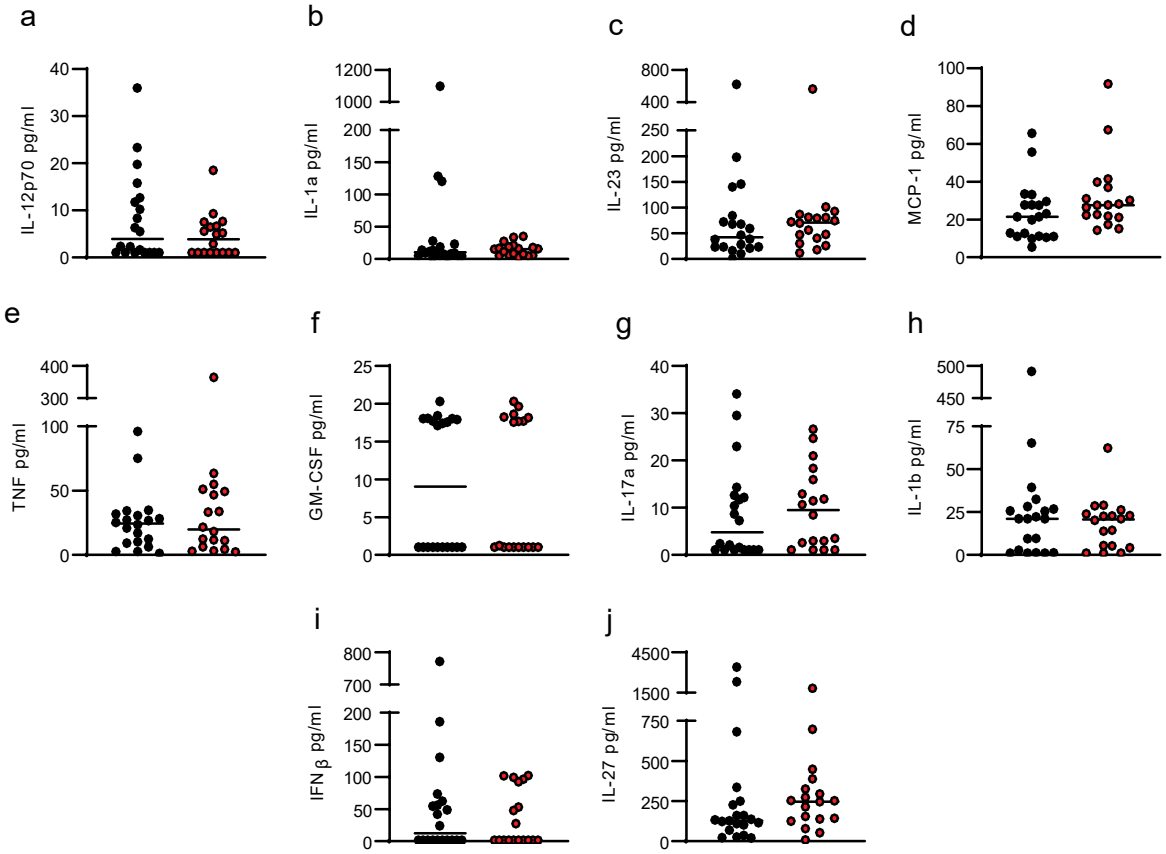


FIGURE 19: Other blood cytokines show no difference between WT and *Calhm6*$^{-/-}$ mice at peak infection. Serum collected from WT and *Calhm6*$^{-/-}$ mice 72 h after i.p. infection with 3x10^5 CFU of *L. monocytogenes* was run on a LEGENDplex Mouse Inflammation Panel assay to determine a) IL-12p70 b) IL-1α c) IL-23 d) MCP-1 e) TNF f) GM-CSF g) IL-17a h) IL-1β i) IFN-β and j) IL-27 concentrations (pooled results of 2 independent experiment n=16 vs 17, Mann Whitney test).

6.3.6 CALHM6 absence causes a shift in the kinetic of the immune response

IFN-γ production in *L. monocytogenes* infection over time suggests that the lack of CALHM6 causes a shift in the kinetic of the innate immune response: at early stages post infection the system fails to be activated to produce IFN-γ and in consequence *Calhm6*$^{-/-}$ mice fail to control early bacterial burden efficiently. Three days later though, at the peak of infection, IFN-γ production is compensated and the serum levels of IFN-γ are even higher in the *Calhm6*$^{-/-}$ mice, possibly due to the higher bacterial burden. To test if this delay in the kinetic of the innate immune response holds in other infection models, that do not have the confounding factor of different bacterial burden, I injected WT and *Calhm6*$^{-/-}$ mice with Poly(I:C) and measured the percentage of IFN-γ^{+} NK cells this time after 12 instead of 3 hours (Figure 20.a). Unlike in the 3 h post stimulation when *Calhm6*$^{-/-}$ NK cells failed to produce IFN-γ (Figure 13.f and g), by 12 h there was no longer a difference between the percentage of WT and *Calhm6*$^{-/-}$ NK cells producing IFN-γ (Figure 20.b and c). Once again, the amount of Granzyme B produced by WT and *Calhm6*$^{-/-}$ NK cells was the same (Figure 20.d) Taken together, these results suggest that CALHM6 is important only in the very early stages of the infection and affects the kinetic of the innate immune response by slowing it down.

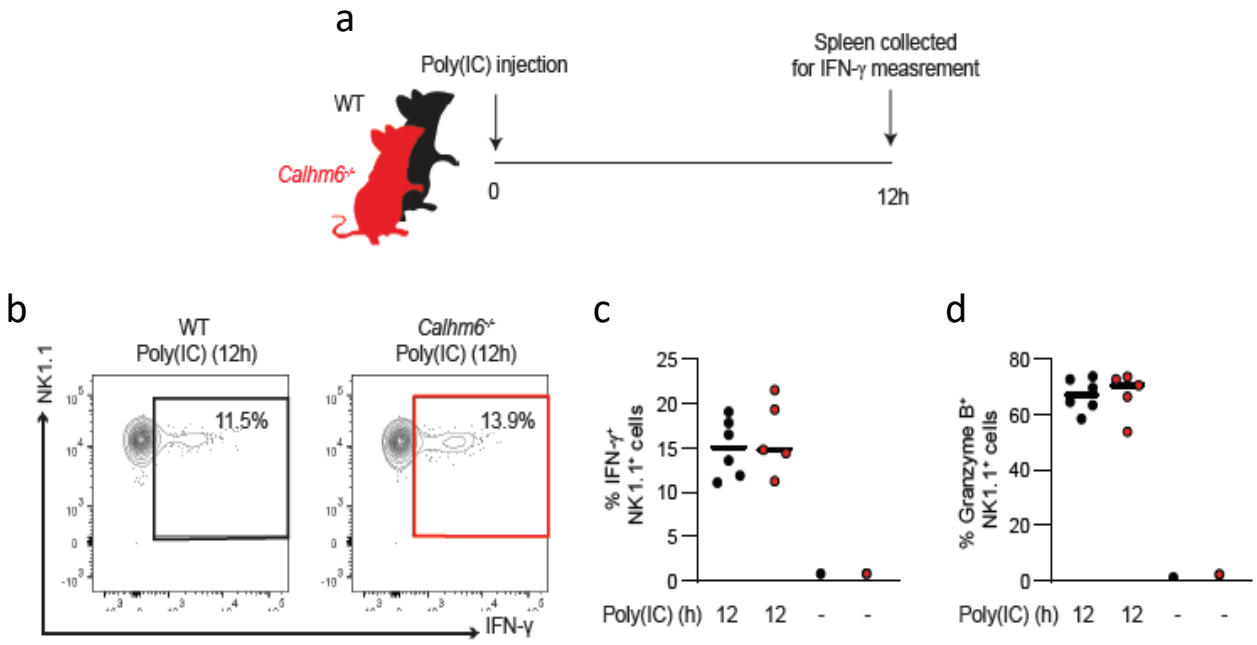


Figure 20: No difference in NK cell-dependent IFN-γ production after 12 h of Poly(I:C). a) Experimental scheme: WT and *Calhm6*$^{-/-}$ mice were injected i.p. with Poly(I:C) (100 ug/ml) or PBS, f) representative flow cytometry panels and g) pooled frequencies of IFN-γ^{+} NK1.1^{+} cells or h) Granzyme B^{+} NK1.1^{+} cells (results from 1 experiment n= 6 vs 5, One-way ANOVA with multiple comparisons).

6.3.7 *Calhm6*$^{-/-}$ mice can efficiently clear *L. monocytogenes* in the later phase of the infection

To look whether *Calhm6*$^{-/-}$ can achieve the sterilising immunity to *L. monocytogenes* I assessed the bacterial load at day 7 (Figure 21.a), when WT mice are known to typically clear the infection completely. At this stage of infection there was no difference anymore between the two mouse strains and both have basically cleared the pathogen (Figure 21.b). By day 7 the burden of the response to *L. monocytogenes* infection has shifted towards the adaptive immune system[303], these results seem to indicate that CALHM6 does not play a role at this stage. Furthermore, the defect that we detected at peak NK cell IFN-γ production (18 h) was completely compensated by day 3 (Figure 18.b), and this was likely a contributing factor in the ability of *Calhm6*$^{-/-}$ mice to clear *L. monocytogenes* at later stages of the infection. These results show that *Calhm6*$^{-/-}$ mice are capable of sterilising immunity against *L. monocytogenes.*

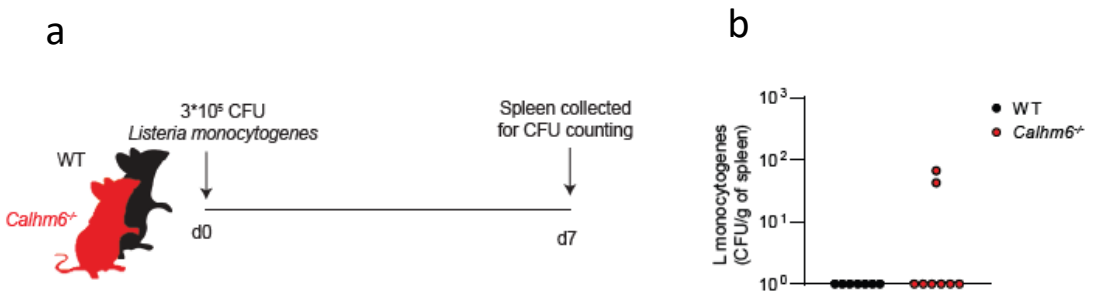


Figure 21: Calhm6-/- can clear L. monocytogenes at day 7. a) Experimental scheme: Mice were infected i.p. with 3x10^5 CFU of *L. monocytogenes*. At day 7 mice were sacrificed and spleens collected with b) Spleens from day 7 were mechanically lysed, and the lysate was grown on antibiotic free BHI agar plates for 24 h at 37°C before CFU count. (Results from one experiment n=7 vs 8, Mann Whitney test).

6.3.8 Absence of CALHM6 does not impair memory response to *L. monocytogenes* infection

I have shown that at day 7, when the immune response has shifted to a mostly adaptive one[303], both WT and *Calhm6*$^{-/-}$ mice are capable of clearing *L. monocytogenes* efficiently. After systemic *L. monocytogenes* infection, T cells get primed in the white pulp zone of the spleen by activated DCs that have migrated from the RP and marginal zone (MZ)[176,323,335,446]. After a primary infection with *L. monocytogenes* mice develop immune memory against the bacteria by creating a long-lived pool of memory T and B cells that can quickly react to subsequent infections[303]. That is why a second infection with much higher doses of *L. monocytogenes* is usually cleared way more efficiently[303]. During re-infection, the main producers of IFN-γ at early stages are not NK cells anymore but *Listeria*-specific memory T cells[303]. T cell activation in many respects, is not dissimilar from NK cell activation: both cell types need accessory cells to supply contact- and soluble-signals and both cell types can form activating immune synapses with DCs[148,449]. I was then interested in ascertaining if the defect seen in NK cell activation was also present in T cells or other adaptive cells. To test whether in *Calhm6*$^{-/-}$ immune memory could be developed efficiently I first infected WT and *Calhm6*$^{-/-}$ mice with a non-lethal dose of *L. monocytogenes* and left the mice to recover for 6 weeks, enough time for the memory response to form. After 42 days mice were re-infected with 10 times more *L. monocytogenes* ($3x10^6$ CFU). Mice were monitored for 3 days (Figure 22.b) and on day 3 spleen (Figure 22.c) and liver (Figure 22.d) were collected to measure the bacterial burden. No significant difference in spleen and liver CFU or in weight loss were observed. Taken together these results indicate that *Calhm6*$^{-/-}$ are capable of mounting a functioning memory response and priming and activating T cells.

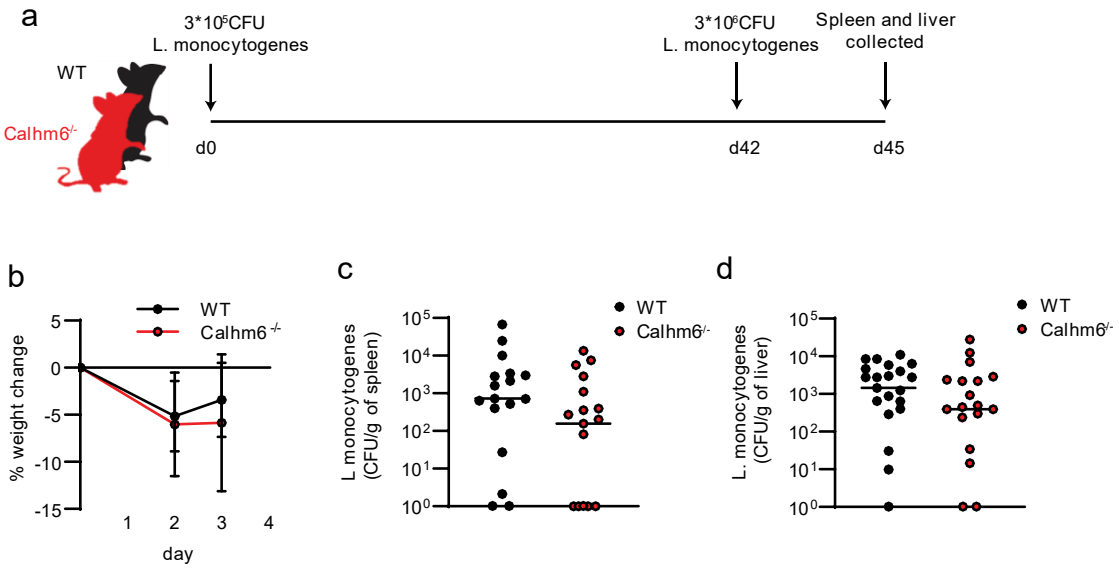


Figure22: *Calhm6*$^{-/-}$ mice can efficiently mount memory response and clear *L. monocytogenes* when re-challenged with higher doses, 42 days after primary infection. a) Experimental scheme: WT and *Calhm6*$^{-/-}$ mice were infected with 3x10^5 CFU of *L. monocytogenes* i.p. and left to recover. After 6 weeks the mice were re-challenged with 3x10^6 CFU. b) The weight was observed for 3 days after the re-challenge and c) spleen and d) liver were collected. Spleens and liver were mechanically lysed, and the lysate was grown on antibiotic free BHI agar plates for 24h at 37°C before CFU count. (pooled results from 3 independent experiments n= 20 vs 18, Mann Whitney test).

6.3.9 CALHM6 is not required for control of the flu virus H3N2 infection *in vivo*

In vitro and *in vivo* studies and my own results, have shown that CALHM6 is upregulated following Poly(I:C) stimulation and Type I IFN response, mostly via IRF3 upregulation[32,33]. Because Poly(I:C) is a viral-associated stimulus that mimics infection of double strand RNA viruses[433] and type I IFN response is important for the ability of organism to respond to viral infections[450] I was interested in testing if CALHM6 was important for the early response to RNA viruses . To study this, I chose the mouse H3N2 strain as model of flu infection[451]. In the early stages of influenza infection, NK cells get recruited to the lungs[452] and once activated, release high quantities of IFN-γ. While the physiological importance of IFN-γ in influenza infection is unclear, and some studies suggest it might be dispensable[453] or even deleterious, due to immunopathology[454], other show that IFN-γ deficiency in early stages increases viral burden and mortality[230,335,427,455]. In our model we intranasally inoculated sedated WT and *Calhm6*$^{-/-}$ mice with 1x10^{4} plaque forming units (PFU) of H3N2 virus (Figure 23.a), I then monitored weight loss daily and viral burden in the lung was measured at day 4 with qPCR (Figure 23.b). There was no difference in either viral burden or weight loss (Figure 23.c) between WT and *Calhm6*$^{-/-}$ mice suggesting that, at least in this specific infection model, CALHM6 deficiency does not affect the immune control of viral infection. Whether this is because for example, there are intact Granzyme B responses in *Calhm6*$^{-/-}$ mice or because other cells could compensate for IFN-γ, it is not clear at this time.

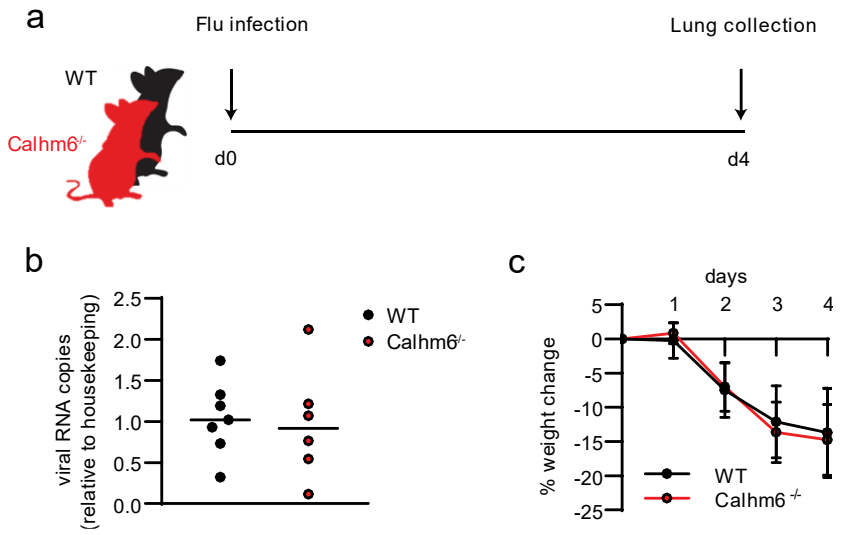


FIGURE 23: *Calhm6*$^{-/-}$ mice can clear H3N2 Influenza A virus. a) Experimental scheme: WT and *Calhm6*$^{-/-}$ mice were infected intranasally with 2x10^4 PFU of H3N2 Influenza A virus. b) At day 4 mice were sacrificed and lungs collected. Single cell suspension was made from the lungs and RNA extracted. Viral RNA was quantified by qPCR (pooled results from 2 independent experiments n=7 vs 6, Mann Whitney test). c) Mouse weight was measured once a day during the 4 days of the experiment (two-way ANOVA)

6.3.10 *Calhm6*$^{-/-}$ NK cells are capable of producing normal levels of IFN-γ in response to contact-independent, soluble stimuli

NK cells can be activated by contact-dependent signals delivered through the IC between NK cells and accessory cells [148], or by contact-independent, soluble signals such as cytokines[84,120,122,456]. To test whether *Calhm6*$^{-/-}$ NK cells are intrinsically deficient in responding to soluble any signals, I first tested whether CALHM6 deficiency causes differences in NK cell maturation. Mouse NK cells can be divided into four subsets based on the expression of the CD27 and CD11b markers on the surface[111]. During the maturation process NK cells start as CD27^{low}CD11b^{low} then in sequence upregulate CD27 and CD11b. In the final stage of maturation NK cells are CD27^{low}CD11^{high}. Because CD27^{high} NK cells are the most involved in cytokine secretion[69,117], I verified whether the lack of IFN-γ production in NK cells could be traced back to the absence of this population. CD27 and CD11b expression in NK cells on WT and *Calhm6*$^{-/-}$ mice was measured by flow cytometry in naïve mice or 3h after Poly(I:C) injection (Figure 24.a and b). No phenotypic differences due to genotype or stimulation were observed in the abundance of the four populations. Once established that maturation is not hindered in *Calhm6*$^{-/-}$ NK cells, I tested if there was a NK cell-intrinsic role of CALHM6 in their ability to respond to soluble signals, or if the defect depended on the cell-mediated activation of NK cells. The main soluble signals produced by macrophages and DCs after *L. monocytogenes* infection are IL-1β, IL-18, IL-12, type I IFN, IL-2 and TNF[84,148,330,428]. I FACS sorted naïve NK1.1^{+}CD3^{-} NK from WT and *Calhm6*$^{-/-}$ mouse spleens and then stimulated them *in vitro* for 6 hours with various soluble pro-inflammatory stimuli known to upregulate IFN-γ production (Figure 24.c). IL-12/IL-18 stimulation was the most efficient in upregulating IFN-γ production, but there was no difference between WT and *Calhm6*$^{-/-}$ NK cells, thus suggesting that *Calhm6*$^{-/-}$ NK cells are capable of producing IFN-γ if provided the right soluble signals. I also tested the efficacy of cell-independent NK stimulation *ex vivo* in cells primed *in vivo*. Mice were injected for 3h with Poly(I:C) or PBS, spleens were then collected and single cell suspension treated with the activating compound PMA/Ionomycin, in the presence of Brefeldin A (Figure 24.d). *Ex vivo*

stimulated NK cells largely (albeit not completely) corrected the defect in IFN-γ production that was evident after *in vivo* Poly(I:C) stimulation alone (Figure 13.f and g). Taken together these results indicate that CALHM6 is not important for the maturation of NK cells and is not required for the activation of NK cells when enough activating soluble factors are present. This suggests that the defect seen in early NK cell responses *in vivo* could be either a result of an inability of accessory cells (macrophages or DC) to produce soluble stimuli or a defect in the contact-dependent communication in the IS between accessory cells and NK cells.

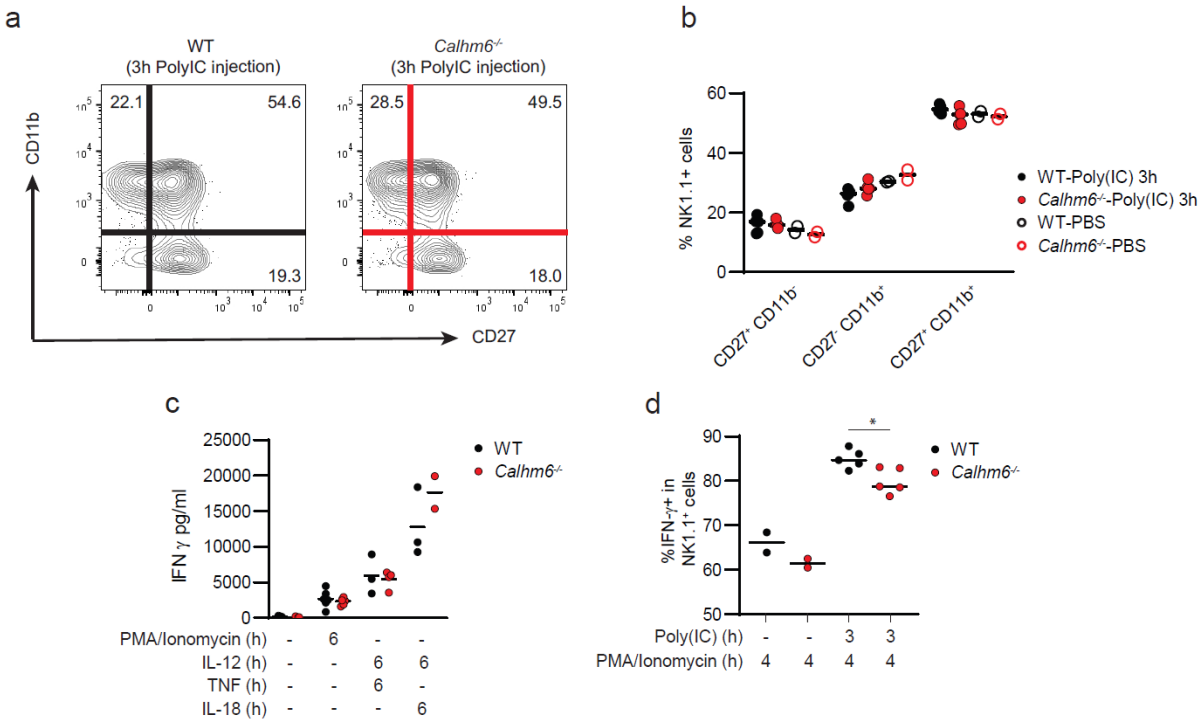


FIGURE 24: *Calhm6*$^{-/-}$ NK cells can produce IFN-γ in response to contact-independent, soluble stimuli.

WT and *Calhm6*$^{-/-}$ mice were injected i.p. with Poly(I:C) (100 µg/mouse) or PBS. At day 3 mice were sacrificed and spleen collected. single cell suspension was obtained from the spleen and cells were stained for flow cytometry. a) Representative flow cytometry panels b) pooled flow cytometry results (results from one experiment n=2, 2, 5 and 5, one-way ANOVA with multiple comparisons) c) CD3^{-} NK1.1^{+} cells were isolated from mouse spleen and cultured *in vitro* with PMA/ionomycin, IL-12 (50ng/ml), TNF (50ng/ml), or IL-18 (50ng/ml) for 6h. The supernatant was collected, and IFN-γ measured with an ELISA (pooled results from 2 independent experiments n=6, one-way ANOVA with multiple comparisons). d) single cell suspension of cells obtained like in FIGURE 23.a were incubated for 1h with PMA/Ionomycin 1x followed by 3h of BFA. Cells were stained for flow cytometry. Above is shown the pooled frequency of IFN-γ^{+} in NK1.1^{+} cells. (Results from one experiment n=2, 2, 5 and 5, one-way ANOVA with multiple comparisons).

6.3.11 *Calhm6*$^{-/-}$ macrophages are capable of responding to Poly(I:C) and developing normal Type I IFN responses *in vivo*.

I then decided to test whether the defect in early NK cell response to Poly(I:C) *in vivo* is a result of an inability of accessory cells (macrophages or DC) to detect Poly(I:C), and react to it. *In vivo* Poly(I:C) induces strong Type I IFN response in DC[457] and macrophages via TLR3 stimulation[458]. Canonical type I IFN signalling transduces through the JAK-STAT pathway leading to transcription of IFN-stimulated genes (ISG)[450]. I measured the upregulation of some ISG (*Ifnar4, Ifnar14, Ifnb1, Il1r2*) in macrophages, as a proxy of their ability of produce systemic Type I IFN and to respond to them. Mice were injected with Poly(I:C) and after 3 or 6 hours sacrificed to magnetically isolate splenic F4/80^{+} macrophages (Figure 25.a). There was no difference in ISG between WT and *Calhm6*$^{-/-}$ macrophages (Figure 25.b to e). I also checked *Il10* expression because IL-10[255] is known to downregulate IFN-γ production when secreted by macrophages, but there was no difference in *Il-10* after 3 or 6 hours of Poly(I:C) stimulation (Figure 25.f). As expected *Calhm6* was highly upregulated in F4/80^{+} cells after Poly(I:C) injection (Figure 25.g) and we confirmed that *Calhm6* was indeed absent in the *Calhm6*$^{-/-}$ mice. These results suggest that *Calhm6*$^{-/-}$ mice respond normally to Poly(I:C) and that early type I IFN responses are not impaired.

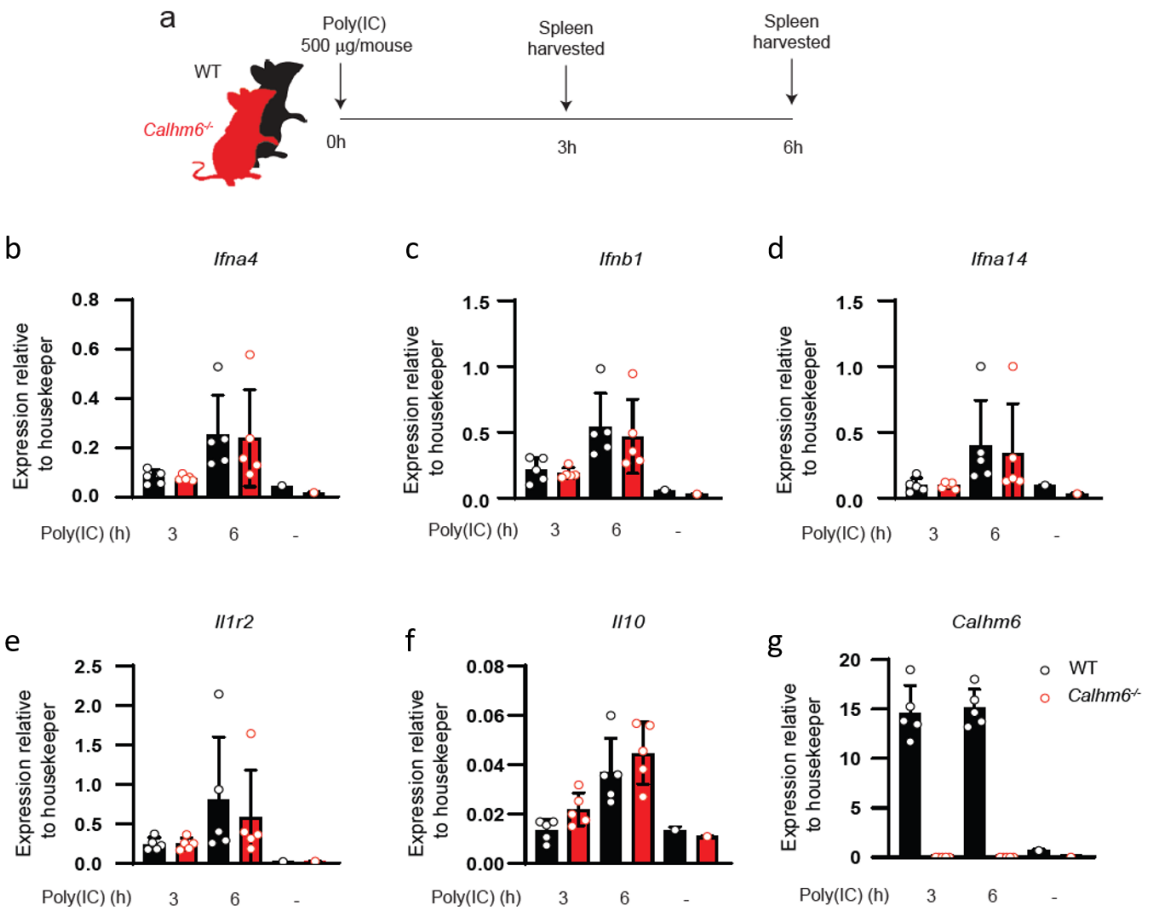


Figure 25: F4/80⁺ *Calhm6*$^{-/-}$ macrophages can respond to Poly(I:C) and develop normal Type I IFN response *in vivo*. a) experimental scheme: WT and *Calhm6*$^{-/-}$ mice were injected with Poly(I:C) 200 µg/mouse or PBS i.p. Spleens were collected 3 and 6 hours after injection and F4/80⁺ cells isolated with magnetic beads selection to collect RNA. Gene expression was assessed by qPCR. Gene expression of b) *Ifna4*, c) *Ifnb1*, d) *Ifna14*, e) *Il1r2*, f) *Il10* and g) *Calhm6* (results from one experiment, n= 5, 5, 5, 5, 1 and 1, one-way ANOVA with multiple comparisons)

6.3.12 *Calhm6*$^{-/-}$ macrophages and DC are capable of responding to *L. monocytogenes* and developing normal pro-inflammatory and anti-microbial response *in vitro*.

To test whether defect in early NK cell response to *L. monocytogenes in vivo* is a result of an inability of accessory cells (macrophages or DC) to detect the bacterium and react to it, we looked *in vivo.* I infected WT or *Calhm6*$^{-/-}$ mice with *L. monocytogenes* and after 24 hours,measured a large array of cytokines known to be important for NK cells activation, like IL-1β, IL-12p70, IL-12p40 and TNF (Figure 26.a to k). There was no significant difference in circulating cytokines between WT and *Calhm6*$^{-/-}$ mice. We need to keep in mind that measuring cytokine levels in serum gives us only a general idea of the inflammation status of the mice and NK cell activation is a local process, where soluble proteins are exchanged at a short distance and most cytokines are removed from the circulation by the targeted cells.

To confirm the serum data and look at cytokine producing-cells in isolation I established an *in vitro* system with BMDM and BMDC as the cells of interest. In the very first phase of infection macrophages and DC are the only cells infected by *L. monocytogenes* in spleen, thus these are the cells that can produce the contact and soluble factor necessary to activate effector cells[148,176,228,237,238,324,445,446]. To mimic natural infection, I infected BMDM with *L. monocytogenes* for 30 min, then killed extracellular/non-phagocytosed *L. monocytogenes* with gentamycin, and left BMDMs for 24 hours to handle and respond to the intracellular bacteria. When *L. monocytogenes* infects macrophages, it binds several PRR causing downstream activation of pro-inflammatory pathways. One of these, particularly effective for the production of pro-inflammatory cytokines is the assembly of the inflammasome complex. *L. monocytogenes* activates a series of inflammasomes due to its pore-forming toxin, flagellin and cytoplasmic DNA release[256,459,460]. The main downstream products of inflammasome activation are IL-1β (Figure 27.a) and IL-18 (not present in our previous cytokine panel, Figure 27.b), that we measured *in vitro* in the supernatant of infected BMDM. I found that both WT

and *Calhm6*$^{-/-}$ BMDM were capable of responding to *L. monocytogenes* infection *in vitro* and releasing similar levels of IL-1β and IL-18. Cytokine stimulation or bacterial infection also upregulate iNOS in macrophages and some DC[461]. iNOS is required to produce NO, an important effector in the killing of intracellular pathogens like *L. monocytogenes*[462]. To test whether the lack of CALHM6 could affect NO production in BMDM, I stimulated BMDM with LPS and Poly(I:C) for 24 h and performed a Griess test on the supernatant (Figure 27.c). Once again there was no difference between WT and *Calhm6*$^{-/-}$ BMDM. Another cytokine important for NK cell activation and production of IFN-γ, that I was not able to detect in the serum because it is sequestered on the cell surface and trans-presented to NK cells as a contact stimulus on the surface of accessory cells, is IL-15[182,463]. To check the concentration of IL-15 on our cells I measured IL-15ra expression on BMDC membrane. IL-15Rα is a high affinity IL-15 binding protein that mediates its function by presenting IL-15 on the surface of accessory cells, like a chaperone, to the responder cells that express the IL-15 signalling receptor complex IL-15Rβγ[463] (Figure 27.d; gating strategy for flow cytometry Figure 28). There was no difference in IL-15Rα extracellular expression between WT and *Calhm6*$^{-/-}$ cells after LPS or Poly(I:C) stimulation.

Finally, I tested if the increased burden of *L. monocytogenes* that we observed in *Calhm6*$^{-/-}$ mice at day 3 could have been due to the intrinsic incapability of *Calhm6*$^{-/-}$ macrophages to respond to IFN-γ and kill bacteria. Macrophages require IFN-γ stimulation to efficiently kill *Listeria*[427], without IFN-γ priming, the pathogen can escape rapidly from the phagosome and can efficiently survive and reproduce[427]. I set-up an *in vitro* infection system with WT and *Calhm6*$^{-/-}$ BMDM, naïve or pre-treated overnight with IFN-γ. Cells were infected with *L. monocytogenes* and CFUs present in the culture were measured after 0, 4 and 8 hours (Figure 27.e). As expected IFN-γ pre-treated macrophages were better at controlling *L. monocytogenes* infection, and had a significantly lower bacterial burden after 8 hours, but both WT and *Calhm6*$^{-/-}$ BMDM were equal in their ability to respond to IFN-γ and control *L. monocytogenes* replication. Taken together these results suggest that *Calhm6*$^{-/-}$ macrophages and DC are intrinsically capable of responding to Poly(I:C) and *L. monocytogenes*; they are also capable of producing soluble factors needed for activation of NK cells, and they can control bacteria, if provided with IFN-γ.

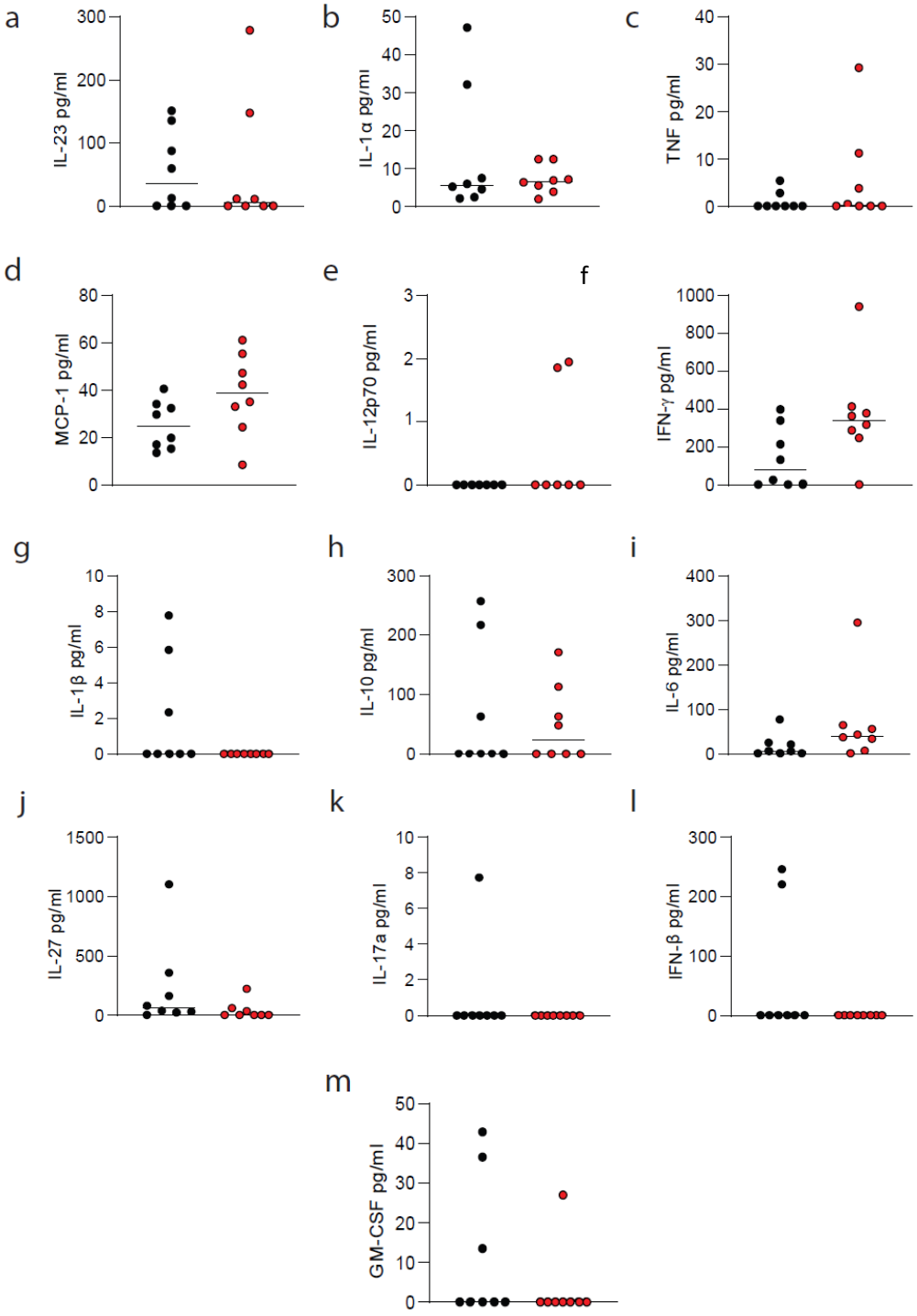


Figure 26: No differences in serum cytokine concentration between WT and Calhm6-/- mice after 24 h L. monocytogenes infection. Serum collected from WT and *Calhm6*$^{-/-}$ mice 24 h after i.p. infection with 3x10^{5} CFU of *L. monocytogenes* was run on a LEGENDplex Mouse Inflammation Panel assay to determine a) IL-23 b) IL-1α c) TNF d) MCP-1 e) TNF f) IFN-γ g) IL-1β h) IL-10 i) IL-6 and j) IL-27 k) IL-17a l) IFN-β m) GM-CSF concentrations (results of 1 experiment n=8 vs 8, Mann Whitney test).

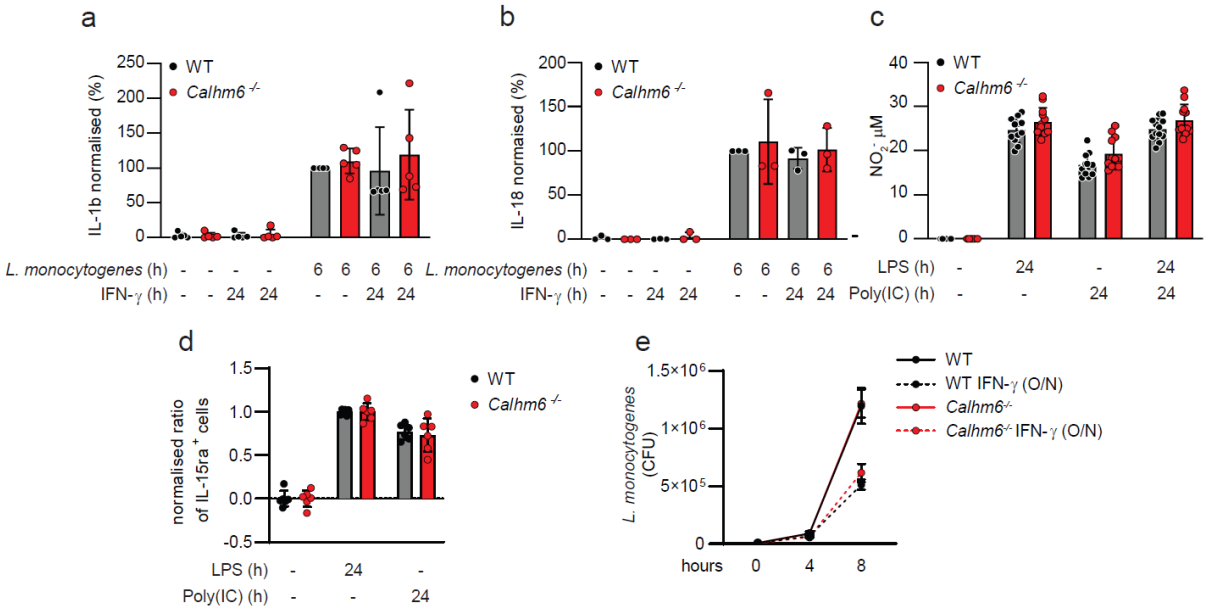


FIGURE 27: *Calhm6*$^{-/-}$ macrophages and DC are capable of responding to *L. monocytogenes* and developing normal pro-inflammatory and anti-microbial response *in vitro*. a) BMDM with or without IFN-γ (10 ng/ml) pre-treatment were grown overnight in antibiotic free medium. The cells were infected with *L. monocytogenes* (MOI 1). After 30 min gentamicin (10 ng/ml) was added to the medium to kill extracellular bacteria. Supernatant from BMDM infected with *L. monocytogenes* was collected after 6 h. The supernatant was run on ELISA to determine IFN-γ (normalised pooled results of 5 independent experiments. n=5. Kruskal Wallis test with multiple comparisons) or b) IL-18 concentration (normalised pooled results of 3 independent experiments. n=3. Kruskal Wallis test with multiple comparisons). c) NO production in WT and *Calhm6*$^{-/-}$ BMDM treated overnight with LPS or Poly(I:C) was assessed by performing a Griess test on the cell supernatant (results from one experiment n=3, Kruskal Wallis test with multiple comparisons) d) Expression of IL-15ra on BMDC after overnight LPS or Poly(I:C) treatment was measured by flow cytometry (normalised pooled results of 2 independent experiments, one way ANOVA with multiple comparisons) e) 3x10^5 BMDM with or without IFN-γ (10 ng/ml) priming were grown overnight in antibiotic free medium. The cells were infected with *L. monocytogenes* (MOI 1). After 30 min gentamicin (10 ng/ml) was added to the medium to kill extracellular bacteria. At 0, 4 and 8 h cells were harvested, gently lysed with 0.1% Triton X-100 and the lysate was plated on antibiotic free BHI plates overnight at 37°C (representative result of 3 independent experiments, n=3, two-way ANOVA).

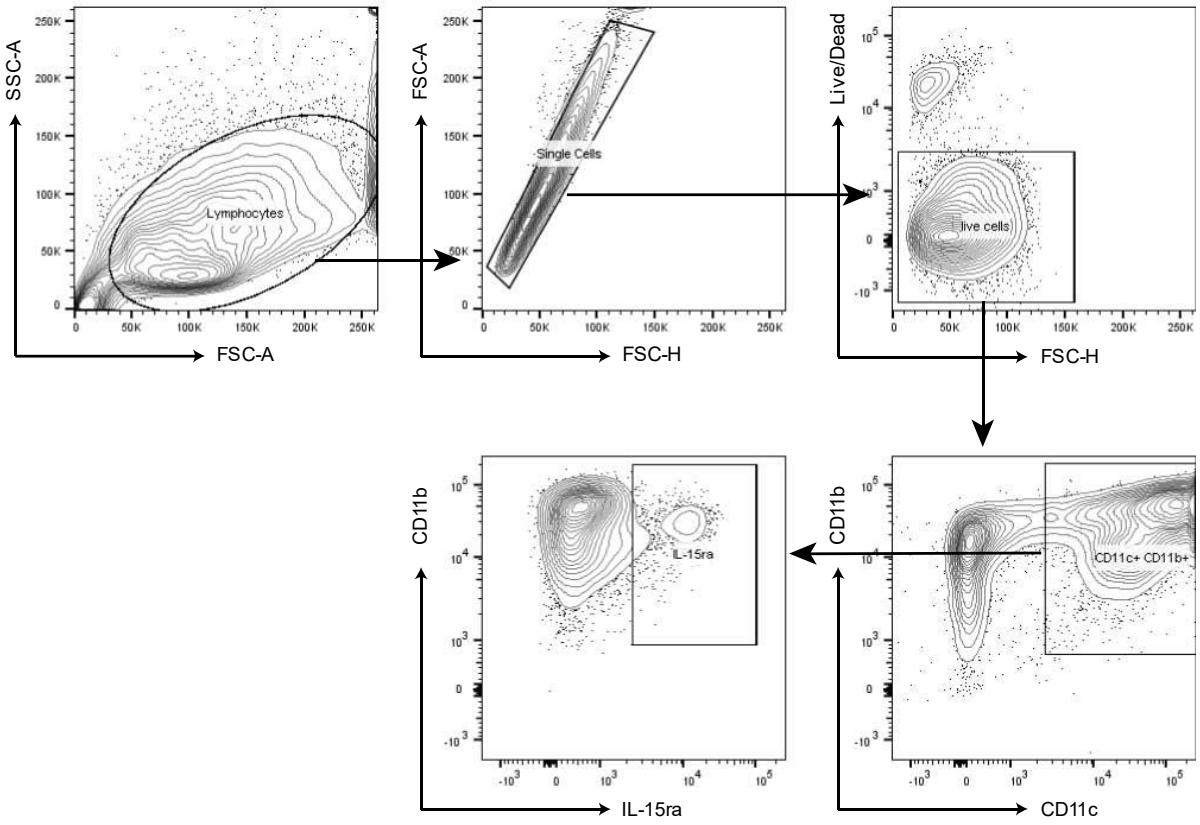


Figure 28: Flow cytometry gating strategy for IL-15ra on BMDC

6.3.13 CALHM6 expression in CD11c$^+$ cells is not required for NK-dependent IFN-γ production

I have shown how *Calhm6*$^{-/-}$ mice have reduced IFN-γ production following pro-inflammatory stimulation *in vivo*. This defect is not due to *Calhm6*$^{-/-}$ NK cells intrinsic defects, seen that they can mature normally and produce normal levels of IFN-γ following contact/cell-independent stimulation. The problem also does not seem to lay in the ability of DC and macrophages to produce soluble factors that can activate NK cells. It is possible that, as only hypothesised by Ebihara[32] and Kasamatsu[33] in discussion of their papers, CALHM6 plays a role at the interface: in the IS between macrophages/DC and NK cells. In our model, macrophages, DC and NK cells are all *Calhm6*$^{-/-}$ so we are unable to identify in which cell type CALHM6 plays a role. The fact that the highest CALHM6 expression is in macrophages would make them the most obvious candidate. To formally solve this problem, we could to use our *Calhm6*$^{fl/fl}$ mice to create conditional KO strain that could selectively eliminate CALHM6 in specific cell type. The first conditional KO strain that we created was CD11c specific. We obtained this mouse by first crossing our original *Calhm6*$^{fl/fl}$ with a flippase-expressing C57BL6/J strain. The FLP-FRT system for DNA recombination is similar to the Cre-lox one[464]. In this case we needed to excise the Flip cassette because it was interfering with CALHM6 expression by adding a LacZ cassette between exon 1 and 2 (Figure 28). Mice so obtained were then crossed with an *Itgax*$^{cre/-}$ expressing strain to obtain *Itgax*$^{cre/-}$ *Calhm6*$^{fl/fl}$ mice that had specific deletion of CALHM6 in CD11c$^+$ cells (Figure 29).

The choice of CD11c specific KO was dictated by the fact that Ebihara and Kasamatsu had used BMDC and CD8$^+$CD11c$^+$ cells in their studies[32,33]. In their *in vitro* cultures, WT NK cells failed to produce normal levels of IFN-γ when co-cultured with activated *Calhm6*$^{-/-}$ BMDC or CD8$^+$CD11c$^+$ cells. Taking this to account I hypothesised that NK cells from *Itgax*$^{cre/-}$*Calhm6*$^{fl/fl}$ would produce less IFN-γ *in vivo* 3 hours after Poly(I:C) stimulation, when we see the strongest NK cells IFN-γ defect in complete *Calhm6*$^{-/-}$ mice (Figure 30.a). We were surprised to see that there was no difference in the percentage of NK cells positive for IFN-γ between WT and *Itgax*$^{cre/-}$*Calhm6*$^{fl/fl}$ mice (Figure 30.b). As expected we also did not

see differences in Granzyme B (Figure 30.c). We can conclude that, unlike previously suggested, CALHM6 expression in $CD11c^+$ cells is not required for NK cells activation. It is possible that in the spleen NK cells are mostly activated by other CALHM6 positive cells, like RPM, MZM or MMM. This conclusion is also well in line with my own data from Chapter 3 showing that highest expression of CALHM6 both *in vivo* and *in vitro* is actually in macrophages, and is rather negligent in DC.

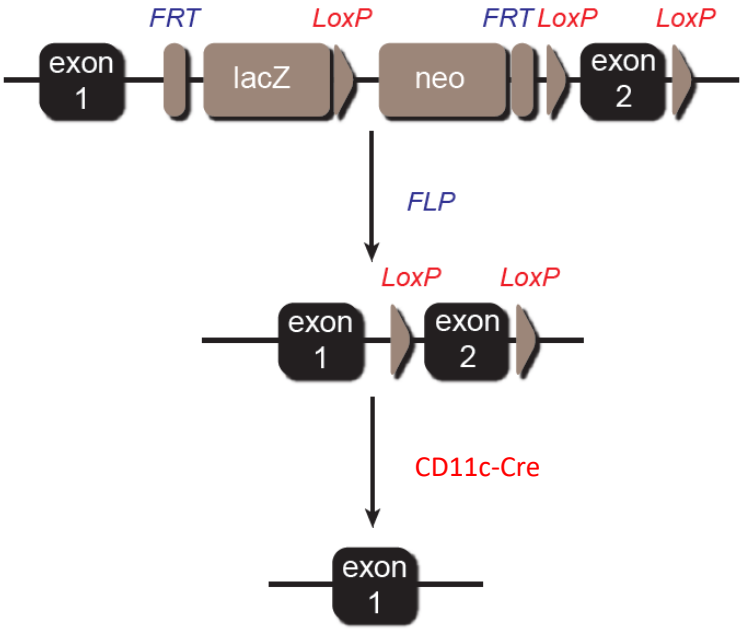


Figure 29: Breeding strategy for *Itgax$^{cre/-}$Calhm6$^{fl/fl}$*. Calhm6fl/fl were crossed with flippase-expressing mice to excise the LacZ and Neo cassette. The resulting mouse strain was then crossed with a line expressing a CD11c-specific Cre (*Itgax$^{cre/-}$*) to obtain a CD11c conditional CALHM6 KO.

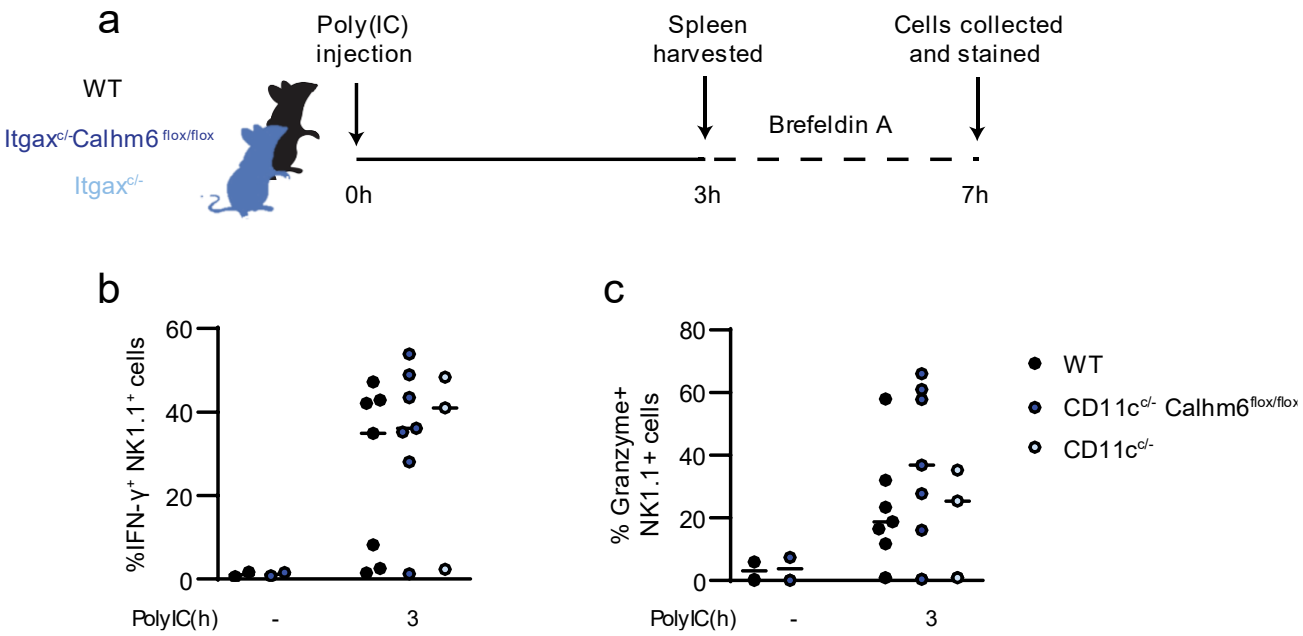


FIGURE 30: CALHM6 expression in CD11c+ cells is not required for NK cells-dependent IFN-γ production after Poly(I:C) stimulation *in vivo*. a) Experimental setup: WT *Itgaxre$^{c-/}$Calhm6$^{fl/fl}$* and *Itgax$^{cre/-}$* control mice were injected i.p. with Poly(I:C) (250 µg/mouse) or PBS. After 3 h spleens were harvested and single cell suspension obtained and cultured in Brefeldin A. After 4 h of incubaion cells were collected and stained for flow cytometry. Pooled flow cytometry results showing percentage of b) IFN-γ$^+$ or c) Granzyme B$^+$ in NK1.1$^+$ cells. (pooled results from 2 independent experiments n=2, 2, 7, 7, 3, Kruskal-Wallis test with multiple comparisons)

6.3.14 *In vitro* models of co-culture between macrophages/DC and NK cells are not suitable to study the role of CALHM6 in NK cells activation.

Due to the time-consuming nature of creating conditional KO mice for CALHM6 I tried to optimise an *in vitro* co-culture system to study the role of CALHM6 in different cell types, this would allow to mix and match WT and *Calhm6*$^{-/-}$ macrophages or NK cells for more advanced mechanistic studies. I based my attempts on the co-culture system established in the 2014 Kasamatsu paper[33], in which BMDC or freshly isolated CD11c^{+} and F4/80^{+} cells were co-cultured with primary NK cells from mouse spleens for 24 hours after Poly(I:C) stimulation. After 24 h the supernatant was collected, and IFN-γ measured via ELISA. The authors of the study showed that, when either DC/macrophages or NK cells are *Calhm6*$^{-/-}$, the IFN-γ concentration is reduced and the biggest reduction was measured when both cell types were *Calhm6*$^{-/-}$. Kasamatsu's results suggested that CALHM6 was important in both cell types but mostly in macrophages and DC[33]. After several attempts we had to conclude that none of these co-culture conditions were reproducible in my hands. I first tried co-culturing negatively selected NK cells with BMDM and BMDC for 24 hours after Poly(I:C) stimulation (Figure 31.a and b). The IFN-γ concentration in the supernatant was the same. Using different doses of Poly(I:C) or switching to positive beads selection for NK cells to increase cell purity also did not show any difference. Even when we used *L. monocytogenes* or LPS as stimulus instead of Poly(I:C) there was no difference in the IFN-γ concentration. All the experiments performed showed a very high variability between biological and technical replicates, it is possible that very small initial variation in the cell number or purity had an amplified effect after prolonged co-culture. To address whether variation was caused by contaminated T cells and or other adaptive cells possibly producing cytokines like IL-2, we generated *Rag*$^{-/-}$*Calhm6*$^{-/-}$ mice. Rag mice lack mature B and T lymphocytes because of their inability to perform V(D)J recombination[465]. When I magnetically isolated F4/80^{+} cells from these mice and co-cultured them with flow cytometry sorted NK1.1^{+}CD3^{-} cells (Figure 31.c) to further increase the purity of the populations, again, I did not see any difference between co-cultures of WT and *Calhm6*$^{-/-}$ cells. This

was true at both 6 and 24 hours. To avoid the possibility that the sorting, being done magnetically or by FACS, could activate the cells independently of Poly(I:C), thus masking the *Calhm6*$^{-/-}$ phenotype, I also cultured whole *Rag*$^{-/-}$ and *Rag*$^{-/-}$*Calhm6*$^{-/-}$ spleens with Poly(I:C) (Figure 31.d). Again, variability was quite high, and there was no difference between WT and *Calhm6*$^{-/-}$ cells. Regrettably we were not able to reproduce the data from Ebihara or Kasamatsu[32,33]. I hypothesised that any differences in contact-dependent activation of NK cells in WT and *Calhm6*$^{-/-}$ cultures must happen quite early on during the co-culture, as shown by the kinetic of the *in vivo* responses to Poly(I:C), and, because both WT and *Calhm6*$^{-/-}$ macrophages and DC are capable of producing soluble cytokines that can activate NK cells, the accumulation quickly compensates for any initial defect or delay. I might not be able to pick up such delay due to the fact that at very early time points the IFN-γ is not yet detectable by ELISA.

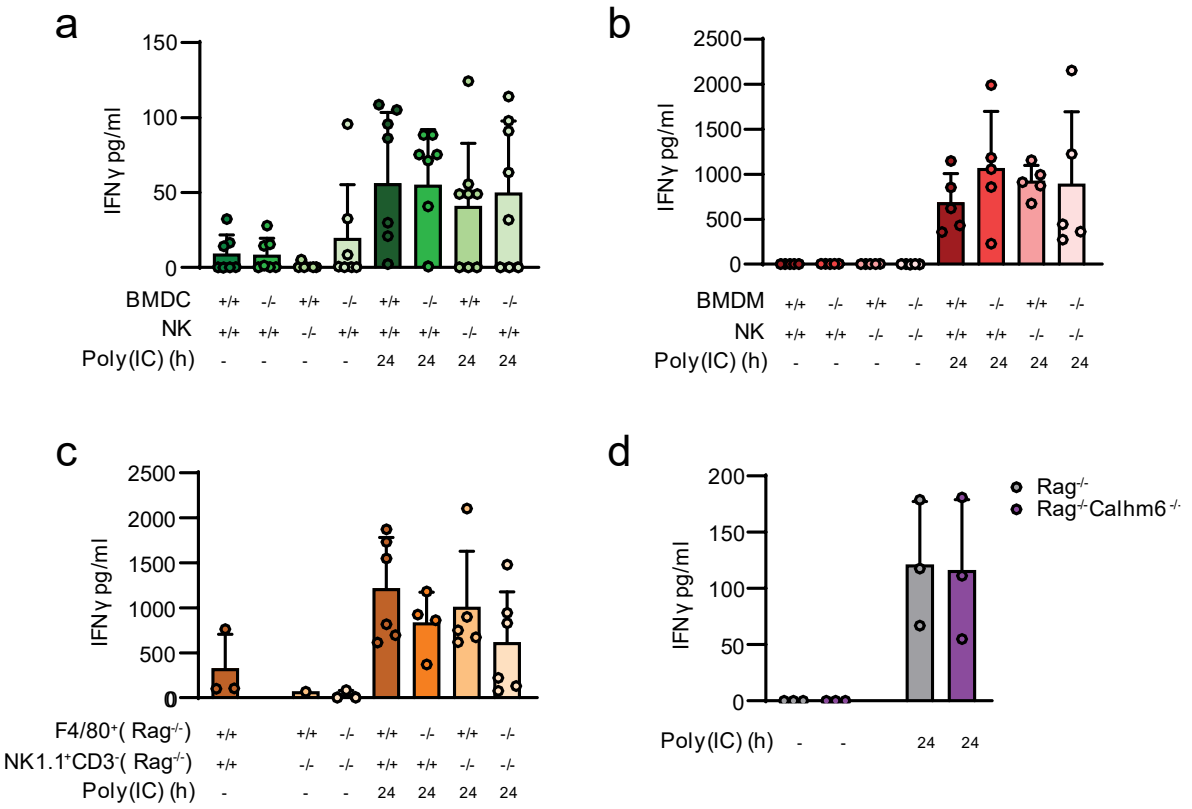


FIGURE 31: *In vitro* co-culture of macrophages/DC and NK cells are not suitable to study difference in IFN-γ production between WT and *Calhm6*$^{-/-}$ mice. a) 1.5x10^5 WT and *Calhm6*$^{-/-}$ BMDC or b) BMDM were co-cultured with 3x10^5 primary WT and *Calhm6*$^{-/-}$ NK cells negatively isolated with magnetic beads from mouse spleen. The genotype of the cells in the co-culture is indicated in the graph legend. The cells were left untreated or stimulated with Poly(I:C) (50 mM/ml) for 24 h. The supernatant was collected, and IFN-γ measured with ELISA. a) (pooled results from 3 independent experiments n=7 vs 8, Kruskal-Wallis test with multiple comparisons) b) (pooled results from 2 independent experiments n= 5 vs 5). The primary cells from c) and d) come from Rag$^{-/-}$ and Rag$^{-/-}$Calhm6$^{-/-}$ mice. c) 1.5x10^5 primary F4/80$^+$ magnetically isolated from mice spleen were co-cultured with 3x10^5 NK1.1$^+$CD3$^-$ FACS sorted cells. The cells were left untreated or stimulated with Poly(I:C) for 24 h. The supernatant was collected, and IFN-γ measured with ELISA. (Pooled results from 2 independent experiments n=6 vs 6, Kruskal-Wallis test with multiple comparisons) d) Spleen harvested from naïve mice were mashed to obtain single cell suspension and 3x10^5 cells cultured with or without Poly(I:C) stimulation. After 24 h the supernatant was collected, and IFN-γ measured with ELISA. (results from one experiment n= 3 vs 3, Kruskal-Wallis test with multiple comparisons)

6.4 Discussion

6.4.1 CALHM6 is important for NK cell-derived early production of IFN-γ in infections

In this study we show for the first time that CALHM6 is important for the early innate response to bacterial infection. When *Calhm6*$^{-/-}$ mice were infected with *L. monocytogenes* NK cells failed to produce normal levels of IFN-γ compared to the WT. The same phenotype was present when the mice were injected with Poly(I:C) instead of *L. monocytogenes*. With both stimulations the defect in IFN-γ production appears very early into the immune response (3 h for Poly(I:C) and 18 h for *L. monocytogenes*). In later stages of the infection (12 h for Poly(I:C) and 3 days for *L. monocytogenes*) this difference disappears, implying that CALHM6 is important for the control of the kinetic of the response, with *Calhm6*$^{-/-}$ mice struggling to initiate their immune activation and so lagging behind in the bacteria control. The shift in the kinetic is also supported by the higher IL-10 concentration in serum of day 3 infected WT mice compared to *Calhm6*$^{-/-}$ mice. IL-10 is produced by NK cells once they have exhausted their IFN-γ production function[256,466] and *Calhm6*$^{-/-}$ NK cells delay both early IFN-γ production and the subsequent switch to IL-10.

Following *L. monocytogenes* infection, IFN-γ production peak is driven almost entirely by NK cells, and happens in 20-24 hours[255,330,446,467] when adaptive immunity is not required for bacterial control yet[303]. By activating TLR3 signalling[468] the infection should guarantee early upregulation of CALHM6 in infected macrophages, as shown by us in chapter 1. MZM and MMM are the first cells to be infected by *L. monocytogenes,* after the infection has disseminated in blood[323,324,469]. Subsequently, *L. monocytogenes* is transferred from macrophages to CD11c^{+} DC that migrate to the PALS of the WP to form clusters that can prime T cells to start the adaptive response[176,324,446]. It is unclear exactly where and when NK cell activation happens in this model or which cells are responsible for it. Both macrophages and DC once infected by *L. monocytogenes* are capable of inducing IFN-γ secretion from NK cells *in vitro*[238,470,471] and both cell types get infected by *L. monocytogenes* in the first phases of

infection, albeit macrophages are the first ones to do so. NK cells activation could happen directly in the RP where NK cells reside at steady state[444,446,472] or at the boundary between RP and WP, near the MZ where they cluster with $CD11b^+$ cells[330]. In this case macrophages would be the cells mainly responsible for activation. Imaging experiments though, have shown that RP NK cells do not yet produce IFN-γ 12 hours after infection[446]. Alternatively, NK cells could produce IFN-γ after migration to the WP where their action helps sustaining activation of DC and macrophages to allow optimal T cell priming[446,472]. In this case DC and macrophages could activate NK cells because they are both part of innate cell clusters in the PALS[444,446,473]. The fact that the defect in IFN-γ production in *Calhm6*$^{-/-}$ mice happens early in the infection, together with our data showing that CALHM6 is mostly expressed in splenic macrophages and our genetic data showing that conditional deletion of CALHM6 in $CD11c^+$ DC cells does not affect NK cell activation, suggests that the lack of IFN-γ production could be driven by a failure of CALHM6-deficient macrophages to activate, or properly prime, NK cells. Taken together these results show that CALHM6 is important for NK cell-mediated production of IFN-γ in the early stages of *L. monocytogenes* infection.

While IFN-γ production in NK cells was deficient after *L. monocytogenes* and Poly(I:C) stimulation, such defect was not detected in Granzyme B production. As already suggested by Kasamatsu et al[33] CALHM6 deficiency only affects the IFN-γ-producing ability and not the cytotoxicity of NK cells. Granzyme B is a serine protease most commonly found in NK cells and Cytotoxic T cells granules usually secreted together with perforin to cause apoptosis of target cells mainly via caspases cleavage[474], so in this study we used Granzyme B production as a proxy for cytotoxic activity.[32,33]. Our flow cytometry data show how activated NK cells are divided in two distinct sub-population, an IFN-γ^+ "pro-inflammatory" population, and a Granzyme B^+ "cytotoxic" one. Albeit, most stimulation can upregulate both cytokines production and cytotoxicity because activation of STAT1/4 and 5 causes increase in IFN-γ secretion and perforin expression[148] studies of human NK cells found that some NK cells are naturally poised to become more pro-inflammatory or more cytotoxic based on their levels

of transcription factors Eomes and T-bet[106]. In brief we can say that CALHM6 deficiency does not affect NK cells cytotoxicity in the early phases of infection.

6.4.2 CALHM6 is important for the control of *L. monocytogenes* in the early phases of infection

In this chapter we showed for the first time that *Calhm6*$^{-/-}$ mice fail to control *L. monocytogenes* burden in the early stages of infection. 72 hours post-infection *Calhm6*$^{-/-}$ mice had significantly higher bacterial burden in the spleen and greater weight loss compared to the WT controls. This was true for both high and low initial doses of *L. monocytogenes* infection. Knowing the importance of IFN-γ in the first phases of infection for the activation of macrophages , we can probably put the difference between WT and *Calhm6*$^{-/-}$ mice down to the early lack of IFN-γ. Macrophages need IFN-γ stimulation to efficiently kill *L. monocytogenes* that has been phagocyted, but as yet to escape the vacuole[327,427,430,431], and mice that are *Ifngr*$^{-/-}$, *Itax*$^{cre/-}$*Ifngr1*$^{fl/fl}$ or that are injected with anti-IFN-γ antibodies are more susceptible to *L. monocytogenes* infection[335,427,475]. Right after infection the bacterium is mostly contained in MZM and MMM[323,324,446,469,473], failure to keep *L. monocytogenes* replication under control at this stage would result in a higher bacterial burden at peak infection. We did not measure time points for IFN-γ production earlier than 18 hours but data from *Itax*$^{cre/-}$*Ifngr1*$^{fl/fl}$ mice in which DC are incapable of responding to IFN-γ, show that a defect in IFN-γ production from NK cells earlier than 18 h can increase the bacterial burden by disrupting the IL-12 feedback produced early on[335]. The defect is also already present 3 h after Poly(I:C) stimulation, so we can speculate that CALHM6 is required for this very early IFN-γ wave that could be initiated by *L. monocytogenes*-infected CALHM6 positive macrophages.

We showed for the first time that, at day 3 post-infection, *Calhm6*$^{-/-}$ had higher serum levels of the pro-inflammatory cytokines IFN-γ and IL-6 while the anti-inflammatory IL-10 was lower than in the WT controls. No other cytokines tested showed any difference. When NK cells-specific IFN-γ production at day 3 was tested by flow cytometry there was no significant difference between WT and *Calhm6*$^{-/-}$

mice, if anything, there was a slightly higher production of IFN-γ from Calhm6$^{-/-}$ cells. The higher bacterial burden could explain the increase pro-inflammatory cytokines production, the higher inflammation and the increased weight loss in *Calhm6*$^{-/-}$ from day 2 onwards. We believe that CALHM6 is involved only in the very early activation of NK cells and by day 3, when the immune reaction to *L. monocytogenes* is well established, there are compensatory factors, likely soluble ones (e.g. cytokines), that can efficiently activate NK cells despite CALHM6 deficiency. The reduction in IL-10 production that we see in *Calhm6*$^{-/-}$ is of interest. While *L. monocytogenes* induces basal levels of IL-10 production from CD11b^{+} and CD11c^{+} cells in the spleen few hours after the infection[335,427], after 72 h a large part of IL-10 is produced by the NK cells themselves that switch from producing IFN-γ to IL10[286,256,476,477] rarely producing both at the same time[255]. IL-10 is a traditionally anti-inflammatory cytokine that function on both innate and adaptive immune cells by reducing tissue damage that can be caused by excessive and uncontrolled immune response[478]. In the case of *L. monocytogenes*, timing of IL-10 production matters to balance anti-pathogen responses and immunopathology. Both innate and acquired immunity to *L. monocytogenes* are increased in IL-10-deficient mice[479,480] and a series of studies from the Lenz group[255,256,467] and others[481] have shown that NK cell-derived IL-10 also makes mice more susceptible to infection. This explains why in some cases, depleting NK cells ameliorate the phenotype after *L. monocytogenes* infection[255,353,426], despite their beneficial role in IFN-γ production. Unfortunately, we were not able to measure IL-10 release from NK cells specifically by flow cytometry because the antibodies against it are not adequate[482]. It is possible that in our model the delay in IFN-γ production at early stages also causes a delay in NK cell-switch to IL-10 production at day 3.

6.4.3 Calhm6-/- mice can mount an effective T cell memory response

Even if bacterial burden in *Calhm6*$^{-/-}$ mice at day 3 is higher, the mice are still capable of efficiently clearing the infection by day 7. The complete clearance of *L. monocytogenes* is generally attributed to the activation of the adaptive immune system, especially IFN-γ producing and cytotoxic CD8^{+} T cells[303,483], but also CD4^{+} T cells[303,484], are required for sterilising immunity. SCID mice, that lack mature

B and T lymphocytes, can survive the primary infection but develop chronic disease[485]. In *L. monocytogenes* infection T cells are primed in the first 3 days of infection by antigen-presenting $CD11c^+$ that have migrated in the PALS[247,303,428,446]. These APC require IFN-γ stimulation to mature and effectively prime T cells[83,245] but we know that, despite an early defect in IFN-γ production, *Calhm6*$^{-/-}$ cells can compensate and produce physiological levels of IFN-γ by day 3. It looks likely that *Calhm6*$^{-/-}$ mice are capable of clearing *L. monocytogenes* because CALHM6 deficiency does not cause a defect in T cell priming as it does for NK cell priming.

In support of this conclusion is the fact that when mice are re-challenged with *L. monocytogenes* 6 weeks after primary infection, there is no difference in the response between WT and *Calhm6*$^{-/-}$ mice, suggesting that induction of specific memory T and B cells is intact. While the production of anti-*L. monocytogenes* antibodies is not particularly important, being the bacterium life cycle intracellular[303], the T cell response is key for the clearance. Re-challenge with *L. monocytogenes* promotes a rapid expansion of the memory T cell population that start to produce IFN-γ few hours after infection, thus bypassing the need for NK cells during re-challenge[303]. This is why we were able to inject our mice with a ten times higher dose of *L. monocytogenes,* compared to primary infection, without causing a severe phenotype. These results taken together, indicate that *Calhm6*$^{-/-}$ mice can mount a T cell memory response that is efficient enough to clear *L. monocytogenes* infection at the same rate as WT mice do. There are many similarities between cell mediated activation of NK cell and T cells so it will be interesting to define *in vitro* T cell activation dependency on CALHM6.

6.4.4 CALHM6 is important for the accessory cell-mediated activation of NK cells

While *Calhm6*$^{-/-}$ NK cells *in vivo* cannot be efficiently activated to produce IFN-γ after Poly(I:C) or *L. monocytogenes* stimulation, they are not intrinsically incapable to respond to soluble stimuli by secreting normal levels of IFN-γ. While some viruses can directly activate NK cell by binding membrane ligands like NKp44 or NKp46[120,122] no such direct activation has been recognised in the case of *L. monocytogenes* infection. In this model NK cells, like T cells, require both soluble and contact stimuli

to be activated [84,148,223,228]. Both macrophages and DC, once infected by *L. monocytogenes* can activate NK cells and the main soluble factors used by these cells are IL-12 and IL-18[224,228,229,231,237,238,281,486], with IL-15[182,240,487,488], Type I IFN[281,486,489,490], IL-2 and TNF[148] also important albeit to a lesser extent. IL-15 is an unconventional soluble signal because it is presented to NK cells bound to the IL-15R upregulated on the membrane of the activating DC[182,240,488]. Some of these soluble factor, like IL-12 and IL-18 require the formation of an IS in which the cytokines are delivered in a targeted way via vesicle release[223,237]. The macrophage/DC-NK IS, like the DC-T cell one requires binding of integrins, like LFA-1-ICAM1[491], at the cellular interface and rearrangement of the actin cytoskeleton to form a ring-shaped structure[248,250,491] that surrounds a synaptic cleft in which soluble and contact-signal can be presented efficiently[223–225,237]. The cause of *Calhm6*$^{-/-}$ faulty activation could be then the concentration of soluble factors that macrophages and DC provide, a splenic anatomical defect that does not allow NK cells to co-localise effectively with activating cells, or a defect in the immunological synapse formation and in the presentation of contact stimuli.

Serum level of pro-inflammatory cytokines is the same between *Calhm6*$^{-/-}$ and WT mice 24 hours post-infection. While serum levels of cytokines are not always indicative of local concentration in inflamed sites, this data suggest that *Calhm6*$^{-/-}$ innate cells are capable of producing soluble stimuli that can activate NK cells (IL-12 in particular). WT and *Calhm6*$^{-/-}$ BMDM and BMDC can also produce the same amount of IL-1β, IL-18 and membrane-bound IL-15 after pro-inflammatory stimulation *in vitro*. As we discussed, the defect seen in NK cells IFN-γ production must be due to a defect in the activation process and not to an intrinsic incapability of NK cells to upregulate or secrete IFN-γ. With this second series of data we can exclude that it is a lack of soluble stimuli produced by DC or macrophages that causes the defect in activation. These results suggest that CALHM6 deficiency causes a failure in the cell-dependent activation process. This could be due to a failure to form a stable synapse all together, or to a problem in recruiting the right activating molecules to the cellular interface. For example we know that IL-12 and IL-18 are directionally secreted in the synaptic cleft to increase their efficacy[223,237].

There is also no difference in Type I IFN levels in the serum 24 hours post-infection and F4/80^{+} macrophages have the same levels of Type I IFN response gene upregulation in WT and *Calhm6*$^{-/-}$ sorted macrophages after 3 and 6 h of Poly(I:C) stimulation *in vivo*. It was important to establish this because, first it tells us that macrophages can sense and react to Poly(I:C) normally, and second that they can elicit physiological Type I IFN response. Type I IFNs were proposed to activate NK cells in the right condition[281,486,489,490], and more recently have been linked to early IL-10 upregulation in *L. monocytogenes* infection[256,285]. We can then exclude that the defect that we see in *L. monocytogenes* control is due to differences in innate sensing or the type I IFN pathway activation.

6.4.5 *Calhm6*$^{-/-}$ mice can control H3N2 Influenza A infection efficiently

Calhm6$^{-/-}$ mice can control Influenza A infection as well as WT mice. *Calhm6*$^{-/-}$ mice do not have a higher viral burden in the lungs at day 4 post-infection and they do not lose more weight than the control mice. This is an interesting result because, like in the case of *L. monocytogenes*, NK cells are important in the early phases of Influenza infection, together with CD8^{+} they produce IFN-γ[438] that is required to stimulate ISG like IRF1, that are key for the viral clearance[68]. Like in the *L. monocytogenes* model, DC and alveolar macrophages are necessary to activate NK cells due to contact signal and the production of soluble stimuli, especially IL-12[249,257,452]. Unlike in the *L. monocytogenes* model though, Influenza A viruses can directly activate NK cells by the binding of the surface protein hemagglutinin to the NKp46 activating receptor on the NK cell surface[120], thus helping the formation of the DC-NK cells activating IS[249]. It is possible that this direct activation bypasses the requirement of CALHM6 in the cell-mediated activation of NK cells. Furthermore, contrary to the *L. monocytogenes* model, the benefits of IFN-γ in Influenza infection are more nebulous. IFN-γ might not be required for an early control of the infection, or Granzyme B may be compensating for any IFN-γ defect. IFN- γ was even reported to be deleterious[492] for its blocking of IL-5 production[454], that affects the formation of an appropriate memory response[453]. For example *Ifng*$^{-/-}$ or *ifngr*$^{-/-}$ mice do not undergo normal contraction of the memory T cell pool after primary infection and in consequence have a stronger

recall response[493]. To test CALHM6 effect on the Influenza A response then, we might have to investigate the strength of the recall instead of the primary infection. It is also possible that, considering the specific time frame in which CALHM6 is important in *L. monocytogenes* infection, we are looking at the wrong time point. If there was a substantial difference in the viral burden at earlier time points though, we would expect to see it reflected by differences in weight loss. After these initial experiments we can say that CALHM6 is not important in the early control of Influenza A infection.

6.5 Limitation of the study

While *L. monocytogenes* is a very well-known model of infection there are discrepancies in the literature on exactly which type of cells are infected *in vivo*, in which time fashion, and what cytokines are exactly required or dispensable to upregulate IFN-γ. Some of these discrepancies can be explained by the bacterial load used for the initial infection, the strain of mice used in the study, for example BALB/c mice are more susceptible than C57BL/6 to *L. monocytogenes*[293,294]. Most relevant for our study, the way of administering *L. monocytogenes* influences the kinetics of the infection. Most of the published studies on *L. monocytogenes* infection of spleen were performed after intravenous injections while we used an intraperitoneal one. This could mean that there are some discrepancies in *L. monocytogenes* uptake and processing between our model and the ones published.

While we were able to measure levels of cytokines in serum 24 hours after infection, these levels do not necessarily recapitulate the concentrations of cytokines that NK cells are exposed to in their spleen niche. This is especially true for important cytokines like IL-12 and IL-18 that get delivered to the NK cells through the synaptic cleft and so are often non-detectable in the supernatant. To answer the question whether the lack of NK cells activation could be due to a defect in synaptic IL-12 and IL-18 delivery, we plan to perform macrophage-NK cell synapse confocal imaging in WT and *Calhm6*$^{-/-}$ cells.

A cytokine that we could not measure satisfactory is IL-10 to confirm that the differences in IL-10 production were due to NK cells specifically. Unfortunately, we were not able to stain IL-10 for flow cytometry measurement, this is a well-known problem usually resolved by using IL-10 reporter mice. Being the question only marginally connected to our main aim of defining CALHM6 role in infection, we decided not to undergo the expensive and time-consuming measure to generate *Calhm6*$^{-/-}$ IL-10 reporter mice.

Although we tested whether *Calhm6*$^{-/-}$ mice were capable of generating a memory response to *L. monocytogenes* infection by re-challenging mice after six weeks, we did not check whether *Calhm6*$^{-/-}$ and WT mice are capable to maintain this memory response at the same rate for longer stretches of time. While the initial recall response is mostly $CD8^+$-mediated, correct priming of $CD4^+$ T cells is important for the long-term maintenance of the memory response[494,495]. Because other preliminary unpublished data from members of our lab suggested that there was no difference in the priming of $CD4^+$ T cells between *Calhm6*$^{-/-}$ and WT mice we decided that this was not the most interesting line of questions to follow up on.

Our exploration of the role of CALHM6 in anti-viral immunity was limited to one condition of Influenza A virus. While this did not show any defect, it is possible that other dsRNA viruses or the same virus but with a different concentration or at different time points, would have highlighted a role for CALHM6 in protection from viral infection. While this is an interesting line of questioning, we believed that the in-depth investigation of not one but two infection models, was not possible in the time allocated for this DPhil project. This was especially true because the *in vivo* role of CALHM6 was just a part of my bigger investigation of the role of CALHM6 in the immune system.

The most frustrating part of this project was our failure to reproduce the published *in vitro* co-culture experiment, despite trying many different conditions. This is not only an obstacle for the understanding of which cells need CALHM6 expression to function *in vivo*, but, more disappointingly, this took away an important tool to study the mechanism of CALHM6 function *in vitro*. If we had a

functioning model, we could have tested various NK cells activating factors that might have rescued our phenotype, as well as trying to develop CALHM6 inhibitors that we could then test *in vivo*. Unfortunately, we had to limit our study to the measurement of NK cell activating factors in our *in vivo* system, making the experiments more complicated, time consuming, and subjected to more variables.

6.6 Conclusions

The main aim of this chapter was to define the role of CALHM6 in the immune system during infections. We discovered that CALHM6 is important for NK cell-dependent production of IFN-γ in the early phases of *L. monocytogenes* infection but was compensated for at later stages and IFN-γ production increased 3 days later. We also found that this early deficiency in IFN-γ affects the immune response of *Calhm6*$^{-/-}$ mice to *L. monocytogenes.* These mice have a higher bacterial burden at day 3 post infection (peak infection) as well as higher serum levels of the pro-inflammatory cytokines IL-6 and IFN-γ and lower levels of the anti-inflammatory cytokine IL-10. The fact that IL-10 is also produced by NK cells around day 3 of infection, as negative feedback to their early IFN-γ secretion, suggests that the initial delay in NK cells activation continues to day 3 and NK cells at this stage have not yet fully switched to resolution phase and IL-10 production.

We also demonstrate that CALHM6 is likely involved in the cell-cell interaction between macrophages/DC and NK cells. *Calhm6*$^{-/-}$ NK cells can be fully activated when stimulated in isolation by contact-independent soluble signals. Similarly, *Calhm6*$^{-/-}$ macrophages and DC can produce these signals when stimulated *in vitro*. They can also efficiently kill invading *L. monocytogenes in vitro*, if provided with IFN-γ So, *in vitro*, when stimulated experimentally, both cells are capable of performing their anti-microbial functions, but somehow, they fail to communicate and elicit these functions from each other *in vivo*.

We could not optimise an *in vitro* system to mechanistically in which cell type CALHM6 is most important, but, genetically, when we tested Poly(I:C) dependent NK cell activation in *Itgax*$^{cre/-}$ *Calhm6*$^{fl/fl}$ mice we could exclude CD11c^{+} DC as the cell type of interest.

7 Mechanism of CALHM6 function in macrophages

7.1 Introduction

7.1.1 The CALHM6 proteins function

After we established that CALHM6 is highly expressed in macrophages, and showed that it is important for cell-mediated activation of NK cells in *L. monocytogenes* infection, in this chapter we want to investigate the cellular role of CALHM6 and its mechanism of action. There is close to no literature on this topic so, to start our investigation, we decided to look at other CALHM proteins whose function had already been established as a way to build our hypothesis. We considered this a sound choice because all CALHM proteins have a high sequence and structural homology[22,23,26,92] and the resolution of their three-dimensional structure has shown that all CALHM proteins form similar membrane channels. The smallest CALHM channel is formed by eight (CALHM1/3)[496] monomers but they can go all the way up to 12 (CALHM2, CALHM5)[22,25]. Interestingly, the best-known of these channels is the CALHM1/3 one that localised in taste bud cells where it helps forming the neuronal synapse between taste cells and sensory neurons. CALHM1/3 channel releases ATP from the taste cell into the synaptic cleft where it works as a neurotransmitter and activate sensory neurons. Our first hypothesis then, is that CALHM6 could also be important at the cell synapse, in this case at the immunological synapse between macrophages/DC and NK cells, necessary for efficient NK cell activation.

Both the CALHM1/3 and CALHM2 channels have been defined in the literature as non-selective ion channel, large enough to secrete ATP[12,18,30]. In the case of CALHM2 the ATP secretion might not happen at the synapse but it is important for microglial activation in the central nervous system (CNS)[30,31]. Because extracellular ATP is also an important pro-inflammatory signal in immune system [1,497] and has been shown to be an actor in DC-mediated T cell activation[95,498] our second hypothesis was that CALHM6 would behave like an ATP channel in IS. Judging by its structure, we can say that the pore formed by CALHM6 is wide enough to allow the passage of ATP or even bigger metabolites[22].

Another function suggested for CALHM2 by Cheng et al. very recently, was that of a chaperone protein for the ATP receptor P2X7 (P2X7R). In CALHM2 absence P2X7 receptor is not trafficked efficiently to

the plasma membrane and, because ATP signalling is important for inflammasome activation, *Calhm2*$^{-/-}$ microglial are less capable of assembling the inflammasome machinery. The idea that CALHM6 could be involved not only in the release of ATP, but also in its downstream sensing, is compelling. Considering how important is the inflammasome pathway in immune responses we decided to test the third hypothesis that CALHM6 may be involved in the control of P2X7R signalling.

7.1.2 Phagocytosis in macrophages

Phagocytosis is the process through which macrophages recognise and ingest particles larger than 0.5 μm[326]. This process is important for bacterial clearance, like in the case of *L. monocytogenes*[499], and for tissue homeostasis: macrophages can recognise and phagocyte apoptotic cells in a process called efferocytosis[326]. Only a handful of immune cells are considered professional phagocytes: monocytes, macrophages, neutrophils, DC and eosinophils are the main ones[500]. The recognition of phagocytic targets can be carried out by opsonic or non-opsonic receptors. Non-opsonic receptors recognise the target particle directly, CD163 for example is important for the recognition of apoptotic cells while Dectin-1 recognise fungal-wall structures[501,502]. Opsonic receptors instead, recognise host-derived opsonin and the best known opsonic receptors are FcRs that bind the Fc invariant portion of antibodies and complement factors[326]. After a phagocytosis target is identified by phagocytes, the phagocytic cup, a membrane invagination, is formed[503] and the actin filaments at the base of the cup re-nucleate closer to the target where they form pseudopodia, under the control of the Arp2/3 complex[504], that have the function to incapsulate the target. Once the phagosome has closed around the target particle it undergoes maturation. The proteins that need to be recycled or directed to the proteasome are ubiquitinated and removed, while the extracellular cargo that needs to be eliminated is broken down in the phagolysosome[326]. The formation of the phagolysosome is a gradual process, first the early phagosomes fuse with endosomes in a process mediated by Rab5[505] and later by Rab7[506]. The acidification of the phagosome starts after the fusion and the pH of the compartment decreases gradually thanks to the progressive accumulation of the Vacuolar-type H^+-ATPase pump until the

internal pH is as low as 4.5[507]. The final stage of phagosome maturation is their fusion with lysosomes to become phagolysosomes, here not only the environment is extremely acidic but it is also rich in hydrolytic enzymes like lysozyme and lipases, and reactive oxygen species[326].

Our interest in phagocytosis of *Calhm6*$^{-/-}$ macrophages stemmed from the discovery, by Cheng and colleagues, that *Calhm2*$^{-/-}$ microglial cells have increased phagocytosis, together with reduced pro-inflammatory activation[31]. Phagocytosis is a key process in *L. monocytogenes* control and ATP has been recognised as one of the signals required for efficient phagocytosis of apoptotic cells as well as pathogen-derived molecules[1,326,508]. In this chapter, as a final hypothesis we will then investigate the role of CALHM6 in macrophage phagocytosis

7.2 Aims

1. Assess whether CALHM6 localises to the IS between macrophages/DC and NK cells

2. Test whether biochemically CALHM6 behaves similar to other CALHM proteins

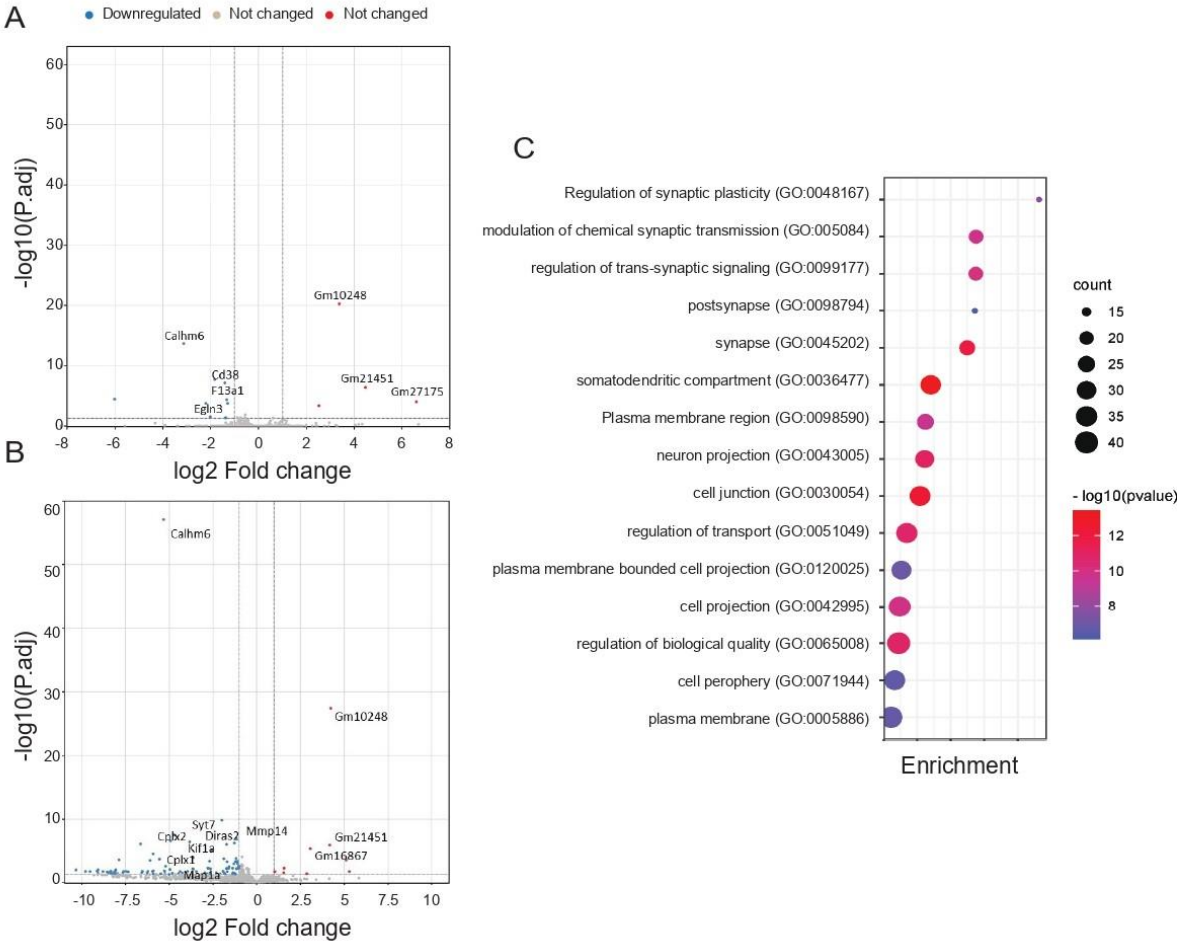
3. Test if CALHM6 function as an ATP channel

7.3 Results

7.3.1 *Calhm6*$^{-/-}$ macrophages fail to upregulate synaptic pathway related genes in response to inflammatory stimuli.

I have shown in my work that CALHM6 is important for the contact-mediated activation of NK cells. Macrophages and DC can both activate NK cells but we know that CALHM6 expression is higher in macrophages after stimulation, and that specific deletion of CALHM6 in CD11c^{+} DC do not affect NK cells activation. So, I focused my attention on macrophages. In order to check if the absence of CALHM6 could cause changes in macrophages that could explain their inability to activate NK cells, I performed an unbiased analysis of WT vs *Calhm6*$^{-/-}$ BMDM, naïve or stimulated for 24 hours, with Poly(I:C), IFN-γ, LPS, LPS + IFN-γ , Zymosan, or Zymosan + IFN-γ . All the stimulations used were known to upregulate CALHM6 expression. When I performed RNAseq analysis of the RNA extracted from resting WT and *Calhm6*$^{-/-}$ BMDMs I saw in the volcano plot (Figure 32.a, Appendix Table 1) that at steady state, there are no differentially expressed genes (DEG) between WT and *Calhm6*$^{-/-}$ BMDM. This is expected and reassuring, as CALHM6 expression is very low in steady state. On the contrary after Poly(I:C) stimulation *Calhm6*$^{-/-}$ failed to upregulate the expression of several genes (Figure 32.b, Appendix Table 3) I have shown in the first chapter that Poly(I:C) is one of the strongest stimuli to generate long lasting upregulation of CALHM6, and in this experiment we find that, of all inflammatory stimuli, this one causes the highest amount of DEG between WT and *Calhm6*$^{-/-}$ BMDM (Appendix tables 5, 7, 9, 11 and 13). Independently of the stimulation conditions, the absence of CALHM6 does not seem to affect any obvious immune pathway, so to look at the possible significance of the DEG, I performed a Gene Ontology enrichment analysis[509,510]. It was extremely interesting to find that the highest DEG enrichment after Poly(I:C) stimulation was for genes involved in synaptic pathways (Figure 32.c and d, Appendix Table 4). These DEG were mostly genes traditionally associated with neuronal synapses. This was true not only for Poly(I:C) but, in smaller measure, for all other stimulations (Appendix Tables 6, 8, 10, 12, 14). The genes that failed to be upregulated in *Calhm6*$^{-/-}$ BMDM are involved for example, in such functions as vesicle trafficking and fusion (*Rab15, syt1/7*)[511,512], endo- and exocytosis (*Add2, Cplx2, Trim9*)[513–515] or formation of synaptic contacts

(*Map1a/b*)[516]. As an example of genes, the expression of which is controlled by CALHM6, we show in figure 30.e the synaptic vesicle cycle from the Kyoto Encyclopaedia of Genes and Genome (KEGG), using neuronal synapse as a graphical guide, highlighted in green are the genes that failed to be upregulated in activated CALHM6 deficient cells. Taken together these data suggest that CALHM6 could be implicated in the synapse-formation process in BMDM after stimulation, possibly by regulating vesicle trafficking or fusion.


A
Downregulated
Not changed
Not changed
-log10(P.adj)
log2 Fold change
Gm10248
Calhm6
Cd38
F13a1
Egln3
Gm21451
Gm27175
B
-log10(P.adj)
log2 Fold change
Calhm6
Gm10248
Syt7
Cplx2
Diras2
Mmp14
Kif1a
Cplx1
Map1a
Gm21451
Gm16867
C
Regulation of synaptic plasticity (GO:0048167)
modulation of chemical synaptic transmission (GO:005084)
regulation of trans-synaptic signaling (GO:0099177)
postsynapse (GO:0098794)
synapse (GO:0045202)
somatodendritic compartment (GO:0036477)
Plasma membrane region (GO:0098590)
neuron projection (GO:0043005)
cell junction (GO:0030054)
regulation of transport (GO:0051049)
plasma membrane bounded cell projection (GO:0120025)
cell projection (GO:0042995)
regulation of biological quality (GO:0065008)
cell perophery (GO:0071944)
plasma membrane (GO:0005886)
Enrichment
count
- log10(pvalue)

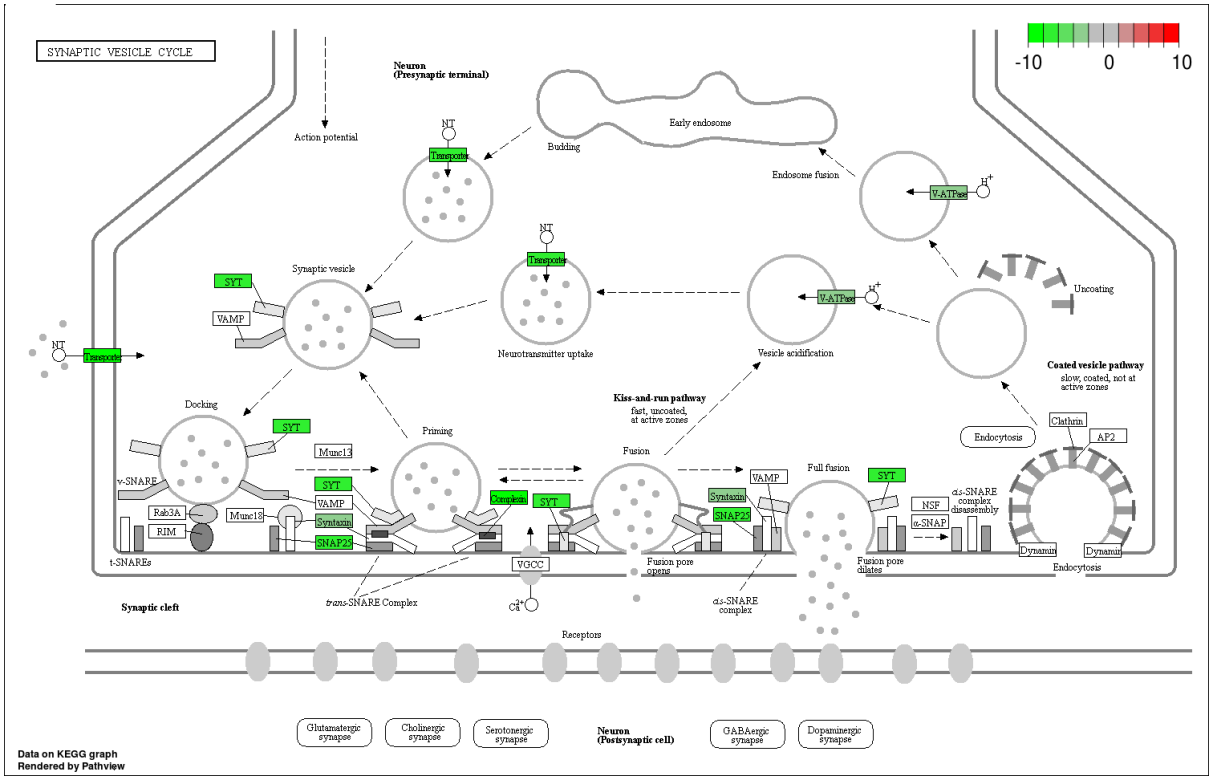


FIGURE 32: *Calhm6*$^{-/-}$ BMDM fail to upregulate mRNA linked to synaptic pathways following Poly(I:C) stimulation. 3x10^6 WT and BMDM were left untreated or stimulated for 24 h with Poly(I:C) (10 µg/ml). RNA was extracted for RNAseq analysis. Volcano plot of differentially expressed genes between a) untreated or b) Poly(I:C) stimulated WT and *Calhm6*$^{-/-}$ BMDM. c) Bubble plot of Gene Ontology analysis of differentially expressed genes between WT and *Calhm6*$^{-/-}$ Poly(I:C) treated BMDM. d) scheme of synaptic vesicle cycle from KEGG rendered by pathview, in green are highlighted all the genes downregulated in *Calhm6*$^{-/-}$ BMDM. (results from one experiment n=3, 3, 3 and 3).

7.3.2 CALHM6 polarises to the contact synapses of macrophages

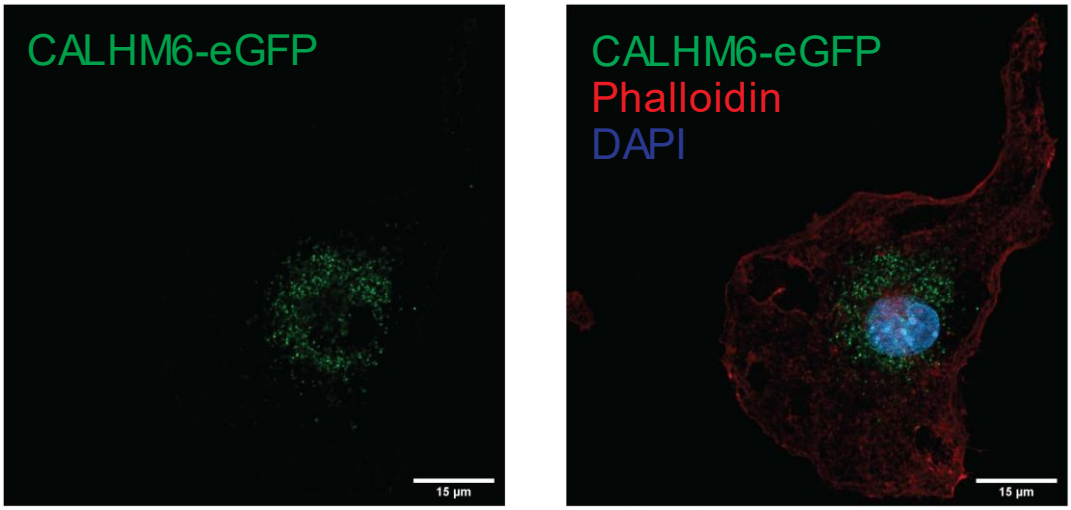
CALHM6 implication in the formation of macrophage/DC-NK cells synapse is suggested by its role in controlling synaptic gene expression and by the fact that CALHM6 absence disrupts accessory cell-mediated NK cell activation. CALHM6 is a transmembrane protein[22] that can be expressed on the extracellular membrane[22,32]. For this reason, I wanted to test whether CALHM6 could localise at the macrophage-NK cell IS. Unfortunately, I could not use commercially available antibodies to stain endogenous CALHM6 for imaging purposes. So, I generated or purchased C-terminal tagged forms of CALHM6 (CALHM6-FLAG and CALHM6-eGFP) and then retrovirally transduced WT BMDM with one of these constructs to have a primary cell system that overexpressed a form of CALHM6 that I could visualise via confocal imaging. Surprisingly, when I looked at tagged CALHM6 expression in these nonactivated BMDM, I could not see any expression in the extracellular membrane like in Ebihara et al.[32]. The expression was exclusively intracellular, largely in the peri-nuclear area (Figure 33.a and b). The protein does not appear to be freely circulating in the cytoplasm but instead segregated in vesicle-like structures. There was no difference in expression between CALHM6-eGFP and CALHM6-FLAG so for the following experiments I decided to use CALHM6-eGFP to avoid unspecific staining due to conjugated antibodies.

After establishing a system to visualise CALHM6 in BMDM I tested whether CALHM6-eGFP would localise at the BMDM-NK cells interface during IS formation. I sorted fresh NK cells from WT mice spleens and co-cultured them with CALHM6-eGFP transduced BMDM pre-stimulated with IFN-γ and LPS for 6 h. NK cells were added on top of a BMDM monolayer that had been left to adhere overnight to microscope coverslips. The much smaller NK cells were easily distinguishable from BMDM based on cell size and morphology (Figure 34.a). My co-cultures were imaged by taking serial Z-sections, and in top sections, where we identified NK cell contact with the BMDM, I assessed polarisation of CALHM6 from BMDM towards the NK cells 10, 20 and 40 min post co-culture. Images were blinded and polarisation was scored manually and defined as presence of polarised GFP staining towards the NK

cell membrane (Figure 34.b). While at 0 min there was no polarisation towards NK cells in any of the contact imaged, the percentage of IS that shows polarisation of CALHM6 towards NK cells increases significantly with time (significance calculated with a two-way ANOVA using time and percentage polarisation as variables).

To check whether the polarisation of CALHM6 towards the BMDM-NK cells synapse was unique to NK cells or if CALHM6 also polarises to other known BMDM synapses, the best characterised of which are phagocytic synapse, I tested the same co-culture system but instead of NK cells we used 3 µm polystyrene beads (Figure 34.c and d), non-opsonised sheep sRBC (Figure 34.e and f) or IgG opsonised sRBC (Figure 34.g and h). All these targets can be phagocyted by BMDM, polystyrene beads and sRBC are recognised by nonopsonic receptors while opsonised sRBC are recognised by the opsonic FcgR[326]. For the phagocytosis to happen, an interphase very similar to IS needs to form[517], actin needs to be remodelled around the target where it polymerises to form pseudopodia. We can see this actin accumulation around the phagocytic targets in my images. Like in the BMDM-NK cells synapse, CALHM6 polarises at the phagocytic synapse in a time-dependent manner, the highest polarisation was after 40 min. In the case of opsonised sRBC the phagocytosis happens so quickly that at 20 min all the cells have already been internalised and hence they cannot be analysed. The results from my imaging experiments point towards CALHM6 being a protein that is recruited to the extracellular membrane of BMDM synapses.

a



b

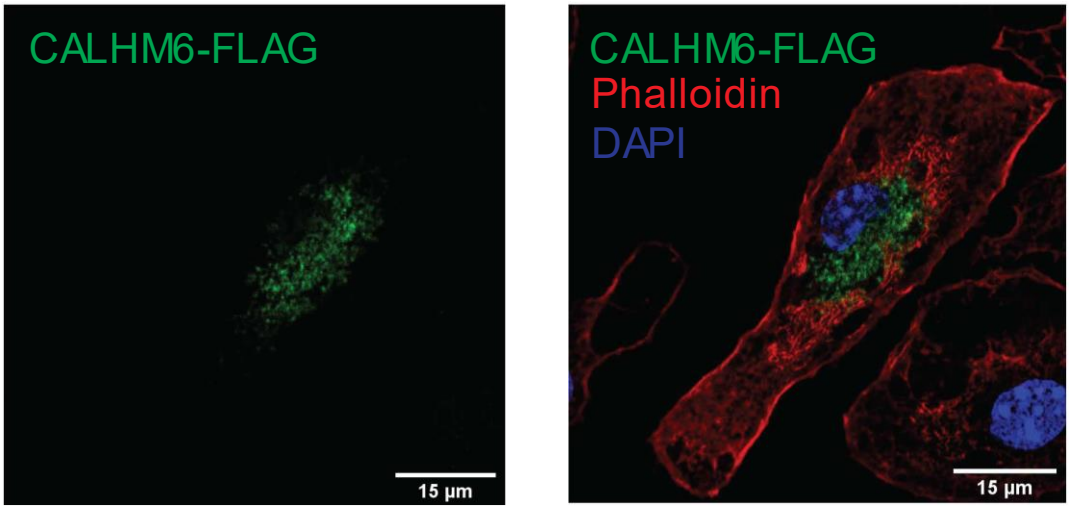
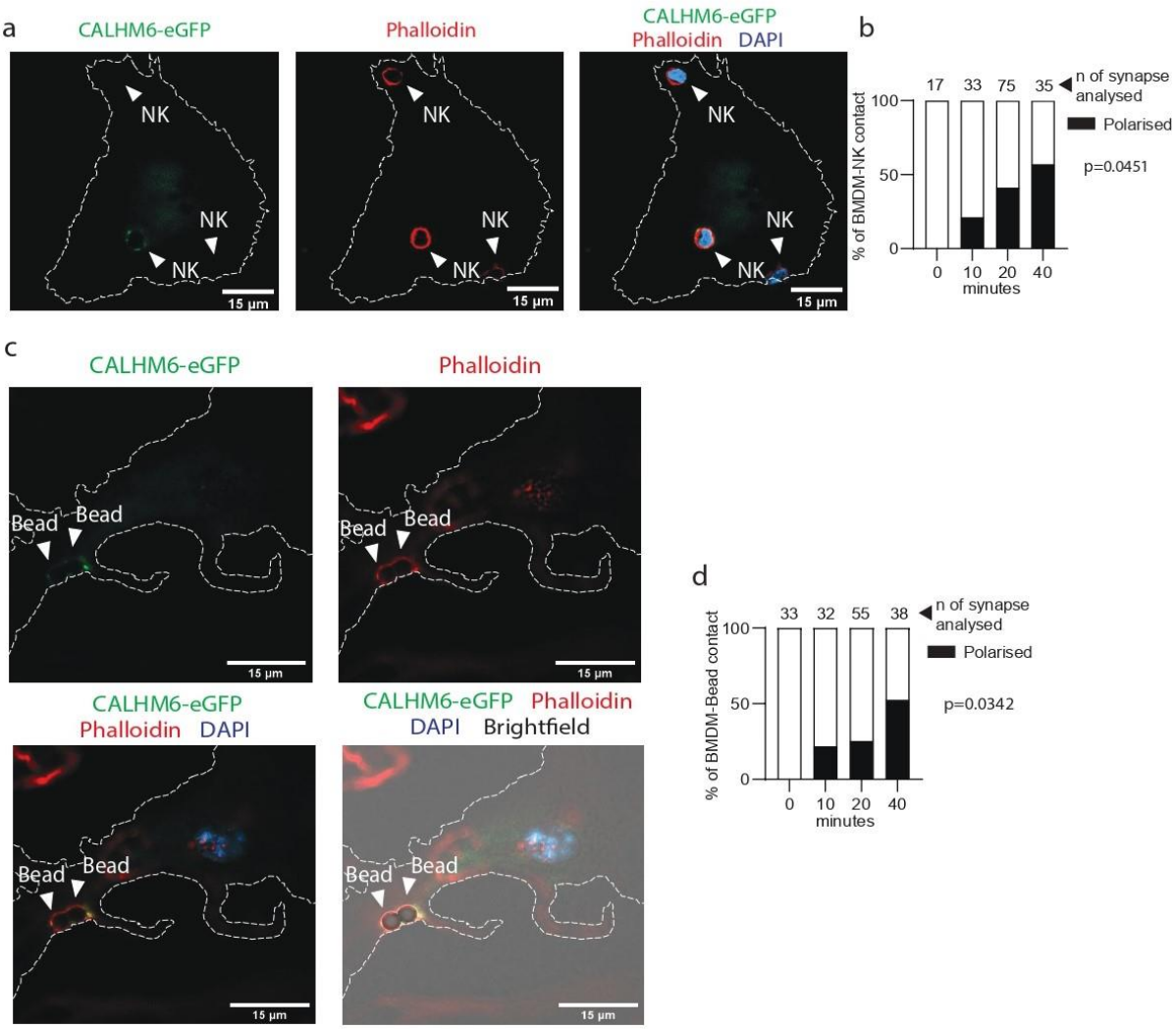


FIGURE 33: CALHM6 is mostly expressed intracellularly I non activated BMDM. Freshly isolated BM cells were transduced with a retroviral vector expressing a) CALHM6-eGFP or b) CALHM6-FLAG and then differentiated into BMDM. Differentiated cells were plated on a coverslip, fixed with 4% PFA and permeabilised with 0.1% Triton before being stained with phalloidin, DAPI and, in the case of CALHM6-FLAG, fluorescently conjugated αFLAG ab. Pictures were taken with a 60x objective. (Representative images)


a
CALHM6-eGFP
Phalloidin
CALHM6-eGFP
Phalloidin DAPI
NK
15 µm
b
17 33 75 35
n of synapse analysed
Polarised
p=0.0451
% of BMDM-NK contact
100
50
0
0 10 20 40
minutes
c
CALHM6-eGFP
Phalloidin
Bead
CALHM6-eGFP
Phalloidin DAPI
CALHM6-eGFP Phalloidin
DAPI Brightfield
d
33 32 55 38
n of synapse analysed
Polarised
p=0.0342
% of BMDM-Bead contact
0 10 20 40
minutes

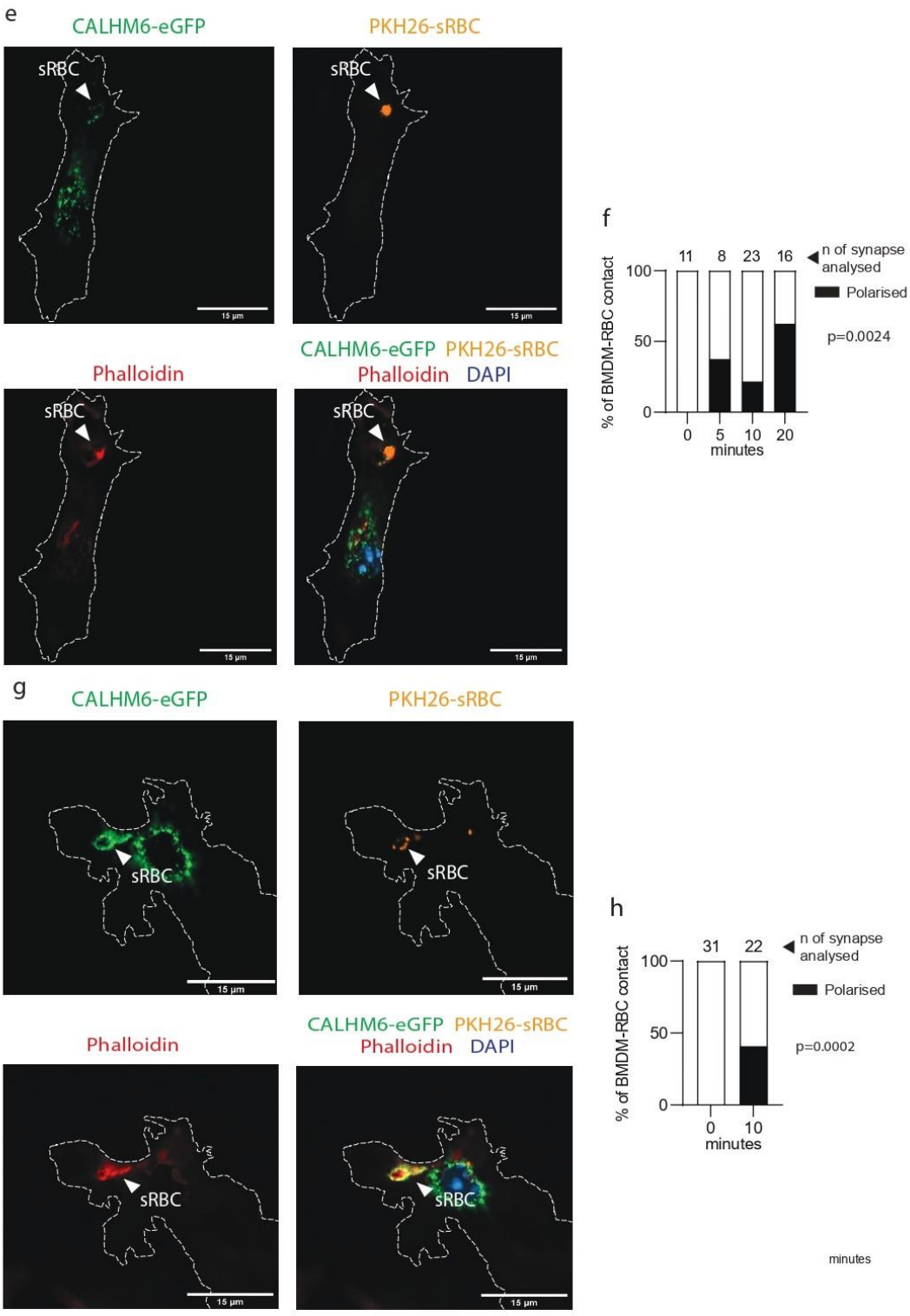


FIGURE 34: CALHM6 polarises towards BMDM synapses. BMDM are transduced with a retroviral vector expressing CALHM6-eGFP. 2.5x10^5 BMDM are plated on coverslips in 6 well plates and pre-treated with IFN-γ and LPS for 6 h. a) primary NK1.1$^+$CD3$^-$ cells isolated from mouse spleens were co-cultured with the transduced BMDM for 10, 20 or 40 min. The co-culture was fixed with 4% PFA, permeabilised with 0.1% Triton and stained with phalloidin and DAPI. Pictures were taken with a 60x

objective. (Representative image) b) Images were blinded and CALHM6-eGFP polarisation towards $NK1.1^{+}CD3^{-}$ quantified. (Pooled results from 3 independent experiments, two-way ANOVA). In the same way transduced BMDM were co-cultured with c), d) 3mM polystyrene beads (Representative image and pooled results from 3 independent experiments, two-way ANOVA), e) and f) PHK26 labelled sRBC (Representative image and pooled results from 3 independent experiments, two-way ANOVA) or g) and h) PHK26 labelled opsonised sRBC (Representative image and pooled results from 2 independent experiments, two-way ANOVA). The white arrowheads indicate the location of respectively NK, beads and sRBC synapses. The numbers above the bars indicate the number of synapses analysed for each condition. The statistics represent the significance of the interaction between the percentage of synapses towards which CALHM6 is polarised and the time points.

7.3.3 CALHM6 is not required for phagocytosis or endocytosis in macrophages

I showed that CALHM6 is recruited to the phagocytic synapse, and there are differences in the expression of vesicle trafficking genes between activated WT and *Calhm6*$^{-/-}$ macrophages. A paper from Cheng et al. also showed that absence of CALHM2 in microglia increased their phagocytotic potential[31]. The next point to address then, was CALHM6 requirement by BMDM to carry out phagocytosis efficiently. To answer this question, I used fluorescently labelled sRBC (Figure 35.a) opsonised or not, and Zymosan particles (Figure 35.b), as targets of phagocytosis. sRBC were labelled with the generic membrane dye PHK26 and left in normal medium or opsonised with anti sRBC IgG2s. WT and *Calhm6*$^{-/-}$ BMDM were then stimulated with IFN-γ for 6 h to upregulate endogenous CALHM6 expression and co-cultured with the sRBC for 0, 5, 15 or 45 min. Extracellular sRBCs were removed by quick lysis, using red cell lysis buffer, and the amount of sRBC internalised by BMDM was measured by flow cytometry (Figure 35.a). There was no difference in the MFI, or percent, of sRBC/PKH26 positive BMDM between WT and *Calhm6*$^{-/-}$ cells, indicating that the phagocytosis happened at the same rate. As expected BMDM can internalise opsonised sRBC far more efficiently than the non-opsonised one, due to their recognition by the FcgR[326]. A similar experiment was repeated with fluorescent zymosan, in this case naïve or IFN-γ pre-treated BMDM were co-cultured with Zymosan for 0, 5, 10, 20 and 40 min. I chose Zymosan as a pathogen particle because it is recognised for internalisation by Dectin-1[399] which stimulation also upregulates CALMH6[87]. Zymosan was conjugated with pHrodo, a fluorophore optimised for phagocytosis assays, its fluorescence is minimal outside the cells but dramatically increases when it is exposed to a low pH environment[518]. In this way it can be used to assess the entrance of the phagocyted Zymosan into the lysosome, where the pH can be as low as 4.5[326]. As it was the case for sRBC there was no difference in the MFI, or percent of Zymosan/pHrodo positive cells between WT and *Calhm6*$^{-/-}$ BMDM. These results not only tell us that the speed with which particles are taken up is the same between WT and *Calhm6*$^{-/-}$ BMDM but also it indicates that the trafficking and fusion of the phagosomes with the lysosomes happens at normal rates and so does their acidification.

Finally, we tested if there was a difference in endocytosis between WT and *Calhm6*$^{-/-}$ BMDM. Endocytosis is an internalisation process used by cells to sample the environment. Unlike phagocytosis the endosomes formed during endocytosis are of small size and do not happen around specific targets[519]. Clatrin and dynamin-mediated endocytosis are the best known of the endocytic processes[519]. I chose to study endocytosis by looking at 10 kDa Dextran uptake, because it is known to go through clatrin-mediated uptake[520]. Like Zymosan before, Dextran was conjugated with fluorescent pHrodo. Similar to the previous experiment naïve and IFN-γ pre-treated BMDM were incubated with Dextran for 0, 10 and 20 min (Figure 35.c). Again there was no difference in endocytosis level between WT and *Calhm6*$^{-/-}$ BMDM. These results taken together tell us that CALHM6, despite localising at the phagocytic cup, is not required for the efficient phagocytic or endocytic role of BMDM.

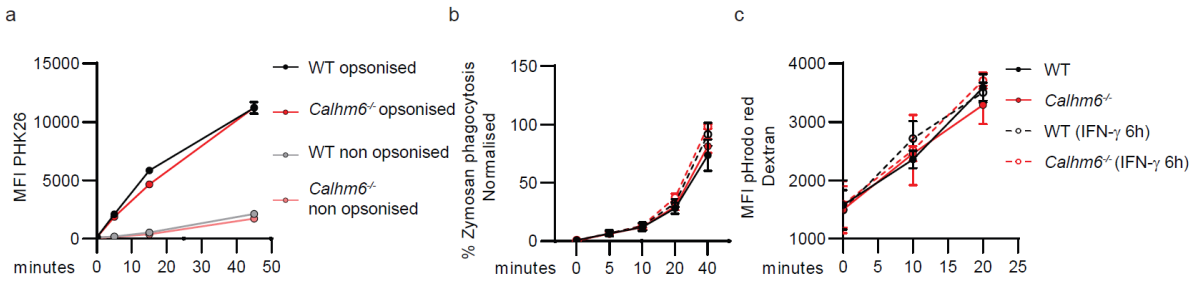


FIGURE 35: There is no difference in phago- and endocytosis rate between WT and *Calhm6*$^{-/-}$ BMDM. a) sRBC were stained with the membrane staining reagent PHK26 and left untreated or opsonised with IgG2s for 2 h. sRBC were then co-cultured with WT and *Calhm6*$^{-/-}$ BMDM for 5, 15 and 45 minutes. At the end of the co-culture cells were washed with PBS, fixed with 4% PFA and analysed by flow cytometry. (Representative of 2 independent experiments, n=2 vs 2, two-way ANOVA). WT and *Calhm6*$^{-/-}$ BMDM were co-cultured with b) pHrodo Red Zymosan bioparticles (pooled normalised results from 3 independent experiments, n=3 vs 3, two-way ANOVA) or c) pHrodo Red Dextran 10000 MW (pooled results from 2 independent experiments, n=2 vs 2, two-way ANOVA).

7.3.4 CALHM6 forms a higher order molecular complexes similar to those make by other members of CALHM family.

Only very recently, during the course of our studies, the structure of the CALHM6 protein has been defined by Cryo-EM analysis of human placental CALHM6 expressed in HEK293S cells[22]. CALHM6 monomer is a four-time membrane spanning protein that forms very big channel-like structures composed of ten or eleven monomers[22]. Because there are no data in the literature on the structure of endogenous CALHM6 in immune cells I tested whether, in BMDM, CALHM6 could also form a big supramolecular complex. I lysed IFN-γ or LPS stimulated BMDM in non-denaturing condition, run the lysate on a Native BluePAGE gel and probed using CALHM6 specific antibody (Figure 36.a). In these conditions CALHM6 run much higher (>720 kDa) than its monomeric form (about 37kDa, or 50 kDa when glycosylated, Figure 8). This suggests that endogenous CALHM6 is part of a much bigger complex in murine BMDM. Interestingly this complex is much bigger than the CALHM1 one (242kDa), when analysed on a similar Native BluePAGE gel[18]. This could be explained by CALHM1 forming only a octameric channel[23] instead of decamers and undecamers formed by CALHM6, or by CALHM6 being part of a bigger complex that involves other proteins. We know that for the integrity of CALHM channels, disulphide bonds in the inter-helix loops are important[18,20,22,521] so I next tested if this was true also in the case of CALHM6. I ran non-denatured lysate from IFN-γ stimulated BMDM on a SDS Page western blot with growing concentration of DTT, a reducing agent that can break disulfate bonds[522] (Figure 36.b). Like for CALHM1, the presence of a reducing agent broke down the complex, and the disappearance of the bigger complex was proportional to the concentration of DTT. Boiling the samples also denatures the proteins and the bigger complexes disappear in all conditions except the one without DTT. Even after incubation with DTT when we do not boil the sample, we can see a final protein product that is higher than 100 kDa, this suggest that we could still be looking at a dimer of two glycosylated CALHM6 monomers.

When the structure of CALHM6 was resolved the authors of the study did not find any glycosylated residues on the protein[22] but my BMDM data clearly show that, while the protein monomer on WB forms a 37kDa band, the largest fraction of the protein runs at around 50 kDa, I hypothesized that the 50 kDa one is a glycosylated form of CALHM6, both fractions are absent in *Calhm6*$^{-/-}$ (Figure 9.b). To confirm that the extra band that we see is due to glycosylation I treated our BMDM cell lysate with Peptide-N-Glycosidase F (PNGase F), an amidase that can cleave high mannose, hybrid, and complex oligosaccharides from N-linked proteins[523]. I used PNGase because a single potential N-glycosylation site is predicted for CALHM6[92]. As shown in Figure 36.c after PNGase treatment the 50 kDa band completely disappears and CALHM6 only appears as 37 kDa monomer, thus showing that larger fraction is indeed due to the N-glycosylation of CALHM6.

I also showed that tagged proteins could form higher molecular complexed in non-reducing conditions similar to endogenous CALHM6 (Figure 36.d). Thus, CALHM6 protein at least biochemically behaves like other CALHMs and the tagged forms of CALHM6 are suitable for functional experiments.

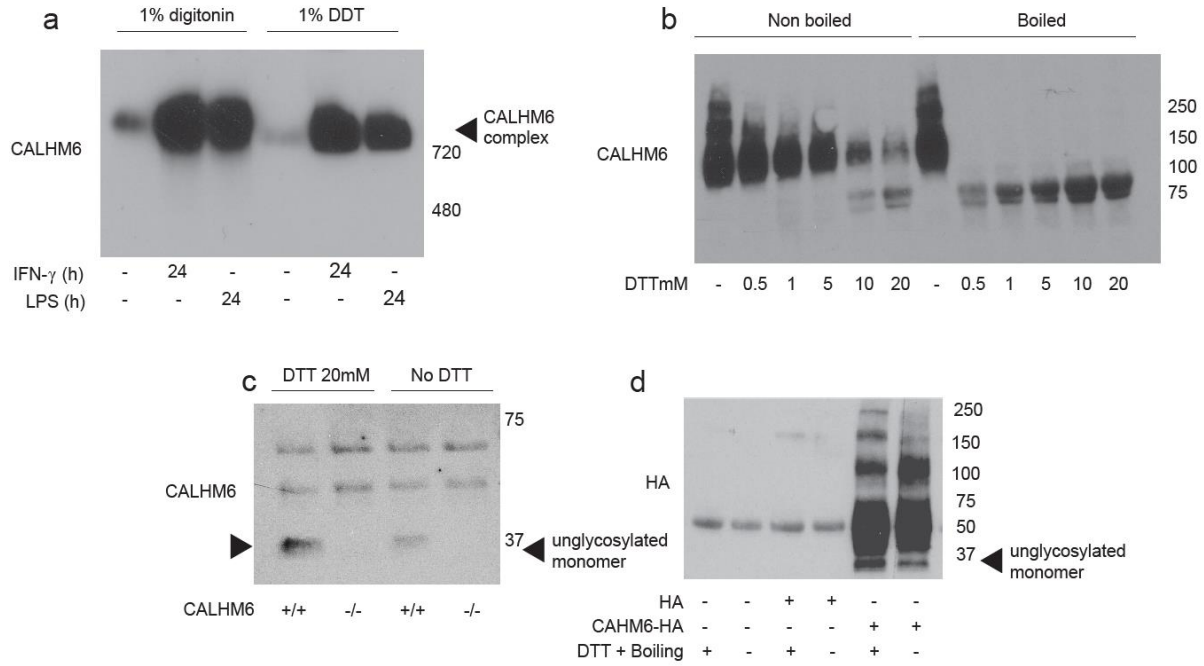


FIGURE 36: Like other members of the CALHM family in BMDM CALHM6 forms a higher order oligomeric complex. BMDM were stimulated for 24 h with IFN-γ or LPS and harvested in 1% digitonin or 1% DDT buffer, with cOmplete protease inhibitor cocktail. a) The lysate was run on a non-denaturing Blu page gel and blotted for CALHM6. (Representative of 2 independent experiments). b) Cells were lysate in a 1% triton x100 buffer with cOmplete protease inhibitor cocktail, prepared with growing concentrations of DTT. Half of the samples were heated to 95° for 5 min. The resulting samples were run on an SDS gel (Representative of one experiment n=1). c) WT and Calhm6-/- BMDM stimulated overnight with IFN-g, cells were lysed, and proteins collected in denaturing conditions. The lysates were treated with PNGase F for 20 h to achieve glycosylation. Cell lysate was run on a SDS gel with or without DTT addition and CALHM6 visualised by immunoblotting (Representative of one experiment n=1). d) BMDMs from *Calhm6*$^{-/-}$ mice were transduced with plasmids containing only a HA-tag or HA-tagged CALHM6 constructs. Cells lysed in non-denaturing conditions and run on an SDS PAGE blotted with aCALHM6. (Representative of 2 independent experiments)

7.3.5 CALHM6 channel does not open in response to the same stimuli that open the CALHM1/3 channel

The best known of the CALHM channels is the CALHM1/3 that forms a ion- and ATP channel[11,12,36] opened by changes in extracellular calcium, membrane voltage and pressure[12,13,34,52]. CALHM2 has also been identified as a novel ATP channel in the brain[30,31], even if its opening mechanism has yet to be discovered[22]. In light of these data, especially considering the similarity between the CALHM6 and CALHM2 structure[22,496], I hypothesized that CALHM6 works as a membrane ATP channel in vivo. I tested my hypothesis by measuring ATP release from WT vs *Calhm6*$^{-/-}$ BMDM that had been stimulated with IFN-γ to upregulate CALHM6. The cells were cultured for 20 min in a Ca^{2+}-depleted isotonic buffer, a condition that it is known to open the CALHM1/3 channel[21,22]. ATP release was measured with the ENLITEN Luciferin-Luciferase assay system (Figure 37.a). I could not detect any difference in the level of ATP released between WT and *Calhm6*$^{-/-}$ BMDM. Because BMDM express many other ATP channels that could mask the phenotype, I next tested ATP release in HEK293T cells. In this system I overexpressed CALHM6 so as to overcome the contribution of other ATP channels. HEK293T cells were transfected with empty vector or plasmids containing CALHM6-HA or CALHM1-HA, as a positive control (Figure 37.b), and the transfection efficiency was measured by flow cytometry. While I detected significant upregulation of ATP release in CALHM1-HA transfected cells, there was no difference between CALHM6-HA and non-transfected cells. It is possible that, to function as an ATP channel, CALHM6 needs additional cellular components not present in HEK293T cells, so I repeated the same experiment, this time in primary WT BMDM, using lentivirus carrying CALHM6-GFP or GFP alone. The BMDM were stimulated with IFN-γ before ATP measurement (Figure 37.c). Overexpression of CALHM1-HA in primary BMDM is mostly lethal, probably due to the poorly selective nature of the large CALHM1 channel, so we could not use it as a positive control. In BMDM overexpressing CALHM6 there is no difference in ATP release compared to baseline.

It is possible that the depletion of extracellular Ca^{2+} is not the right stimulus to open CALHM6 channel. A Cryo-EM study of CALHM6 structure shows that inside the CALHM6 pore, the trans-membrane helix 1 (TM1) of CALHM6 creates a plug that closes the pore, with a possible lipid like density under the TM1, suggesting that the opening mechanism may be more complex than for CALHM1 and mere removal of extracellular Ca^{2+} may not be sufficient. Droździyk and colleagues in their paper[22] suggest two possible models for CALHM channel gating (Figure 37.d). The first one (likely applies to conical pore of CALHM6) envisages a change in conformation of the first a-helix that protrudes into the channel with an angle close to 60^{o}. If this is the gating strategy the N-terminal fragment of the protein, which position cannot be defined clearly by Cryo-EM, should be particularly important considering its position in the three-dimensional structure. Alternatively, it is possible that the removal of the lipid plug from the channel is needed for the opening (likely applies to cylindrical pore of CALHM4). I decided to test the first gating hypothesis by creating a recombinant CALHM6 (CALHM6-ΔNT-HA) protein that lacked the short N-terminal region (aa 1-8) and expressed it in Plat-E cells together with empty vector, CALHM6-HA and CALHM1-HA. In the eventuality that low extracellular Ca^{2+} was not the right trigger to open CALHM6 I also tested Ionomycin stimulation and high extracellular K^{+} conditions. Both these stimuli have been shown to trigger ATP release from CALHM1 (Figure 37.e). All three stimulations increased ATP release from CALMH1 transfected Plat-E but still there was no difference between CALHM6-ΔNT-HA and control cells. These results tell us that, if CALHM6 is an ATP channel, it cannot be opened by stimuli that work for CALHM1. Also, the removal of the short N-terminal fragment of CALHM6, is not sufficient to open the channel.

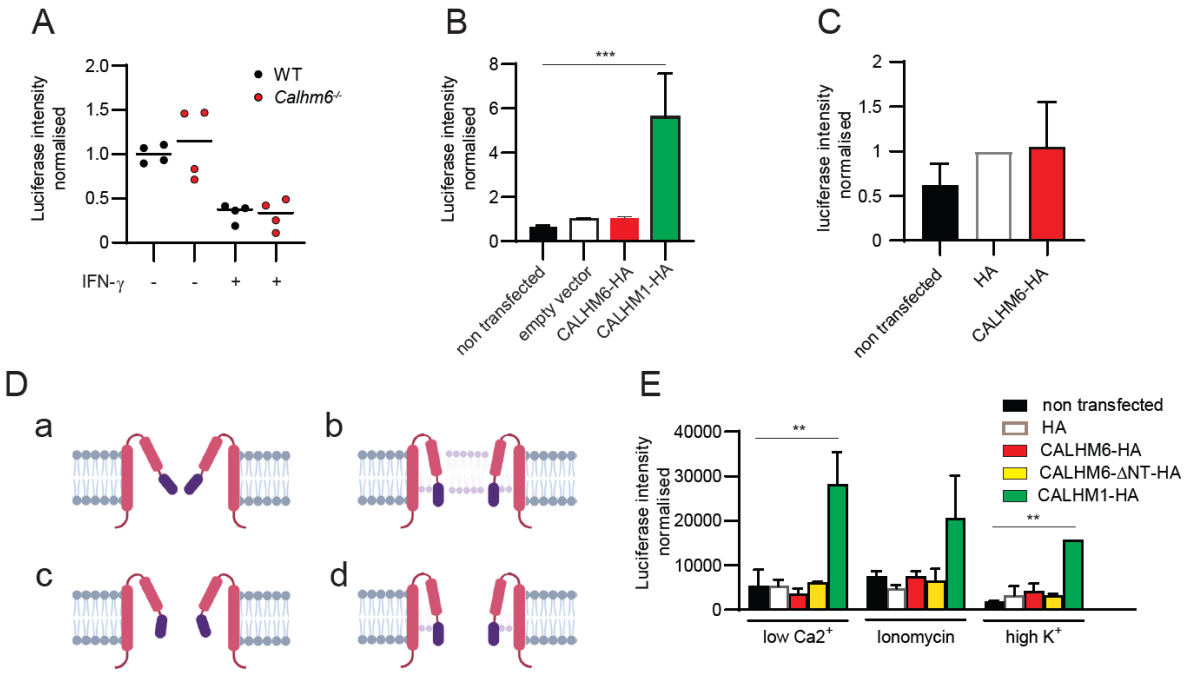


FIGURE 37: CALHM6 is not opened by the same stimuli that open CALHM1 a) 1x10^5 naïve or overnight IFN-γ primed BMDM from WT and *Calhm6*$^{-/-}$ mice were exposed to isotonic medium containing 5 mM of EDTA and 1 mM of the ATPase inhibitor ARL67156 for 20 min. ATP concentration in the medium was measured with ENLITEN Luciferase/rLuciferin assay. (Normalised pooled results from 2 independent experiments, n=4, Kruskall-Wallis test with multiple comparisons). b) HEK293T cells were transfected with GFP-labelled plasmids. containing only a HA, HA-tagged CALHM6 or HA-tagged CALHM1 constructs. Transduction efficiency was measured by flow cytometry. ATP release was measured like in Figure 36.a (Normalised pooled results from 3 independent experiments, Kruskal-Wallis test with multiple comparisons). c) BMDMs from *Calhm6*$^{-/-}$ mice were transduced with plasmids containing only a HA-tag or HA-tagged CALHM6 constructs and ATP release measured after 20 min in low-calcium buffer (Normalised pooled results from 2 independent experiments, Kruskal-Wallis test with multiple comparisons) (Normalisation was calculated by considering the value of the empty vector control as 1). d) scheme of possible CALHM6 and CALHM4 open and close configuration. i) iii) the TM1 and short N-terminal domain work as a gate, likely in CALHM6 ii) and iv) the channel is gated by a lipid plug, likely in CALHM4. e) Plat-E cells were transfected with GFP-labelled plasmids containing only a HA-tag, HA-tagged CALHM6, HA tagged CALHM6-ΔNT or HA tagged CALHM1 construct. The cells were cultured for 20 min in isotonic medium containing either EDTA, Ionomycin or excess K^+. ATP release was measured as previously (representative results of 2 (for EDTA medium) or 1 independent experiments, Kruskal-Wallis test with multiple comparisons).

7.3.6 CALHM6 does not act as a P2X7R chaperone

A recent study from Cheng and colleagues from the Yuan lab[31] has uncovered a brand new function for the CALHM6 homologue CALHM2: that of chaperone of the ATP-gated P2X7R channel. In *Calhm2*$^{-/-}$ microglial cells the expression of P2X7R on the cell surface is lowered causing a reduction in the ATP triggered potassium fluxes required for inflammasome activation. Thus, microglial cells from *Calhm2*$^{-/-}$ mice have less proinflammatory activity and less severe AD symptoms. Considering the structural similarities between CALHM2 and CALHM6 I explored the hypothesis that CALHM6 could also act as a chaperone for P2X7R in BMDMs, facilitating P2X7R expression on the extracellular membrane. To test this, I measured P2X7R expression on the plasma membrane of WT and *Calhm6*$^{-/-}$ BMDM stimulated with Poly(I:C) or LPS for 6 or 12 hours (Figure 38.a and b). Contrary to my hypothesis we did not see any difference in the surface expression of P2X7R. Because P2X7R is required for inflammasome activation downstream of ATP signalling[524], I also checked if CALHM6 was affecting the activation of the inflammasome complex by measuring the rate of cell death in BMDM after inflammasome-activating stimulations. I first used Poly(I:C) as signal one because it is the strongest upregulator of CALHM6, inflammasome activation by Poly(I:C) only works for short stimulations[525] so I pre-treated WT and *Calhm6*$^{-/-}$ BMDM with Poly(I:C) for an 1 h followed by stimulation with ATP (Figure 38.c). ATP here was used as a second signal because of it is a ligand for P2X7R. We did not see any difference in cell death measured by LDH assay 1 h after ATP stimulation. I did not use IL-1β release as a proxy of inflammasome activation because the first stimulation is too short to see accumulation of pro-IL-1β in the cells. Other forms of inflammasome activation, with Nigericin as a second signal, were also tested (Figure 38.d and e) and once again, CALHM6 deficiency did not cause a significant difference in cell death. Taken together these results suggest that CALHM6 does not act as chaperone for P2X7R trafficking and is not required for classical inflammasome pathway activation.

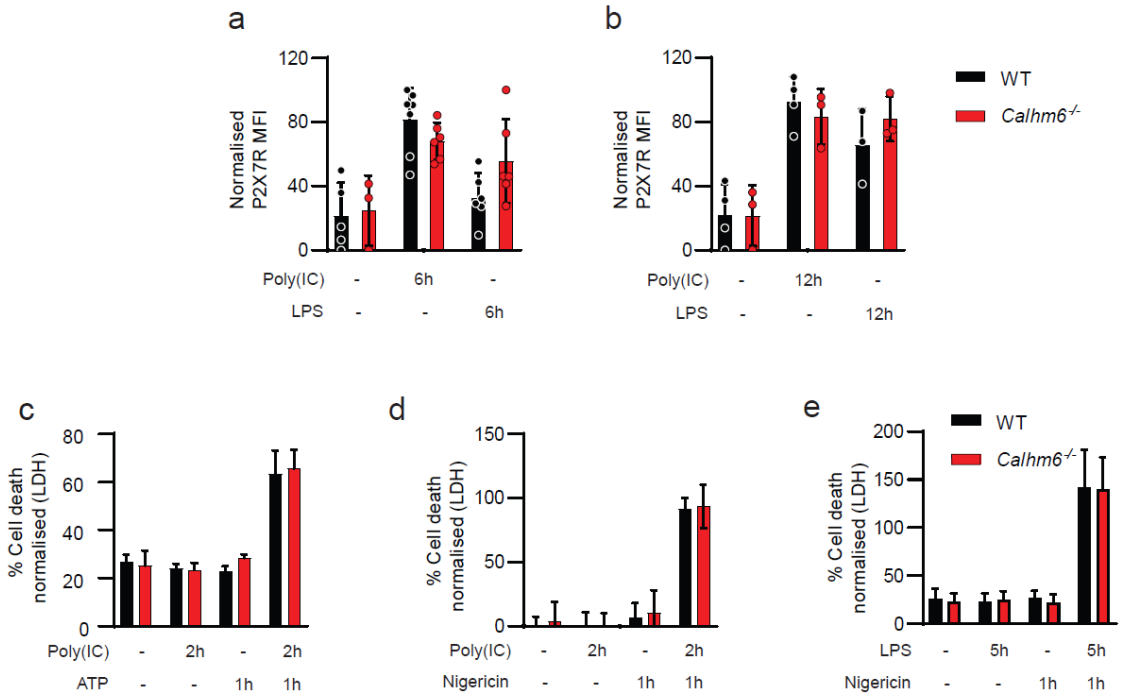


FIGURE 38: CALHM6 deficiency does not affect P2X7R expression or inflammasome activation in BMDM. BMDM were stimulated for a) 6 or b) 12 h with Poly(I:C) or LPS and extracellular concentration of P2X7R measured by flow cytometry. The graphs represent pooled values of P2X7R MFI (pooled values from 3 independent experiments n=3 vs 3, Kruskal-Wallis test with multiple comparisons), (pooled values from 2 independent experiments n=2 vs 2, Kruskal-Wallis test with multiple comparisons). % of cell deaths measured with LDH assay after inflammasome activation in BMDM: cells were treated with Poly(I:C) for 2 h followed by one-hour c) ATP (2.5mM), or d) 1 h Nigericin (value from 1 experiment, n= 3 vs 3, Kruskal-Wallis test with multiple comparisons) (pooled normalised values from 2 independent experiments n=4 vs 4, Kruskal-Wallis test with multiple comparisons). e) BMDM were stimulated with LPS for 5 h in total and Nigericin was added 1 h before harvest (pooled normalised values from 3 independent experiments n=3 vs 3, Kruskal-Wallis test with multiple comparisons)

7.4 Discussion

7.4.1 CALHM6 is a synaptic protein in macrophages

In this study we performed for the first time, an unbiased transcriptome sequencing of WT vs *Calhm6*$^{-/-}$ cells. We sequenced RNA from BMDM activated with several pro-inflammatory stimuli for 24 hours. Interestingly the main pathways that failed to be upregulated upon stimulation of *Calhm6*$^{-/-}$ BMDMs identified by gene ontology analysis, were synaptic pathways. This was true not only for Poly(I:C) stimulation, the one that caused the highest amount of DEG, but it was also true for any other pro-inflammatory stimulus. Reassuringly there were no real differences between unstimulated WT and *Calhm6*$^{-/-}$ BMDM: as we showed, CALHM6 is not expressed at steady state. The great majority of DEG are not traditionally implicated in immune processes but are instead associated with neurological synapses. Several genes are involved in vesicle fusion, exocytosis and cytoskeletal binding and remodelling (Table 4). While most of these genes were traditionally studied in brain, it is plausible that some of them have retained a role in immune-synaptic function, as immune synapse require rearrangement and processes that are similar to the ones in neuronal synapses[96,148]. For example, IL-12 is contained into vesicles that get released in the synaptic cleft and IL-18 is polarised towards the NK cells after the formation of the DC-NK cell immune synapse [237,526]. Several proteins need to be trafficked and cluster at the cell-cell interface[148,258], and cytoskeleton remodelling is required to allow actin polymerisation at the IS[526]. As an example, SNAREs proteins control fusion of synaptic vesicle to the membrane and accumulate both at the neurological and immune synapse[268]. CALHM6 is the only member of the CALHM family specifically expressed in the immune system, all the other protein have been detected exclusively in the CNS[92] (and in placenta in the case of CALHM2 and CALHM4[22]) where their function is known in taste bud cells[10] and microglia[31]. It is interesting that, even when CALHM6 is expressed in immune cells, it seems to have retained control over the same processes controlled by other CALHMs in CNS.

Gene name	*Function*
Syn7	Control Ca^{2+} driven release of neurotransmitter from vesicles by exocytosis[512,527] Also found in lysosomal and secretory granules membranes[528]
Cplx1/2	Regulates vesicles fusogenicity and lower the energy barrier for Ca2+ evoked release of vesicle at the synapse[515]
Map1a *Map1b*	Anchors ion channels and signal complexes to the cytoskeleton. Regulates dendritic growth[529]. Binds microtubules without being a motor-molecules and maintains synaptic plasticity[530]
Snph	Component of the synaptic vesicle docking/fusion machinery, binds SNAP25[531] Important for docking of axonal mitochondrial in the synapse[532]
Cntn1	Important for axon-glia communication[533] Neural and epithelial cell adhesion protein[534]
Obsl1	Link the cytoskeleton to the cell membrane especially at cell-cell and cell-matrix interaction[535]
En2	Transcription factor with a role in cell-cell communication, guides temporal axon formation[536]
Rph3a	Implicated in Ca^{2+} dependent neurotransmitter release. Interact with a-Actinin to crosslink Actin[537] Bind SNAP25 and it is involved in vesicle fusion and release[538]
Clstn2	Part of the Cadherin family, KO causes aberrant morphology of neural synapses and alter number of vesicles in the synapse[539]

Table 4: Selection of DEG between Poly(I:C) stimulated WT and *Calhm6*$^{-/-}$ BMDM.

Some of the DEG like *Snph*, control trafficking of mitochondria along the microtubules. We know that in the case of the taste bud synapse formed by CALHM1, the accumulation of mitochondria just below the surface is fundamental to create an ATP rich environment that increases the specificity of the channel for ATP[10]. Accumulation of mitochondria has also been observed at both ends of the immunological synapse, on DC[98] and NK cells[99]. For future studies it would be interesting to test whether this is true for macrophage-NK cell synapses and whether CALHM6 influences this clustering. There also must be some low level of autocrine signalling by molecules released through CALHM6, as gene expression differences were detected in pure cultures of activated BMDM, without the presence of NK cells.

When we overexpressed an eGFP-tagged form of CALHM6 in BMDM we found that, without an external stimulus, it did not localise at the extracellular membrane but it was distributed in vesicle-like particles mostly around the nucleus. This intracellular localisation was not due to the specific tag because FLAG-tagged CALHM6 imaging showed the same pattern. Unfortunately, it was not possible to assess cellular localisation of endogenous CALHM6 because the available commercial antibody is not suitable for confocal staining. Also, endogenous CALHM6 is not expressed in steady state, so it is possible that newly synthesised endogenous protein travels to the cell surface more upon appropriate stimulation. Interestingly, Ebihara[32] and Droździżyk[22] suggested that ectopically expressed CALHM6 localises on the extracellular membrane, but they looked at the BMDC and NK cells, cells that have very little cytoplasm and, from the available pictures, it is difficult to establish whether the protein is effectively on the membrane or inside the cell and also they did not see glycosylation. The puncta-like appearance of the CALHM6-GFP staining in our BMDM suggests that it is not diffused in the cytoplasm, something that we expect considering that it is a transmembrane protein, further studies are necessary to establish the exact membrane compartment in which CALHM6 is localised. Co-staining experiments with EEA-1 and MitoTracker Red allowed us to exclude early endosomes and mitochondria as the site of CALHM6 localisation (data not shown).

In this study we showed for the first time that CALHM6 gets recruited towards the BMDM-NK cell synapse in a time-dependent manner. After incubation with NK cells a portion of the cytoplasmic CALHM6 relocalise around the actin ring that defines the IS. Since the IS was discovered by Poo and Kupfer in their respective 1988 and 1991 works[540,541], it has been one of the most studied immunological phenomena. The DC-T cell IS has been the focus of most of the studies and we have an in-depth knowledge of the molecules involved in its formation as well as the remodelling that occurs to make the IS possible. This knowledge though, is mostly focused on events that happen on the T cell side[267,542], what are the changes in conformation of APCs following contact with T cells is much less understood[543,544]. Even less investigated is the NK cells activating synapse, especially when it is formed between macrophages and NK cells. The synaptic structures formed in all these cases follow the same generic pattern: recognition by effectors cells of receptors on macrophages/DC, clustering of receptors at the point of contact, exclusion of molecules that are too big or are inhibitory from the synapse, remodelling of actin, formation of concentric structures of integrins to stabilise the contact[96,148,222,542,545], so it is likely that some of the same molecular processes are at play in all the different IS. It has been shown that, in particular in DC-T cell IS, endosomal transport of synaptic machinery is important to generate signalling complexes[268,546547] and can also regulate actin remodelling to shape the synapse[548]. The importance of vesicle trafficking to the immune synapse has also been elucidated on the DC side of the IS, were many molecules need to traffic and polarise, like MHCII[543]. MHCII assembles in the ER and Golgi and through endosomes moves to the MHCII containing compartments MIIC[549,550], DC activation causes tubulation of vesicles that extend along microtubules and fuse with the plasma membrane at the IS site[368]. Interestingly MHCII is not the only molecule to move the IS along microtubules, IL-12 and ICAM-1 also follow this route[551]. The mitochondrial trafficking could be facilitated by the MTOC reorientation towards the IS guided by the GTPase Cdc42[551] that moves the whole endosomal compartment just underneath the IS[551–553]. The MTOC migration towards the IS is a phenomenon well studied also on the T and NK cell side present in both activating and cytotoxic IS[554,555]. It is possible that the MTOC remodelling, together with the increase

in endo- and exocytosis around the IS[267] could explain how CALHM6, normally expressed intracellularly becomes polarised towards the NK cell synapse.

While we do not yet have data on the function of CALHM6 in the macrophage-NK cell synapse, we can speculate that CALHM6 is not important to establish the initial cell-cell contact (it is not expressed on the membrane at the very initial stages) or as a receptor for NK cells ligands (it is highly glycosylated extracellularly). The cryo-EM structure and our own biochemical analysis of CALHM6 suggests that instead we are looking at a channel-like protein[22], it is possible that the channel activity of CALHM6 is important at the IS. As we mentioned, other members of the CALHM family are ATP channels and ATP has been recognised as an activating stimulus in the DC-T cell synapse: after IS formation P2X1 and P2X4 receptors are translocated at the IS together with Pannexin1 and the ATP released through Pannexin1 function as an autocrine activation signal by driving Ca^{2+} entrance through the ATP-dependent P2Xs channels[95,498]. While this effect has only been shown in T cells, Tittarelli et al. found that also the ATP channel Cx43 clusters at the cytotoxic NK cell synapse[556] while other classic ATP channels: Connexins and Gap junctions, are active in the T cell IS[557]. Thus, it is interesting to hypothesise that CALHM6 works as an ATP channel at the IS.

CALHM6 polarises not only towards the IS but also at the "phagocytic synapse". Our imaging show time-dependent polarisation of CALHM6 towards polystyrene beads and opsonised or non-opsonised sRBC. The first identification of a phagocytic synapse was by Goodbridge and colleagues in 2011[558], they identified that clustering of phagocytic receptors in a synapse-like structure from which regulatory molecules like CD45 are excluded, is an initial step required for phagocytosis[558]. The formation of a synapse-like structure was then confirmed for TLR1/2 and FcgR-mediated phagocytosis[559,560]. Like in the IS in the phagocytic synapse we have reorientation of the MTOC that moves underneath the phagocytic cup, driven by Cdc42, PI3K and mPAR-6[561]. We could speculate that this cytoskeletal reorganisation is what, in both synapses helps polarising CALHM6 towards it.

CALHM6 absence does not prejudicate the rate of phagocytosis in BMDM, nor their ability to form mature phagolysosomes. Despite CALHM6 influencing the transcription of genes linked to vesicular trafficking and its localisation at the phagocytic cup, its role is not required for efficient phagocytosis, either Dectin-1- or FcgR-mediated. It is possible that while it is present in both IS and Phagocytic synapse its role is only important in the first one.

7.4.2 CALHM6 forms a channel-like structure similar to other CALHM proteins

Here we showed for the first time, that mouse CALHM6 can form oligomers in immune cells. When run on non-denaturing gel CALHM6 from BMDM forms a complex of about 700 kDa that is compatible with the decameric structure of human CALHM6, resolved by Cryo-EM[22]. We also showed that disulphide bonds are required for the integrity of the oligomeric structure, when we treat BMDM cell lysate with the reducing agent DTT we see a breakdown of the complex. The reliance on disulphide bonds for the maintenance of the structural integrity is not unique to CALM6, CHLM1, CALHM1, CALHM2 and CALHM4 have been shown to require disulphide bonds for their stability[20,22,521]. It is possible that, like for the CALHM1/3 channel[11], CALHM6 is capable of forming channel-like structures with other members of the CALHM family but, the fact that after immune stimulation CALHM6 is the only member of the family to be extensively upregulated, seems to suggest the contrary. CALHM amino acid sequence is highly conserved between species and similar conformations of CALHM1 have been observed in chicken (*Gallus gallus domesticus*), killifish (*Oryzias latipes*), and *C. elegans*[20], these are strong indicators that we can use the working hypothesis that the structure of the CALHM6 oligomer in mice resembles the human one and, as in CALHM2 and CALHM4[22], the addition of a C-terminal tag does not affect the formation of the channel.

CALHM6 is N-glycosylated in mouse cells. In silico analysis identify a predicted glycosylation site on the asparagine residue 143[92]. The monomeric structure of CALHM6, that has a molecular weight of around 37 kDa appears on SDS gels as a double band, one sharp at 37 and a larger one at around 50 kDa. The second band is the glycosylated form of CALHM6, when we treat our cells with

deglycosylating enzymes specific for N-glycosylation the 50 kDa band disappears. Time courses of CALHM6 expression in BMDM after stimulation also shows that the non-glycosylated form is the first one to appear (Figure 7.b and d) probably because the protein is still in the ER and needs to mature before being glycosylated. CALHM1 and CALHM3 are also N-glycosylated in one extracellular residue and in their case, the glycosylation affects the gating kinetics of the channel[562]. Interestingly the published structure of human CALHM6 does not show any glycosylation when expressed ectopically in *X laevis*, as seen in Droździżyk et al[22]. It is possible that in order to obtain proper maturation of CALHM6, the protein has to be expressed in a physiological environment. In this case the function of the CALHM6 channel could be affected by lack of glycosylation.

7.4.3 CALHM6 channel does not open in response to the same conditions that open CALHM1.

Expression of CALHM6 in BMDM, HEK293T or Plat-E cells does not cause release of ATP in the extracellular environment in response to low extracellular Ca^{2+} concentration. This is true both for physiological levels of CALHM6 in IFN-γ stimulated BMDM and for overexpressed CALHM6 in all the cell types examined. Ionomycin or excess of extracellular K^+ also do not increase ATP release from BMDM. All the stimuli used in this chapter are known to open the better studied CALHM1/3 channel[18,27,34] but clearly are not sufficient for CALHM6. As of today we know the function of only four of the six CALHM channels studied: CALHM1/3[10], CALHM2[30] and of *the C. Elegans* CHLM1[16]. They are all channels with an unusually large pores with low selectivity of the channel. CALHM channels are permeable to ATP, and some ions like Ca^{2+}, Cl^-, and K^+ (in that order of affinity). The physiological function of CALHM1/3 and CALHM2 channels though, seems predominantly linked to the release of ATP[10,30], even if more recent studies point to CALHM2 as more of a chaperone for the bona-fide ATP channel P2X7R[31]. Our data indicate that, either CALHM6 is not permeable to ATP, or it needs a different set of stimuli to open, otherwise it is possible that it does not function as a channel in the context of mouse BMDM.

The structure of CALHM6 shows how the first TM helix, to which the N-terminal fragment is attached, protrudes into the channel opening with a 60^{o} angle, thus restricting the width of the channel and possibly preventing passage of large size molecules[22]. It was not possible to obtain conformational data on the N-terminal fragment of TM1 because it is not part of the αHelix and shows a disorganised structure. Drożdżyk at al.[22] hypothesise that the various conformation of this fragment could be the switch between open/closed states of the channel. We deleted the 8 amino acids which make the N-terminal fragment of CALHM6 , but this was not sufficient to open the channel to the passage of ATP. Judging by the structure of CALHM6 it is unlikely that its mechanism of opening could resemble the one of the CALHM1/3 channel. The CALHM6 oligomer is much bigger, being formed by 10/11 instead of eight subutnits[22,23]. Like CALHM2/4 and 5, CALHM6 shows densities in the middle of the channel pore that are compatible with a TM1 and a lipid density in CALHM6 and lipid bilayer in CALHM4, that could function as a plug for the channel. It is possible that changes in membrane voltage, extracellular ionic composition or pressure (all stimuli that open CALHM1) will not be enough to remove the TM1 and any possible lipid plug under it, and that changes in lipid composition of the membrane might be required for the bigger CALHM channels to open. While we have no data to confirm the role of lipids in CALHM6 channel opening we know that, upon immune synapse formation, there is a change in lipid composition of the plasma membrane. For example we see accumulation of Phosphatidylinositol 4,5-bisphosphate on the DC side of the IS[563] and lipid raft formation on NK is required for efficient macrophage-dependent activation[564], this changes could be the key of CALHM6 channel function. We know that, to work correctly, CALHM1/3 channel needs to be palmitoylated intracellularly and palmitoylation is a reversible modification that allows the anchoring of proteins to lipid rafts[52,562]. Alternatively, to the lipid hypothesis, the opening could be caused by protein binding or post-translational protein modification driven by the formation of the IS or other activating stimuli that we failed to reproduce *in vitro*.

7.4.4 CALHM6 is not a chaperone for ATP receptor P2X7 in BMDM

One final hypothesis was that CALHM6, despite its pore-like structure, would not form a functioning channel on the plasma membrane but instead would be important for the trafficking/assembly/signalling of other molecules in the synapse. The only indications that we have in this direction come from the non-channel function showed by CALHM2. A very recent study from the Yuan group[31] demonstrated that the CALHM2 oligomer works as a chaperon molecule to bring the ATP receptor, P2X7R to the cell membrane where it can signal in response to ATP and activate the downstream NLRP3 inflammasome complex, thus having a pro-inflammatory effect.

In our study, we excluded function of CALHM6 as P2X7R chaperone, at least *in vitro*. Although we have not excluded the possibility that CALHM6 may play that role for another client protein. P2X7R is the best known of the P2X family of ATP receptors, it is expressed in all immune cells and, among other functions, it is key for the activation of the NLRP3 inflammasome pathway in response to ATP[565]. Structural knowledge of the P2X7R derives from three-dimensional structures of homologous proteins like P2XR3[566], or of the same protein in other mammalian species[567]. P2X7R forms a trimer that can bind ATP at the interfaces of its extracellular domains and, upon ligation, change conformation allowing the rapid inward flux of Na^+ and Ca^{2+} and the outward flux of K^+[524]. The K^+ flux functions as a second signal for the activation of the inflammasome pathway causing cell death as well as the release of IL-1β and IL-18. The calcium flux instead, modulates intracellular signalling pathways, such as MyD88/NF-κB, PI3K/Akt/mTOR, and the MAPK pathway proteins[568–570]. Independently of inflammasome, P2X7R activation also promotes the secretion of IL-6, TNF and CCL2[571]. Interestingly, both NLRP3 inflammasome and IL-18 are required for NK cells activation upon *L. monocytogenes* infection in mice[256], i.e. the same stimulus that also require CALHM6 for NK cells activation. While CALHM6 does not regulate the trafficking of P2X7R to the extracellular membrane, it is possible that it affects its function in other ways. Janks and colleagues[572] showed that ATP treatment of BMDM expressing P2X7R causes the opening of channels that allow the passage of large cations across the

membrane as well as big fluorescent dyes like YO-PRO-1. While there are indications that P2X7R itself could be the channel in question, the molecular identity of the protein involved remains yet unknown[572,573]. It is intriguing to speculate that the CALHM protein could be involved not in the release of ATP but in the autocrine sensing of it, by acting in concert with P2X receptors like CALHM2 does.

7.5 Limitations

The main limitation with our RNAseq data is that it has been done on cultures of BMDM alone. While CALHM6 may have a role in autocrine signalling in BMDM, our study has shown that the most interesting role of CALHM6 is in cell-mediated activation of NK cells. Thus, it is likely that the main differences between WT and *Calhm6*$^{-/-}$ BMDM transcriptome would appear only after co-culture with NK cells. To circumvent this problem, we did try to sequence the transcriptome of splenic NK1.1^{+}CD3^{-} and F4/80^{+} cells from WT and *Calhm6*$^{-/-}$ mice after 6 h of Poly(I:C) or PBS injection but unfortunately the Poly(I:C) stimulation did not work uniformly and we were unable to use the data (data not shown).

While we demonstrated that CALHM6 localises at the IS between BMDM and NK cells on the BMDM side we did not test whether this was true for the NK side as well. We decided to start by looking at BMDM because we knew that they expressed the highest level of CALHM6 and because, for the scope of this project, we were mostly interested in the role of CALHM6 in accessory cells, any role it may play in NK cells we might address in the future.

All the imaging of CALHM6 proteins have been done in systems in which the proteins were overexpressed. This could create artefacts due to the non-physiological amount of CALHM6 present in the system. It is for example possible that the high perinuclear accumulation of endogenous CALHM6 is not present in non-transfected BMDM and the newly synthesised CALHM6 produced could be transferred directly to the extracellular membrane by the cells. To avoid this problem in future

experiments we are developing an iBMDM cell line with a CRISPR-Cas9 driven Knock-In of CALHM6-split GFP tag in only one of the *Calhm6* alleles. In this way we should have an easy-to-handle system that expresses tagged CALHM6 at physiological levels.

Following up our data on CALHM6 presence on the phagocytic cup we tested whether it had a role in endocytosis. We found none, but we have yet to test if CALHM6 role is instead in exocytosis, in particular at the stage of vesicular fusion with the plasma membrane at IS, as the genes regulated by CALHM6 seem to suggest. Preliminary results on glucuronidase release suggests that there is no difference (data not shown) but more suitable models will need to be investigated.

As mentioned in the discussion, we only investigated if CALHM6 is an ATP channel but failed to test whether other molecules or metabolites could be transported through CALHM6. This was entirely due to lack of time, we think that it would be extremely interesting to test whether Ca^{2+} in particular could be released through CALHM6. Several studies suggest that other CALHM proteins are permeable to calcium ions and the diameter of Ca^{2+} is much smaller than the one of ATP making it more suitable for channel release.

7.6 Conclusions

In this chapter we make a strong case for CALHM6 being important in the IS between accessory cells and NK cells. We also showed that *Calhm6*$^{-/-}$ BMDM are less capable to upregulate genes linked to synaptic pathways after immune stimulation, in particular genes involved in vesicular trafficking and fusion. We also showed for the first time that CALHM6, normally present in the cytoplasm, is polarised towards the membrane surrounding NK cells after the formation of a BMDM-NK IS. The polarisation is time-dependent and increases in the first 40 minutes of co-culture.

We showed that CALHM6 is polarised not only towards the BMDM-NK cell synapse but also to the phagocytic synapse. CALHM6 likely plays only a signalling role there as it was not required for particle uptake, the rate of phagocytosis between WT and *Calhm6*$^{-/-}$ BMDM is the same.

Looking at the supramolecular organisation of murine CALHM6 for the first time, we showed that it forms a big complex that requires disulphide bonds for its stability. Taken together our results suggest that the murine CALHM6 structure recapitulates the human one that has been resolved by Cryo-EM.

When we tested ATP release from CALHM6 we found that, unlike CALHM1/3, it does not function as an ATP channel following extracellular calcium depletion, exposure to high K^+ levels or Ionomycin. Even after deletion of the N-terminal fragment of CALHM6 that had been put forward as a possible gating mechanism, there is no ATP release from CALHM6 channels. It is likely that the stimuli needed to open the CALHM6 channel are more complex and different from the ones needed for the much smaller CALHM1/3.

CALHM6 does not influence the initiation of inflammation by acting as a chaperone of ATP-gated channel P2X7R like CALHM2 does. Because of this *Calhm6*$^{-/-}$ BMDM are capable to respond to ATP stimuli by activating canonical inflammasome pathways at the same rate as WT BMDM.

8 Future directions

While the work that we described represents a great leap forward in the understanding of the biology of CALHM6 and adds to the knowledge of the under-studied macrophage-NK cell IS, there are some fundamental question that our study has not yet addressed, mostly for lack of time or experimental models that would allow it. First and foremost, the main question that remain unanswered is the one of the functions of CALHM6. We showed that CALHM6 does not behave like the ATP channel CALHM1/3 or the chaperon molecule CALHM2, but we have yet to determine if it can work at all as a channel *in vivo* or *in vitro*. The second interesting question that we failed to address, due to the lack of a functional in vitro model, is in which cell type CALHM6 is important after the formation of the IS. We studied CALHM6 biology in macrophages, as they are the cells that express it most, we showed that it is dispensable in $CD11c^{+}$ cells, but we do not know what is CALHM6 role, if any, in NK cells.

Other equally interesting, albeit not as pressing, questions still unanswered regard how exactly CALHM6 is important at the IS, is it possible that its presence influence the construction of a successful IS? Could the absence of CALHM6 create aberration in the IS morphology or in the trafficking of molecules to the IS?

Our data indicates that CALHM6 is important in determining the kinetic of the immune response. In its absence the inflammatory response lags behind and the peak of inflammation happens later than in the WT. This is particularly dangerous when we have fast acting infection that could escape the defences orchestrated by the innate immune system and become too severe before the body is poised to act appropriately. Alternatively, this delayed peak could be causing problems in the case of co-infections. Many severe symptoms of infections, for example in the case viral pneumonia, are not caused by the primary infection but by opportunistic viral or bacterial co-infections[574]. The absence of CALHM6 could affect the response to secondary infections by changing the kinetics of the primary one.

Finally, it would be of the outmost interest to study CALHM6 protein interaction network. We know that CALHM6 forms a big complex that is trafficked intracellularly and there is the possibility, looking at RNAseq data and CALHM2 function, that CALHM6 is implicated in the trafficking of other proteins. To study the interactome of CALHM6, especially in the context of the IS would help answering questions on the function of CALHM6.

8.1 Determine if CALHM6 is an ATP or ion channel in macrophages

All the characterised members of the CALHM family are somewhat promiscuous channels, akin to Pannexins and Connexins, and other than ATP, can let through many different ions, the best studied of which is Ca^{2+}[16,36,575], that has the reported highest affinity for CALHMs. The large pore of CALHM6, and the fact that calcium signalling is important at the IS[223,237,576] and for immune cell activation, points towards CALHM6 being also a Ca^{2+} channel. It is possible that CALHM6 would exert this function only when expressed at the plasma membrane so, to test whether CALHM6 could allow for the passage of calcium fluxes we think that the best strategy would be the real-time monitoring of cellular calcium fluxes, done by microscopy or flow cytometry using calcium-sensitive fluorescent dyes like Fluo-4 or Fura Red. This will ideally be done all throughout the formation of the BMDM-NK cell IS.

It is possible that the ATP release, or the ionic current generated by CALHM6 is not macroscopic enough to be measured by whole-cell experiments, techniques targeted to small CALHM6-containing membrane fraction might be needed to detect the opening of CALHM6. One way to detect localised ATP release in the IS, is to use WT and *Calhm6*$^{-/-}$ BMDMs expressing membrane tethered ATP sensor (in collaboration with Prof Broz laboratory, Switzerland) and capture local, synaptic ATP by live imaging as the IS formed between macrophages and NK cells. Another way to detect local ion current is to use patch-clamp experiments. Most of the discoveries regarding CALHM1/3 gating and kinetic have been obtained through patch-clamp experiments on *X. Laevis* oocyte overexpressing CALHM1. This system has no other ion channels that can mask CALHM1 function and the oocyte cell is big enough to be

easily examined by patch-clamp techniques. Unfortunately, when Droździyc and colleagues tried the same experiment with CALHM6-expressing oocytes they could not see any current through the channel[22]. We have already shown that the form of CALHM6 ectopically expressed in *X. Laevis* is not the physiological (lacks N-glycosylation) so we are, in collaboration with Prof Foskett lab at the University of Pennsylvania, setting up a system to measure currents in WT vs *Calhm6*$^{-/-}$ BMDM through patch-clamp techniques. This will be a much more sensitive system than the fluorophores that we are equipped to use in our lab.

8.2 Define in which cell type CALHM6 is important *in vivo*

8.2.1 Generation of conditional KO mice

Unfortunately, our effort to establish an in vitro system that could clarify the role of CALHM6 in different cell types was unsuccessful. To address this question *in vivo*, we proceeded to generate specific conditional KO mice that lack CALHM6 only in defined cell population. Due to this approach, we have already established that CD11c^{+} DC are not important for CALHM6-mediated IFN-γ production. Our next step will be to generate NK cell-specific CALHM6 KO mice, this could be obtained by crossing our *Calhm6*$^{fl/fl}$ mice with Ncr1-Cre[577] mice that are already at the Kennedy Institute of Rheumatology. Looking at NK cell-dependent IFN-γ production after Poly(I:C)/*L. monocytogenes* injection will be a quick model to test the role of CALHM6 in NK cells. Future studies will generate macrophage and monocyte-specific CALHM6 KO mice using either LysMCre or CCR2 Cre mice, all available at Kennedy Institute of Rheumatology.

8.2.2 Unbiased approach to the study of macrophage and NK cells transcriptome in *Calhm6*$^{-/-}$ mice

Three hours after Poly(I:C) injection NK cells from *Calhm6*$^{-/-}$ mice produce less IFN-γ. To identify CALHM6-dependent gene expression programmes in both activating and effector cells we will perform

RNA sequencing, of splenic F4/80^{+} and NK1.1^{+} cells in naïve vs Poly(I:C) injected mice. Optimisation of this experiment is underway.

8.3 Define CALHM6 role at the immune synapse

8.3.1 Avoiding artefacts caused by CALHM6 overexpression

As we mentioned already, all our IS images have been obtained by overexpressing a tagged form of CALHM6 in BMDM, because the antibody against the endogenous form does not work for confocal microscopy. This could cause several artefacts in the cellular localisation and behaviour of CALHM6. To avoid this problem in the future we are developing an immortalised BMDM cell line that expresses, a fluorescently tagged form of CALHM6 knocked into one of the endogenous CALHM6 alleles under its natural promoter. This will allow for the study of the IS in more physiological conditions.

8.3.2 Imaging the immune synapse

While we showed that CALHM6 is recruited at the immune synapse in BMDM-NK cell model we have not yet established whether its absence causes aberration in the establishment or the maturation of the IS itself. We have optimised an *in vitro* model in which we can image the IS, it would be interesting to use this model to check if there are identifiable difference in the BMDM-NK synapse between WT and *Calhm6*$^{-/-}$ cells. In light of the RNA seq data we suspect that CALHM6 could influence vesicle trafficking and fusion, it would be of particular interest to test whether IL-12 can efficiently polarise and be released in the *Calhm6*$^{-/-}$ synapse. IL-12 needs to be trafficked to the synapse in vesicles and it is only released in the synaptic cleft[223], so attempting to look at whole cell or extracellular IL-12 content would not give us an indication of a defect in IL-12 delivery at the synapse. Knowing how important IL-12 is for IFN-γ production this is a priority. Other molecules also polarise towards the IS and should be checked via microscopy, for example IL-18 is another cytokine important for NK cells activation that polarises at the IS[237]. It would also be interesting to check whether the rearrangement of microtubules towards the IS is altered by the absence of CLAHM6.

8.4 Investigate further the physiological consequences of delayed innate responses in Calhm6$^{-/-}$ mice

8.4.1 Establish how CALHM6 affect the accessory cell response to Poly(I:C)

We have shown that CALHM6 deficiency causes the delay in the production of IFN-γ upon Poly(I:C) stimulation or *Listeria* infection. We know that in these experimental models NK cell activation and IFN-γ production are dependent on accessory cells. Future studies should define how the response of accessory cells to Poly(I:C) is different in the very early phases of stimulation (30 min, 1 or 3 h), even before they start to communicate with NK cells, and also after they have failed to receive NK cell derived IFN-γ help . This could be obtained by isolating RNA from splenic macrophages and DC at different time points after Poly(I:C) injection and measuring by qPCR the expression of genes that we know be the signature of Poly(I:C) response, like IL-1β, IL-6, TNF or more type I IFN regulated genes.

8.4.2 Test how delayed innate responses in *Calhm6*$^{-/-}$ mice affect their response to a subsequent co-infection.

In humans, co-infections are common (e.g. viral, followed by bacterial co-infection). They cause severe diseases because response to a primary infection affect the immune system readiness to respond to a second insult. The timing of the second insult is key to the type of response the organism exhibit. When it happens at peak inflammation a second stimulus can cause devastating effect starting a cytokine storm and sepsis response, alternatively if the first infection is already receding and the immune system has activated negative feedback loops to dampen inflammation and reduce response to pro-inflammatory stimuli, then the second pathogen might be advantaged by the lack of a proper immune response[578,579]. To test whether CALHM6 plays a role in the time-dependent degree of secondary response we could use well established lethal co-infection mimic models, simplest one being lethal model of Poly(I:C) injection, followed by LPS, with the second stimulus administered at different times after the first one.

8.5 Define the interactome of CALHM6

CALHM6 forms a big oligomeric structure in cells and it is trafficked in the cell to the IS. Being such a big complex it is likely that it could establish several interactions with other proteins, especially in the crowded environment of the IS. Knowing what are the other proteins that can bind CALHM6 would be a huge step forward in the understanding of CALHM6 function. This is especially true now that CALHM2 has been identified as a chaperone protein that can bind P2X7R[22]. When we tried to analyse the interactome of CALHM6 using the endogenous protein we could not obtain enough material to submit a sample for Mass Spectrometry analysis. We suspect this was in part due to the inadequate affinity of the antibody against the three-dimensional structure of CALHM6 in the cells. It is also difficult to obtain enough cells for a Mass Spectrometry analysis when working with primary cells. For this reason, we are developing an iBMDM cell line that express physiological levels of a tagged form of CALHM6, that we will be able to use to identify the its interactome.

8.6 Test possible functional interaction between CALHM6 and other CALHM proteins

While CALHM6 is the only member of the CALHM family to be upregulated by pro-inflammatory stimuli in BMDM we can still measure in these cells baseline expression of the *Calhm2* gene, albeit at much lower levels. CALHM2 is the only other member of the CALHM family that is not exclusively expressed in the CNS and it is possible that its interaction with CALHM6 affects its function. The fact that CALHM1 can polymerise with CALHM3 to form a heteromeric channel, together with the structural similarities between the members of the family, suggest that an heteromeric channel might be possible in the case of CALHM6 as well. To test this hypothesis, we could use short interference RNA to knock down the level of CALHM2 in BMDM and check whether a double KO affects the response to pro-inflammatory stimuli in a more prominent way.

9 Final comments

In this study we found a novel synaptic channel-like protein that affects the kinetic of the immune response to infection. We demonstrated that CALHM6 deficiency slows the reaction to *L. monocytogenes* infection by delaying the production of NK cell specific IFN-γ, and we showed how this delay has a domino effect on the subsequent immune response. In *Calhm6*$^{-/-}$ the pathogen is allowed to hyper proliferate in the early stages, thus probably reducing their lethal concentration 50 and making the mice more susceptible to *L. monocytogenes* infection. Furthermore, the delay in IFN-γ production postpone the appearance of the resolving-cytokine IL-10 (Figure 38). The importance of CALHM6 is not limited to *L. monocytogenes* infection but it is also key following the viral-mimicking compound Poly(I:C). We know that the prompt reaction of the immune system to infection is fundamental for the efficient control of the infection. The immune system is a well-oiled machine that needs all its cogs to work in synchrony to obtain the ideal response, IFN-γ is one of the main component of the initial pro-inflammatory feedback against pathogens and its pleiotropic effects are required to kick-start and boost the immune response[580]. There are many ways in which IFN-γ is fundamental in establishing the downstream immune response, first of all during *L. monocytogenes* infection, is required to activate macrophages and enable them to kill phagocyted bacteria[431,475]. Without this action *L. monocytogenes* can escape the vacuole, proliferate in the cytoplasm, and use macrophages as a vector of infection[288,303]. This requirement for IFN-γ in the early stages of infection is not a prerogative of *L. monocytogenes* response but a more generic immune mechanism. For example, during early response to *M. tuberculosis* in the lungs, alternatively activated macrophages (AAM) that have an immunosuppressive phenotype, need to be quickly substituted by classically activated ones (CAM) that have bactericidal properties[581]. The key cytokine for the activation of CAM is IFN-γ and it is likely that an early delay in IFN-γ production, could impair the immune response by increasing the switching time between AAM and CAM, worsening the outcome of the disease[581,582]

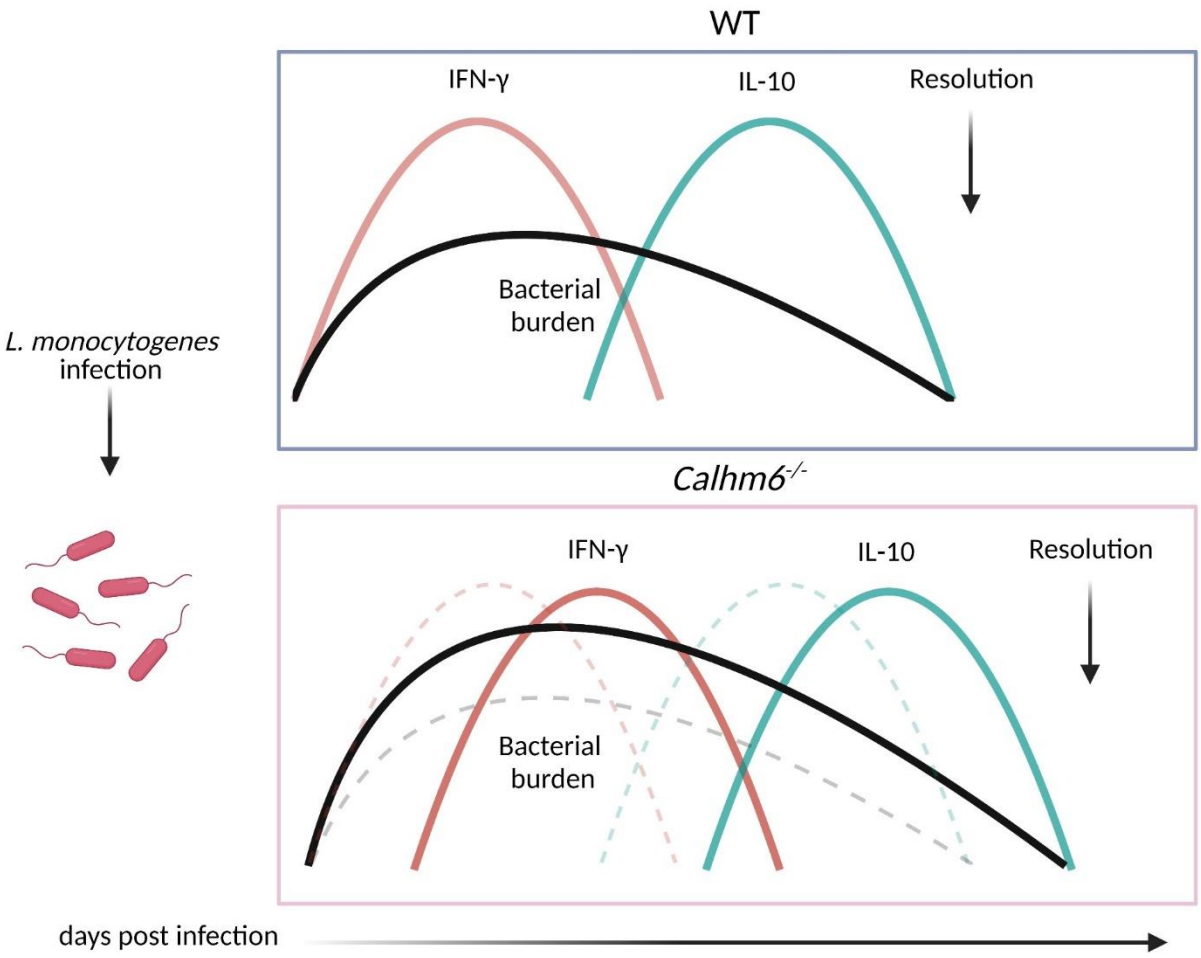


Figure 39: Effect of CALHM6 deficiency in *L. monocytogenes* infection. When *Calhm6*$^{-/-}$ mice are infected with *L. monocytogenes* the production of IFN-γ and IL-10 from NK cells is delayed and the initial bacterial burden increased for the inability of the immune system to efficiently react to the infection. both WT and *Calhm6*$^{-/-}$ mice though, can clear the infection by day 7.

The change in the kinetic of the response caused by the absence CALHM6 becomes of particular relevance when we consider the case of superinfections. Multiple infections with different pathogens are often the cause of serious disease in the real world. The case of influenza infections, especially before the introduction of modern antibiotics, is emblematic: during the 1918 H1N1 pandemic between 85-95% of all lethal cases manifested bronchopneumonia mostly caused by co-infection with influenza virus and *Staphylococcus aureus* or *Streptococcus pneumoniae*[583]. For bacterial infection following influenza infection the timing between viral and bacterial exposure is key in determining the disease outcome[584]: co-infection that occurs 2-3 days post viral encounter decrease susceptibility to the pathogen, 7 days later patients become more susceptible to the bacterial disease[585,586]. While this difference in susceptibility has multiple causes, from virulence factors to neutrophilia[583,584,587,588], the timely production of IFN-γ is itself a factor[589,590]. IFN-γ appears very early and it is a fast-action cytokine, messenger RNA induced by IFN-γ in responsive cells appears after only 30 min of exposure and the thousands of genes upregulated accumulate in 5 h[386,591], among those genes there are a significant number that increase the preparedness of the organism to bacterial infections. For example, IFN-γ shifts the dose-response curve to LPS, allowing macrophages to respond to lower doses of bacteria[592,593] by increasing TLR4 expression[594,595], and by promoting the expression of proteins like guanylate binding proteins that can sense cytosolic LPS[596,597]. These literature findings suggest that the absence of CALHM6, by changing the kinetic of the immune response, would affect the response of an organism to co-infection depending on the timing of the second infection. While we are only beginning to test this hypothesis now, we believe that it is of the utmost relevance to further investigate the role of CALHM6 in the context of co-infections.

By showing that CALHM6 localises at the interface between macrophage and NK cells after stimulation, we suggest a role for CALHM6 as a synaptic protein. The activating immunological synapse between macrophage and NK cells is one of the least well-known IS, especially when compared with the DC-T cell or the cytotoxic synapse. Our study adds another tile to the very incomplete mosaic that is the macrophage-NK cell IS and for the first time associates a channel-like protein with this structure.

In this study we also go a step further in the characterisation of the already well-studied innate response to *L. monocytogenes*. While most of its mechanism have been elucidated, our study highlights the importance of the macrophage-driven NK cell activation compared to the DC one, that has already been observed and described[444,446,473]. Our conditional KO experiments as well as gene expression analysis, suggests a direct interaction, possibly carried out in the RP, between *L. monocytogenes* infected macrophages and naïve NK cells in vivo. Without this interaction the initial pro-inflammatory feedback loop driven by IFN-γ is delayed. Given the importance that NK cells have as first responders against intracellular pathogens as well as tumours[84,107,113], especially seeing the increasingly promising results in NK cell-based cancer immunotherapy[86] the exact understanding of the mechanism of cell-mediated NK cell activation could be key to the development of effective therapies.

While we fell short of exactly defining CALHM6 mechanism of action in the immunological synapse we are aware that the reason why it was so difficult to pinpoint the function of CALHM6, is the same that drives our interest in it: the absolute uniqueness of the CALHM protein structures. Save from the CALHM1/3 channel, that compared to CALHM6, forms a significantly smaller oligomer[22], several groups have failed to find an opening mechanism for any of the other CALHM oligomers[18,22]. While there are many examples of resolved structures of gated ion channels that bind lipids[598–600] we are unaware of any with this pore size that use lipids as a "plug" in the internal pore like CALHM2 and 4, or possible combination of inward conformational orientation of TM1 plus the lipids underneath, that somehow closes the CALHM6 pore. Unfortunately, unlike other ion channels in which the resolution of the structure gives hints into the possible gating mechanism, this is not the case for CALHM6, where inner pore structure is not resolved clearly. It is possible that various CALHM proteins have evolved from the taste receptor complexes present in taste bud cells of which CALHM1/3 is a part. In recent years taste receptors of this kind have been identified in the airways[601], gastrointestinal tract[602], lungs[56] and CNS[603] where their function has moved from that of taste receptors to innate immune sensors of compound of pathogen origin[601], this would go some way into explaining CALHM6 function

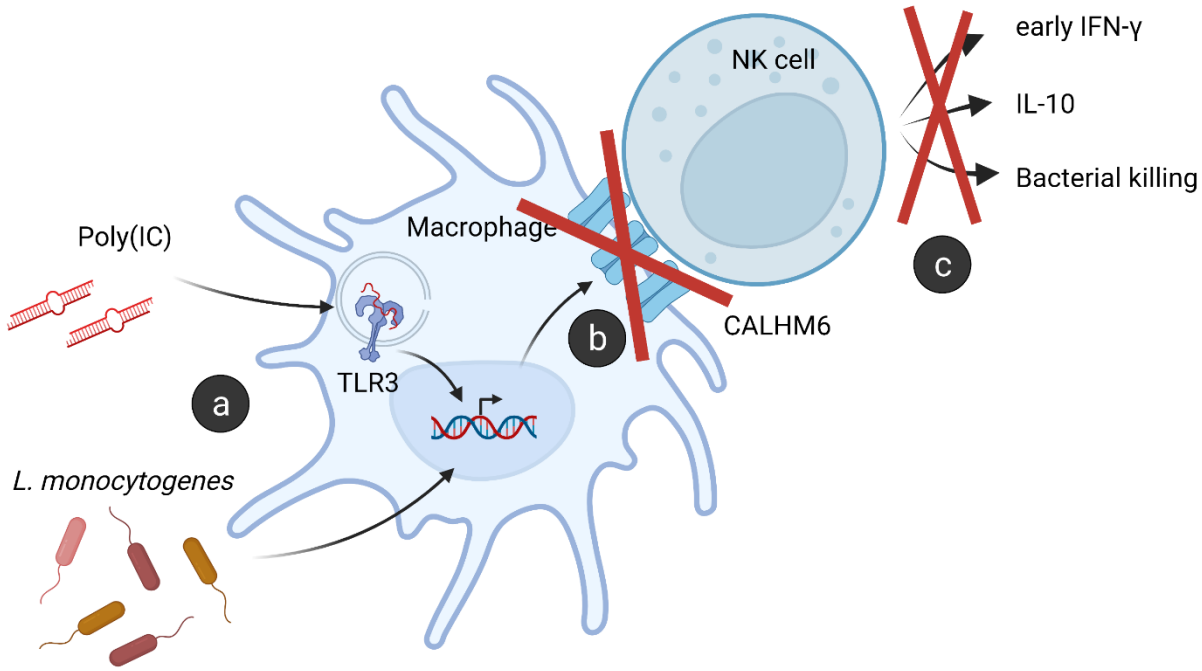


Figure 40: CALHM6 deficiency impair mice response to L. monocytogenes infection. a) pro-inflammatory stimuli like Poly(I:C) and systemic *L. monocytogenes* infection activate macrophages and upregulate CALHM6 expression in macrophages. b) Infected macrophages can, in turn, activate NK cells in the spleen through the formation of an IS in which CALHM6 proteins are recruited. c) In the absence of CALHM6 macrophages do not properly activate NK cells that fail to produce IFN-γ in the early stages of the infection. This causes a defect in *L. monocytogenes* killing and increases the bacterial burden at peak infection. At the same time CALHM6 deficiency, by delaying the production of IFN-γ, also cause a reduction in IL-10 production at peak infection.

in the immune system, and why it is different from the one of his homologue CALHM1 in taste bud cells.

Structural analysis suggests that slight modification in the interface at which CALHM monomers interact with each other has caused a progressive increase in the angle at which the subunit can bind each other. This in turn, has increased the number of monomers that form the channel, causing an expansion in the pore diameter, possibly creating space for the infiltration of the lipid plug. It is yet unclear if these channel-like structures of CALHM2, 4, 5 and 6 have retained the channel properties of CALHM1/3 and have adapted their gating strategy, or if the permeability of the structure has been completely abrogated in order to protect the cells from indiscriminate loss of ions. An intriguing hypothesis is that CALHM structures could work not as channels but as protein chaperons possibly, in the case of CALHM6, organising proteins at the IS.

In this work we have gone a long way to elucidate the role of CALHM6 in the immune system during infections and we have considerably increased our degree of biological knowledge of this understudied protein.

10 List of figures

FIGURE 1: Oligomeric structure of CALHM proteins..... 19

FIGURE 2: CALHM1/3 channel in taste sensing..... 22

FIGURE 3: CALHM6 in the immune system..... 29

Figure 4: Activation of NK cells..... 35

Figure 5: Schematic representation of a murine accessory cell-NK cell activating immune synapse..... 44

Figure 6. *Calhm6* expression in immune cells..... 88

Figure 7. *Calhm6* expression is induced by pro- and suppressed by anti-inflammatory cytokines..... 91

Figure 8. *Calhm6* expression is boosted by IFN-γ pre-treatment..... 93

Figure 9: Generation and characterisation of *Calhm6*$^{-/-}$ mice..... 96

Figure 10: Flow cytometry gating strategy for spleen adaptive cells..... 97

Figure 11: Flow cytometry gating strategy for spleen innate cells..... 98

Figure 12: Flow cytometry gating strategy for thymus..... 99

Figure 13: CALHM6 is important for IFN-γ production in early response to infection..... 112

Figure 14: Flow cytometry gating strategy for splenic IFN-γ^{+} NK cells..... 113

Figure 15: CALHM6 deficiency impairs IFN-γ but not Granzyme B production from NK cell in earl..... 115

Figure 16: *Calhm6*$^{-/-}$ mice fail to control early stages of *L. Monocytogenes* infection..... 117

Figure 17: *Calhm6*$^{-/-}$ mice fail to control early stages of *L. Monocytogenes* infection even with a lower initial burden of infection..... 119

Figure 18: *Calhm6*$^{-/-}$ NK cells can produce normal levels of IFN-γ at peak infection allowing for *L. monocytogenes* clearance 121

Figure 19: Other blood cytokines show no difference between WT and *Calhm6*$^{-/-}$ mice at peak infection..... 122

Figure 20: No difference in NK cell-dependent IFN-γ production after 12 h of Poly(I:C)..... 124

Figure 21: *Calhm6*$^{-/-}$ can clear L. monocytogenes at day 7..... 126

Figure22: *Calhm6*$^{-/-}$ mice can efficiently mount memory response and clear *L. monocytogenes* when re-challenged with higher doses, 42 days after primary infection.... 128

Figure 23: *Calhm6*$^{-/-}$ mice can clear H3N2 Influenza A virus…….. 130

Figure 24: *Calhm6*$^{-/-}$ NK cells can produce IFN-γ in response to contact-independent, soluble stimuli…… 133

Figure 25: F4/80^{+} *Calhm6*$^{-/-}$ macrophages can respond to Poly(I:C) and develop normal Type I IFN response *in vivo*…… 135

Figure 26: No differences in serum cytokine concentration between WT and *Calhm6*$^{-/-}$ mice after 24 h L. monocytogenes infection…….. 139

Figure 27: *Calhm6*$^{-/-}$ macrophages and DC are capable of responding to *L. monocytogenes* and developing normal pro-inflammatory and anti-microbial response *in vitro*…… 140

Figure 28: Flow cytometry gating strategy for IL-15ra on BMDC…… 141

Figure 29: Breeding strategy for *Itgax*$^{cre/-}$*Calhm6*$^{fl/fl}$…… 144

Figure 30: CALHM6 expression in CD11c+ cells is not required for NK-dependent IFN-γ production after Poly(I:C) stimulation *in vivo*…… 145

Figure 31: *In vitro* co-culture of macrophages/DC and NK cells are not suitable to study difference in IFN-γ production between WT and *Calhm6*$^{-/-}$ mice…… 148

Figure 32: *Calhm6*$^{-/-}$ BMDM fail to upregulate mRNA linked to synaptic pathways following Poly(I:C) stimulation…… 165

Figure 33: CALHM6 is mostly expressed in BMDM cytoplasm in nonactivated BMDMs…… 169

Figure 34: CALHM6 polarises towards BMDM synapses…… 170

Figure 35: There is no difference in phago- and endocytosis rate between WT and *Calhm6*$^{-/-}$ BMDM…….. 173

Figure 36: Like other members of the CALHM family in BMDM CALHM6 forms a higher order oligomeric complex…….. 176

Figure 37: CALHM6 is not opened by the same stimuli that open CALHM1…… 179

Figure 38: CALHM6 deficiency does not affect P2X7R expression or inflammasome activation in BMDM…… 181

Figure 39: Effect of CALHM6 deficiency in *L. monocytogenes* infection…… 202

Figure 40: CALHM6 deficiency impair mice response to L. monocytogenes infection……. 205

11 Appendix

11.1 Untreated BMDM

Table 1: List of Differentially expressed genes in WT vs *Calhm6*$^{-/-}$ BMDM

gene_name	baseMean	FC	log2FoldChange	pvalue	padj	gene_description
Gm10248	133.52	10.41	3.38	2.92467E-25	5.51301E-21	predicted gene 10248
Fam26f	2424.5	0.114	-3.132	2.25885E-18	2.12897E-14	calcium homeostasis modulator family member 6
Gm21451	34.9	22.22	4.474	1.02032E-10	3.84659E-07	predicted gene, 21451
Gm21887	261.08	0.015	-6.012	1.04399E-08	3.27988E-05	-
Gm27175	15.14	96.915	6.599	4.01821E-08	9.40898E-05	-
Gm37847	15.06	96.908	6.599	4.49235E-08	9.40898E-05	-
Egln3	542.5	0.218	-2.199	1.01221E-07	0.000173456	egl-9 family hypoxia-inducible factor 3
Gm16867	55.96	5.762	2.527	2.75534E-07	0.000432817	predicted gene, 16867
Mgarp	123.38	0.248	-2.014	2.22084E-05	0.029902038	mitochondria localized glutamic acid rich protein

Table 2: Gene Ontology enrichment analysis in WT vs *Calhm6*$^{-/-}$ BMDM

Description	Count	GeneRatio	BgRatio	pvalue	p.adjust
filamentous actin	2	2/22	28/13042	0.001	0.04799

11.2 Poly(I:C) stimulated BMDM

Table 3: List of the 50 highest Differentially expressed genes in WT vs *Calhm6*$^{-/-}$ BMDM

gene_name	baseMean	FC	log2FoldChange	pvalue	padj	gene_description
Fam26f	2424.5	0.025	-5.331	4.198E-62	7.91323E-58	calcium homeostasis modulator family member 6
Gm10248	133.52	18.791	4.232	4.02848E-32	3.79684E-28	predicted gene 10248
Syt7	355.92	0.038	-4.717	6.6899E-12	3.15261E-08	synaptotagmin VII
Kif1a	283.05	0.033	-4.933	8.31909E-11	2.61358E-07	kinesin family member 1A
Diras2	194.04	0.07	-3.835	1.38222E-10	3.72211E-07	DIRAS family, GTP-binding RAS-like 2
Ak3l2-ps	94.22	0.01	-6.637	3.89623E-10	8.16045E-07	-
Gm21451	34.9	18.038	4.173	7.04692E-10	1.20759E-06	predicted gene, 21451
Gm16867	55.96	8.357	3.063	2.84207E-09	4.46443E-06	predicted gene, 16867
Egln3	542.5	0.168	-2.574	6.17344E-09	8.95148E-06	egl-9 family hypoxia-inducible factor 3
Gm21887	261.08	0.016	-5.925	2.08714E-08	2.81018E-05	-
Vgf	58.87	0.08	-3.64	9.13446E-08	0.000107615	VGF nerve growth factor inducible
Rph3a	32.56	0.021	-5.563	1.97264E-07	0.000195706	rabphilin 3A
Cplx2	133.19	0.004	-7.883	2.61345E-07	0.000246317	complexin 2
Gm27175	15.14	34.535	5.11	2.8159E-07	0.00025276	-
Gm37847	15.06	34.535	5.11	3.15965E-07	0.000270725	-

Cplx1	59.04	0.015	-6.094	3.9494E-07	0.000323679	complexin 1
Mgarp	123.38	0.153	-2.707	5.31723E-07	0.000417624	mitochondria localized glutamic acid rich protein
Chrm1	34.17	0.027	-5.213	4.84812E-06	0.002687855	cholinergic receptor, muscarinic 1, CNS
Map1a	136.18	0.145	-2.787	1.096E-05	0.005065179	microtubule-associated protein 1 A
Robo2	45.41	0.16	-2.648	1.87427E-05	0.007066014	roundabout guidance receptor 2
Ndrg4	156.97	0.08	-3.645	1.91916E-05	0.007093381	N-myc downstream regulated gene 4
Gm3764	43.3	0.032	-4.961	2.37739E-05	0.008455451	-
Gm26953	27.58	0.002	-9.078	2.76319E-05	0.009470193	-
Ddn	131.37	0.004	-8.061	2.81573E-05	0.009477954	dendrin
Gria1	99.82	0.001	-10.327	2.97837E-05	0.009849507	glutamate receptor, ionotropic, AMPA1 (alpha 1)
Enpp2	56.43	0.026	-5.29	3.95497E-05	0.012425208	ectonucleotide pyrophosphatase/phosphodiesterase 2
Trim9	28.87	0.017	-5.91	4.1074E-05	0.012692545	tripartite motif-containing 9
Ndrg2	46.29	0.002	-9.138	4.37635E-05	0.013305525	N-myc downstream regulated gene 2
Fam107a	20.99	0.003	-8.345	5.14381E-05	0.014917045	family with sequence similarity 107, member A
Il33	28.4	0.016	-5.957	5.75012E-05	0.015708648	interleukin 33
Snph	38.73	0.013	-6.226	5.73469E-05	0.015708648	syntaphilin
Car2	121.51	0.064	-3.957	5.59749E-05	0.015708648	carbonic anhydrase 2
Ntrk2	40.99	0.011	-6.547	5.51888E-05	0.015708648	neurotrophic tyrosine kinase, receptor, type 2
Gprin1	12.94	0.006	-7.456	6.10702E-05	0.016213705	G protein-regulated inducer of neurite outgrowth 1
Miat	49.65	0.001	-9.788	6.10346E-05	0.016213705	myocardial infarction associated transcript (non-protein coding)
Apba2	19.92	0.005	-7.607	6.20787E-05	0.016252537	amyloid beta (A4) precursor protein-binding, family A, member 2
Grin1	49.51	0.048	-4.388	6.36066E-05	0.016424456	glutamate receptor, ionotropic, NMDA1 (zeta 1)
Phyhip	35.5	0.002	-8.791	7.19439E-05	0.016951789	phytanoyl-CoA hydroxylase interacting protein
Hspa12a	82.52	0.091	-3.462	7.04759E-05	0.016951789	heat shock protein 12A
Sh3gl2	25.21	0.004	-8.141	7.17566E-05	0.016951789	SH3-domain GRB2-like 2
En2	30.76	39.206	5.293	7.06284E-05	0.016951789	engrailed 2
Tenm2	49.14	0.026	-5.264	7.01915E-05	0.016951789	teneurin transmembrane protein 2
Hpcal4	66.88	0.001	-9.527	7.28922E-05	0.01696319	hippocalcin-like 4
Clstn2	22.02	0.004	-8.094	8.22066E-05	0.018230517	calsyntenin 2
Atp1a2	78.64	0.006	-7.357	9.07483E-05	0.019438695	ATPase, Na+/K+ transporting, alpha 2 polypeptide
Plppr4	33.5	0.003	-8.548	9.41532E-05	0.01994144	phospholipid phosphatase related 4
Pcp4	41.37	0.011	-6.566	0.000116948	0.024224989	Purkinje cell protein 4
Cntn1	27.92	0.003	-8.478	0.000119209	0.024424802	contactin 1
Hpca	103.1	0.005	-7.654	0.000121939	0.024452601	hippocalcin
Obsl1	29.93	0.2	-2.321	0.000130264	0.025556214	obscurin-like 1

Table 4: Gene Ontology enrichment analysis in WT vs *Calhm6*$^{-/-}$ BMDM (first 20 pathways)

Description	*Count*	*GeneRatio*	*BgRatio*	*pvalue*	*p.adjust*
synaptic membrane	67	67/258	343/13042	2.3E-48	1E-45
trans-synaptic signaling	76	76/253	480/12857	2E-48	5.6E-45
chemical synaptic transmission	75	75/253	471/12857	6.1E-48	5.6E-45
anterograde trans-synaptic signaling	75	75/253	471/12857	6.1E-48	5.6E-45
synaptic signaling	76	76/253	488/12857	6.9E-48	5.6E-45

glutamatergic synapse	66	66/258	390/13042	2.1E-43	4.5E-41
presynapse	65	65/258	406/13042	3.7E-41	5.4E-39
intrinsic component of synaptic membrane	43	43/258	142/13042	1.4E-39	1.5E-37
integral component of synaptic membrane	39	39/258	130/13042	9.5E-36	7E-34
regulation of trans-synaptic signaling	56	56/253	363/12857	1.4E-34	7.9E-32
axon part	53	53/258	341/13042	1.1E-32	6.8E-31
intrinsic component of postsynaptic membrane	33	33/258	97/13042	2.2E-32	1.2E-30
postsynaptic specialization	51	51/258	341/13042	1.3E-30	6.4E-29
neuron to neuron synapse	50	50/258	341/13042	1.4E-29	6.1E-28
integral component of postsynaptic membrane	30	30/258	89/13042	2.3E-29	9E-28
asymmetric synapse	47	47/258	325/13042	1.6E-27	4.9E-26
synapse organization	46	46/253	306/12857	8E-28	3.8E-25
behavior	52	52/253	424/12857	4.4E-27	1.8E-24
intrinsic component of presynaptic membrane	25	25/258	77/13042	3.7E-24	1.1E-22
distal axon	40	40/258	277/13042	1.9E-23	5.3E-22

11.3 LPS stimulated BMDM

Table 5: List of the 50 highest Differentially expressed genes in WT vs *Calhm6*$^{-/-}$ BMDM

gene_name	*baseMean*	*FC*	*log2FoldChange*	*pvalue*	*padj*	*gene_description*
Fam26f	2424.5	0.066	-3.932	2.59E-46	2.44E-42	calcium homeostasis modulator family member 6
Gm10248	133.52	18.597	4.217	2.07E-46	2.44E-42	predicted gene 10248
AC161884.1	397.23	0.242	-2.044	2.16E-16	1.36E-12	-
Gm21451	34.9	19.253	4.267	4.61E-11	2.17E-07	predicted gene, 21451
Cd38	5623.72	0.539	-0.892	4.36E-10	1.64E-06	CD38 antigen
Gm21887	261.08	0.014	-6.172	6.73E-09	2.11E-05	-
Gm16867	55.96	6.662	2.736	1.2E-08	3.23E-05	predicted gene, 16867
Gja1	291.91	0.441	-1.181	1.89E-07	0.000445	gap junction protein, alpha 1
AC168059.1	178.68	0.43	-1.216	4.46E-07	0.000933	-
Gm4131	18.98	0.012	-6.327	1.39E-06	0.002614	predicted gene 4131
Rgs9	109.05	0.228	-2.133	1.64E-06	0.002645	regulator of G-protein signaling 9
Scd2	9058.26	0.467	-1.099	1.68E-06	0.002645	stearoyl-Coenzyme A desaturase 2
Gm37847	15.06	14.949	3.902	1.94E-06	0.00281	-
Lzts2	193.07	0.493	-1.019	2.48E-06	0.003334	leucine zipper, putative tumor suppressor 2
Scd1	195.57	0.314	-1.669	3.21E-06	0.004035	stearoyl-Coenzyme A desaturase 1
C1qtnf6	480.21	0.556	-0.848	4.12E-06	0.004857	C1q and tumor necrosis factor related protein 6
F13a1	519.84	0.476	-1.071	4.5E-06	0.00499	coagulation factor XIII, A1 subunit
Brca1	1428.43	1.386	0.471	5.4E-06	0.005656	breast cancer 1, early onset
Fcrls	2186.48	0.531	-0.912	6.53E-06	0.006477	Fc receptor-like S, scavenger receptor
Aldoc	691.72	0.39	-1.357	7.92E-06	0.007461	aldolase C, fructose-bisphosphate
Psrc1	404.88	0.616	-0.7	9.41E-06	0.008447	proline/serine-rich coiled-coil 1
Egln3	542.5	0.285	-1.813	1.06E-05	0.009114	egl-9 family hypoxia-inducible factor 3
Capsl	214.29	2.848	1.51	1.17E-05	0.009617	calcyphosine-like
Timeless	1031.34	1.488	0.573	1.24E-05	0.009721	timeless circadian clock 1

Gm27175	15.14	10.232	3.355	1.34E-05	0.010083	-
Upp1	3353.3	0.595	-0.748	1.56E-05	0.011286	uridine phosphorylase 1
Epas1	89.13	0.312	-1.68	2.17E-05	0.015171	endothelial PAS domain protein 1
Slc6a9	64.08	0.342	-1.549	2.78E-05	0.018714	solute carrier family 6 (neurotransmitter transporter, glycine), member 9
Scn1b	284.02	0.548	-0.867	2.88E-05	0.018721	sodium channel, voltage-gated, type I, beta
Rgs1	5254.57	1.554	0.636	3.77E-05	0.023701	regulator of G-protein signaling 1
Tgfbr2	8564.31	0.763	-0.391	4.32E-05	0.026244	transforming growth factor, beta receptor II
Emb	4184.28	0.679	-0.559	4.5E-05	0.026519	embigin
Prr5l	2501.09	1.488	0.573	5.53E-05	0.031563	proline rich 5 like
Ndrg1	2017.59	0.562	-0.832	6.42E-05	0.033402	N-myc downstream regulated gene 1
Epb41l3	90.06	0.468	-1.096	6.91E-05	0.033402	erythrocyte membrane protein band 4.1 like 3
Syt16	47.78	0.084	-3.566	6.74E-05	0.033402	synaptotagmin XVI
E230016K23Rik	5171.93	0.6	-0.738	6.64E-05	0.033402	RIKEN cDNA E230016K23 gene
Kcnc3	42.32	0.27	-1.889	6.1E-05	0.033402	potassium voltage gated channel, Shaw-related subfamily, member 3
Gm17509	413.47	0.579	-0.788	6.73E-05	0.033402	-
Gm9574	347.39	1.724	0.786	7.1E-05	0.033476	-
P4ha2	610.51	0.498	-1.007	7.57E-05	0.034799	procollagen-proline, 2-oxoglutarate 4-dioxygenase (proline 4-hydroxylase), alpha II polypeptide
Ccl6	5033.25	0.597	-0.744	8.05E-05	0.035308	chemokine (C-C motif) ligand 6
Stra6l	1627.71	1.51	0.595	7.92E-05	0.035308	STRA6-like
Zmat3	4758.86	0.717	-0.479	8.42E-05	0.036065	zinc finger matrin type 3
Vwf	3616.39	1.534	0.617	8.76E-05	0.036714	Von Willebrand factor
Tmem176a	487.59	0.464	-1.107	9.54E-05	0.038348	transmembrane protein 176A
Myo1e	21009.69	1.462	0.548	9.56E-05	0.038348	myosin IE
Tmem176b	755	0.527	-0.924	9.93E-05	0.03864	transmembrane protein 176B
Gm17035	1013.04	0.47	-1.09	0.0001	0.03864	-
Mir5114	407.33	0.517	-0.951	0.000106	0.0401	microRNA 5114

Table 6: Gene Ontology enrichment analysis in WT vs *Calhm6*$^{-/-}$ BMDM (first 20 pathways)

Description	*Count*	*GeneRatio*	*BgRatio*	*pvalue*	*p.adjust*
synaptic membrane	19	19/85	343/13042	5.1E-13	1.24E-10
trans-synaptic signaling	22	22/84	480/12857	2.62E-13	3.5E-10
synaptic signaling	22	22/84	488/12857	3.66E-13	3.5E-10
regulation of trans-synaptic signaling	19	19/84	363/12857	1.42E-12	5.49E-10
anterograde trans-synaptic signaling	21	21/84	471/12857	1.72E-12	5.49E-10
glutamatergic synapse	18	18/85	390/13042	4.77E-11	3.86E-09
presynapse	17	17/85	406/13042	7.96E-10	4.84E-08
integral component of synaptic membrane	10	10/85	130/13042	1.14E-08	5.52E-07
postsynaptic density	14	14/85	324/13042	2E-08	7.2E-07
asymmetric synapse	14	14/85	325/13042	2.08E-08	7.2E-07
intrinsic component of synaptic membrane	10	10/85	142/13042	2.66E-08	8.07E-07
axon part	14	14/85	341/13042	3.79E-08	8.38E-07
neuron to neuron synapse	14	14/85	341/13042	3.79E-08	8.38E-07
synapse organization	14	14/84	306/12857	9.87E-09	2.1E-06
behavior	16	16/84	424/12857	1.21E-08	2.31E-06

regulation of membrane potential	13	13/84	271/12857	2E-08	3.49E-06
regulation of AMPA receptor activity	5	5/84	17/12857	6.14E-08	9.8E-06
regulation of glutamate receptor signaling pathway	6	6/84	35/12857	9.05E-08	1.24E-05
regulation of ion transport	15	15/84	441/12857	1.43E-07	1.71E-05
positive regulation of nervous system development	15	15/84	450/12857	1.85E-07	2.09E-05

11.4 LPS and IFN-γ stimulated BMDM

Table 7: List of Differentially expressed genes in WT vs *Calhm6*$^{-/-}$ BMDM

gene_name	*baseMean*	*FC*	*log2FoldChange*	*pvalue*	*padj*	*gene_description*
Fam26f	2424.5	0.05	-4.317	1.5E-67	2.84E-63	calcium homeostasis modulator family member 6
Gm10248	133.52	18.52	4.211	2.22E-43	2.09E-39	predicted gene 10248
En2	30.76	167.847	7.391	7.8E-19	4.9E-15	engrailed 2
AC161884.1	397.23	0.231	-2.112	3.14E-17	1.48E-13	-
Gm16867	55.96	11.624	3.539	6.12E-13	2.31E-09	predicted gene, 16867
Gm21451	34.9	21.451	4.423	8.15E-13	2.56E-09	predicted gene, 21451
Gm27177	13.78	81.855	6.355	4.01E-11	1.08E-07	-
AC241593.2	280.58	4.959	2.31	1.24E-10	2.92E-07	-
Gm27175	15.14	43.411	5.44	9.75E-10	2.04E-06	-
Gm37847	15.06	43.835	5.454	1.08E-09	2.04E-06	-
Gm21887	261.08	0.013	-6.257	5.84E-09	1E-05	-
Gm15247	152.15	0.171	-2.549	3.01E-07	0.000472	-
Tmem267	1182.78	3.63	1.86	7.84E-07	0.001137	transmembrane protein 267
C1qtnf6	480.21	0.557	-0.845	5.62E-06	0.007562	C1q and tumor necrosis factor related protein 6
Arhgef18	352.58	0.57	-0.811	2.03E-05	0.025456	rho/rac guanine nucleotide exchange factor (GEF) 18
Gm23935	5685.86	0.493	-1.02	3.72E-05	0.043865	-

Table 8: Gene Ontology enrichment analysis in WT vs *Calhm6*$^{-/-}$ BMDM (first 20 pathways)

Description	*Count*	*GeneRatio*	*BgRatio*	*pvalue*	*p.adjust*
protein localization to synapse	4	4/25	69/12857	8.83E-06	0.008094
excitatory synapse	3	3/27	57/13042	0.000215	0.016046
gap junction	2	2/27	11/13042	0.000224	0.016046
synaptic cleft	2	2/27	14/13042	0.00037	0.017631
glutamatergic synapse	5	5/27	390/13042	0.001093	0.031005
postsynaptic cytosol	2	2/27	25/13042	0.001202	0.031005
parallel fiber to Purkinje cell synapse	2	2/27	26/13042	0.001301	0.031005
profilin binding	2	2/26	12/12763	0.00026	0.031212
cell cortex region	2	2/27	43/13042	0.003537	0.033552
dendritic spine	3	3/27	155/13042	0.003906	0.033552
neuron spine	3	3/27	158/13042	0.004122	0.033552
collagen type I trimer	1	1/27	2/13042	0.004136	0.033552
insulin-like growth factor binding protein complex	1	1/27	2/13042	0.004136	0.033552

growth factor complex	1	1/27	2/13042	0.004136	0.033552
insulin-like growth factor ternary complex	1	1/27	2/13042	0.004136	0.033552
rod spherule	1	1/27	2/13042	0.004136	0.033552
postsynaptic density	4	4/27	324/13042	0.004177	0.033552
asymmetric synapse	4	4/27	325/13042	0.004223	0.033552
neuron to neuron synapse	4	4/27	341/13042	0.005008	0.03581
site of polarized growth	3	3/27	178/13042	0.005747	0.036889
terminal bouton	2	2/27	56/13042	0.005933	0.036889
dendritic filopodium	1	1/27	3/13042	0.006198	0.036932
protein localization to postsynaptic membrane	3	3/25	45/12857	8.73E-05	0.040037

11.5 Zymosan stimulated BMDM

Table 9: List of Differentially expressed genes in WT vs *Calhm6*$^{-/-}$ BMDM

gene_name	*baseMean*	*FC*	*log2FoldChange*	*pvalue*	*padj*	*gene_description*
Fam26f	2424.5	0.067	-3.895	5.07E-54	9.56E-50	calcium homeostasis modulator family member 6
Gm10248	133.52	13.529	3.758	2.74E-37	2.58E-33	predicted gene 10248
AC161884.1	397.23	0.185	-2.433	8.47E-22	5.32E-18	-
Gm21451	34.9	35.803	5.162	2.06E-14	9.72E-11	predicted gene, 21451
Gm16867	55.96	14.084	3.816	1.35E-13	5.08E-10	predicted gene, 16867
Gm27175	15.14	98.838	6.627	5.96E-12	1.87E-08	-
Gm37847	15.06	96.67	6.595	9.95E-12	2.68E-08	-
AC241593.2	280.58	4.579	2.195	1.41E-10	3.33E-07	-
Gm15247	152.15	0.118	-3.081	7.06E-10	1.48E-06	-
En2	30.76	35.237	5.139	1.52E-09	2.87E-06	engrailed 2
Tmem267	1182.78	3.915	1.969	1.59E-07	0.000272	transmembrane protein 267
Ncam2	70.77	4.894	2.291	3.99E-07	0.000626	neural cell adhesion molecule 2
Flnb	6207.07	1.594	0.673	5.8E-07	0.000781	filamin, beta
Gm21887	261.08	0.03	-5.04	5.41E-07	0.000781	-
Rcl1	677.33	1.656	0.728	8.96E-06	0.011263	RNA terminal phosphate cyclase-like 1
Gm27177	13.78	10.541	3.398	9.94E-06	0.011716	-
Kcnh6	73.44	0.346	-1.532	1.72E-05	0.019072	potassium voltage-gated channel, subfamily H (eag-related), member 6
Kcnh7	133.91	2.187	1.129	1.93E-05	0.020254	potassium voltage-gated channel, subfamily H (eag-related), member 7
Bik	12.98	0.021	-5.571	2.42E-05	0.024019	BCL2-interacting killer
C1qtnf6	480.21	0.587	-0.769	2.61E-05	0.024561	C1q and tumor necrosis factor related protein 6
Cysltr2	821.61	2.035	1.025	3.66E-05	0.032818	cysteinyl leukotriene receptor 2
Plag1	453.6	1.574	0.654	3.96E-05	0.033949	pleiomorphic adenoma gene 1
Fah	47.12	2.683	1.424	5.58E-05	0.042814	fumarylacetoacetate hydrolase
2810474O19Rik	10738.03	1.336	0.418	5.68E-05	0.042814	retroelement silencing factor 1
5730522E02Rik	102.95	4.497	2.169	5.39E-05	0.042814	-

Table 10: Gene Ontology enrichment analysis in WT vs *Calhm6*$^{-/-}$ BMDM (first 20 pathways)

Description	Count	GeneRatio	BgRatio	pvalue	p.adjust
presynaptic membrane organization	4	4/34	12/12857	1.99E-08	1.64E-05
intrinsic component of synaptic membrane	6	6/35	142/13042	1.88E-06	0.000137
synaptic membrane	8	8/35	343/13042	2.67E-06	0.000137
glutamatergic synapse	8	8/35	390/13042	6.9E-06	0.000237
heterophilic cell-cell adhesion via plasma membrane cell adhesion molecules	4	4/34	30/12857	1.06E-06	0.000385
presynaptic membrane assembly	3	3/34	9/12857	1.4E-06	0.000385
neurotransmitter-gated ion channel clustering	3	3/34	11/12857	2.75E-06	0.000468
trans-synaptic signaling	9	9/34	480/12857	2.98E-06	0.000468
synaptic signaling	9	9/34	488/12857	3.41E-06	0.000468
positive regulation of synapse assembly	4	4/34	42/12857	4.25E-06	0.0005
integral component of synaptic membrane	5	5/35	130/13042	2.33E-05	0.000599
postsynaptic specialization membrane	4	4/35	78/13042	5.38E-05	0.001109
anterograde trans-synaptic signaling	8	8/34	471/12857	2.39E-05	0.001478
postsynaptic specialization assembly	3	3/34	22/12857	2.51E-05	0.001478
ionotropic glutamate receptor complex	3	3/35	35/13042	0.000109	0.001608
neurotransmitter receptor complex	3	3/35	35/13042	0.000109	0.001608
intrinsic component of postsynaptic membrane	4	4/35	97/13042	0.000126	0.001624
postsynapse assembly	3	3/34	25/12857	3.73E-05	0.001628
regulation of trans-synaptic signaling	7	7/34	363/12857	3.76E-05	0.001628
anchored component of membrane	4	4/35	101/13042	0.000148	0.001688

11.6 Zymosan + IFN-ɣ stimulated BMDM

Table 11: List of the 50 highest Differentially expressed genes in WT vs *Calhm6*$^{-/-}$ BMDM

gene_name	baseMean	FC	log2FoldChange	pvalue	padj	gene_description
Fam26f	2424.5	0.045	-4.488	8.12E-72	1.53E-67	calcium homeostasis modulator family member 6
Gm10248	133.52	11.909	3.574	1.56E-32	1.47E-28	predicted gene 10248
En2	30.76	1538.171	10.587	1.36E-21	8.57E-18	engrailed 2
Gm16867	55.96	12.614	3.657	1.2E-12	4.54E-09	predicted gene, 16867
Gm21451	34.9	23.119	4.531	7.8E-12	2.45E-08	predicted gene, 21451
Gm15247	152.15	0.098	-3.345	2.37E-11	6.38E-08	-
AC241593.2	280.58	4.513	2.174	1.55E-10	3.64E-07	-
Gm27175	15.14	43.201	5.433	1.48E-09	3.09E-06	-
Gm37847	15.06	43.201	5.433	1.81E-09	3.41E-06	-
Tmem267	1182.78	4.454	2.155	1.15E-08	1.96E-05	transmembrane protein 267
Gm27177	13.78	49.797	5.638	1.62E-08	2.54E-05	-
Gm21887	261.08	0.021	-5.569	6.53E-08	9.46E-05	-
Gm38405	30.03	12.235	3.613	9.88E-07	0.001035	-
Hist1h4m	408.41	0.237	-2.076	1.5E-06	0.001489	histone cluster 1, H4m
Rtn1	241.8	0.156	-2.681	5.7E-06	0.004743	reticulon 1
Hdac11	95.65	0.226	-2.144	1E-05	0.007574	histone deacetylase 11
Hist1h3h	657.88	0.217	-2.203	2.19E-05	0.013269	histone cluster 1, H3h

Gm34280	121.55	0.021	-5.585	2.32E-05	0.013269	-
Mir3100	71.86	4.302	2.105	2.98E-05	0.016538	microRNA 3100
Chn1os3	57.39	0.002	-9.287	4.07E-05	0.019914	chimerin 1, opposite strand 3
Chn1	92.71	0.014	-6.183	4.27E-05	0.020128	chimerin 1
Slc22a17	48.17	0.059	-4.075	7.48E-05	0.025931	solute carrier family 22 (organic cation transporter), member 17
Camk2a	376.38	0.149	-2.75	7.7E-05	0.025931	calcium/calmodulin-dependent protein kinase II alpha
Grin1	49.51	0.045	-4.489	6.37E-05	0.025931	glutamate receptor, ionotropic, NMDA1 (zeta 1)
Apba2	19.92	0.004	-7.87	7.3E-05	0.025931	amyloid beta (A4) precursor protein-binding, family A, member 2
Plp1	151.92	0.083	-3.593	7.45E-05	0.025931	proteolipid protein (myelin) 1
Thy1	44.27	0.002	-9.058	7.38E-05	0.025931	thymus cell antigen 1, theta
Grin1os	34.12	0.016	-5.951	6.93E-05	0.025931	glutamate receptor, ionotropic, NMDA1 (zeta 1), opposite strand
Disp2	31.93	0.017	-5.88	9.63E-05	0.029201	dispatched RND tramsporter family member 2
Gm26953	27.58	0.003	-8.501	0.000107	0.029201	-
Adam11	36.18	0.159	-2.657	0.000114	0.029952	a disintegrin and metallopeptidase domain 11
Cacna1e	58.69	0.086	-3.541	0.00014	0.035013	calcium channel, voltage-dependent, R type, alpha 1E subunit
Hist1h2ai	215.67	0.249	-2.005	0.000138	0.035013	histone cluster 1, H2ai
Tro	24.48	0.13	-2.939	0.000165	0.03781	trophinin
Gria2	74.78	0.001	-9.399	0.000168	0.03781	glutamate receptor, ionotropic, AMPA2 (alpha 2)
Rgs7bp	72.45	0.085	-3.553	0.000207	0.040802	regulator of G-protein signalling 7 binding protein
Scrn1	45.14	0.002	-9.189	0.000251	0.041721	secernin 1
Add2	25.89	0.003	-8.431	0.000243	0.041721	adducin 2 (beta)
Phf24	36.56	0.079	-3.656	0.000246	0.041721	PHD finger protein 24
Depdc1a	175.6	37.375	5.224	0.00029	0.044387	DEP domain containing 1a
Ncam1	37.41	0.074	-3.749	0.000289	0.044387	neural cell adhesion molecule 1
Cntn1	27.92	0.003	-8.172	0.000286	0.044387	contactin 1
4930558J18Rik	26.52	37.792	5.24	0.000336	0.045911	RIKEN cDNA 4930558J18 gene
Nptxr	176.02	0.24	-2.061	0.000347	0.046762	neuronal pentraxin receptor
Peg3	26.34	0.003	-8.629	0.000373	0.048166	paternally expressed 3
Enho	28.35	0.099	-3.338	0.000376	0.048166	energy homeostasis associated
Syn2	62.98	0.024	-5.371	0.000395	0.048594	synapsin II
Pex5l	19.93	0.006	-7.349	0.000397	0.048594	peroxisomal biogenesis factor 5-like
Rnf112	31.57	0.002	-9.043	0.000445	0.051086	ring finger protein 112
Svop	17.88	0.068	-3.884	0.000447	0.051086	SV2 related protein

Table 12: Gene Ontology enrichment analysis in WT vs *Calhm6*$^{-/-}$ BMDM (first 20 pathways)

Description	*Count*	*GeneRatio*	*BgRatio*	*pvalue*	*p.adjust*
glutamatergic synapse	55	55/219	390/13042	1.09E-35	4.88E-33
synaptic membrane	50	50/219	343/13042	4.56E-33	1.03E-30
trans-synaptic signaling	56	56/215	480/12857	4.88E-32	1.3E-28
synaptic signaling	56	56/215	488/12857	1.18E-31	1.3E-28
chemical synaptic transmission	55	55/215	471/12857	1.83E-31	1.3E-28
anterograde trans-synaptic signaling	55	55/215	471/12857	1.83E-31	1.3E-28
presynapse	51	51/219	406/13042	1.59E-30	1.79E-28
neuron to neuron synapse	44	44/219	341/13042	8.95E-27	6.71E-25

postsynaptic specialization	44	44/219	341/13042	8.95E-27	6.71E-25
intrinsic component of synaptic membrane	31	31/219	142/13042	4.1E-26	2.64E-24
asymmetric synapse	41	41/219	325/13042	1.45E-24	7.27E-23
intrinsic component of postsynaptic membrane	25	25/219	97/13042	3.74E-23	1.68E-21
integral component of synaptic membrane	27	27/219	130/13042	3.15E-22	1.29E-20
regulation of trans-synaptic signaling	41	41/215	363/12857	8.65E-23	4.11E-20
synapse organization	38	38/215	306/12857	1.27E-22	5.2E-20
axon part	38	38/219	341/13042	7.54E-21	2.83E-19
behavior	42	42/215	424/12857	4E-21	1.43E-18
integral component of postsynaptic membrane	22	22/219	89/13042	4.64E-20	1.6E-18
transmembrane transporter complex	27	27/219	159/13042	8.37E-20	2.69E-18
transporter complex	27	27/219	166/13042	2.69E-19	8.07E-18

References

1. Junger, W. G. Immune cell regulation by autocrine purinergic signalling. *Nat. Rev. Immunol.* **11**, 201–212 (2011).

2. Vitiello, L., Gorini, S., Rosano, G. & La Sala, A. Immunoregulation through extracellular nucleotides. *Blood* vol. 120 511–518 (2012).

3. Burnstock, G., Nistri, A., Khakh, B. S. & Giniatullin, R. ATP-gated P2X receptors in health and disease. *Front. Cell. Neurosci.* **8**, (2014).

4. Lazarowski, E. R. Vesicular and conductive mechanisms of nucleotide release. *Purinergic Signalling* vol. 8 359–373 (2012).

5. Taruno, A., Taruno & Akiyuki. ATP Release Channels. *Int. J. Mol. Sci.* **19**, 808 (2018).

6. Dosch, M., Gerber, J., Jebbawi, F. & Beldi, G. Mechanisms of ATP release by inflammatory cells. *International Journal of Molecular Sciences* vol. 19 (2018).

7. Idzko, M., Ferrari, D. & Eltzschig, H. K. Nucleotide signalling during inflammation. *Nature* vol. 509 310–317 (2014).

8. Illes, P., Burnstock, G. & Tang, Y. Astroglia-Derived ATP Modulates CNS Neuronal Circuits. *Trends Neurosci.* (2019) doi:10.1016/j.tins.2019.09.006.

9. Inoue, K., Tsuda, M. & Koizumi, S. ATP receptors in pain sensation: Involvement of spinal microglia and P2X4 receptors. *Purinergic Signalling* vol. 1 95–100 (2005).

10. Romanov, R. A. *et al.* Chemical synapses without synaptic vesicles: Purinergic neurotransmission through a CALHM1 channel-mitochondrial signaling complex. *Sci. Signal.* **11**, eaao1815 (2018).

11. Ma, Z. *et al.* CALHM3 Is Essential for Rapid Ion Channel-Mediated Purinergic Neurotransmission of GPCR-Mediated Tastes. *Neuron* (2018) doi:10.1016/j.neuron.2018.03.043.

12. Taruno, A. *et al.* CALHM1 ion channel mediates purinergic neurotransmission of sweet, bitter and umami tastes. *Nature* **495**, 223–226 (2013).

13. Sana-Ur-Rehman, H., Markus, I., Moore, K. H., Mansfield, K. J. & Liu, L. Expression and localization of pannexin-1 and CALHM1 in porcine bladder and their involvement in modulating ATP release. *Am. J. Physiol. Integr. Comp. Physiol.* **312**, R763–R772 (2017).

14. Jeon, Y. K. *et al.* Thermosensitivity of the voltage-dependent activation of calcium homeostasis modulator 1 (calhm1) ion channel. *Biochem. Biophys. Res. Commun.* **534**, 590–596 (2021).

15. Dreses-Werringloer, U. *et al.* A Polymorphism in CALHM1 Influences Ca2+ Homeostasis, Aβ Levels, and Alzheimer's Disease Risk. *Cell* **133**, 1149–1161 (2008).

16. Tanis, J. E. *et al.* CLHM-1 is a functionally conserved and conditionally toxic Ca2+-permeable ion channel in Caenorhabditis elegans. *J. Neurosci.* **33**, 12275–86 (2013).

17. Ma, Z., Tanis, J. E., Taruno, A. & Foskett, J. K. Calcium homeostasis modulator (CALHM) ion channels. *Pflügers Arch. - Eur. J. Physiol.* **468**, 395–403 (2016).

18. Siebert, A. P. *et al.* Structural and functional similarities of calcium homeostasis modulator 1 (CALHM1) ion channel with connexins, pannexins, and innexins. *J. Biol. Chem.* **288**, 6140–53 (2013).

19. Beyer, E. C. & Berthoud, V. M. Gap junction gene and protein families: Connexins, innexins, and pannexins. *Biochim. Biophys. Acta - Biomembr.* **1860**, 5–8 (2018).

20. Yang, W. *et al.* Cryo-EM structure of CLHM1 ion channel from Caenorhabditis elegans. *Protein Sci.* pro.3904 (2020) doi:10.1002/pro.3904.

21. Ma, Z. *et al.* Calcium homeostasis modulator 1 (CALHM1) is the pore-forming subunit of an ion channel that mediates extracellular Ca2+ regulation of neuronal excitability. *Proc. Natl. Acad. Sci. U. S. A.* **109**, E1963-71 (2012).

22. Drożdżyk, K. *et al.* Cryo-EM structures and functional properties of CALHM channels of the human placenta. *Elife* **9**, (2020).

23. Syrjanen, J. L. *et al.* Structure and assembly of calcium homeostasis modulator proteins. *Nat. Struct. Mol. Biol.* **27**, 150–159 (2020).

24. Demura, K. *et al.* Cryo-EM structures of calcium homeostasis modulator channels in diverse oligomeric assemblies. *bioRxiv* 2020.01.31.928093 (2020) doi:10.1101/2020.01.31.928093.

25. Liu, J. *et al.* Cryo-EM structures of human calcium homeostasis modulator 5. *Cell Discovery* vol. 6 1–4 (2020).

26. Choi, W., Clemente, N., Sun, W., Du, J. & Lü, W. The structures and gating mechanism of human calcium homeostasis modulator 2. *Nature* 1–5 (2019) doi:10.1038/s41586-019-1781-3.

27. Tanis, J. E., Ma, Z. & Foskett, J. K. The NH_2 terminus regulates voltage-dependent gating of CALHM ion channels. *Am. J. Physiol. Physiol.* **313**, C173–C186 (2017).

28. Nomura, K., Nakanishi, M., Ishidate, F., Iwata, K. & Taruno, A. All-Electrical Ca2+-Independent Signal Transduction Mediates Attractive Sodium Taste in Taste Buds. *Neuron* (2020) doi:10.1016/j.neuron.2020.03.006.

29. Wu, J. *et al.* Generation of Calhm1 knockout mouse and characterization of calhm1 gene

expression. *Protein Cell* **3**, 470–480 (2012).

30. Jun, M. *et al.* Calhm2 governs astrocytic ATP releasing in the development of depression-like behaviors. *Mol. Psychiatry* **23**, 883–891 (2018).

31. Cheng, J. *et al.* Microglial Calhm2 regulates neuroinflammation and contributes to Alzheimer's disease pathology. *Sci. Adv.* **7**, eabe3600 (2021).

32. Ebihara, T. *et al.* Identification of a polyI:C-inducible membrane protein that participates in dendritic cell-mediated natural killer cell activation. *J. Exp. Med.* **207**, 2675–87 (2010).

33. Kasamatsu, J. *et al.* INAM plays a critical role in IFN-γ production by NK cells interacting with polyinosinic-polycytidylic acid-stimulated accessory cells. *J. Immunol.* **193**, 5199–207 (2014).

34. Workman, A. D. *et al.* CALHM1-Mediated ATP Release and Ciliary Beat Frequency Modulation in Nasal Epithelial Cells. *Sci. Rep.* **7**, 6687 (2017).

35. Ma, Z., Saung, W. T. & Foskett, J. K. Action potentials and ion conductances in wild-type and CALHM1-knockout type II taste cells. *J. Neurophysiol.* **117**, 1865–1876 (2017).

36. Dreses-Werringloer, U. *et al.* CALHM1 controls the Ca 2+-dependent MEK, ERK, RSK and MSK signaling cascade in neurons. *J. Cell Sci.* **126**, 1199–1206 (2012).

37. Vingtdeux, V. *et al.* CALHM1 ion channel elicits amyloid-β clearance by insulin-degrading enzyme in cell lines and in vivo in the mouse brain. *J. Cell Sci.* **128**, 2330–2338 (2015).

38. Lambert, J.-C. *et al.* The CALHM1 P86L polymorphism is a genetic modifier of age at onset in Alzheimer's disease: a meta-analysis study. *J. Alzheimers. Dis.* **22**, 247–55 (2010).

39. Xu, H., Chen, J., Wang, Y., Wu, Y. & Liang, Y. SELL and IFI44 as potential biomarkers of Sjögren's syndrome and their correlation with immune cell infiltration. *Genes Genet. Syst.* **96**, 71–80 (2021).

40. Kim, M. J. *et al.* Villitis of Unknown Etiology Is Associated with a Distinct Pattern of Chemokine Up-Regulation in the Feto-Maternal and Placental Compartments: Implications for Conjoint Maternal Allograft Rejection and Maternal Anti-Fetal Graft-versus-Host Disease. *J. Immunol.* **182**, 3919–3927 (2009).

41. Javed, A. *et al.* Pre-infection transcript levels of FAM26F in peripheral blood mononuclear cells inform about overall plasma viral load in acute and post-acute phase after simian immunodeficiency virus infection. *J. Gen. Virol.* **97**, 3400–3412 (2016).

42. Tordoff, M. G. *et al.* Salty Taste Deficits in CALHM1 Knockout Mice. *Chem. Senses* **39**, 515–528 (2014).

43. Sclafani, A., Marambaud, P. & Ackroff, K. Sucrose-conditioned flavor preferences in sweet ageusic T1r3 and Calhm1 knockout mice. *Physiol. Behav.* **126**, 25–29 (2014).

44. Sclafani, A. & Ackroff, K. Greater reductions in fat preferences in CALHM1 than CD36 knockout mice. *Am. J. Physiol. Regul. Integr. Comp. Physiol.* **315**, R576–R585 (2018).

45. Hellekant, G., Schmolling, J., Marambaud, P. & Rose-Hellekant, T. A. CALHM1 Deletion in Mice Affects Glossopharyngeal Taste Responses, Food Intake, Body Weight, and Life Span. *Chem. Senses* **40**, 373–379 (2015).

46. Kinnamon, S. C. Taste receptor signalling - from tongues to lungs. *Acta Physiol.* **204**, 158–168 (2012).

47. Iwamoto, M., Takashima, M. & Ohtubo, Y. A subset of taste receptor cells express biocytin-permeable channels activated by reducing extracellular Ca^{2+} concentration. *Eur. J. Neurosci.* ejn.14672 (2020) doi:10.1111/ejn.14672.

48. Andres-Barquin, P. J. & Conte, C. Molecular Basis of Bitter Taste: The T2R Family of G Protein-Coupled Receptors. *Cell Biochem. Biophys.* **41**, 099–112 (2004).

49. Gaete, P. S. *et al.* A novel voltage clamp/dye uptake assay reveals saturable transport of molecules through CALHM1 and connexin channels. doi:10.1101/2020.02.15.950923.

50. Kinnamon, S. C. Neurosensory transmission without a synapse: New perspectives on taste signaling. *BMC Biol.* **11**, (2013).

51. Kashio, M., Wei-qi, G., Ohsaki, Y., Kido, M. A. & Taruno, A. CALHM1/CALHM3 channel is intrinsically sorted to the basolateral membrane of epithelial cells including taste cells. *Sci. Rep.* **9**, 2681 (2019).

52. Taruno, A. *et al.* Post-translational palmitoylation controls the voltage gating and lipid raft association of the CALHM1 channel. *J. Physiol.* **595**, 6121–6145 (2017).

53. Taruno, A., Sun, H., Kashio, M. & Marunaka, Y. *N-Linked Glycosylation Regulates CALHM1 Channel Function and Subcellular Localization*. (2016) doi:10.1016/j.bpj.2015.11.3250.

54. Schneider, C., O'Leary, C. E. & Locksley, R. M. Regulation of immune responses by tuft cells. *Nat. Rev. Immunol.* 1 (2019) doi:10.1038/s41577-019-0176-x.

55. Elizondo-Vega, R. J., Recabal, A. & Oyarce, K. Nutrient sensing by hypothalamic tanycytes. *Frontiers in Endocrinology* vol. 10 (2019).

56. Delyle, S. G. *et al.* Characterization Of The Expression And The Role Of Bitter Taste Receptors In Human Lung Parenchyma And Macrophages. *Am J Respir Crit Care Med* **189**, A5749 (2014).

57. Lazutkaite, G., Soldà, A., Lossow, K., Meyerhof, W. & Dale, N. Amino acid sensing in hypothalamic tanycytes via umami taste receptors. *Mol. Metab.* **6**, 1480–1492 (2017).

58. Cui, P. J. *et al.* CALHM1 P86L polymorphism is a risk factor for Alzheimer's disease in the Chinese population. *J. Alzheimer's Dis.* **19**, 31–35 (2010).

59. Lin, K. *et al.* Association between the polymorphisms of CALHM1 and GOLPH2 genes and Alzheimer's disease. *Psychiatr. Genet.* **20**, 190 (2010).

60. Wang, J., Gu, B. J., Masters, C. L. & Wang, Y. J. A systemic view of Alzheimer disease - Insights from amyloid-β metabolism beyond the brain. *Nature Reviews Neurology* vol. 13 612–623 (2017).

61. Beecham, G. W., Schnetz-Boutaud, N., Haines, J. L. & Pericak-Vance, M. A. CALHM1 polymorphism is not associated with late-onset Alzheimer disease. *Ann. Hum. Genet.* **73**, 379–81 (2009).

62. Bertram, L. *et al.* No association between CALHM1 and Alzheimer's disease risk. *Cell* **135**, 993–4; author reply 994-6 (2008).

63. Giedraitis, V. *et al.* CALHM1 P86L polymorphism does not alter amyloid-β or tau in cerebrospinal fluid. *Neurosci. Lett.* **469**, 265–267 (2010).

64. Inoue, K. *et al.* The P86L common allele of *CALHM1* does not influence risk for Alzheimer disease in Japanese cohorts. *Am. J. Med. Genet. Part B Neuropsychiatr. Genet.* **153B**, 532–535 (2010).

65. Minster, R. L., Demirci, F. Y., DeKosky, S. T. & Kamboh, M. I. No association between CALHM1 variation and risk of Alzheimer disease. *Hum. Mutat.* **30**, E566-9 (2009).

66. Nacmias, B. *et al.* Lack of implication for calhm1 p86l common variation in italian patients with early and late onset alzheimer's disease. *J. Alzheimer's Dis.* **20**, 37–41 (2010).

67. Tan, E. K. *et al.* CALHM1 variant is not associated with Alzheimer's disease among Asians. *Neurobiol. Aging* **32**, 546.e11-546.e12 (2011).

68. Ripke, S. *et al.* Genome-wide association analysis identifies 13 new risk loci for schizophrenia. *Nat. Genet.* **45**, 1150–1159 (2013).

69. Lv, R. *et al.* A polymorphism in CALHM1 is associated with temporal lobe epilepsy. *Epilepsy Behav.* **20**, 681–685 (2011).

70. Calero, O. *et al.* Genetic variability of the gene cluster CALHM1–3 in sporadic Creutzfeldt-Jakob disease. *Prion* **6**, 407–412 (2012).

71. Moreno-Ortega, A. J., Ruiz-Nuño, A., García, A. G. & Cano-Abad, M. F. Mitochondria sense with different kinetics the calcium entering into HeLa cells through calcium channels CALHM1 and mutated P86L-CALHM1. *Biochem. Biophys. Res. Commun.* **391**, 722–726 (2010).

72. Marambaud, P., Dreses-Werringloer, U. & Vingtdeux, V. Calcium signaling in neurodegeneration. *Molecular Neurodegeneration* vol. 4 (2009).

73. Stanley, E. F. Presynaptic calcium channels and the depletion of synaptic cleft calcium ions. *J.*

Neurophysiol. **83**, 477–482 (2000).

74. Vingtdeux, V. *et al.* CALHM1 deficiency impairs cerebral neuron activity and memory flexibility in mice. *Sci. Rep.* **6**, 24250 (2016).

75. Xue-bin, Y. *Preliminary Study of Calcium Homeostasis Modulator 1 Involvement in Trigeminal Neuralgia*.

76. Garrosa, J., Paredes, I., Marambaud, P., López, M. G. & Cano-Abad, M. F. Molecular and Pharmacological Modulation of CALHM1 Promote Neuroprotection against Oxygen and Glucose Deprivation in a Model of Hippocampal Slices. *Cells* **9**, 664 (2020).

77. Bartoli, F., Burnstock, G., Crocamo, C. & Carrà, G. Purinergic Signaling and Related Biomarkers in Depression. *Brain Sci.* **10**, 160 (2020).

78. Cui, Q. *et al.* Hippocampal CD 39/ENTPD1 promotes mouse depression-like behavior through hydrolyzing extracellular ATP. *EMBO Rep.* (2020) doi:10.15252/embr.201947857.

79. Sawynok, J. & Liu, X. J. Adenosine in the spinal cord and periphery: release and regulation of pain. *Prog. Neurobiol.* **69**, 313–40 (2003).

80. Egelman, D. M. & Montague, P. R. Calcium dynamics in the extracellular space of mammalian neural tissue. *Biophys. J.* **76**, 1856–1867 (1999).

81. Wan, C.-K. *et al.* Opposing roles of STAT1 and STAT3 in IL-21 function in CD4+ T cells. *Proc. Natl. Acad. Sci. U. S. A.* **112**, 9394–9 (2015).

82. Guinn, Z., Lampe, A. T., Brown, D. M. & Petro, T. M. Significant role for IRF3 in both T cell and APC effector functions during T cell responses. *Cell. Immunol.* **310**, 141–149 (2016).

83. Wehner, R., Dietze, K., Bachmann, M. & Schmitz, M. The Bidirectional Crosstalk between Human Dendritic Cells and Natural Killer Cells. *J Innate Immun* **3**, 258–263 (2011).

84. Horowitz, A., Stegmann, K. A. & Riley, E. M. Activation of Natural Killer Cells during Microbial Infections. *Front. Immunol.* **2**, 88 (2012).

85. Hammer, Q., Rückert, T. & Romagnani, C. Natural killer cell specificity for viral infections. *Nat. Immunol.* **19**, 800–808 (2018).

86. Chiossone, L., Dumas, P.-Y., Vienne, M. & Vivier, E. Natural killer cells and other innate lymphoid cells in cancer. *Nat. Rev. Immunol.* **18**, 671–688 (2018).

87. Chiba, S. *et al.* Recognition of tumor cells by Dectin-1 orchestrates innate immune cells for anti-tumor responses. *Elife* **3**, e04177 (2014).

88. Belone, A. de F. F. *et al.* Genome-Wide Screening of mRNA Expression in Leprosy Patients.

Front. Genet. **6**, 334 (2015).

89. Julia, A. *et al.* A genome-wide association study identifies a novel locus at 6q22.1 associated with ulcerative colitis. *Hum. Mol. Genet.* **23**, 6927–6934 (2014).

90. Dufek, S. *et al.* Genetic Identification of Two Novel Loci Associated with Steroid-Sensitive Nephrotic Syndrome. *J. Am. Soc. Nephrol.* **30**, 1375–1384 (2019).

91. Fritsch-Stork, R. D. E. *et al.* Expression of ERAP2 and LST1 is increased before start of therapy in rheumatoid arthritis patients with good clinical response to glucocorticoids. *Clin. Exp. Rheumatol.* **34**, 685–689 (2016).

92. Malik, U., Javed, A., Ali, A. & Asghar, K. Structural and functional annotation of human FAM26F: A multifaceted protein having a critical role in the immune system. *Gene* **597**, 66–75 (2017).

93. Burnstock, G. & Boeynaems, J.-M. Purinergic signalling and immune cells. (2014) doi:10.1007/s11302-014-9427-2.

94. Cekic, C. & Linden, J. Purinergic regulation of the immune system. *Nat. Rev. Immunol.* **16**, 177–192 (2016).

95. Woehrle, T. *et al.* Pannexin-1 hemichannel-mediated ATP release together with P2X1 and P2X4 receptors regulate T-cell activation at the immune synapse. *Blood* **116**, 3475–84 (2010).

96. Dustin, M. L. & Long, E. O. Cytotoxic immunological synapses. *Immunol. Rev.* **235**, 24–34 (2010).

97. Foley, J. F. Mitochondrial Positioning in T Cells. *Sci. Signal.* **4**, ec99–ec99 (2011).

98. Gómez-Cabañas, L. *et al.* Immunological Synapse Formation Induces Mitochondrial Clustering and Mitophagy in Dendritic Cells. *J. Immunol.* **202**, 1715–1723 (2019).

99. Abarca-Rojano, E. *et al.* Re-organization of mitochondria at the NK cell immune synapse. *Immunol. Lett.* **122**, 18–25 (2009).

100. Smith, H. J. Antigenicity of carcinogen-induced and spontaneous tumours in inbred mice. *Br. J. Cancer* **20**, 831 (1966).

101. Trinchieri, G. Biology of Natural Killer Cells. *Adv. Immunol.* **47**, 187–376 (1989).

102. Thomas, R. & Yang, X. NK-DC Crosstalk in Immunity to Microbial Infection. *J. Immunol. Res.* **2016**, 1–7 (2016).

103. Scoville, S. D., Freud, A. G. & Caligiuri, M. A. Modeling human natural killer cell development in the era of innate lymphoid cells. *Front. Immunol.* **8**, 360 (2017).

104. Sojka, D. K., Tian, Z. & Yokoyama, W. M. Tissue-Resident Natural Killer Cells and Their Potential Diversity. *Semin. Immunol.* **26**, 127 (2014).

105. Paul, S. & Lal, G. The molecular mechanism of natural killer cells function and its importance in cancer immunotherapy. *Front. Immunol.* **8**, 1124 (2017).

106. Simonetta, F., Pradier, A. & Roosnek, E. T-bet and eomesodermin in NK cell development, maturation, and function. *Front. Immunol.* **7**, 241 (2016).

107. Vivier, E., Tomasello, E., Baratin, M., Walzer, T. & Ugolini, S. Functions of natural killer cells. *Nat. Immunol.* **9**, 503–510 (2008).

108. Kalkunte, S. S. *et al.* Vascular Endothelial Growth Factor C Facilitates Immune Tolerance and Endovascular Activity of Human Uterine NK Cells at the Maternal-Fetal Interface. *J. Immunol.* **182**, 4085–4092 (2009).

109. Hanna, J. *et al.* Decidual NK cells regulate key developmental processes at the human fetal-maternal interface. *Nat. Med. 2006 129* **12**, 1065–1074 (2006).

110. Robson, A. *et al.* Uterine natural killer cells initiate spiral artery remodeling in human pregnancy. *FASEB J.* **26**, 4876–4885 (2012).

111. Zhang, C. & Tian, Z. NK cell subsets in autoimmune diseases. *Journal of Autoimmunity* vol. 83 22–30 (2017).

112. Lanier, L. L., Testi, R., Bindl, J. & Phillips, J. H. Identity of Leu-19 (CD56) leukocyte differentiation antigen and neural cell adhesion molecule. *J. Exp. Med.* **169**, 2233–2238 (1989).

113. Abel, A. M., Yang, C., Thakar, M. S. & Malarkannan, S. Natural killer cells: Development, maturation, and clinical utilization. *Front. Immunol.* **9**, 1869 (2018).

114. Mace, E. M. *et al.* Mutations in GATA2 cause human NK cell deficiency with specific loss of the CD56bright subset. *Blood* **121**, 2669–2677 (2013).

115. Cooper, M. A., Fehniger, T. A. & Caligiuri, M. A. The biology of human natural killer-cell subsets. *Trends Immunol.* **22**, 633–640 (2001).

116. Ferlazzo, G. & Münz, C. NK Cell Compartments and Their Activation by Dendritic Cells. *J. Immunol.* **172**, 1333–1339 (2004).

117. Chiossone, L. *et al.* Maturation of mouse NK cells is a 4-stage developmental program. *Blood* **113**, 5488–5496 (2009).

118. Hayakawa, Y. & Smyth, M. J. CD27 Dissects Mature NK Cells into Two Subsets with Distinct Responsiveness and Migratory Capacity. *J. Immunol.* **176**, 1517–1524 (2006).

119. Mody, C. H. *et al.* Microbial killing by NK cells. *J. Leukoc. Biol.* **105**, 1285–1296 (2019).

120. Mandelboim, O. *et al.* Recognition of haemagglutinins on virus-infected cells by NKp46 activates lysis by human NK cells. *Nature* **409**, 1055–1060 (2001).

121. Jarahian, M. *et al.* Modulation of NKp30- and NKp46-Mediated Natural Killer Cell Responses by Poxviral Hemagglutinin. *PLOS Pathog.* **7**, e1002195 (2011).

122. Hershkovitz, O. *et al.* NKp44 receptor mediates interaction of the envelope glycoproteins from the West-Nile and dengue viruses with Natural Killer cells. *J. Immunol.* **183**, 2610 (2009).

123. Fischer, A. Human Primary Immunodeficiency Diseases - ScienceDirect. *Immunity* **27**, 835–845 (2007).

124. Moon, W. Y. & Powis, S. J. Does Natural Killer Cell Deficiency (NKD) Increase the Risk of Cancer? NKD May Increase the Risk of Some Virus Induced Cancer. *Front. Immunol.* **10**, 1703 (2019).

125. Orange, J. S. Natural killer cell deficiency. *J. Allergy Clin. Immunol.* **132**, 515–525 (2013).

126. Kim, S. *et al.* Licensing of natural killer cells by host major histocompatibility complex class I molecules. *Nature* **436**, 709–713 (2005).

127. Wong, S., Freeman, J. D., Kelleher, C., Mager, D. & Takei, F. Ly-49 multigene family. New members of a superfamily of type II membrane proteins with lectin-like domains. *J. Immunol.* **147**, (1991).

128. Christiansen, F. T., Tait, B. D. & Rajalingam, R. Overview of the Killer Cell Immunoglobulin-Like Receptor System. *Methods Mol. Biol.* **882**, 391–414 (2012).

129. Braud, V. M. *et al.* HLA-E binds to natural killer cell receptors CD94/NKG2A, B and C. *Nat. 1998 3916669* **391**, 795–799 (1998).

130. Vance, R. E., Kraft, J. R., Altman, J. D., Jensen, P. E. & Raulet, D. H. Mouse CD94/NKG2A is a natural killer cell receptor for the nonclassical major histocompatibility complex (MHC) class I molecule Qa-1(b). *J. Exp. Med.* **188**, 1841–1848 (1998).

131. Veillette, A., Latour, S. & Davidson, D. Negative Regulation of Immunoreceptor Signaling. *https://doi.org/10.1146/annurev.immunol.20.081501.130710* **20**, 669–707 (2003).

132. Kwon, H.-J. & Kim, H. S. Signaling for Synergistic Activation of Natural Killer Cells. *Immune Netw.* **12**, 240 (2012).

133. Bryceson, Y. T., March, M. E., Ljunggren, H. G. & Long, E. O. Activation, coactivation, and costimulation of resting human natural killer cells. *Immunol. Rev.* **214**, 73–91 (2006).

134. Kruse, P. H., Matta, J., Ugolini, S. & Vivier, E. Natural cytotoxicity receptors and their ligands. *Immunol. Cell Biol.* **92**, 221–229 (2014).

135. Nakao, T. *et al.* DAP12/TREM2 Expression by Mouse and Human Liver DC: Functional Implications and Regulation of Liver Ischemia-Reperfusion Injury. *Hepatology* **70**, 696 (2019).

136. Zompi, S. & Colucci, F. Anatomy of a murder—signal transduction pathways leading to activation of natural killer cells. *Immunol. Lett.* **97**, 31–39 (2005).

137. Upshaw, J. L. *et al.* NKG2D-mediated signaling requires a DAP10-bound Grb2-Vav1 intermediate and phosphatidylinositol-3-kinase in human natural killer cells. *Nat. Immunol. 2006 75* **7**, 524–532 (2006).

138. Billadeau, D. D., Upshaw, J. L., Schoon, R. A., Dick, C. J. & Leibson, P. J. NKG2D-DAP10 triggers human NK cell–mediated killing via a Syk-independent regulatory pathway. *Nat. Immunol. 2003 46* **4**, 557–564 (2003).

139. Kwon, H. J. *et al.* Stepwise phosphorylation of p65 promotes NF-κB activation and NK cell responses during target cell recognition. *Nat. Commun. 2016 71* **7**, 1–15 (2016).

140. Cerwenka, A. *et al.* Retinoic Acid Early Inducible Genes Define a Ligand Family for the Activating NKG2D Receptor in Mice. *Immunity* **12**, 721–727 (2000).

141. Cosman, D. *et al.* ULBPs, Novel MHC Class I–Related Molecules, Bind to CMV Glycoprotein UL16 and Stimulate NK Cytotoxicity through the NKG2D Receptor. *Immunity* **14**, 123–133 (2001).

142. Song, H., Kim, J. K., Cosman, D. & Choi, I. Soluble ULBP suppresses natural killer cell activity via down-regulating NKG2D expression. *Cell. Immunol.* **239**, 22–30 (2006).

143. Groh, V. *et al.* Broad tumor-associated expression and recognition by tumor-derived γδ T cells of MICA and MICB. *Proc. Natl. Acad. Sci.* **96**, 6879–6884 (1999).

144. Koretzky, G., Billadeau, D. D. & Leibson, P. J. ITAMs versus ITIMs: striking a balance during cell regulation. *J. Clin. Invest.* **109**, 161–168 (2002).

145. Daniels, K. A. *et al.* Murine cytomegalovirus is regulated by a discrete subset of natural killer cells reactive with monoclonal antibody to Ly49H. *J. Exp. Med.* **194**, 29–44 (2001).

146. Esin, S. *et al.* Direct binding of human NK cell natural cytotoxicity receptor NKp44 to the surfaces of mycobacteria and other bacteria. *Infect. Immun.* **76**, 1719–1727 (2008).

147. Chalifour, A. *et al.* Direct bacterial protein PAMP recognition by human NK cells involves TLRs and triggers alpha-defensin production. *Blood* **104**, 1778–1783 (2004).

148. Newman, K. C. & Riley, E. M. Whatever turns you on: accessory-cell-dependent activation of NK cells by pathogens. *Nat. Rev. Immunol.* **7**, 279–291 (2007).

149. Steinman, R. M. & Cohn, Z. A. Identification of a Novel Cell Type in Peripheral Lymphoid Organs of Mice. *J. Exp. Med.* **137**, 1142–1162 (1973).

150. Banchereau, J. & Steinman, R. M. Dendritic cells and the control of immunity. *Nat. 1998 3926673* **392**, 245–252 (1998).

151. Klechevsky, E. Functional Diversity of Human Dendritic Cells. *Adv. Exp. Med. Biol.* **850**, 43–54 (2015).

152. Paul, W. E. Bridging Innate and Adaptive Immunity. *Cell* **147**, 1212–1215 (2011).

153. Janeway, C. A. Approaching the asymptote? Evolution and revolution in immunology. *Cold Spring Harb. Symp. Quant. Biol.* **54 Pt 1**, 1–13 (1989).

154. Cabeza-Cabrerizo, M., Cardoso, A., Minutti, C. M., Pereira da Costa, M. & Reis Sousa, C. Annual Review of Immunology Dendritic Cells Revisited. (2021) doi:10.1146/annurev-immunol-061020.

155. Edwards, A. D. *et al.* Relationships Among Murine CD11chigh Dendritic Cell Subsets as Revealed by Baseline Gene Expression Patterns. *J. Immunol.* **171**, 47–60 (2003).

156. Merad, M., Sathe, P., Helft, J., Miller, J. & Mortha, A. The Dendritic Cell Lineage: Ontogeny and Function of Dendritic Cells and Their Subsets in the Steady State and the Inflamed Setting. *Annu. Rev. Immunol.* **31**, 563–604 (2013).

157. Vremec, D., Pooley, J., Hochrein, H., Wu, L. & Shortman, K. CD4 and CD8 Expression by Dendritic Cell Subtypes in Mouse Thymus and Spleen. *J. Immunol.* **164**, 2978–2986 (2000).

158. Sallusto, F. & Lanzavecchia, A. Efficient presentation of soluble antigen by cultured human dendritic cells is maintained by granulocyte/macrophage colony-stimulating factor plus interleukin 4 and downregulated by tumor necrosis factor alpha. *J. Exp. Med.* **179**, 1109–18 (1994).

159. Guilliams, M., Lambrecht, B. N. & Hammad, H. Division of labor between lung dendritic cells and macrophages in the defense against pulmonary infections. *Mucosal Immunol. 2013 63* **6**, 464–473 (2013).

160. Chieppa, M., Rescigno, M., Huang, A. Y. C. & Germain, R. N. Dynamic imaging of dendritic cell extension into the small bowel lumen in response to epithelial cell TLR engagement. *J. Exp. Med.* **203**, 2841–2852 (2006).

161. Voedisch, S. *et al.* Mesenteric Lymph Nodes Confine Dendritic Cell-Mediated Dissemination of Salmonella enterica Serovar Typhimurium and Limit Systemic Disease in Mice. *Infect. Immun.* **77**, 3170 (2009).

162. Liu, J. & Cao, X. Cellular and molecular regulation of innate inflammatory responses. *Cell. Mol. Immunol.* **13**, 711–721 (2016).

163. Nace, G., Evankovich, J., Eid, R. & Tsung, A. Dendritic cells and damage-associated molecular patterns: endogenous danger signals linking innate and adaptive immunity. *J. Innate Immun.* **4**, 6–15 (2012).

164. Matzinger, P. Tolerance, Danger, and the Extended Family. *http://dx.doi.org/10.1146/annurev.iy.12.040194.005015* **12**, 991–1045 (2003).

165. Zelenay, S. & Reis e Sousa, C. Adaptive immunity after cell death. *Trends Immunol.* **34**, 329–335 (2013).

166. Jarrossay, D., Napolitani, G., Colonna, M., Sallusto, F. & Lanzavecchia, A. Specialization and complementarity in microbial molecule recognition by human myeloid and plasmacytoid dendritic cells. doi:10.1002/1521-4141.

167. Reis E Sousa, C. *et al.* In vivo microbial stimulation induces rapid CD40 ligand-independent production of interleukin 12 by dendritic cells and their redistribution to T cell areas. *J. Exp. Med.* **186**, 1819–1829 (1997).

168. Mashayekhi, M. *et al.* CD8α+ Dendritic Cells Are the Critical Source of Interleukin-12 that Controls Acute Infection by Toxoplasma gondii Tachyzoites. *Immunity* **35**, 249–259 (2011).

169. Sancho, D. *et al.* Identification of a dendritic cell receptor that couples sensing of necrosis to immunity. *Nat. 2009 4587240* **458**, 899–903 (2009).

170. Waskow, C. *et al.* FMS-like tyrosine kinase 3 is required for dendritic cell development in peripheral lymphoid tissues. *Nat. Immunol.* **9**, 676 (2008).

171. Schaupp, L. *et al.* Microbiota-Induced Type I Interferons Instruct a Poised Basal State of Dendritic Cells. *Cell* **181**, 1080-1096.e19 (2020).

172. Vermaelen, K. Y., Carro-Muino, I., Lambrecht, B. N. & Pauwels, R. A. Specific Migratory Dendritic Cells Rapidly Transport Antigen from the Airways to the Thoracic Lymph Nodes. *J. Exp. Med.* **193**, 51–60 (2001).

173. Allenspach, E. J., Lemos, M. P., Porrett, P. M., Turka, L. A. & Laufer, T. M. Migratory and Lymphoid-Resident Dendritic Cells Cooperate to Efficiently Prime Naive CD4 T cells. *Immunity* **29**, 795–806 (2008).

174. Sixt, M. *et al.* The Conduit System Transports Soluble Antigens from the Afferent Lymph to Resident Dendritic Cells in the T Cell Area of the Lymph Node. *Immunity* **22**, 19–29 (2005).

175. Lewis, S. M., Williams, A. & Eisenbarth, S. C. Structure and function of the immune system in the spleen. *Sci. Immunol.* **4**, eaau6085 (2019).

176. Neuenhahn, M. *et al.* CD8α+ Dendritic Cells Are Required for Efficient Entry of Listeria monocytogenes into the Spleen. *Immunity* **25**, 619–630 (2006).

177. Heath, W. R., Kato, Y., Steiner, T. M. & Caminschi, I. Antigen presentation by dendritic cells for B cell activation. *Curr. Opin. Immunol.* **58**, 44–52 (2019).

178. Andrews, D. M., Scalzo, A. A., Yokoyama, W. M., Smyth, M. J. & Degli-Esposti, M. A. Functional interactions between dendritic cells and NK cells during viral infection. *Nat. Immunol. 2002 42* **4**, 175–181 (2002).

179. Del Fresno, C. *et al.* DNGR-1 in dendritic cells limits tissue damage by dampening neutrophil recruitment. *Science (80-.).* **362**, 351–356 (2018).

180. Caux, C. *et al.* CD34+ hematopoietic progenitors from human cord blood differentiate along two independent dendritic cell pathways in response to GM-CSF+TNF alpha. *J. Exp. Med.* **184**, 695–706 (1996).

181. Caux, C. *et al.* CD34+ Hematopoietic Progenitors From Human Cord Blood Differentiate Along Two Independent Dendritic Cell Pathways in Response to Granulocyte-Macrophage Colony-Stimulating Factor Plus Tumor Necrosis Factor α: II. Functional Analysis. *Blood* **90**, 1458–1470 (1997).

182. Lucas, M., Schachterle, W., Oberle, K., Aichele, P. & Diefenbach, A. Dendritic Cells Prime Natural Killer Cells by trans-Presenting Interleukin 15. *Immunity* **26**, 503–517 (2007).

183. Segura, E. *et al.* Differential expression of pathogen-recognition molecules between dendritic cell subsets revealed by plasma membrane proteomic analysis. *Mol. Immunol.* **47**, 1765–1773 (2010).

184. Liu, K. *et al.* In vivo analysis of dendritic cell development and homeostasis. *Science* **324**, 392–397 (2009).

185. Perry, J. S. A. *et al.* Distinct contributions of Aire and antigen-presenting-cell subsets to the generation of self-tolerance in the thymus. *Immunity* **41**, 414–426 (2014).

186. Scott, C. L., Aumeunier, A. M. & Mowat, A. M. I. Intestinal CD103+ dendritic cells: master regulators of tolerance? *Trends Immunol.* **32**, 412–419 (2011).

187. Wendland, M. *et al.* Lymph node T cell homeostasis relies on steady state homing of dendritic cells. *Immunity* **35**, 945–957 (2011).

188. Benahmed, F. *et al.* Multiple CD11c+ cells collaboratively express IL-1β to modulate stromal vascular endothelial growth factor and lymph node vascular-stromal growth. *J. Immunol.* **192**, 4153–4163 (2014).

189. Okabe, Y. & Medzhitov, R. Tissue biology perspective on macrophages. *Nat. Immunol. 2016 171* **17**, 9–17 (2015).

190. Cox, N., Pokrovskii, M., Vicario, R. & Geissmann, F. Origins, Biology, and Diseases of Tissue Macrophages. *https://doi.org/10.1146/annurev-immunol-093019-111748* **39**, 313–344

(2021).

191. Muñoz-Espín, D. *et al.* Programmed Cell Senescence during Mammalian Embryonic Development. *Cell* **155**, 1104–1118 (2013).

192. Nagata, S., Hanayama, R. & Kawane, K. Autoimmunity and the Clearance of Dead Cells. *Cell* **140**, 619–630 (2010).

193. Morioka, S., Maueröder, C. & Ravichandran, K. S. Living on the Edge: Efferocytosis at the Interface of Homeostasis and Pathology. *Immunity* **50**, 1149–1162 (2019).

194. Kohyama, M. *et al.* Role for Spi-C in the development of red pulp macrophages and splenic iron homeostasis. *Nat. 2008 4577227* **457**, 318–321 (2008).

195. Ikegami, M. *et al.* Surfactant metabolism in transgenic mice after granulocyte macrophage-colony stimulating factor ablation. *https://doi.org/10.1152/ajplung.1996.270.4.L650* **270**, (1996).

196. Tauber, A. I. Metchnikoff and the phagocytosis theory. *Nat. Rev. Mol. Cell Biol. 2003 411* **4**, 897–901 (2003).

197. Bilej, M., De Baetselier, P. & Beschin, A. Antimicrobial defense of the earthworm. *Folia Microbiol. 2000 454* **45**, 283–300 (2000).

198. Gomez Perdiguero, E. *et al.* Tissue-resident macrophages originate from yolk-sac-derived erythro-myeloid progenitors. *Nat. 2014 5187540* **518**, 547–551 (2014).

199. Yona, S. *et al.* Fate Mapping Reveals Origins and Dynamics of Monocytes and Tissue Macrophages under Homeostasis. *Immunity* **38**, 79–91 (2013).

200. Jenkins, S. J. *et al.* Local macrophage proliferation, rather than recruitment from the blood, is a signature of T H2 inflammation. *Science (80-.).* **332**, 1284–1288 (2011).

201. Jakubzick, C. *et al.* Minimal Differentiation of Classical Monocytes as They Survey Steady-State Tissues and Transport Antigen to Lymph Nodes. *Immunity* **39**, 599–610 (2013).

202. Lavin, Y. *et al.* Tissue-resident macrophage enhancer landscapes are shaped by the local microenvironment. *Cell* **159**, 1312–26 (2014).

203. Glass, C. K. Genetic and genomic approaches to understanding macrophage identity and function. *Arterioscler. Thromb. Vasc. Biol.* **35**, 755–762 (2015).

204. Pollard, J. W. Trophic macrophages in development and disease. *Nat. Rev. Immunol. 2009 94* **9**, 259–270 (2009).

205. Boyle, W., Simonet, W., Nature, D. L.- & 2003, undefined. Osteoclast differentiation and

activation. *nature.com*.

206. Han, Y. *et al.* Paracrine and endocrine actions of bone—the functions of secretory proteins from osteoblasts, osteocytes, and osteoclasts. *nature.com*.

207. Mosser, D. M. & Edwards, J. P. Exploring the full spectrum of macrophage activation. *Nat. Rev. Immunol.* **8**, 958 (2008).

208. Zhang, X. & Mosser, D. M. Macrophage activation by endogenous danger signals. *J. Pathol.* **214**, 161–178 (2008).

209. Kono, H. & Rock, K. L. How dying cells alert the immune system to danger. *Nat. Rev. Immunol.* **8**, 279 (2008).

210. Chen, C. J. *et al.* Identification of a key pathway required for the sterile inflammatory response triggered by dying cells. *Nat. Med.* **13**, 851–856 (2007).

211. Edwards, J. P., Zhang, X., Frauwirth, K. A. & Mosser, D. M. Biochemical and functional characterization of three activated macrophage populations. *J. Leukoc. Biol.* **80**, 1298–1307 (2006).

212. O'Shea, J. J. & Murray, P. J. Cytokine signaling modules in inflammatory responses. *Immunity* **28**, 477–487 (2008).

213. Dale, D. C., Boxer, L. & Conrad Liles, W. The phagocytes: neutrophils and monocytes. *Blood* **112**, 935–945 (2008).

214. Filipe-Santos, O. *et al.* Inborn errors of IL-12/23- and IFN-gamma-mediated immunity: molecular, cellular, and clinical features. *Semin. Immunol.* **18**, 347–361 (2006).

215. Nandan, D. & Reiner, N. E. Attenuation of gamma interferon-induced tyrosine phosphorylation in mononuclear phagocytes infected with Leishmania donovani: selective inhibition of signaling through Janus kinases and Stat1. *Infect. Immun.* **63**, 4495 (1995).

216. Yamamoto, M. *et al.* Role of adaptor TRIF in the MyD88-independent toll-like receptor signaling pathway. *Science* **301**, 640–643 (2003).

217. Swanson, K. V., Deng, M. & Ting, J. P. Y. The NLRP3 inflammasome: molecular activation and regulation to therapeutics. *Nat. Rev. Immunol. 2019 198* **19**, 477–489 (2019).

218. Langrish, C. L. *et al.* IL-23 drives a pathogenic T cell population that induces autoimmune inflammation. *J. Exp. Med.* **201**, 233–240 (2005).

219. Szekanecz, Z. & Koch, A. E. Macrophages and their products in rheumatoid arthritis. *Curr. Opin. Rheumatol.* **19**, 289–295 (2007).

220. Ouimet, M. *et al.* Autophagy regulates cholesterol efflux from macrophage foam cells via lysosomal acid lipase. *Elsevier*.

221. Pekala, P. H., Kawakamit, M., Angus', C. W., Laneo, M. D. & Ceramit, A. Selective inhibition of synthesis of enzymes for de novo fatty acid biosynthesis by an endotoxin-induced mediator from exudate cells. *Natl. Acad Sci.* **80**, 2743–2747 (1983).

222. Dustin, M. L. & Colman, D. R. Neural and immunological synaptic relations. *Science* **298**, 785–9 (2002).

223. Borg, C. *et al.* NK cell activation by dendritic cells (DCs) requires the formation of a synapse leading to IL-12 polarization in DCs. *Blood* **104**, 3267–3275 (2004).

224. Lapaque, N., Walzer, T., Méresse, S., Vivier, E. & Trowsdale, J. Interactions between Human NK Cells and Macrophages in Response to Salmonella Infection 1. *J. Immunol.* **182**, 4339–4348 (2009).

225. Nedvetzki, S. *et al.* Reciprocal regulation of human natural killer cells and macrophages associated with distinct immune synapses. *Blood* **109**, 3776–85 (2007).

226. Newman, K. C., Korbel, D. S., Hafalla, J. C. & Riley, E. M. Cross-Talk with Myeloid Accessory Cells Regulates Human Natural Killer Cell Interferon-γ Responses to Malaria. *PLoS Pathog.* **2**, e118 (2006).

227. Haller, D., Serrant, P., Granato, D., Schiffrin, E. J. & Blum, S. Activation of Human NK Cells by Staphylococci and Lactobacilli Requires Cell Contact-Dependent Costimulation by Autologous Monocytes. *Clin. Diagn. Lab. Immunol.* **9**, 649 (2002).

228. Amakata, Y., Fujiyama, Y., Andoh, A., Hodohara, K. & Bamba, T. Mechanism of NK cell activation induced by coculture with dendritic cells derived from peripheral blood monocytes. *Clin. Exp. Immunol.* **124**, 214–222 (2001).

229. Nomura, T. *et al.* Essential role of interleukin-12 (IL-12) and IL-18 for gamma interferon production induced by listeriolysin O in mouse spleen cells. *Infect. Immun.* **70**, 1049–1055 (2002).

230. Tripp, C. S., Wolf, S. F. & Unanue, E. R. Interleukin 12 and tumor necrosis factor alpha are costimulators of interferon gamma production by natural killer cells in severe combined immunodeficiency mice with listeriosis, and interleukin 10 is a physiologic antagonist. *Proc. Natl. Acad. Sci. U. S. A.* **90**, 3725–3729 (1993).

231. Scharton-Kersten, T., Afonso, L. C., Wysocka, M., Trinchieri, G. & Scott, P. IL-12 is required for natural killer cell activation and subsequent T helper 1 cell development in experimental leishmaniasis. *J. Immunol.* **154**, (1995).

232. Manna, P. P., Chakrabarti, G. & Bandyopadhyay, S. Innate immune defense in visceral leishmaniasis: cytokine mediated protective role by allogeneic effector cell. *Vaccine* **28**, 803–

810 (2010).

233. Mohan, K., Moulin, P. & Stevenson, M. M. Natural killer cell cytokine production, not cytotoxicity, contributes to resistance against blood-stage Plasmodium chabaudi AS infection. *J. Immunol.* **159**, (1997).

234. Orange, J. S. & Biron, C. A. An absolute and restricted requirement for IL-12 in natural killer cell IFN-gamma production and antiviral defense. Studies of natural killer and T cell responses in contrasting viral infections. *J. Immunol.* **156**, (1996).

235. Lusty, E. *et al.* IL-18/IL-15/IL-12 synergy induces elevated and prolonged IFN-γ production by ex vivo expanded NK cells which is not due to enhanced STAT4 activation. *Mol. Immunol.* **88**, 138–147 (2017).

236. Chan, A. H. & Schroder, K. Inflammasome signaling and regulation of interleukin-1 family cytokines. *J. Exp. Med.* **217**, (2020).

237. Semino, C., Angelini, G., Poggi, A. & Rubartelli, A. NK/iDC interaction results in IL-18 secretion by DCs at the synaptic cleft followed by NK cell activation and release of the DC maturation factor HMGB1. *Blood* **106**, 609–16 (2005).

238. Humann, J. & Lenz, L. L. Activation of Naive NK Cells in Response to Listeria monocytogenes Requires IL-18 and Contact with Infected Dendritic Cells. *J Immunol* **184**, 5172–5178 (2018).

239. Liang, S., Wei, H., Sun, R. & Tian, Z. IFNα regulates NK cell cytotoxicity through STAT1 pathway. *Cytokine* **23**, 190–199 (2003).

240. Mortier, E., Woo, T., Advincula, R., Gozalo, S. & Ma, A. IL-15Rα chaperones IL-15 to stable dendritic cell membrane complexes that activate NK cells via trans presentation. *J. Exp. Med.* **205**, 1213–1225 (2008).

241. Hamerman, J. A., Ogasawara, K. & Lanier, L. L. Cutting Edge: Toll-Like Receptor Signaling in Macrophages Induces Ligands for the NKG2D Receptor. *J. Immunol.* **172**, 2001–2005 (2004).

242. Vankayalapati, R. *et al.* Role of NK cell-activating receptors and their ligands in the lysis of mononuclear phagocytes infected with an intracellular bacterium. *J. Immunol.* **175**, 4611–4617 (2005).

243. Basu, S. *et al.* Human Uterine NK cells Interact with Uterine Macrophages via NKG2D upon stimulation with PAMPs. *Am. J. Reprod. Immunol.* **61**, 52 (2009).

244. Atochina, O. & Harn, D. LNFPIII/LeX-stimulated macrophages activate natural killer cells via CD40-CD40L interaction. *Clin. Diagn. Lab. Immunol.* **12**, 1041–1049 (2005).

245. Bellora, F. *et al.* The interaction of human natural killer cells with either unpolarized or polarized macrophages results in different functional outcomes. *Proc. Natl. Acad. Sci. U. S. A.* **107**, 21659–21664 (2010).

246. Romo, N. *et al.* Natural killer cell-mediated response to human cytomegalovirus-infected macrophages is modulated by their functional polarization. *J. Leukoc. Biol.* **90**, 717–726 (2011).

247. Michel, T., Hentges, F. & Zimmer, J. Consequences of the crosstalk between monocytes/macrophages and natural killer cells. *Front. Immunol.* **3**, 403 (2012).

248. Pallandre, J. R. *et al.* Dendritic cell and natural killer cell cross-talk: A pivotal role of CX3CL1 in NK cytoskeleton organization and activation. *Blood* **112**, 4420–4424 (2008).

249. Draghi, M. *et al.* NKp46 and NKG2D recognition of infected dendritic cells is necessary for NK cell activation in the human response to influenza infection. *J. Immunol.* **178**, 2688–98 (2007).

250. Hadad, U. *et al.* NKp46 clusters at the immune synapse and regulates NK cell polarization. *Front. Immunol.* **6**, 25 (2015).

251. Holger Warschkau and Albrecht F. Kiderlen. No TA Monoclonal Antibody Directed Against the Murine Macrophage Surface Molecule F4/80 Modulates Natural Immune Response to Listeria monocytogenesitle. *J. Immunol. (Baltimore, Md. 1950* **163**, 3409–3416 (1999).

252. Bellone, G., Aste-Amezaga, M., Trinchieri, G. & Rodeck, U. Regulation of NK cell functions by TGF-beta 1. *J. Immunol.* **155**, (1995).

253. Song, H. *et al.* IL-2/IL-18 prevent the down-modulation of NKG2D by TGF-β in NK cells via the c-Jun N-terminal kinase (JNK) pathway. *Cell. Immunol.* **242**, 39–45 (2006).

254. Neyer, L. E. *et al.* Role of interleukin-10 in regulation of T-cell-dependent and T-cell-independent mechanisms of resistance to Toxoplasma gondii. *Infect. Immun.* **65**, 1675 (1997).

255. Clark, S. E. *et al.* Bacterial Manipulation of NK Cell Regulatory Activity Increases Susceptibility to Listeria monocytogenes Infection. *PLOS Pathog.* **12**, e1005708 (2016).

256. Clark, S. E., Schmidt, R. L., McDermott, D. S. & Lenz, L. L. A Batf3/Nlrp3/IL-18 Axis Promotes Natural Killer Cell IL-10 Production during Listeria monocytogenes Infection. *Cell Rep.* **23**, 2582–2594 (2018).

257. Gerosa, F. *et al.* The Reciprocal Interaction of NK Cells with Plasmacytoid or Myeloid Dendritic Cells Profoundly Affects Innate Resistance Functions. *J. Immunol.* **174**, 727–734 (2005).

258. Piccioli, D., Sbrana, S., Melandri, E. & Valiante, N. M. Contact-dependent stimulation and inhibition of dendritic cells by natural killer cells. *J. Exp. Med.* **195**, 335–41 (2002).

259. Ferlazzo, G. *et al.* Human dendritic cells activate resting natural killer (NK) cells and are recognized via the NKp30 receptor by activated NK cells. *J. Exp. Med.* **195**, 343–351 (2002).

260. Jiao, L. *et al.* NK cells promote type 1 T cell immunity through modulating the function of dendritic cells during intracellular bacterial infection. *J. Immunol.* **187**, 401–411 (2011).

261. Zhou, Z. *et al.* Granzyme A from cytotoxic lymphocytes cleaves GSDMB to trigger pyroptosis in target cells. *Science* **368**, (2020).

262. Zhang, Z. *et al.* Gasdermin E suppresses tumour growth by activating anti-tumour immunity. *Nature* **579**, 415–420 (2020).

263. Liu, D. *et al.* Integrin-Dependent Organization and Bidirectional Vesicular Traffic at Cytotoxic Immune Synapses. *Immunity* **31**, 99–109 (2009).

264. Jiang, K. *et al.* Pivotal role of phosphoinositide-3 kinase in regulation of cytotoxicity in natural killer cells. *Nat. Immunol. 2000 15* **1**, 419–425 (2000).

265. Tuli, A. *et al.* Arf-like GTPase Arl8b regulates lytic granule polarization and natural killer cell-mediated cytotoxicity. *Mol. Biol. Cell* **24**, 3721–3735 (2013).

266. Sanborn, K. B. *et al.* Myosin IIA associates with NK cell lytic granules to enable their interaction with F-actin and function at the immunological synapse. *J. Immunol.* **182**, 6969–6984 (2009).

267. Griffiths, G. M., Tsun, A. & Stinchcombe, J. C. The immunological synapse: a focal point for endocytosis and exocytosis. *J. Cell Biol.* **189**, 399–406 (2010).

268. Das, V. *et al.* Activation-Induced Polarized Recycling Targets T Cell Antigen Receptors to the Immunological Synapse: Involvement of SNARE Complexes. *Immunity* **20**, 577–588 (2004).

269. Alter, G., Malenfant, J. M. & Altfeld, M. CD107a as a functional marker for the identification of natural killer cell activity. *J. Immunol. Methods* **294**, 15–22 (2004).

270. Osińska, I., Popko, K. & Demkow, U. Perforin: an important player in immune response. *Cent. J. Immunol.* **39**, 109–115 (2014).

271. Walch, M. *et al.* Cytotoxic Cells Kill Intracellular Bacteria through Granulysin-Mediated Delivery of Granzymes. *Cell* **157**, 1309–1323 (2014).

272. Cullen, S. P. & Martin, S. J. Mechanisms of granule-dependent killing. *Cell Death Differ. 2008 152* **15**, 251–262 (2007).

273. Goping, I. S. *et al.* Granzyme B-Induced Apoptosis Requires Both Direct Caspase Activation and Relief of Caspase Inhibition. *Immunity* **18**, 355–365 (2003).

274. Ogbomo, H. *et al.* Granule-Dependent NK Cell Killing of Cryptococcus Requires Kinesin to Reposition the Cytolytic Machinery for Directed Cytotoxicity. *Cell Rep.* **24**, 3017–3032 (2018).

275. Lu, C.-C. *et al.* NK cells kill mycobacteria directly by releasing perforin and granulysin. *J. Leukoc. Biol.* **96**, 1119–1129 (2014).

276. Dotiwala, F. *et al.* Granzyme B Disrupts Central Metabolism and Protein Synthesis in Bacteria to Promote an Immune Cell Death Program. *Cell* **171**, 1125-1137.e11 (2017).

277. Prager, I. & Watzl, C. Mechanisms of natural killer cell-mediated cellular cytotoxicity. *J. Leukoc. Biol.* **105**, 1319–1329 (2019).

278. Peter, M. E. & Krammer, P. H. The CD95(APO-1/Fas) DISC and beyond. *Cell Death Differ. 2003 101* **10**, 26–35 (2003).

279. Lugini, L. *et al.* Immune Surveillance Properties of Human NK Cell-Derived Exosomes. *J. Immunol.* **189**, 2833–2842 (2012).

280. Von Karstedt, S., Montinaro, A. & Walczak, H. Exploring the TRAILs less travelled: TRAIL in cancer biology and therapy. *Nat. Rev. Cancer 2017 176* **17**, 352–366 (2017).

281. Orange, J. S. & Biron, C. A. Characterization of early IL-12, IFN-alphabeta, and TNF effects on antiviral state and NK cell responses during murine cytomegalovirus infection. *J. Immunol.* **156**, (1996).

282. Fauriat, C., Long, E. O., Ljunggren, H. G. & Bryceson, Y. T. Regulation of human NK-cell cytokine and chemokine production by target cell recognition. *Blood* **115**, 2167–2176 (2010).

283. Bluman, E. M., Bartynski, K. J., Avalos, B. R. & Caligiuri, M. A. Human natural killer cells produce abundant macrophage inflammatory protein-1 alpha in response to monocyte-derived cytokines. *J. Clin. Invest.* **97**, 2722–2727 (1996).

284. Bär, E., Whitney, P. G., Moor, K., ReiseSousa, C. & LeibundGut-Landmann, S. IL-17 Regulates Systemic Fungal Immunity by Controlling the Functional Competence of NK Cells. *Immunity* **40**, 117–127 (2014).

285. Clark, S. E. *et al.* Bacterial Manipulation of NK Cell Regulatory Activity Increases Susceptibility to Listeria monocytogenes Infection. *PLoS Pathog.* **12**, (2016).

286. Perona-Wright, G. *et al.* Systemic but Not Local Infections Elicit Immunosuppressive IL-10 Production by Natural Killer Cells. *Cell Host Microbe* **6**, 503–512 (2009).

287. Swaminathan, B. & Gerner-Smidt, P. The epidemiology of human listeriosis. *Microbes Infect.* **9**, 1236–1243 (2007).

288. Radoshevich, L. & Cossart, P. Listeria monocytogenes: towards a complete picture of its physiology and pathogenesis. *Nat. Publ. Gr.* **16**, (2017).

289. Hamon, M., Bierne, H. & Cossart, P. Listeria monocytogenes: a multifaceted model. *Nat. Rev. Microbiol.* **4**, 423–434 (2006).

290. Gandhi, M. & Chikindas, M. L. Listeria: A foodborne pathogen that knows how to survive. *Int. J. Food Microbiol.* **113**, 1–15 (2007).

291. D'Orazio, S. E. F. Innate and Adaptive Immune Responses during Listeria monocytogenes Infection. *Microbiol. Spectr.* **7**, (2019).

292. Lecuit, M. *et al.* A transgenic model for listeriosis: role of internalin in crossing the intestinal barrier. *Science* **292**, 1722–1725 (2001).

293. Liu, T., Nishimura, H., Matsuguchi, T. & Yoshikai, Y. Differences in Interleukin-12 and -15 Production by Dendritic Cells at the Early Stage of Listeria monocytogenes Infection between BALB/c and C57 BL/6 Mice. *Cell. Immunol.* **202**, 31–40 (2000).

294. Liu, T., Matsuguchi, T., Tsuboi, N., Yajima, T. & Yoshikai, Y. Differences in expression of toll-like receptors and their reactivities in dendritic cells in BALB/c and C57BL/6 mice. *Infect. Immun.* **70**, 6638–6645 (2002).

295. Munder, A. *et al.* Murine pulmonary infection with Listeria monocytogenes: differential susceptibility of BALB/c, C57BL/6 and DBA/2 mice. *Microbes Infect.* **7**, 600–611 (2005).

296. Nikitas, G. *et al.* Transcytosis of Listeria monocytogenes across the intestinal barrier upon specific targeting of goblet cell accessible E-cadherin. *J. Exp. Med.* **208**, 2263–2277 (2011).

297. Jones, G. S. & D'Orazio, S. E. F. Monocytes Are the Predominant Cell Type Associated with Listeria monocytogenes in the Gut, but They Do Not Serve as an Intracellular Growth Niche. *J. Immunol.* **198**, 2796–2804 (2017).

298. Mengaud, J., Ohayon, H., Gounon, P., Mege, R. M. & Cossart, P. E-cadherin is the receptor for internalin, a surface protein required for entry of L. monocytogenes into epithelial cells. *Cell* **84**, 923–932 (1996).

299. Shen, Y., Naujokas, M., Park, M. & Ireton, K. InIB-dependent internalization of Listeria is mediated by the Met receptor tyrosine kinase. *Cell* **103**, 501–510 (2000).

300. Kühbacher, A. *et al.* Genome-Wide siRNA Screen Identifies Complementary Signaling Pathways Involved in Listeria Infection and Reveals Different Actin Nucleation Mechanisms during Listeria Cell Invasion and Actin Comet Tail Formation. *MBio* **6**, 1–14 (2015).

301. Goldfine, H., Bannam, T., Johnston, N. C. & Zuckert, W. R. Bacterial phospholipases and intracellular growth: the two distinct phospholipases C of Listeria monocytogenes. *Symp. Ser. Soc. Appl. Microbiol.* **27**, (1998).

302. Hamon, M. A., Ribet, D., Stavru, F. & Cossart, P. Listeriolysin O: the Swiss army knife of Listeria. *Trends Microbiol.* **20**, 360–368 (2012).

303. Pamer, E. G. Immune responses to Listeria monocytogenes. *Nat. Rev. Immunol.* **4**, 812–823 (2004).

304. Shaughnessy, L. M. & Swanson, J. A. The role of the activated macrophage in clearing Listeria monocytogenes infection. *Front. Biosci.* **12**, 2683–92 (2007).

305. Geoffroy, C., Gaillard, J. L., Alouf, J. E. & Berche, P. Purification, characterization, and toxicity of the sulfhydryl-activated hemolysin listeriolysin O from Listeria monocytogenes. *Infect. Immun.* **55**, 1641–1646 (1987).

306. Jones, S. & Portnoy, D. A. Characterization of Listeria monocytogenes pathogenesis in a strain expressing perfringolysin O in place of listeriolysin O. *Infect. Immun.* **62**, 5608–5613 (1994).

307. Rabinovich, L., Sigal, N., Borovok, I., Nir-Paz, R. & Herskovits, A. A. Prophage excision activates Listeria competence genes that promote phagosomal escape and virulence. *Cell* **150**, 792–802 (2012).

308. Welch, M. D., Iwamatsu, A. & Mitchison, T. J. Actin polymerization is induced by Arp 2/3 protein complex at the surface of Listeria monocytogenes. *Nat. 1997 3856613* **385**, 265–269 (1997).

309. Truong, D., Copeland, J. W. & Brumell, J. H. Bacterial subversion of host cytoskeletal machinery: Hijacking formins and the Arp2/3 complex. *BioEssays* **36**, 687–696 (2014).

310. Fattouh, R. *et al.* The diaphanous-related formins promote protrusion formation and cell-to-cell spread of Listeria monocytogenes. *J. Infect. Dis.* **211**, 1185–1195 (2015).

311. Czuczman, M. A. *et al.* Listeria monocytogenes exploits efferocytosis to promote cell-to-cell spread. *Nat. 2014 5097499* **509**, 230–234 (2014).

312. Pankla, R. *et al.* Genomic transcriptional profiling identifies a candidate blood biomarker signature for the diagnosis of septicemic melioidosis. *Genome Biol.* **10**, R127 (2009).

313. Edelson, B. T. & Unanue, E. R. MyD88-dependent but Toll-like receptor 2-independent innate immunity to Listeria: no role for either in macrophage listericidal activity. *J. Immunol.* **169**, 3869–3875 (2002).

314. Flo, T. H. *et al.* Human Toll-Like Receptor 2 Mediates Monocyte Activation by Listeria monocytogenes, But Not by Group B Streptococci or Lipopolysaccharide. *J. Immunol.* **164**, 2064–2069 (2000).

315. Kawai, T. & Akira, S. The role of pattern-recognition receptors in innate immunity: update on Toll-like receptors. *Nat. Immunol. 2010 115* **11**, 373–384 (2010).

316. Seki, E. *et al.* Critical Roles of Myeloid Differentiation Factor 88-Dependent Proinflammatory Cytokine Release in Early Phase Clearance of Listeria monocytogenes in Mice. *J. Immunol.* **169**, 3863–3868 (2002).

317. Hayashi, F. *et al.* The innate immune response to bacterial flagellin is mediated by Toll-like receptor 5. *Nat. 2001 4106832* **410**, 1099–1103 (2001).

318. Chen, S. T. *et al.* CLEC5A is a critical receptor in innate immunity against Listeria infection. *Nat. Commun. 2017 81* **8**, 1–13 (2017).

319. Meixenberger, K. *et al.* Listeria monocytogenes-Infected Human Peripheral Blood Mononuclear Cells Produce IL-1β, Depending on Listeriolysin O and NLRP3. *J. Immunol.* **184**, 922–930 (2010).

320. Wu, J., Fernandes-Alnemri, T. & Alnemri, E. S. Involvement of the AIM2, NLRC4, and NLRP3 inflammasomes in caspase-1 activation by Listeria monocytogenes. *J. Clin. Immunol.* **30**, 693–702 (2010).

321. Kobayashi, K. S. *et al.* Nod2-dependent regulation of innate and adaptive immunity in the intestinal tract. *Science (80-.).* **307**, 731–734 (2005).

322. Hansen, K. *et al.* Listeria monocytogenes induces IFNβ expression through an IFI16-, cGAS- and STING-dependent pathway. *EMBO J.* **33**, 1654–1666 (2014).

323. Aichele, P. *et al.* Macrophages of the Splenic Marginal Zone Are Essential for Trapping of Blood-Borne Particulate Antigen but Dispensable for Induction of Specific T Cell Responses. *J. Immunol.* **171**, 1148–1155 (2003).

324. Aoshi, T. *et al.* The cellular niche of Listeria monocytogenes infection changes rapidly in the spleen. *Eur. J. Immunol.* **39**, 417–425 (2009).

325. Ebe, Y. *et al.* The role of Kupffer cells and regulation of neutrophil migration into the liver by macrophage inflammatory protein-2 in primary listeriosis in mice. *Pathol. Int.* **49**, 519–532 (1999).

326. Rosales, C. & Uribe-Querol, E. Phagocytosis: A Fundamental Process in Immunity. *Biomed Res. Int.* **2017**, (2017).

327. Portnoy, D. A., Schreiber, R. D., Connelly, P. & Tilneys, L. G. Gamma interferon limits access of Listeria monocytogenes to the macrophage cytoplasm. *J. Exp. Med.* **170**, 2141–2146 (1989).

328. Harty, J. T. & Bevant, M. J. Specific immunity to listeria monocytogenes in the absence of IFNγ. *Immunity* **3**, 109–117 (1995).

329. Roesler, J. *et al.* Listeria monocytogenes and recurrent mycobacterial infections in a child with complete interferon-γ-receptor (IFNγR1) deficiency: Mutational analysis and evaluation of therapeutic options. *Exp. Hematol.* **27**, 1368–1374 (1999).

330. Kubota, K. & Kadoya, Y. Innate IFN-γ-producing cells in the spleen of mice early after Listeria monocytogenes infection: Importance of microenvironment of the cells involved in the production of innate IFN-γ. *Front. Immunol.* **2**, (2011).

331. Schmidt, R. L. & Lenz, L. L. Distinct Licensing of IL-18 and IL-1β Secretion in Response to NLRP3 Inflammasome Activation. *PLoS One* **7**, e45186 (2012).

332. Cheers, Y. Z. and C. Control of IL-12 and IFN-γ Production in Response to Live or Dead Bacteria by TNF and Other Factors. *J. Immunol.* **1**, 1447–1453 (1998).

333. Ghanem, E. N. B., Nelson, C. C. & D'Orazio, S. E. F. T Cell-Intrinsic Factors Contribute to the Differential Ability of CD8+ T Cells To Rapidly Secrete IFN-γ in the Absence of Antigen. *J. Immunol.* **186**, 1703–1712 (2011).

334. Seregin, S. S., Chen, G. Y. & Laouar, Y. Dissecting CD8+ NKT Cell Responses to Listeria Infection Reveals a Component of Innate Resistance. *J. Immunol.* **195**, 1112–20 (2015).

335. Lee, S. H. *et al.* Identifying the Initiating Events of Anti-Listeria Responses Using Mice with Conditional Loss of IFN-γ Receptor Subunit 1 (IFNGR1). *J. Immunol.* **191**, 4223–4234 (2013).

336. Wagner, R. D., Steinberg, H., Brown, J. F. & Czuprvnski, C. J. Recombinant interleukin-12 enhances resistance of mice to Listeria monocytogenes infection. *Microb. Pathog.* **17**, 175–186 (1994).

337. Li, X., Lyons, A. B., Woods, G. M. & Körner, H. The absence of TNF permits myeloid Arginase 1 expression in experimental L. monocytogenes infection. *Immunobiology* **222**, 913–917 (2017).

338. Aoshi, T. *et al.* Bacterial Entry to the Splenic White Pulp Initiates Antigen Presentation to CD8+ T Cells. *Immunity* **29**, 476–486 (2008).

339. Edelson, B. T. *et al.* CD8α+ Dendritic Cells Are an Obligate Cellular Entry Point for Productive Infection by Listeria monocytogenes. *Immunity* **35**, 236–248 (2011).

340. Stockinger, S. *et al.* Characterization of the Interferon-Producing Cell in Mice Infected with Listeria monocytogenes. *PLOS Pathog.* **5**, e1000355 (2009).

341. Dresing, P., Borkens, S., Kocur, M., Kropp, S. & Scheu, S. A Fluorescence Reporter Model Defines "Tip-DCs" as the Cellular Source of Interferon β in Murine Listeriosis. *PLoS One* **5**, e15567 (2010).

342. Carrero, J. A., Calderon, B. & Unanue, E. R. Listeriolysin O from Listeria monocytogenes Is a Lymphocyte Apoptogenic Molecule. *J. Immunol.* **172**, 4866–4874 (2004).

343. Carrero, J. A., Calderon, B. & Unanue, E. R. Lymphocytes are detrimental during the early innate immune response against Listeria monocytogenes. *J. Exp. Med.* **203**, 933–940 (2006).

344. Auerbuch, V., Brockstedt, D. G., Meyer-Morse, N., O'Riordan, M. & Portnoy, D. A. Mice lacking the type I interferon receptor are resistant to Listeria monocytogenes. *J. Exp. Med.* **200**, 527–33 (2004).

345. Witter, A. R., Okunnu, B. M. & Berg, R. E. The Essential Role of Neutrophils during Infection with the Intracellular Bacterial Pathogen Listeria monocytogenes. *J. Immunol.* **197**, 1557–1565 (2016).

346. Liu, M. *et al.* Formylpeptide receptors are critical for rapid neutrophil mobilization in host defense against Listeria monocytogenes. *Sci. Reports 2012 21* **2**, 1–7 (2012).

347. Carr, K. D. *et al.* Specific depletion reveals a novel role for neutrophil-mediated protection in the liver during Listeria monocytogenes infection. *Eur. J. Immunol.* **41**, 2666–2676 (2011).

348. Serbina, N. V & Pamer, E. G. Monocyte emigration from bone marrow during bacterial infection requires signals mediated by chemokine receptor CCR2. *Nat. Immunol.* **7**, 311–317 (2006).

349. Barsig, J., Flesch, I. E. A. & Kaufmann, S. H. E. Macrophages and Hepatocytic Cells as Chemokine Producers in Murine Listeriosis. *Immunobiology* **199**, 87–104 (1998).

350. Rosen, H., Gordon, S. & North, R. J. Exacerbation of murine listeriosis by a monoclonal antibody specific for the type 3 complement receptor of myelomonocytic cells. Absence of monocytes at infective foci allows Listeria to multiply in nonphagocytic cells. *J. Exp. Med.* **170**, 27–37 (1989).

351. Berg, R. E., Cordes, C. J. & Forman, J. Contribution of CD8+ T cells to innate immunity: IFN-γ secretion induced by IL-12 and IL-18. *Eur. J. Immunol.* **32**, 2807–2816 (2002).

352. Thäle, C. & Kiderlen, A. F. Sources of interferon-gamma (IFN-γ) in early immune response to Listeria monocytogenes. *Immunobiology* **210**, 673–683 (2005).

353. Takada, H., Matsuzaki, G., Hiromatsu, K. & Nomoto, K. Analysis of the role of natural killer cells in Listeria monocytogenes infection: relation between natural killer cells and T-cell receptor gamma delta T cells in the host defence mechanism at the early stage of infection. *Immunology* **82**, 106–12 (1994).

354. Perona-Wright, G. *et al.* Systemic but Not Local Infections Elicit Immunosuppressive IL-10 Production by Natural Killer Cells. *Cell Host Microbe* **6**, 503–512 (2009).

355. D'Orazio, S. E. F., Troese, M. J. & Starnbach, M. N. Cytosolic Localization of Listeria monocytogenes Triggers an Early IFN-γ Response by CD8+ T Cells That Correlates with Innate Resistance to Infection. *J. Immunol.* **177**, 7146–7154 (2006).

356. Berg, R. E., Crossley, E., Murray, S. & Forman, J. Memory CD8+ T Cells Provide Innate Immune Protection against Listeria monocytogenes in the Absence of Cognate Antigen. *J. Exp. Med.* **198**, 1583–1593 (2003).

357. Berg, R. E., Cordes, C. J. & Forman, J. Contribution of CD8+ T cells to innate immunity: IFN-γ secretion induced by IL-12 and IL-18. *Eur. J. Immunol.* **32**, 2807–2816 (2002).

358. Bancroft, G. J., Bosma, M. J., Bosma, G. C. & Unanue, E. R. Regulation of macrophage Ia expression in mice with severe combined immunodeficiency: induction of Ia expression by a T cell-independent mechanism. *J. Immunol.* **137**, (1986).

359. Miller, D. C. & Czuprynski, C. J. Passive immunization with convalescent serum, or oral immunization with formalin-killed organisms, does not protect mice against gastrointestinal challenge with Listeria monocytogenes. *Comp. Immunol. Microbiol. Infect. Dis.* **25**, 69–75

(2002).

360. Leong, M. L. *et al.* Impact of preexisting vector-specific immunity on vaccine potency: Characterization of Listeria monocytogenes-specific humoral and cellular immunity in humans and modeling studies using recombinant vaccines in mice. *Infect. Immun.* **77**, 3958–3968 (2009).

361. Chen, L. & Flies, D. B. Molecular mechanisms of T cell co-stimulation and co-inhibition. *Nat. Rev. Immunol.* **13**, 227–242 (2013).

362. Keppler, S. J., Rosenits, K., Koegl, T., Vucikuja, S. & Aichele, P. Signal 3 Cytokines as Modulators of Primary Immune Responses during Infections: The Interplay of Type I IFN and IL-12 in CD8 T Cell Responses. *PLoS One* **7**, e40865 (2012).

363. Busch, D. H. & Pamer, E. G. T lymphocyte dynamics during Listeria monocytogenes infection. *Immunol. Lett.* **65**, 93–98 (1999).

364. Škoberne, M., Holtappels, R., Hof, H. & Geginat, G. Dynamic Antigen Presentation Patterns of Listeria monocytogenes-Derived CD8 T Cell Epitopes In Vivo. *J. Immunol.* **167**, 2209–2218 (2001).

365. Badovinac, V. P., Porter, B. B. & Harty, J. T. Programmed contraction of CD8+ T cells after infection. *Nat. Immunol. 2002 37* **3**, 619–626 (2002).

366. Jensen, E. R. *et al.* Fas (CD95)-Dependent Cell-Mediated Immunity toListeria monocytogenes. *Infect. Immun.* **66**, 4143–4150 (1998).

367. Kägi, D., Ledermann, B., Bürki, K., Hengartner, H. & Zinkernagel, R. M. CD8+ T cell-mediated protection against an intracellular bacterium by perforin-dependent cytotoxicity. *Eur. J. Immunol.* **24**, 3068–3072 (1994).

368. Neefjes, J., Jongsma, M. L. M., Paul, P. & Bakke, O. Towards a systems understanding of MHC class I and MHC class II antigen presentation. *Nat. Rev. Immunol. 2011 1112* **11**, 823–836 (2011).

369. Safley, S. A., Jensen, P. E., Reay, P. A. & Ziegler, H. K. Mechanisms of T cell epitope immunodominance analyzed in murine listeriosis. *J. Immunol.* **155**, (1995).

370. Way, S. S., Havenar-Daughton, C., Kolumam, G. A., Orgun, N. N. & Murali-Krishna, K. IL-12 and Type-I IFN Synergize for IFN-γ Production by CD4 T Cells, Whereas Neither Are Required for IFN-γ Production by CD8 T Cells after Listeria monocytogenes Infection. *J. Immunol.* **178**, 4498–4505 (2007).

371. Pepper, M. *et al.* Different routes of bacterial infection induce long-lived TH1 memory cells and short-lived TH17 cells. *Nat. Immunol. 2009 111* **11**, 83–89 (2009).

372. Bajénoff, M., Narni-Mancinelli, E., Brau, F. & Lauvau, G. Visualizing Early Splenic Memory

CD8+ T Cells Reactivation against Intracellular Bacteria in the Mouse. *PLoS One* **5**, e11524 (2010).

373. Mittrücker, H.-W., Köhler, A. & Kaufmann, S. H. E. Substantial in vivo proliferation of CD4 + and CD8 + T lymphocytes during secondary Listeria monocytogenes infection. doi:10.1002/(SICI)1521-4141(200004)30:4.

374. Joshi, N. S. *et al.* Inflammation Directs Memory Precursor and Short-Lived Effector CD8+ T Cell Fates via the Graded Expression of T-bet Transcription Factor. *Immunity* **27**, 281–295 (2007).

375. DiSpirito, J. R. & Shen, H. Histone Acetylation at the Single-Cell Level: A Marker of Memory CD8+ T Cell Differentiation and Functionality. *J. Immunol.* **184**, 4631–4636 (2010).

376. Chandrabos, C. *et al.* The p60 and NamA autolysins from Listeria monocytogenes contribute to host colonization and induction of protective memory. *Cell. Microbiol.* **17**, 147–163 (2015).

377. Williams, M. A., Tyznik, A. J. & Bevan, M. J. Interleukin-2 signals during priming are required for secondary expansion of CD8+ memory T cells. *Nat. 2006 4417095* **441**, 890–893 (2006).

378. Meek, S. M. & Williams, M. A. IFN-Gamma-Dependent and Independent Mechanisms of CD4+ Memory T Cell-Mediated Protection from Listeria Infection. *Pathog. 2018, Vol. 7, Page 22* **7**, 22 (2018).

379. Morita, S., Kojima, T. & Kitamura, T. Plat-E: an efficient and stable system for transient packaging of retroviruses. *Gene Ther.* **7**, 1063–1066 (2000).

380. Tabone, O. *et al.* Blood transcriptomics reveal the evolution and resolution of the immune response in tuberculosis. *J. Exp. Med.* **218**, (2021).

381. Rashidian, M. *et al.* Immuno-PET identifies the myeloid compartment as a key contributor to the outcome of the antitumor response under PD-1 blockade. *Proc. Natl. Acad. Sci.* 201905005 (2019) doi:10.1073/pnas.1905005116.

382. Mccarthy, M. M. *et al.* Virus infection of the CNS disrupts the immune-neural-synaptic axis via induction of pleiotropic gene regulation of host responses. (2021) doi:10.7554/eLife.62273.

383. Dong, X., Liu, M., Chen, H. & Zhou, A. Integrative gene network analysis identies TIMP1 as key factors for Haemophilus parasuis infection. doi:10.21203/rs.3.rs-152593/v1.

384. Javed, A. *et al.* Pre-infection transcript levels of FAM26F in peripheral blood mononuclear cells inform about overall plasma viral load in acute and post-acute phase after simian immunodeficiency virus infection. *J. Gen. Virol.* **97**, 3400–3412 (2016).

385. Sayed, D. El & Badr, F. A. Interpreting Macrophage Transcripts In Human T Cell-Mediated Rejection.

386. Martinez, F. O. & Gordon, S. The M1 and M2 paradigm of macrophage activation: time for

reassessment. *F1000Prime Rep.* **6**, 13 (2014).

387. Murray, P. J. Macrophage Polarization. *http://dx.doi.org/10.1146/annurev-physiol-022516-034339* **79**, 541–566 (2017).

388. Schroder, K., Hertzog, P. J., Ravasi, T. & Hume, D. A. Interferon-γ: an overview of signals, mechanisms and functions. *J. Leukoc. Biol.* **75**, 163–189 (2004).

389. Erwig, L.-P., Kluth, D. C., Walsh, G. M. & Rees, A. J. Initial Cytokine Exposure Determines Function of Macrophages and Renders Them Unresponsive to Other Cytokines. *J. Immunol.* **161**, (1998).

390. Murray, P. J. *et al.* Macrophage Activation and Polarization: Nomenclature and Experimental Guidelines. *Immunity* **41**, 14–20 (2014).

391. Hanahan, D., Wagner, E. F. & Palmiter, R. D. The origins of oncomice: a history of the first transgenic mice genetically engineered to develop cancer. *Genes Dev.* **21**, 2258–2270 (2007).

392. J W Gordon, G A Scangos, D J Plotkin, J A Barbosa, and F. H. R. Genetic transformation of mouse embryos by microinjection of purified DNA. *PNAS* **December 1**, 12 (1980).

393. M, Y. & R, H. The Legacy of Nat Sternberg: The Genesis of Cre-lox Technology. *Annu. Rev. Virol.* **2**, 25–40 (2015).

394. Sternberg, N. Demonstration and Analysis of P1 Site-specific Recombination Using λ-P1 Hybrid Phages Constructed In Vitro. *Cold Spring Harb. Symp. Quant. Biol.* **43**, 1143–1146 (1979).

395. Heng, T. S. P. *et al.* The Immunological Genome Project: networks of gene expression in immune cells. *Nat. Immunol.* **9**, 1091–1094 (2008).

396. Bezbradica, J. S., Rosenstein, R. K., DeMarco, R. A., Brodsky, I. & Medzhitov, R. A role for the ITAM signaling module in specifying cytokine-receptor functions. *Nat. Immunol.* **15**, 333–342 (2014).

397. Haan, J. M. M. den & Kraal, G. Innate Immune Functions of Macrophage Subpopulations in the Spleen. *J. Innate Immun.* **4**, 437–445 (2012).

398. Kurotaki, D., Uede, T. & Tamura, T. Functions and development of red pulp macrophages. *Microbiol. Immunol.* **59**, 55–62 (2015).

399. S, D. *et al.* Yeast zymosan, a stimulus for TLR2 and dectin-1, induces regulatory antigen-presenting cells and immunological tolerance. *J. Clin. Invest.* **116**, 916–928 (2006).

400. D, K. *et al.* CSF-1-dependent red pulp macrophages regulate CD4 T cell responses. *J. Immunol.* **186**, 2229–2237 (2011).

401. Karlmark, K. R., Tacke, F. & Dunay, I. R. Monocytes in health and disease – Minireview. *Eur. J. Microbiol. Immunol. (Bp).* **2**, 97 (2012).

402. Kapellos, T. S. *et al.* Human Monocyte Subsets and Phenotypes in Major Chronic Inflammatory Diseases. *Front. Immunol.* **0**, 2035 (2019).

403. Ziegler-Heitbrock, L. *et al.* Nomenclature of monocytes and dendritic cells in blood. (2010) doi:10.1182/blood-2010-02-258558.

404. Cros, J. *et al.* Human CD14dim Monocytes Patrol and Sense Nucleic Acids and Viruses via TLR7 and TLR8 Receptors. *Immunity* **33**, 375 (2010).

405. Carlin, L. M. *et al.* Nr4a1-Dependent Ly6Clow Monocytes Monitor Endothelial Cells and Orchestrate Their Disposal. *Cell* **153**, 362 (2013).

406. Thomas, G., Tacke, R., Hedrick, C. C. & Hanna, R. N. Nonclassical Patrolling Monocyte Function in the Vasculature. *Arterioscler. Thromb. Vasc. Biol.* **35**, 1306 (2015).

407. Auffray, C. *et al.* Monitoring of blood vessels and tissues by a population of monocytes with patrolling behavior. *Science* **317**, 666–670 (2007).

408. Hamilton, J. A. GM-CSF-Dependent Inflammatory Pathways. *Front. Immunol.* **0**, 2055 (2019).

409. Ribechini, E. *et al.* Novel GM-CSF signals via IFN-γR/IRF-1 and AKT/mTOR license monocytes for suppressor function. *Blood Adv.* **1**, 947–960 (2017).

410. Sun, L. *et al.* GM-CSF Quantity Has a Selective Effect on Granulocytic vs. Monocytic Myeloid Development and Function. *Front. Immunol.* **0**, 1922 (2018).

411. Bosteels, C. *et al.* Early treatment with inhaled GM-CSF improves oxygenation and anti-viral immunity in COVID-19 induced lung injury-a randomized clinical trial. doi:10.21203/rs.3.rs-959220/v1.

412. Pietrocola, G. *et al.* Toll-Like Receptors (TLRs) in Innate Immune Defense Against Staphylococcus Aureus: *https://doi.org/10.5301/ijao.5000030* **34**, 799–810 (2011).

413. Gong, D. *et al.* TGFβ signaling plays a critical role in promoting alternative macrophage activation. *BMC Immunol. 2012 131* **13**, 1–10 (2012).

414. Fujiwara, Y. *et al.* Guanylate-binding protein 5 is a marker of interferon-γ-induced classically activated macrophages. *Clin. Transl. Immunol.* **5**, e111 (2016).

415. Malik, U. & Javed, A. FAM26F: An Enigmatic Protein Having a Complex Role in the Immune System. *Int. Rev. Immunol.* 1–11 (2016) doi:10.1080/08830185.2016.1206098.

416. Flandin, J.-F., Chano, F. & Descoteaux, A. RNA interference reveals a role for TLR2 and TLR3 in

the recognition of Leishmania donovani promastigotes by interferon–γ-primed macrophages. *Eur. J. Immunol.* **36**, 411–420 (2006).

417. Willment, J. A. *et al.* Dectin-1 Expression and Function Are Enhanced on Alternatively Activated and GM-CSF-Treated Macrophages and Are Negatively Regulated by IL-10, Dexamethasone, and Lipopolysaccharide. *J. Immunol.* **171**, 4569–4573 (2003).

418. LP, S. *et al.* Mice deficient in IL-1beta manifest impaired contact hypersensitivity to trinitrochlorobenzone. *J. Exp. Med.* **183**, 1427–1436 (1996).

419. M, K. *et al.* Impaired immune and acute-phase responses in interleukin-6-deficient mice. *Nature* **368**, 339–342 (1994).

420. Takeda, K. *et al.* Defective NK Cell Activity and Th1 Response in IL-18–Deficient Mice. *Immunity* **8**, 383–390 (1998).

421. Sojka, D. K., Yang, L. & Yokoyama, W. M. Uterine Natural Killer Cells. *Front. Immunol.* **0**, 960 (2019).

422. Jiang, Q., Wei, H. & Tian, Z. IFN-producing killer dendritic cells contribute to the inhibitory effect of poly I:C on the progression of murine melanoma. *J. Immunother.* **31**, 555–562 (2008).

423. Kakuta, S., Tagawa, Y. I., Shibata, S., Nanno, M. & Iwakura, Y. Inhibition of B16 melanoma experimental metastasis by interferon-γ through direct inhibition of cell proliferation and activation of antitumour host mechanisms. *Immunology* **105**, 92 (2002).

424. MACKANESS, G. B. Cellular resistance to infection. *J. Exp. Med.* **116**, 381–406 (1962).

425. Schoenborn, J. R. & Wilson, C. B. Regulation of Interferon-γ During Innate and Adaptive Immune Responses. *Adv. Immunol.* **96**, 41–101 (2007).

426. Shegarfi, H. *et al.* The Role of Natural Killer Cells in Resistance to the Intracellular Bacterium *Listeria monocytogenes* in Rats. *Scand. J. Immunol.* **70**, 238–244 (2009).

427. Dai, W. J. *et al.* Impaired macrophage listericidal and cytokine activities are responsible for the rapid death of Listeria monocytogenes-infected IFN-gamma receptor-deficient mice. *J. Immunol.* **158**, 5297–304 (1997).

428. Williams, M. A., Schmidt, R. L. & Lenz, L. L. Early events regulating immunity and pathogenesis during Listeria monocytogenes infection. *Trends Immunol.* **33**, 488–495 (2012).

429. Zhong, M. X., Kuziel, W. A., Pamer, E. G. & Serbina, N. V. Chemokine Receptor 5 Is Dispensable for Innate and Adaptive Immune Responses to Listeria monocytogenes Infection. *Infect. Immun.* **72**, 1057–1064 (2004).

430. Myers, J. T., Tsang, A. W. & Swanson, J. A. Localized reactive oxygen and nitrogen

intermediates inhibit escape of Listeria monocytogenes from vacuoles in activated macrophages. *J. Immunol.* **171**, 5447–5453 (2003).

431. Higginbotham, J. N., Lin, T. L. & Pruett, S. B. Effect of macrophage activation on killing of Listeria monocytogenes. Roles of reactive oxygen or nitrogen intermediates, rate of phagocytosis, and retention of bacteria in endosomes. *Clin. exp. Immunol* **88**, 492–498 (1992).

432. MacMicking, J., Xie, Q. W. & Nathan, C. NITRIC OXIDE AND MACROPHAGE FUNCTION. *http://dx.doi.org/10.1146/annurev.immunol.15.1.323* **15**, 323–350 (2003).

433. Matsumoto, M. & Seya, T. TLR3: Interferon induction by double-stranded RNA including poly(I:C). *Adv. Drug Deliv. Rev.* **60**, 805–812 (2008).

434. Krammer, F. *et al.* Influenza. *Nat. Rev. Dis. Prim.* **4**, 3 (2018).

435. Wisskirchen, C., Ludersdorfer, T. H., Müller, D. A., Moritz, E. & Pavlovic, J. The cellular RNA helicase UAP56 is required for prevention of double-stranded RNA formation during influenza A virus infection. *J. Virol.* **85**, 8646–8655 (2011).

436. Guillot, L. *et al.* Involvement of toll-like receptor 3 in the immune response of lung epithelial cells to double-stranded RNA and influenza A virus. *J. Biol. Chem.* **280**, 5571–5580 (2005).

437. Pichlmair, A. *et al.* RIG-I-mediated antiviral responses to single-stranded RNA bearing 5'-phosphates. *Science* **314**, 997–1001 (2006).

438. Iwasaki, A. & Pillai, P. S. Innate immunity to influenza virus infection. *Nat. Rev. Immunol.* **14**, 315–328 (2014).

439. Schulz, O. *et al.* Toll-like receptor 3 promotes cross-priming to virus-infected cells. *Nature* **433**, 887–892 (2005).

440. Le Goffic, R. *et al.* Detrimental Contribution of the Toll-Like Receptor (TLR)3 to Influenza A Virus–Induced Acute Pneumonia. *PLOS Pathog.* **2**, e53 (2006).

441. Seo, S.-U. *et al.* MyD88 signaling is indispensable for primary influenza A virus infection but dispensable for secondary infection. *J. Virol.* **84**, 12713–12722 (2010).

442. Scholtissek, C., Rohde, W., Von Hoyningen, V. & Rott, R. On the origin of the human influenza virus subtypes H2N2 and H3N2. *Virology* **87**, 13–20 (1978).

443. Nebenführ, A., Ritzenthaler, C. & Robinson, D. G. Brefeldin A: Deciphering an Enigmatic Inhibitor of Secretion. *Plant Physiol.* **130**, 1102–1108 (2002).

444. Berg, R. E., Crossley, E., Murray, S. & Forman, J. Relative Contributions of NK and CD8 T Cells to IFN-γ Mediated Innate Immune Protection against Listeria monocytogenes. *J. Immunol.* **175**, 1751–1757 (2005).

445. Dussurget, O., Bierne, H. & Cossart, P. The bacterial pathogen Listeria monocytogenes and the interferon family: type I, type II and type III interferons. *Front. Cell. Infect. Microbiol.* **4**, 50 (2014).

446. Kang, S.-J., Liang, H.-E., Reizis, B. & Locksley, R. M. Regulation of Hierarchical Clustering and Activation of Innate Immune Cells by Dendritic Cells. *Immunity* **29**, 819–833 (2008).

447. Kubota, K. & Kadoya, Y. Innate IFN-γ-producing cells in the spleen of mice early after Listeria monocytogenes infection: importance of microenvironment of the cells involved in the production of innate IFN-γ. *Front. Immunol.* **2**, 26 (2011).

448. Brombacher, F. *et al.* IL-12 is dispensable for innate and adaptive immunity against low doses of Listeria monocytogenes. *Int. Immunol.* **11**, 325–332 (1999).

449. Smith-Garvin, J. E., Koretzky, G. A. & Jordan, M. S. T Cell Activation. *http://dx.doi.org/10.1146/annurev.immunol.021908.132706* **27**, 591–619 (2009).

450. Ivashkiv, L. B. & Donlin, L. T. Regulation of type I interferon responses. *Nat. Rev. Immunol.* **14**, 36 (2014).

451. Kilbourne, E. D. Future influenza vaccines and the use of genetic recombinants. *Bull. World Health Organ.* **41**, 643–5 (1969).

452. Pribul, P. K. *et al.* Alveolar macrophages are a major determinant of early responses to viral lung infection but do not influence subsequent disease development. *J. Virol.* **82**, 4441–8 (2008).

453. Graham, M. B. *et al.* Response to influenza infection in mice with a targeted disruption in the interferon gamma gene. *J. Exp. Med.* **178**, 1725–32 (1993).

454. Califano, D. *et al.* IFN-γ increases susceptibility to influenza A infection through suppression of group II innate lymphoid cells. *Mucosal Immunol.* **11**, 209–219 (2018).

455. Weiss, I. D. *et al.* IFN-γ Treatment at Early Stages of Influenza Virus Infection Protects Mice from Death in a NK Cell-Dependent Manner. *J. Interf. Cytokine Res.* **30**, 439–449 (2010).

456. Marr, K. J. *et al.* Cryptococcus neoformans Directly Stimulates Perforin Production and Rearms NK Cells for Enhanced Anticryptococcal Microbicidal Activity. *Infect. Immun.* **77**, 2436 (2009).

457. Kadowaki, N., Antonenko, S. & Liu, Y.-J. Distinct CpG DNA and Polyinosinic-Polycytidylic Acid Double-Stranded RNA, Respectively, Stimulate CD11c− Type 2 Dendritic Cell Precursors and CD11c+ Dendritic Cells to Produce Type I IFN. *J. Immunol.* **166**, 2291–2295 (2001).

458. Reimer, T., Brcic, M., Schweizer, M. & Jungi, T. W. poly(I:C) and LPS induce distinct IRF3 and NF-kappaB signaling during type-I IFN and TNF responses in human macrophages. *J. Leukoc. Biol.* **83**, 1249–1257 (2008).

459. Hara, H. *et al.* The NLRP6 Inflammasome Recognizes Lipoteichoic Acid and Regulates Gram-Positive Pathogen Infection. *Cell* **175**, 1651-1664.e14 (2018).

460. Theisen, E. & Sauer, J. D. Listeria monocytogenes and the Inflammasome: From Cytosolic Bacteriolysis to Tumor Immunotherapy. *Curr. Top. Microbiol. Immunol.* **397**, 133–160 (2016).

461. Serbina, N. V., Salazar-Mather, T. P., Biron, C. A., Kuziel, W. A. & Pamer, E. G. TNF/iNOS-producing dendritic cells mediate innate immune defense against bacterial infection. *Immunity* **19**, 59–70 (2003).

462. Tsukada, H., Kawamura, I., Arakawa, M., Nomoto, K. & Mitsuyama, M. Dissociated development of T cells mediating delayed-type hypersensitivity and protective T cells against Listeria monocytogenes and their functional difference in lymphokine production. *Infect. Immun.* **59**, 3589–3595 (1991).

463. Schluns, K. S., Stoklasek, T. & Lefrançois, L. The roles of interleukin-15 receptor α: Trans-presentation, receptor component, or both? *Int. J. Biochem. Cell Biol.* **37**, 1567–1571 (2005).

464. Gronostajskit, R. M. *et al.* The FLP recombinase of the Saccharomyces cerevisiae 2 microns plasmid attaches covalently to DNA via a phosphotyrosyl linkage. *Mol. Cell. Biol.* **5**, 3274 (1985).

465. Mombaerts, P. *et al.* RAG-1-deficient mice have no mature B and T lymphocytes. *Cell* **68**, 869–877 (1992).

466. Perona-Wright, G. *et al.* Systemic but Not Local Infections Elicit Immunosuppressive IL-10 Production by Natural Killer Cells. *Cell Host Microbe* **6**, 503–512 (2009).

467. Humann, J., Bjordahl, R., Andreasen, K. & Lenz, L. L. Expression of the p60 autolysin enhances NK cell activation and is required for listeria monocytogenes expansion in IFN-gamma-responsive mice. *J. Immunol.* **178**, 2407–2414 (2007).

468. Radoshevich, L. & Cossart, P. Listeria monocytogenes: Towards a complete picture of its physiology and pathogenesis. *Nature Reviews Microbiology* vol. 16 32–46 (2018).

469. Jablonska, J., Dittmar, K. E., Kleinke, T., Buer, J. & Weiss, S. Essential role of CCL2 in clustering of splenic ERTR-9+ macrophages during infection of BALB/c mice by Listeria monocytogenes. *Infect. Immun.* **75**, 462–470 (2007).

470. Nishibori, T., Xiong, H., Kawamura, I., Arakawa, M. & Mitsuyama, M. Induction of cytokine gene expression by listeriolysin O and roles of macrophages and NK cells. *Infect. Immun.* **64**, 3188 (1996).

471. Warschkau, H. & Kiderlen, A. F. Listeria monocytogenes Modulates Natural Immune Response to Murine Macrophage Surface Molecule F4/80 A Monoclonal Antibody Directed Against the. *J Immunol Ref.* **3409**, 3409–3416 (1999).

472. Bekiaris, V. *et al.* Ly49H+ NK Cells Migrate to and Protect Splenic White Pulp Stroma from Murine Cytomegalovirus Infection. *J. Immunol.* **180**, 6768–6776 (2008).

473. Muraille, E. *et al.* Distinct in vivo dendritic cell activation by live versus killed Listeria monocytogenes. *Eur. J. Immunol.* **35**, 1463–1471 (2005).

474. Afonina, I. S., Cullen, S. P. & Martin, S. J. Cytotoxic and non-cytotoxic roles of the CTL/NK protease granzyme B. *Immunol. Rev.* **235**, 105–116 (2010).

475. Buchmeier, N. A. & Schreiber, R. D. Requirement of endogenous interferon-gamma production for resolution of Listeria monocytogenes infection. *Proc. Natl. Acad. Sci. U. S. A.* **82**, 7404–7408 (1985).

476. Valderrama, C., Clark, A., Urano, F., Unanue, E. R. & Carrero, J. A. *Listeria monocytogenes* induces an interferon-enhanced activation of the integrated stress response that is detrimental for resolution of infection in mice. *Eur. J. Immunol.* **47**, 830–840 (2017).

477. Soria-Castro, R. *et al.* Valproic acid inhibits interferon-γ production by NK cells and increases susceptibility to Listeria monocytogenes infection. *Sci. Reports 2020 101* **10**, 1–14 (2020).

478. Ouyang, W. & O'Garra, A. IL-10 Family Cytokines IL-10 and IL-22: from Basic Science to Clinical Translation. *Immunity* **50**, 871–891 (2019).

479. Carrero, J. A. & Unanue, E. R. Mechanisms and Immunological Effects of Apoptosis Caused by Listeria Monocytogenes. *Adv. Immunol.* **113**, 157–174 (2012).

480. Dai, W. J., Köhler, G. & Brombacher, F. Both innate and acquired immunity to Listeria monocytogenes infection are increased in IL-10-deficient mice. *J. Immunol.* **158**, (1997).

481. Liu, D. *et al.* IL-10-Dependent Crosstalk between Murine Marginal Zone B Cells, Macrophages, and CD8α+ Dendritic Cells Promotes Listeria monocytogenes Infection. *Immunity* **51**, 64-76.e7 (2019).

482. Bouabe, H. Cytokine Reporter Mice: The Special Case of IL-10. *Scand. J. Immunol.* **75**, 553–567 (2012).

483. Zenewicz, L. A. & Shen, H. Innate and adaptive immune responses to Listeria monocytogenes: a short overview. *Microbes Infect.* **9**, 1208–1215 (2007).

484. Ladel, C. H., Flesch, I. E., Arnoldi, J. & Kaufmann, S. H. Studies with MHC-deficient knock-out mice reveal impact of both MHC I- and MHC II-dependent T cell responses on Listeria monocytogenes infection. *J. Immunol.* **153**, (1994).

485. Vatsala Bhardwaj, Osami Kanagawa, P. E. S. and E. R. U. Chronic Listeria Infection in SCID Mice: Requirements for the Carrier State and the Dual Role of T Cells in Transferring Protection or Suppression. *J. Immunol.* **January 1**, 376–384 (1988).

486. Malmgaard, L. & Paludan, S. R. Short Communication Interferon (IFN)-a/b, interleukin (IL)-12 and IL-18 coordinately induce production of IFN-c during infection with herpes simplex virus type 2. doi:10.1099/vir.0.19251-0.

487. Dhiman, R. *et al.* IL-22 produced by human NK cells inhibits growth of Mycobacterium tuberculosis by enhancing phagolysosomal fusion. *J. Immunol.* **183**, 6639–6645 (2009).

488. Brilot, F., Strowig, T., Roberts, S. M., Arrey, F. & Münz, C. NK cell survival mediated through the regulatory synapse with human DCs requires IL-15Ralpha. *J. Clin. Invest.* **117**, 3316–29 (2007).

489. Marshall, J. D., Heeke, D. S., Abbate, C., Yee, P. & Van Nest, G. Induction of interferon-γ from natural killer cells by immunostimulatory CpG DNA is mediated through plasmacytoid-dendritic-cell-produced interferon-α and tumour necrosis factor-α. *Immunology* **117**, 38 (2006).

490. Freudenberg, M. A. *et al.* Cutting Edge: A Murine, IL-12-Independent Pathway of IFN-γ Induction by Gram-Negative Bacteria Based on STAT4 Activation by Type I IFN and IL-18 Signaling. *J. Immunol.* **169**, 1665–1668 (2002).

491. Brown, A. C. N., Dobbie, I. M., Alakoskela, J. M., Davis, I. & Davis, D. M. Super-resolution imaging of remodeled synaptic actin reveals different synergies between NK cell receptors and integrins. *Blood* **120**, 3729–3740 (2012).

492. Zhou, G., Juang, S. W. W. & Kane, K. P. NK cells exacerbate the pathology of influenza virus infection in mice. *Eur. J. Immunol.* **43**, 929–938 (2013).

493. Prabhu, N. *et al.* Gamma interferon regulates contraction of the influenza virus-specific CD8 T cell response and limits the size of the memory population. *J. Virol.* **87**, 12510–22 (2013).

494. Sun, J. C. & Bevan, M. J. Defective CD8 T Cell Memory Following Acute Infection Without CD4 T Cell Help. *Science* **300**, 339 (2003).

495. Shedlock, D. J. *et al.* Role of CD4 T Cell Help and Costimulation in CD8 T Cell Responses During Listeria monocytogenes Infection. *J. Immunol.* **170**, 2053–2063 (2003).

496. Demura, K. *et al.* Cryo-EM structures of calcium homeostasis modulator channels in diverse oligomeric assemblies. *Sci. Adv.* **6**, 8105 (2020).

497. Trautmann, A. Extracellular ATP in the immune system: more than just a "danger signal". *Sci. Signal.* **2**, pe6 (2009).

498. Schenk, U. *et al.* Purinergic control of T cell activation by ATP released through pannexin-1 hemichannels. *Sci. Signal.* **1**, ra6 (2008).

499. Markers of acute myeloid leukemia stem cells. (2017).

500. Rabinovitch, M. Professional and non-professional phagocytes: an introduction. *Trends Cell Biol.* **5**, 85–87 (1995).

501. Canton, J., Neculai, D. & Grinstein, S. Scavenger receptors in homeostasis and immunity. *Nat. Rev. Immunol.* **13**, 621–634 (2013).

502. Dambuza, I. M. & Brown, G. D. C-type lectins in immunity: recent developments. *Curr. Opin. Immunol.* **32**, 21–27 (2015).

503. García-García, E. & Rosales, C. Signal transduction during Fc receptor-mediated phagocytosis. *J. Leukoc. Biol* **72**, 1092–1108 (2002).

504. Park, H. & Cox, D. Cdc42 regulates Fc gamma receptor-mediated phagocytosis through the activation and phosphorylation of Wiskott-Aldrich syndrome protein (WASP) and neural-WASP. *Mol. Biol. Cell* **20**, 4500–4508 (2009).

505. Kitano, M., Nakaya, M., Nakamura, T., Nagata, S. & Matsuda, M. Imaging of Rab5 activity identifies essential regulators for phagosome maturation. *Nat. 2008 4537192* **453**, 241–245 (2008).

506. Vieira, O. V. *et al.* Modulation of Rab5 and Rab7 Recruitment to Phagosomes by Phosphatidylinositol 3-Kinase. *Mol. Cell. Biol.* **23**, 2501 (2003).

507. Marshansky, V. & Futai, M. The V-type H+-ATPase in vesicular trafficking: targeting, regulation and function. *Curr. Opin. Cell Biol.* **20**, 415–426 (2008).

508. Zumerle, S. *et al.* Intercellular Calcium Signaling Induced by ATP Potentiates Macrophage Phagocytosis. *Cell Rep.* **27**, 1-10.e4 (2019).

509. Consortium, T. gene ontology. The Gene Ontology resource: enriching a GOld mine. *Nucleic Acids Res.* **49**, D325–D334 (2021).

510. Ashburner, M. *et al.* Gene Ontology: tool for the unification of biology. *Nat. Genet. 2000 251* **25**, 25–29 (2000).

511. Bhuin, T. & Roy, J. K. Rab proteins: The key regulators of intracellular vesicle transport. *Exp. Cell Res.* **328**, 1–19 (2014).

512. Courtney, N. A., Bao, H., Briguglio, J. S. & Chapman, E. R. Synaptotagmin 1 clamps synaptic vesicle fusion in mammalian neurons independent of complexin. *Nat. Commun. 2019 101* **10**, 1–14 (2019).

513. Winkle, C. C. *et al.* A novel netrin-1-sensitive mechanism promotes local SNARE-mediated exocytosis during axon branching. *J. Cell Biol.* **205**, 217–232 (2014).

514. Kiang, K. M. Y. & Leung, G. K. K. A Review on Adducin from Functional to Pathological Mechanisms: Future Direction in Cancer. *Biomed Res. Int.* **2018**, (2018).

515. Trimbuch, T. & Rosenmund, C. Should I stop or should I go? The role of complexin in neurotransmitter release. *Nat. Rev. Neurosci. 2016 172* **17**, 118–125 (2016).

516. Bodaleo, F. J., Montenegro-Venegas, C., Henríquez, D. R., Court, F. A. & Gonzalez-Billault, C. Microtubule-associated protein 1B (MAP1B)-deficient neurons show structural presynaptic deficiencies in vitro and altered presynaptic physiology. *Sci. Reports 2016 61* **6**, 1–15 (2016).

517. Niedergang, F., Di Bartolo, V. & Alcover, A. Comparative anatomy of phagocytic and immunological synapses. *Front. Immunol.* **7**, 18 (2016).

518. Loiselle, F. B. & Casey, J. R. Measurement of Intracellular pH. *Methods Mol. Biol.* **637**, 311–331 (2010).

519. Doherty, G. J. & McMahon, H. T. Mechanisms of Endocytosis. *http://dx.doi.org/10.1146/annurev.biochem.78.081307.110540* **78**, 857–902 (2009).

520. Waite, J. C. *et al.* Dynamic Imaging of the Effector Immune Response to Listeria Infection In Vivo. *PLOS Pathog.* **7**, e1001326 (2011).

521. JW, K., YK, J., J, K., SJ, K. & SJ, K. Intramolecular Disulfide Bonds for Biogenesis of CALHM1 Ion Channel Are Dispensable for Voltage-Dependent Activation. *Mol. Cells* **44**, 758–769 (2021).

522. Cleland, W. W. Dithiothreitol, a New Protective Reagent for SH Groups*. *Biochemistry* **3**, 480–482 (2002).

523. Norris, G. E., Stillman, T. J., Anderson, B. F. & Baker, E. N. The three-dimensional structure of PNGase F, a glycosyl asparaginase from Flavobacterium meningosepticum. *Structure* **2**, 1049–1059 (1994).

524. Di Virgilio, F., Dal Ben, D., Sarti, A. C., Giuliani, A. L. & Falzoni, S. The P2X7 Receptor in Infection and Inflammation. *Immunity* **47**, 15–31 (2017).

525. Fernandes-Alnemri, T. *et al.* Cutting edge: TLR signaling licenses IRAK1 for rapid activation of the NLRP3 inflammasome. *J. Immunol.* **191**, 3995–3999 (2013).

526. Borg, C. *et al.* NK cell activation by dendritic cells (DCs) requires the formation of a synapse leading to IL-12 polarization in DCs. *Blood* **104**, 3267–75 (2004).

527. Schwarz, T. L. Synaptotagmin promotes both vesicle fusion and recycling. *Proc. Natl. Acad. Sci.* **101**, 16401–16402 (2004).

528. Andrews, N. W. & Chakrabarti, S. There's more to life than neurotransmission: the regulation of exocytosis by synaptotagmin VII. *Trends Cell Biol.* **15**, 626–631 (2005).

529. Szebenyi, G. *et al.* Activity-Driven Dendritic Remodeling Requires Microtubule-Associated Protein 1A. *Curr. Biol.* **15**, 1820–1826 (2005).

530. Takei, Y., Kikkawa, Y. S., Atapour, N., Hensch, T. K. & Hirokawa, N. Defects in Synaptic Plasticity, Reduced NMDA-Receptor Transport, and Instability of Postsynaptic Density Proteins in Mice Lacking Microtubule-Associated Protein 1A. *J. Neurosci.* **35**, 15539–15554 (2015).

531. Lao, G. *et al.* Syntaphilin: A Syntaxin-1 Clamp that Controls SNARE Assembly. *Neuron* **25**, 191–201 (2000).

532. Kang, J. S. *et al.* Docking of Axonal Mitochondria by Syntaphilin Controls Their Mobility and Affects Short-Term Facilitation. *Cell* **132**, 137–148 (2008).

533. Yan, J., Wong, N., Hung, C., Chen, W. X. Y. & Tang, D. Contactin-1 Reduces E-Cadherin Expression Via Activating AKT in Lung Cancer. *PLoS One* **8**, e65463 (2013).

534. Veny, M. *et al.* Contactin-1 Is Required for Peripheral Innervation and Immune Homeostasis Within the Intestinal Mucosa. *Front. Immunol.* **11**, 1268 (2020).

535. Geisler, S. B. *et al.* Obscurin-like 1, OBSL1, is a novel cytoskeletal protein related to obscurin. *Genomics* **89**, 521–531 (2007).

536. Brunet, I. *et al.* The transcription factor Engrailed-2 guides retinal axons. *Nat. 2005 4387064* **438**, 94–98 (2005).

537. Kato, M. *et al.* Physical and Functional Interaction of Rabphilin-3A with α-Actinin *. *J. Biol. Chem.* **271**, 31775–31778 (1996).

538. Ferrer-Orta, C. *et al.* Structural characterization of the Rabphilin- 3A-SNAP25 interaction. *Proc. Natl. Acad. Sci. U. S. A.* **114**, E5343–E5351 (2017).

539. Ranneva, S. V., Maksimov, V. F., Korostyshevskaja, I. M. & Lipina, T. V. Lack of synaptic protein, calsyntenin-2, impairs morphology of synaptic complexes in mice. *Synapse* **74**, e22132 (2020).

540. Poo, W. J., Conrad, L. & Janeway, C. A. Receptor-directed focusing of lymphokine release by helper T cells. *Nat. 1988 3326162* **332**, 378–380 (1988).

541. Kupfer, A., Mosmann, T. R. & Kupfer, H. Polarized expression of cytokines in cell conjugates of helper T cells and splenic B cells. *Proc. Natl. Acad. Sci.* **88**, 775–779 (1991).

542. Angus, K. L. & Griffiths, G. M. Cell polarisation and the immunological synapse. *Curr. Opin. Cell Biol.* **25**, 85–91 (2013).

543. Verboogen, D. R. J. *et al.* The dendritic cell side of the immunological synapse. *Biomol. Concepts* **7**, 17–28 (2016).

544. Rodríguez-Fernández, J. L., Delgado-Martín, C. & Riol-Blanco, L. What is the function of the dendritic cell side of the immunological synapse? *Sci. Signal.* **3**, (2010).

545. Davis, D. M. *et al.* The human natural killer cell immune synapse. *Proc. Natl. Acad. Sci. U. S. A.* **96**, 15062–7 (1999).

546. Bouchet, J., McCaffrey, M. W., Graziani, A. & Alcover, A. The functional interplay of Rab11, FIP3 and Rho proteins on the endosomal recycling pathway controls cell shape and symmetry. *Small GTPases* **9**, 310–315 (2018).

547. Onnis, A., Finetti, F. & Baldari, C. T. Vesicular trafficking to the immune synapse: How to assemble receptor-tailored pathways from a basic building set. *Front. Immunol.* **7**, 50 (2016).

548. Bouchet, J. *et al.* Rab11-FIP3 Regulation of Lck Endosomal Traffic Controls TCR Signal Transduction. *J. Immunol.* **198**, 2967–2978 (2017).

549. Pannerden, H. E. N. van tot, Geerts, W. J., Kleijmeer, M. J. & Heijnen, H. F. G. Spatial organization of the transforming MHC class II compartment. *Biol. Cell* **102**, 581–591 (2010).

550. Chow, A., Toomre, D., Garrett, W. & Mellman, I. Dendritic cell maturation triggers retrograde MHC class II transport from lysosomes to the plasma membrane. *Nature* **418**, 988–994 (2002).

551. Pulecio, J. *et al.* Cdc42-mediated MTOC polarization in dendritic cells controls targeted delivery of cytokines at the immune synapse. *J. Exp. Med.* **207**, 2719 (2010).

552. Keller, A. M. *et al.* Costimulatory ligand CD70 is delivered to the immunological synapse by shared intracellular trafficking with MHC class II molecules. *Proc. Natl. Acad. Sci. U. S. A.* **104**, 5989 (2007).

553. Vyas, J. M. *et al.* Tubulation of Class II MHC Compartments Is Microtubule Dependent and Involves Multiple Endolysosomal Membrane Proteins in Primary Dendritic Cells. *J. Immunol.* **178**, 7199 (2007).

554. Allan, V. J., Thompson, H. M. & McNiven, M. A. Motoring around the Golgi. *Nat. Cell Biol. 2002 410* **4**, E236–E242 (2002).

555. Allan, V. J. & Kreis, T. E. A microtubule-binding protein associated with membranes of the Golgi apparatus. *J. Cell Biol.* **103**, 2229–2239 (1986).

556. Tittarelli, A., Janji, B., Van Moer, K., Noman, M. Z. & Chouaib, S. The Selective Degradation of Synaptic Connexin 43 Protein by Hypoxia-induced Autophagy Impairs Natural Killer Cell-mediated Tumor Cell Killing. *J. Biol. Chem.* **290**, 23670–23679 (2015).

557. Tittarelli, A., Navarrete, M., Gleisner, M. A., Gebicke-Haerter, P. & Salazar-Onfray, F. Connexin-mediated signaling at the immunological synapse. *International Journal of Molecular Sciences* vol. 21 3736 (2020).

558. HS, G. *et al.* Activation of the innate immune receptor Dectin-1 upon formation of a 'phagocytic synapse'. *Nature* **472**, 471–475 (2011).

559. Li, M., Wang, H., Li, W., Xu, X. G. & Yu, Y. Macrophage activation on “phagocytic synapse” arrays: Spacing of nanoclustered ligands directs TLR1/2 signaling with an intrinsic limit. *Sci. Adv.* **6**, (2020).

560. Barth, N. D., Marwick, J. A., Vendrell, M., Rossi, A. G. & Dransfield, I. The ‘Phagocytic synapse’ and clearance of apoptotic cells. *Front. Immunol.* **8**, 1708 (2017).

561. Eng, E. W., Bettio, A., Ibrahim, J. & Harrison, R. E. MTOC reorientation occurs during FcγR-mediated phagocytosis in macrophages. *Mol. Biol. Cell* **18**, 2389–2399 (2007).

562. Okui, M. *et al.* Posttranslational regulation of CALHM1/3 channel: *N* -linked glycosylation and *S* -palmitoylation. *FASEB J.* **35**, e21527 (2021).

563. Fooksman, D. R., Shaikh, S. R., Boyle, S. & Edidin, M. Cutting Edge: Phosphatidylinositol 4,5-Bisphosphate Concentration at the APC Side of the Immunological Synapse Is Required for Effector T Cell Function. *J. Immunol.* **182**, 5179–5182 (2009).

564. SV, K. *et al.* Colocalization of the IL-12 receptor and FcgammaRIIIa to natural killer cell lipid rafts leads to activation of ERK and enhanced production of interferon-gamma. *Blood* **111**, 4173–4183 (2008).

565. Savio, L. E. B., Mello, P. de A., da Silva, C. G. & Coutinho-Silva, R. The P2X7 receptor in inflammatory diseases: Angel or demon? *Frontiers in Pharmacology* vol. 9 (2018).

566. Mansoor, S. E. *et al.* X-ray structures define human P2X3 receptor gating cycle and antagonist action. *Nat. 2016 5387623* **538**, 66–71 (2016).

567. Karasawa, A. & Kawate, T. Structural basis for subtype-specific inhibition of the P2X7 receptor. *Elife* **5**, (2016).

568. Bradford, M. D. & Soltoff, S. P. P2X 7 receptors activate protein kinase D and p42/p44 mitogen-activated protein kinase (MAPK) downstream of protein kinase C. *Biochem. J* **366**, 745–755 (2002).

569. Liu, Y., Xiao, Y. & Li, Z. P2X7 receptor positively regulates MyD88-dependent NF-κB activation. *Cytokine* **55**, 229–236 (2011).

570. Bian, S. *et al.* P2X7 Integrates PI3K/AKT and AMPK-PRAS40-mTOR Signaling Pathways to Mediate Tumor Cell Death. *PLoS One* **8**, e60184 (2013).

571. Shieh, C. H., Heinrich, A., Serchov, T., van Calker, D. & Biber, K. P2X7-dependent, but differentially regulated release of IL-6, CCL2, and TNF-α in cultured mouse microglia. *Glia* **62**, 592–607 (2014).

572. Janks, L., Sprague, R. S. & Egan, T. M. ATP-Gated P2X7 Receptors Require Chloride Channels To Promote Inflammation in Human Macrophages. *J. Immunol.* **202**, 883–898 (2018).

573. Browne, L. E., Compan, V., Bragg, L. & North, R. A. P2X7 receptor channels allow direct permeation of nanometer-sized dyes. *J. Neurosci.* **33**, 3557–3566 (2013).

574. Manohar, P. *et al.* Secondary Bacterial Infections in Patients With Viral Pneumonia. *Front. Med.* **7**, 420 (2020).

575. Gallego-Sandín, S., Alonso, M. T. & García-Sancho, J. Calcium homoeostasis modulator 1 (CALHM1) reduces the calcium content of the endoplasmic reticulum (ER) and triggers ER stress. *Biochem. J.* **437**, 469–75 (2011).

576. Verron, Q. *et al.* NK cells integrate signals over large areas when building immune synapses but require local stimuli for degranulation. *bioRxiv* 2020.07.29.224618 (2020) doi:10.1101/2020.07.29.224618.

577. Eckelhart, E. *et al.* A novel Ncr1-Cre mouse reveals the essential role of STAT5 for NK-cell survival and development. *Blood* **117**, 1565–1573 (2011).

578. Jamieson, A. M., Yu, S., Annicelli, C. H. & Medzhitov, R. Influenza virus-induced glucocorticoids compromise innate host defense against a secondary bacterial infection. *Cell Host Microbe* **7**, 103–114 (2010).

579. Jamieson, A. M. *et al.* Role of tissue protection in lethal respiratory viral-bacterial coinfection. *Science (80-.).* **340**, 1230–1234 (2013).

580. Schroder, K., Hertzog, P. J., Ravasi, T. & Hume, D. A. Interferon-γ: an overview of signals, mechanisms and functions. *J. Leukoc. Biol.* **75**, 163–189 (2004).

581. Day, J., Friedman, A. & Schlesinger, L. S. Modeling the immune rheostat of macrophages in the lung in response to infection.

582. Marino, S. *et al.* Macrophage polarization drives granuloma outcome during Mycobacterium tuberculosis infection. *Infect. Immun.* **83**, 324–338 (2015).

583. Rynda-Apple, A., Robinson, K. M. & Alcorn, J. F. Influenza and bacterial superinfection: Illuminating the immunologic mechanisms of disease. *Infect. Immun.* **83**, 3764–3770 (2015).

584. McCullers, J. A. The co-pathogenesis of influenza viruses with bacteria in the lung. *Nat. Rev. Microbiol. 2014 124* **12**, 252–262 (2014).

585. Rynda-Apple, A. *et al.* Regulation of IFN-γ by IL-13 dictates susceptibility to secondary postinfluenza MRSA pneumonia. *Eur. J. Immunol.* **44**, 3263–3272 (2014).

586. McNamee, L. A. & Harmsen, A. G. Both influenza-induced neutrophil dysfunction and neutrophil-independent mechanisms contribute to increased susceptibility to a secondary Streptococcus pneumoniae infection. *Infect. Immun.* **74**, 6707–6721 (2006).

587. Kudva, A. *et al.* Influenza A Inhibits Th17-Mediated Host Defense against Bacterial Pneumonia

in Mice. *J. Immunol.* **186**, 1666–1674 (2011).

588. McCullers, J. A. & Rehg, J. E. Lethal Synergism between Influenza Virus and Streptococcus pneumoniae: Characterization of a Mouse Model and the Role of Platelet-Activating Factor Receptor. *J. Infect. Dis.* **186**, 341–350 (2002).

589. Sun, K. & Metzger, D. W. Inhibition of pulmonary antibacterial defense by interferon-gamma during recovery from influenza infection. *Nat. Med.* **14**, 558–564 (2008).

590. Tian, X. *et al.* Poly I:C enhances susceptibility to secondary pulmonary infections by gram-positive bacteria. *PLoS One* **7**, (2012).

591. Luster, A. D., Unkeless, J. C. & Ravetch, J. V. γ-Interferon transcriptionally regulates an early-response gene containing homology to platelet proteins. *Nat. 1985 3156021* **315**, 672–676 (1985).

592. Costelloe, E. O., Stacey, K. J., Antalis, T. M. & Hume, D. A. Regulation of the plasminogen activator inhibitor-2 (PAI-2) gene in murine macrophages. Demonstration of a novel pattern of responsiveness to bacterial endotoxin. *J. Leukoc. Biol.* **66**, 172–182 (1999).

593. Williams, J. G., Jurkovich, G. J., Hahnel, G. B. & Maier, R. V. Macrophage priming by interferon gamma: a selective process with potentially harmful effects. *J. Leukoc. Biol.* **52**, 579–584 (1992).

594. Mita, Y., Dobashi, K., Shimizu, Y., Nakazawa, T. & Mori, M. Toll-like receptor 2 and 4 surface expressions on human monocytes are modulated by interferon-gamma and macrophage colony-stimulating factor. *Immunol. Lett.* **78**, 97–101 (2001).

595. Bosisio, D. *et al.* Stimulation of toll-like receptor 4 expression in human mononuclear phagocytes by interferon-gamma: a molecular basis for priming and synergism with bacterial lipopolysaccharide. *Blood* **99**, 3427–3431 (2002).

596. Liu, B. C. *et al.* Constitutive Interferon Maintains GBP Expression Required for Release of Bacterial Components Upstream of Pyroptosis and Anti-DNA Responses. *Cell Rep.* **24**, 155-168.e5 (2018).

597. Meunier, E. & Broz, P. Interferon-induced guanylate-binding proteins promote cytosolic lipopolysaccharide detection by caspase-11. *DNA Cell Biol.* **34**, 1–5 (2015).

598. Thompson, M. J. & Baenziger, J. E. Ion channels as lipid sensors: from structures to mechanisms. *Nat. Chem. Biol. 2020 1612* **16**, 1331–1342 (2020).

599. Jodaitis, L., van Oene, T. & Martens, C. Assessing the Role of Lipids in the Molecular Mechanism of Membrane Proteins. *Int. J. Mol. Sci. 2021, Vol. 22, Page 7267* **22**, 7267 (2021).

600. Zheng, H., Liu, W., Anderson, L. Y. & Jiang, Q. X. Lipid-dependent gating of a voltage-gated potassium channel. *Nat. Commun. 2011 21* **2**, 1–9 (2011).

601. Lee, R. J. & Cohen, N. A. Taste receptors in innate immunity. *Cell. Mol. Life Sci.* **72**, 217–36 (2015).

602. Wu, S. V. *et al.* Expression of bitter taste receptors of the T2R family in the gastrointestinal tract and enteroendocrine STC-1 cells. *Proc. Natl. Acad. Sci. U. S. A.* **99**, 2392–7 (2002).

603. Welcome, M. O. & Mastorakis, N. E. The taste of neuroinflammation: Molecular mechanisms linking taste sensing to neuroinflammatory responses. *Pharmacological Research* vol. 167 105557 (2021).